High-Throughput Online Monitoring Techniques for Bioprocesses with Spore-Forming Bacteria

Von der Fakultät für Mathematik, Informatik und Naturwissenschaften der RWTH Aachen University zur Erlangung des akademischen Grades einer Doktorin der Naturwissenschaften genehmigte Dissertation

vorgelegt von

Jennifer Goldmanns, M. Sc.
aus
Mönchengladbach

Berichter: Univ.-Prof. Dr. rer. nat. habil. Lars Lauterbach
Univ.-Prof. Dr.-Ing. Dr. h. c. (Osaka) Jochen Büchs

Tag der mündlichen Prüfung: 20.11.2024

Danksagung

Die vorliegende Arbeit entstand während meiner Tätigkeit als wissenschaftliche Mitarbeiterin am Lehrstuhl für Bioverfahrenstechnik der RWTH Aachen University im Rahmen einer Kooperation mit der BASF SE.

Mein besonderer Dank gilt Herrn Professor Büchs für die Möglichkeit am Lehrstuhl für Bioverfahrenstechnik zu promovieren. Seine wissenschaftliche Betreuung und die vielseitigen Diskussionen mit ihm haben zum Gelingen dieser Arbeit beigetragen. Weiterhin möchte ich mich bei Herrn Professor Lauterbach für die Übernahme der Erstprüferschaft sowie bei Herrn Professor Elling als Drittprüfer und bei Herrn Professor Conrath für die Übernahme des Prüfungsvorsitzes bedanken.

Meine Arbeit ist in einer engen Zusammenarbeit mit der BASF SE entstanden. Vor allem danke ich Dr. Tobias May und Dr. Priya Haas für den fachlichen Austausch und die spannenden Diskussionen.

Während meiner Zeit am Lehrstuhl haben mich zahlreiche engagierte Studierende durch Forschungspraktika, Abschlussarbeiten oder als Hilfswissenschaftler unterstützt und zum Erfolg der Arbeit beigetragen. Ein großer Dank geht an -in alphabetischer Reihenfolge- Alexander Deitert, Lina Hollmann, Marie Lipa, Georg Röhling, Benjamin Schick, Patrick Schminder, Theresa Scholand, Monique Schulze und Philipp Wirtz.

Meinen ehemaligen Kolleginnen und Kollegen der BioVT danke ich für die schöne gemeinsame Zeit am Lehrstuhl. Die angenehme und kollegiale Arbeitsatmosphäre, die Hilfsbereitschaft und enge Zusammenarbeit haben zum erfolgreichen Abschluss meiner Promotion beigetragen und meine Promotionszeit bereichert.

Abschließend möchte ich mich bei meiner Familie und bei Georg für die Unterstützung, den steten Rückhalt und das Vertrauen in mich bedanken.

Eidesstattliche Erklärung

Ich, Jennifer Goldmanns, erkläre hiermit, dass diese Dissertation und die darin dargelegten Inhalte die eigenen sind und selbstständig, als Ergebnis der eigenen originären Forschung, generiert wurden.

Hiermit erkläre ich an Eides statt

1. Diese Arbeit wurde vollständig oder größtenteils in der Phase als Doktorandin dieser Universität angefertigt;
2. Sofern irgendein Bestandteil dieser Dissertation zuvor für einen akademischen Abschluss oder eine andere Qualifikation an dieser oder einer anderen Institution verwendet wurde, wurde dies klar angezeigt;
3. Wenn immer andere eigene- oder Veröffentlichungen Dritter herangezogen wurden, wurden diese klar benannt;
4. Wenn aus anderen eigenen- oder Veröffentlichungen Dritter zitiert wurde, wurde stets die Quelle hierfür angegeben. Diese Dissertation ist vollständig meine eigene Arbeit, mit der Ausnahme solcher Zitate;
5. Alle wesentlichen Quellen von Unterstützung wurden benannt;
6. Wenn immer ein Teil dieser Dissertation auf der Zusammenarbeit mit anderen basiert, wurde von mir klar gekennzeichnet, was von anderen und was von mir selbst erarbeitet wurde;
7. Ein Teil oder Teile dieser Arbeit wurden zuvor veröffentlicht und zwar in:

   Goldmanns J, Röhling GA, Lipa MK, Scholand T, Deitert A, May T, Haas EP, Boy M, Herold A, Büchs J. Development of a chemically defined medium for *Paenibacillus polymyxa* by parallel online monitoring of the respiration activity in microtiter plates. BMC Biotechnology. 2023;23(1):25.

Tübingen, 08.02.2025

Jennifer Goldmanns

Zusammenfassung

Die Optimierung von Kultivierungsparametern ist entscheidend für effiziente mikrobielle Prozesse. Hierbei ist der Einsatz von geschüttelten Hochdurchsatz-Kultivierungssystemen in Kombination mit Online-Messtechniken während der initialen Bioprozessentwicklung von großer Bedeutung. In dieser Arbeit wurde das Potential von Online-Messtechniken zur Bewertung des Wachstums und der Sporulation in Kultivierungen sporulierender Bakterien untersucht.

Ein Schlüsselparameter für hohe Zelldichten ist ein an die Nährstoffanforderungen eines Mikroorganismus angepasstes Kultivierungsmedium. Am Beispiel eines industriellen *Paenibacillus polymyxa* Stammes wurde ein chemisch definiertes Medium im Mikrotiterplattenmaßstab entwickelt. Dafür wurde eine Methode, die eine systematische Vorgehensweise mit der Online-Überwachung der Atmungsaktivität kombiniert, erweitert, um Nährstofflimitierungen zu identifizieren. Nach der Verbesserung des Wachstums wurde das Medium auf die wachstumsrelevanten Komponenten reduziert. Die Kultivierung mit der finalen Medienzusammensetzung wurde in den Labor-Fermentermaßstab transferiert.

Neben hohen Zelldichten ist die Charakterisierung der Sporulation relevant, um hohe Sporenkonzentrationen in Bioprozessen mit sporulierenden Bakterien zu erreichen. Jedoch sind konventionelle Methoden zur Bestimmung der Sporenkonzentration aufwendig. Daher wurden in dieser Arbeit spektroskopische Techniken zur Online-Überwachung der Sporulation von *Bacillus subtilis* im Komplexmedium im Mikrotiterplattenmaßstab angewendet. Eine spezifische Fluoreszenzwellenlänge wurde identifiziert, deren Intensität mit der Freilassung der Sporen aus den Mutterzellen korrelierte. Es gibt deutliche Hinweise darauf, dass Siderophore diese charakteristische Fluoreszenz verursachen. Die Anwendbarkeit der Fluoreszenzmessung zur Sporendetektion wurde mit weiteren *Bacillus* Spezies validiert. Die Methode wurde zur Untersuchung des Einflusses der $CaCl_2$-Konzentration und der Sauerstoffverfügbarkeit auf die Sporulation von *B. subtilis* genutzt. Abschließend wurde die Übertragbarkeit der Methode auf ein chemisch definiertes Medium gezeigt.

Die Ergebnisse dieser Arbeit liefern die Grundlage zur effizienten und zuverlässigen Optimierung von Bioprozessen mit sporulierenden Bakterien unter Einsatz von Online-Hochdurchsatz-Messtechniken.

Abstract

The optimization of cultivation parameters is crucial for efficient microbial processes. Therefore, shaken high-throughput cultivation systems combined with online monitoring techniques are required in early bioprocess development. In this thesis, the potential of online monitoring techniques to evaluate growth and sporulation in cultivations of spore-forming bacteria was investigated.

A key parameter for achieving high cell densities is a tailor-made cultivation medium that complies with the specific nutrient requirements of the respective microorganism. A chemically defined medium was developed, exemplarily, for an industrial *Paenibacillus polymyxa* strain in microtiter plate scale. For this purpose, a method, combining a systematic experimental procedure with online monitoring of the respiration activity, was used. The method was extended to identify nutrient limitations. After improving the growth, the medium components were reduced to the growth-relevant ones. The cultivation with the final medium was transferred from the microtiter plate to the laboratory fermenter scale.

In addition to high cell densities, the characterization of sporulation is relevant to achieve high spore concentrations in bioprocesses with spore-forming bacteria. However, conventional spore determination methods are laborious. Therefore, spectroscopic techniques were applied in this thesis for online monitoring of *Bacillus subtilis* sporulation in microtiter plate cultivations with complex medium. A specific fluorescence wavelength was identified. The intensity of this fluorescence wavelength correlated with the release of spores from the mother cells. Strong indications demonstrated that siderophores cause this characteristic fluorescence. The universality of the fluorescence measurement for spore detection was validated with other *Bacillus* species. In addition, the method was used to investigate the influence of the $CaCl_2$ concentration and oxygen availability on the sporulation of *B. subtilis*. Finally, the applicability of the online spore detection method for a chemically defined medium was shown.

The results presented in this work provide the basis for the future usage of high-throughput online measurement techniques to optimize cultivations of spore-forming bacteria in a reliable and time-efficient manner.

Funding, publications, and contributions

The work underlying this thesis was funded by BASF SE (Ludwigshafen am Rhein, Germany). The funding is gratefully acknowledged.

Parts of this thesis (chapter 2) have previously been published:

- Goldmanns J, Röhling GA, Lipa MK, Scholand T, Deitert A, May T, Haas EP, Boy M, Herold A, Büchs J. Development of a chemically defined medium for *Paenibacillus polymyxa* by parallel online monitoring of the respiration activity in microtiter plates. BMC Biotechnology. 2023;23(1):25.[1]

  Authors' contributions: Jennifer Goldmanns designed the study, conducted microtiter plate experiments, analyzed and interpreted data, and drafted the manuscript. Georg Röhling, Marie Lipa, Theresa Scholand, and Alexander Deitert performed microtiter plate experiments and analyzed data. Tobias May and Evangeline Priya Haas designed part of the study, supervised the fermentation, participated in data interpretation, and critically revised the manuscript. Matthias Boy and Andrea Herold participated in data interpretation. Jochen Büchs supervised the study, participated in data interpretation and drafting the manuscript, and critically revised the manuscript. All authors read and approved the final manuscript.

By the time of submission of this thesis, parts of this thesis (chapter 3) are in preparation for submission as a journal article:

- Goldmanns J, Schulze M, Scholand T, May T, Haas EP, Boy M, Herold A, Büchs J. Application of online spectroscopic techniques for detection of *Bacillus* spores in cultivations with complex medium.

[1] Reproduced (adapted) with permission, Open Access CC BY 4.0 https://creativecommons.org/licenses/by/4.0/

Authors' contributions: Jennifer Goldmanns designed the study, conducted experiments, analyzed, and interpreted data, and drafted the manuscript. Monique Schulze and Theresa Scholand performed experiments and analyzed data. Tobias May and Evangeline Priya Haas designed part of the study, participated in data interpretation, and critically revised the manuscript. Matthias Boy and Andrea Herold participated in data interpretation. Jochen Büchs supervised the study, participated in data interpretation, and critically revised the manuscript. All authors read and approved the final manuscript.

Aspects from chapter 2 of this thesis have previously been incorporated into a patent application:

- May T, Haas EP, Heinrich DC, Goldmanns J, Büchs J. Materials and methods for improving plant health. 2022. WO2022029027A1.

Contributions to conferences during the preparation of this thesis (aspects from chapter 2):

- Goldmanns J, May T, Haas EP, Boy M, Büchs J. Identification of growth limiting components for *Paenibacillus* in a chemically defined medium by measuring the oxygen transfer rate in microtiter plates. Oral presentation. 6th European Congress of Applied Biotechnology. Digital conference. 2021.

- Goldmanns J, May T, Haas EP, Boy M, Büchs J. Development of a chemically defined medium for *Paenibacillus* by online monitoring of the breathing activity in microtiter plates. Oral presentation. ACHEMA Pulse. Digital congress. 2021.

Contents

Nomenclature

Abbreviations

Abbreviation	Description
µRAMOS	Respiration Activity MOnitoring System for 48-well microtiter plates
µTOM	Micro-scale(µ) Transfer rate Online Measurement device for 96-well microtiter plates
σ^F	Sigma F factor
ATP	Adenosine triphosphate
B. cereus	*Bacillus cereus*
B. subtilis	*Bacillus subtilis*
B. licheniformis	*Bacillus licheniformis*
B. megaterium	*Bacillus megaterium*
B. pumilus	*Bacillus pumilus*
B. thuringiensis	*Bacillus thuringiensis*
B. velezensis	*Bacillus velezensis*
Bc medium	*Bacillus* complex medium
BGSC	*Bacillus* Genetic Stock Center
CFU	Colony forming unit
CTR	Carbon dioxide transfer rate
DOT	Dissolved oxygen tension
DPA	Dipicolinic acid
DSM	Difco sporulation medium
DSMZ	German collection of Microorganisms and Cell Cultures
E. coli	*Escherichia coli*
exp	Experiment
gr.	Group
HPLC	High-performance liquid chromatography

Abbreviation	**Description**
k_La	Volumetric oxygen transfer coefficient
KEGG	Kyoto Encyclopedia of Genes and Genomes
LB medium	Lysogeny broth medium
MES	2-(*N*-Morpholino)ethanesulfonic acid
MTP	Microtiter plate
Moppa medium	Chemically defined medium for *Paenibacillus polymyxa*
MOPS	3-(*N*-morpholino)propanesulfonic acid
N	Number of replicates
NAD+/NADH	Nicotinamide adenine dinucleotide
NADP/NADPH	Nicotinamide adenine dinucleotide phosphate
nic.	Nicotinic
OD	Optical density
OFAT method	One-factor-at-a-time method
OTR	Oxygen transfer rate
OTR_{max}	Maximum oxygen transfer capacity
P. polymyxa	*Paenibacillus polymyxa*
pantoth.	Pantothenic
p-benz.	p-Aminobenzoic
Pbp complex medium	*Paenibacillus polymyxa* complex medium
RI	Refractive index
RQ	Respiratory quotient
RAMOS	Respiration Activity MOnitoring System
SASP	Small acid-soluble spore proteins
SCFU	Spore colony forming unit
TOC	Total oxygen consumption
VOC	Volatile organic compounds

Symbols

Symbol	Description	Unit
d_0	Shaking diameter	mm
Corrected DOT	DOT after correction	%
DOT	Dissolved oxygen tension	%
DOT_{min}	DOT minimum	%
DOT_{max}	DOT maximum	%
I	Intensity	a.u.
I_0	Initial intensity	a.u.
k_La	Volumetric oxygen transfer coefficient	1/h
L_{O2}	Oxygen solubility	mol/L/bar
n	Shaking frequency	rpm
OTR	Oxygen transfer rate	mmol/L/h
pO_2^{cal}	Head space oxygen partial pressure during calibration	bar
pO_2^{gas}	Oxygen partial pressure in the head space	bar
T	Temperature	K
$t_{0\ h}$ / $t_{67\ h}$	Time (0 h and 67 h)	h
V_L	Filling volume	mL
V_K	Nominal volume of shake flask	mL
V_W	Volume of well of microtiter plate	mL
λ_{em}	Emission wavelength	nm
λ_{ex}	Excitation wavelength	nm

XVIII

List of Figures

List of Tables

1 Introduction

1.1 *Bacillus* spores and their characteristics

Sporulation is a complex biological process triggered under starving conditions in certain bacteria [1, 2]. During sporulation, vegetative cells develop dormant endospores [1, 2], in the following referred to as spores. Known spore-forming bacteria belong, for example, to the genus *Bacillus* and *Clostridium* [3]. *Bacillus* spp. are aerobic or facultative anaerobic, gram-positive bacteria with rod-shaped cells and cylindrical, ellipsoidal, or spherical spores [4, 5]. The discovery of bacterial spores can be traced back to the 19th century. In 1876, the first characterization of *Bacillus* spores was documented by Ferdinand Cohn [6] and Robert Koch [7]. About a century later, the morphological stages of *Bacillus* sporulation were revealed by applying electron microscopy [8]. Over the decades, research on sporulation was mainly performed using the model organism *Bacillus subtilis* [2], as it is well-studied regarding its physiology and genetics [9]. The morphological stages of *Bacillus* sporulation are summarized in review articles [2, 10]. The most crucial stages are the following. Under starving conditions, vegetative cells start sporulation with an asymmetric cell division. A septum is formed, dividing the cell into a larger mother cell and a smaller forespore. The next step is the engulfment, a phagocytosis-like process, of the forespore by the mother cell. The forespore is then located in the cytosol of the mother cell. Cortex formation and coat assembly take place during the development of the mature spore. Subsequently, the mother cell lyses, and the mature spore is released into the environment [2, 10]. As soon as environmental conditions improve, spores can germinate into vegetative cells [11, 12]. The regulation and control of the sporulation process by numerous genes and transcription factors is summarized, for example, by Errington [13].

A major characteristic of spores is their resistance to harsh environmental influences such as heat, radiation, and exposure to various chemicals [14-16]. This resistance arises from the spore's structure and chemical composition [14-16]. The structure of *Bacillus* spores from the outside to the inside consists of an exosporium (not all *Bacillus* species), a coat, an outer membrane, a cortex, a germ cell wall, an inner membrane, and a spore core [17-19]. For example, the spore's inner membrane is a permeability barrier for chemicals, like methylamine [20]. A spore-specific component is dipicolinic acid (pyridine-2,6-dicarboxylic acid, DPA), accounting for up to 5-15 % dry weight of the spore [21]. The acid is represented in the spore core in a chelate, typically, with calcium (calcium-DPA) in a ratio of about 1:1 [21-23]. However, DPA can also form complexes with other divalent cations, like copper, manganese, and iron [24]. DPA is a major factor that is responsible for the spore's resistance to desiccation [25]. The accumulation of calcium-DPA correlates with a low water content in the spore core, which is 28-57 % of the wet weight of the spore core [26, 27]. The high wet heat resistance of the spores is mainly attributable to this low water content [27, 28]. Further components in the spore core are α/β-type small acid-soluble spore proteins (SASP) [29]. Those proteins contribute to the spore's resistance to heat, desiccation, chemicals, and UV radiation by binding on the DNA [30]. Another characteristic of *Bacillus* spores is that they contain almost no high-energy compounds like adenosine triphosphate (ATP) and nicotinamide adenine dinucleotide (triphosphate) (NAD(P)H) [31, 32]. This metabolic inactivity of the spores, together with their resistance to harsh environmental conditions, enable spores to survive long periods in starvation [33, 34].

There are several fields for biotechnological applications of *Bacillus* spores [35]. A well-known application of *Bacillus* spores are probiotics for human and animal health [36]. A further relevant field of application of *Bacillus* spores is their use as biopesticides in agriculture [37, 38]. Biopesticides offer a safer plant protection strategy than chemical pesticides, which harbor risks for humans and the environment [37, 38]. After treatment of the plant with spore-based biopesticides, the plant is protected from pathogens by various modes of action of the germinated *Bacillus* strains [39]. Those modes of action include, for instance, inducing defense mechanisms in the plant [40] and the production of lipopeptides [41] and lytic enzymes [42]. Another interesting application of *Bacillus* spores is self-healing of concrete in civil engineering by calcium carbonate precipitation [43]. The usage of spores

for self-healing of concrete is advantageous as spores can survive the harsh conditions in the cement, like alkaline pH values [43]. Utilizing *Bacillus* spores as a platform for expressing industrial enzymes via spore surface display has become increasingly important [44, 45]. Spore surface display is a technology presenting exogenous proteins on the spore surface by anchoring them with a spore surface protein [46]. This technology enables simple separation of the enzymes from their substrates and improved stability and reusability due to the spore's resistance [45]. Examples of industrial relevant enzymes expressed by *Bacillus* spores with a high stability are the lipase TM1350 from *Thermotoga maritima* [47] and the D-psicose 3-epimerase from *Clostridium scindens* [48]. The spore surface display can also be used in vaccine preparation [35]. For example, the expression of the antigen of *Salmonella* serovar Pullorum, OmpC, on the spore surface of *B. subtilis* as a potential vaccine against *Salmonella* infections was shown by Dai et al. [49]. The broad field of applications shows that nowadays, bioprocesses with spore formers are gaining relevance.

1.2 *Paenibacillus polymyxa*

Paenibacillus polymyxa (only remotely related to *B. subtilis*) is a facultative anaerobic, gram-positive spore-forming bacterium with rod-shaped cells and ellipsoidal spores [50]. *Paenibacillus* species formerly belonged to the genus *Bacillus*, but based on latest sequence analysis, a phylogenetically distinct group was created [50]. *P. polymyxa* is typically found in soils and in the rhizosphere of crop plants [51, 52]. The bacterium has several capabilities that make the organism a plant growth-promoting rhizobacterium (PGPR) [53-55]. Those capabilities include, for instance, the production of siderophores to facilitate iron uptake of the plant [56] and the production of the cytokinin isopentenyl adenine for growth stimulation of the plant [57].

P. polymyxa and its products can be used for numerous biotechnological applications [53-55]. One of those applications is the pathogen control in agriculture [55]. The bacterium protects the plant from pathogens through several modes of action [55]. For example, *P. polymyxa* can produce cell-wall degrading enzymes, like proteases [58] and chitinases [59]. Further modes of action are the production of antifungal compounds, like fusaricidins

[60] and volatile organic compounds (VOCs) [58]. Applications in the pharmaceutical and food industry arise from exopolysaccharides with antioxidant and antitumor activities, produced by *P. polymyxa* [61]. Exopolysaccharides of *P. polymyxa* are also described for applications in wastewater treatment by removing metal ions from wastewater [62]. In addition, *P. polymyxa* can produce valuable chemical compounds, like 2,3-butanediol [63, 64], for applications in the chemical, cosmetic and pharmaceutical industries [65].

1.3 Small-scale online monitoring techniques

In-depth process knowledge is substantial for targeted scale-up from laboratory into industrial scales. Gaining this process knowledge requires an intensive preliminary small-scale process characterization and optimization regarding growth and product formation. Small-scale online monitoring techniques in shaken cultures are a valuable tool in research and development [66]. High-ranking clones [67] and favorable cultivation conditions, like medium compositions [68, 69], can be efficiently screened using those techniques.

Several devices were developed for online monitoring of different cultivation parameters in shake flask and microtiter plate (MTP) scale [70-78]. One important parameter is the respiration activity. By monitoring the respiration activity, information on the metabolic state of the culture, such as on oxygen limitations [79], substrate limitations [80], product inhibitions [81], and diauxic growth [82], is obtained. A frequently applied parameter for the determination of the respiration activity of aerobic microorganisms is the oxygen transfer rate (OTR) [68, 82]. In shake flask scale, the Respiration Activity MOnitoring System (RAMOS) is a well-established device for non-invasive monitoring of the OTR [70, 71]. The oxygen partial pressure in the head space of each customized shake flask is measured with an electrochemical oxygen sensor. The OTR is calculated based on the decrease of the oxygen partial pressure due to the respiration of the microorganisms in the measuring phase. In addition to the OTR, the carbon dioxide transfer rate (CTR) and respiratory quotient (RQ) can be monitored in the RAMOS device in shake flasks [70, 71]. Commercial versions of the system are available from Adolf Kühner AG (Birsfelden, Switzerland) or HiTec Zang GmbH (Herzogenrath, Germany). For high-throughput, non-invasive OTR determination

was implemented for 48-well MTPs (µRAMOS) [73]. Due to the miniaturized dimensions, the wells of the MTP cannot be equipped with electrochemical oxygen sensors. Instead, the µRAMOS device measures the oxygen partial pressure in the head space of each well via fluorescence quenching by applying fluorescence sensor spots in for each well. Optical fibers for each well transmit the signal from the well to the oxygen measuring device via an optical multiplexer [73]. To further increase the throughput, the micro(µ)-scale Transfer rate Online Measurement device (µTOM) was developed, which allows the non-invasive determination of the OTR in 96-well plates [74].

Apart from the OTR measurement, other relevant parameters such as the dissolved oxygen tension (DOT), pH, scattered light, and fluorescence can be measured to monitor a cultivation. Applying devices based on optical measurement techniques allow for the non-invasive detection of these parameters without interrupting the cultivation [72, 75, 76, 78]. For example, the Cell Growth Quantifier (Aquila Biolabs, Baesweiler, Germany) monitors biomass formation in shake flasks, based on backscattered light measurement through the shake flask bottom using a sensor plate [78]. The application of fluorescence dyes as sensor spots in shake flasks allows for monitoring of the pH and DOT of microorganisms (Sensor Flask and SFR vario, PreSens, Regensburg, Germany). In addition, sensor spots for pH and DOT measurement can be integrated in MTPs [83, 84]. As a high-throughput system, the BioLector (commercialized by m2p labs, now part of Beckmann Coulter GmbH, Krefeld, Germany, for example BioLector I) detects non-invasively the scattered light and fluorescence through the transparent bottom in each well of a continuously shaken MTP [72, 75]. Further, pH and DOT can be monitored in the BioLector using MTPs with fluorescence sensor spots (m2p labs, part of Beckmann Coulter GmbH, Krefeld, Germany). In the BioLector, an optical fiber bundle transmits the excitation and emission light between the well of the MTP and a fluorescence reader [72, 75]. During the cultivation, a *x*-*y*-positioning device moves the optical fiber bundle under the MTP from well to well [72, 75]. The commercial versions use an optical filter module system. To allow for individual selection of the wavelength combinations, a BioLector variant using a spectrometer with monochromators instead of a filter module system was developed [76]. Suitable wavelength combinations can be determined beforehand using 2D fluorescence spectroscopy [85, 86]. With the fluorescence measurement in the BioLector, a wide variety of fluorophores can be

monitored, such as the intracellular fluorescence of NADH [72, 75]. In addition, for example, prodigiosin production of *Pseudomonas putida* [85] and pigment formation of *Streptomyces coelicolor* [87] were successfully detected via fluorescence in the BioLector. Scattered light is a commonly used parameter for monitoring biomass formation [75]. In addition, scattered light measurement can uncover morphological changes [88, 89]. To increase the information obtained from cultivations, the BioLector technology and the µRAMOS technology can be combined for measuring the OTR, scattered light and fluorescence within one device (µRAMOS/BioLector combination) [77].

1.4 Objectives and overview

For efficient processes with spore-forming bacteria, intensive preliminary process optimization is necessary to gain in-depth knowledge about the cultivation behavior and the dedicated nutritional requirements of a production strain. To keep the process optimization as fast and simple as possible, online monitoring techniques in high-throughput screenings are promising. Thus, this thesis tests the applicability of different small-scale online monitoring techniques in cultivations of spore-forming bacteria to assess growth and sporulation.

The composition of the cultivation medium is a crucial parameter for optimal growth and product formation of microorganisms [90-92]. Most cultivation protocols of the spore-forming bacterium *P. polymyxa* are based on complex media, yet [63, 93-95]. However, complex media have the disadvantage of an inconsistent fermentation performance, mainly due to the varying composition of undefined components such as soy flour or yeast extract [96-99]. Therefore, chemically defined media are favored, but they often result in lower growth rates, cell densities, and product yields [100-102], making use of these media in industry often not economically viable. Also, the development of chemically defined media is often much more time-intensive compared to the application of nutrient-rich complex media. The objective of chapter 2 was to identify nutrient limitations for growth in a chemically defined medium by extending a medium optimization method, which is based on a systematic procedure combined with online monitoring of the respiration activity in MTPs

[68]. The medium development was performed, exemplarily, for an industrially relevant *P. polymyxa* strain. After determining nutrient limitations, the medium components were reduced to the growth-relevant ones to diminish the costs and effort of medium preparation. The offline parameters optical density (OD), pH, carbon source consumption, and metabolite production were measured to verify the results of the respiration activity online monitoring. The final medium was transferred to a laboratory fermenter to show the applicability of the medium composition at larger scales.

In addition to achieving high cell densities, the characterization of sporulation is an important aspect in optimizing bioprocesses with spore-forming bacteria. Industrial processes that aim to produce spores, require high spore concentrations and sporulation efficiencies. Spore concentrations are typically determined with laborious methods, like agar-plating [103, 104] or microscopy in combination with a counting chamber [105, 106]. In chapter 3, a method for online monitoring of *Bacillus* species sporulation in a complex medium was developed by applying spectroscopic techniques to reduce the effort for assessing spore concentrations and accelerate process optimization. Therefore, conspicuous wavelength combinations were screened in the culture broth of the model organism *B. subtilis*. Then, online fluorescence and scattered light measurement by the BioLector technology was performed in *B. subtilis* cultivations. Samples were taken and microscopic images were recorded to evaluate the sporulation state and to establish correlations with online signals.

In chapter 4, the online spore detection method of chapter 3 was used to assess influence parameters on the sporulation of *B. subtilis*. As calcium is relevant for the heat resistance of *B. subtilis* spores [107] and known to affect spore concentrations [108-110], the effect of additional $CaCl_2$ in the complex medium on *B. subtilis* sporulation was tested. In the past, several studies investigating the influence of oxygen availability on the sporulation of *Bacillus* species were performed in fermenter scale [111-114]. Hence, the experimental throughput is limited. Therefore, the aim of chapter 4 was to assess the influence of the oxygen availability on *B. subtilis* sporulation in-depth in small-scale to allow multiple parallel conditions. Finally, the applicability of the online spore detection method for a chemically defined medium was studied in chapter 5.

The following chapter has previously been published:

- Goldmanns J, Röhling GA, Lipa MK, Scholand T, Deitert A, May T, Haas EP, Boy M, Herold A, Büchs J. Development of a chemically defined medium for *Paenibacillus polymyxa* by parallel online monitoring of the respiration activity in microtiter plates. BMC Biotechnology. 2023;23(1):25.

  The journal article [115] was adapted for this thesis.

Aspects of the following chapter have previously been incorporated into a patent application [116]:

- May T, Haas EP, Heinrich DC, Goldmanns J, Büchs J. Materials and methods for improving plant health. 2022. WO2022029027A1.

Contributions to chapter 2:

The contributions are listed in the chapter “Funding, publications, and contributions”. More detailed experimental contributions from others: Georg Röhling and Marie Lipa assisted with the experiments presented in chapter 2.3.2 (AVT – Biochemical Engineering, RWTH Aachen University, Aachen, Germany). Theresa Scholand, Alexander Deitert, and Georg Röhling assisted with the experiments shown in chapter 2.3.3 (AVT – Biochemical Engineering, RWTH Aachen University, Aachen, Germany). The fermentation, presented in chapter 2.3.4, was performed by BASF SE under the supervision of Dr. Tobias May and Dr. Evangeline Priya Haas (BASF SE, Ludwigshafen am Rhein, Germany).

2 Development of a chemically defined medium for *Paenibacillus polymyxa* by parallel online monitoring of the respiration activity in microtiter plates

2.1 Introduction

Finding suitable process parameters for growth of microorganisms and product formation in microbial cultivations is essential to achieve high product yields. One crucial parameter is the composition of the cultivation medium [90-92]. Often, media containing complex nutrient sources such as yeast extract, meat extract, peptone, and soy flour are applied [117] due to several reasons: It is well known that adding complex components to cultivations leads to high productivities [93]. Furthermore, media recipes are easy-to-use, due to the nutrient-rich composition of complex components. For example, yeast extract contains many nutrients such as carbohydrates, amino acids, peptides, vitamins, growth factors, and trace elements [117]. In contrast to those advantages, the varying composition of complex components often results in an inconsistent fermentation performance [96-98]. Klotz et al. showed the impact of different compositions of yeast extract and peptone from various manufacturers on lactic acid concentrations and productivity of *Sporolactobacillus inulinus* [97]. Furthermore, the composition of soy flour and soy meal is influenced by the soybeans' origin, climate and soil [118] and by their processing methods [119, 120]. Additionally, varying compositions of soy flour were shown over eight years in a single manufacturing plant [99].

To overcome these disadvantages of complex media, the application of chemically defined media is favorable. Chemically defined media are already used in various investigations,

such as in studies of recombinant protein production [121], cell morphology [122], and metabolic engineering [123]. The advantages of chemically defined media were summarized by Zhang and Greasham [124]. As an example, these media can ensure a more reproducible fermentation performance explicitly due to the chemically defined composition. Furthermore, the media components usually are less sensitive to sterilization conditions, in contrast to complex components. Additionally, downstream processing is often simplified, as those media typically do not contain insoluble components, proteins or other cellular compounds [124]. However, cell densities and product yields are often lower in chemically defined media than in complex media [100, 101]. In addition, growth rates are often reduced, compared to complex media [101, 102]. Microorganisms need to synthesize various cellular building blocks on their own, when they are not supplied in the medium [124]. Growth in a chemically defined medium is not possible at all, if microorganisms exhibit auxotrophies and the required nutrient is not added to the medium [68]. In contrast to complex media, which can balance nutritional limitations, a significant challenge of applying a chemically defined medium is to identify the nutrients that the organisms need for high growth rates and product formation [124]. Nutrient requirements and necessary concentrations of nutrients need to be determined to achieve comparable or higher growth rates, cell densities and product yields than in complex media [100, 101, 125]. Additionally, adding unnecessary medium components or components in excess increases costs. As the specific demand for nutrients of microorganisms or strains varies, time-intensive medium optimization is necessary.

To identify and optimize suitable cultivation media, various techniques are established and were summarized by Singh et al. [126]. One classical method is the one-factor-at-a-time (OFAT) method. The technique is known to be easy to use, as only one factor is modified, while all other factors are not changed. Moreover, for analysis, no statistical programs are needed [126]. The method was applied by various groups for medium development [127-129].

Due to laborious experiments and lack of information about correlations between experiments or changed parameters, many other methods were established to optimize fermentations [126, 130]. Statistical methods are applied for medium development [100,

131, 132] and optimization of other crucial parameters, such as pH, temperature, and agitation rate [100, 131, 133]. By varying more than one component at a time and planning experiments strategically, process development is performed more efficiently than with classical methods, because the number of experiments can be reduced [126]. However, drawbacks of those methods are limitations due to a rigidly defined space for parameters to be investigated and local optima [134].

Müller et al. presented a method, which was used to identify auxotrophies for a *Bacillus pumilus* strain in a chemically defined medium [68]. A systematic experimental procedure combined with online monitoring of the OTR as indicator for metabolic behavior was applied. A nutrient-rich chemically defined medium, called complete modified Poolman medium, was used as starting point. The complete modified Poolman medium was based on a medium developed for *Lactobacillus* bacteria [135] and the V3 mineral medium, typically used for *Bacillus* species [136]. Auxotrophies were identified and medium components were reduced to essential ones by grouping the nutrients. Due to the combination with online techniques to monitor the respiration activity, no labor-intensive offline analysis of samples was necessary. However, the applicability of the method to identify growth limitations was not considered as nutrient concentrations were not investigated [68]. Lapierre et al. investigated the nutrient requirements for *Sporosarcina pasteurii* [69], using the systematic method developed by Müller et al. [68]. Essential nutrients and growth limitations were identified by systematically omitting or increasing nutrient groups [69]. As an alternative, online monitoring based on scattered light was performed instead of online monitoring of the OTR [69]. Biomass online monitoring via scattered light measurement can be influenced by cell morphology [137]. Therefore, changes in cell geometry due to sporulation of spore-forming microorganisms might affect the scattered light measurement.

Nutrient requirements of the spore-forming bacterium *P. polymyxa* are not well known as most cultivations are performed in complex media [63, 93-95]. To our knowledge, only few mineral media, which were initially developed for other microbial strains, were used in the past for the cultivation of *P. polymyxa*. For example, Adlakha et al. cultivated *P. polymyxa* in a minimal medium adapted from Schepers et al. with 5 g/L glucose [138, 139]. Alvarez et al. used a chemically defined medium described in von der Weid et al. to investigate

extracellular proteolytic enzyme production [140, 141]. However, none of those studies describes, which nutrients are essential for growth or enhance growth.

This study's objective was to extend the systematic medium optimization method in combination with the µRAMOS technique [68] to identify growth limitations in chemically defined media, exemplarily for an industrial *P. polymyxa* strain. This strain was generated by random-mutagenesis of a wild-type isolate and designated as *P. polymyxa* JG1. In addition, the efficiency of the method of Müller et al. to reduce medium components [68] was confirmed. To best of our knowledge, this study is the first-time report of developing a defined medium for the industrially relevant *P. polymyxa* strain by using this medium optimization method. A screening procedure for *P. polymyxa* was established in MTPs and a reproduction of the cultivation in a laboratory fermenter was performed. The respiration activity of *P. polymyxa* showed good comparability in the µRAMOS and fermenter.

2.2 Materials and Methods

2.2.1 Microbial strain

The cultivations were performed with a *P. polymyxa* strain, which was obtained from BASF SE (Ludwigshafen am Rhein, Germany). This strain was generated by random-mutagenesis of a wild-type isolate, in order to abolish the production of the human last-line antibiotic polymyxin, without affecting growth and sporulation. The strain was designated as *P. polymyxa* JG1. Further information is available from BASF SE (Ludwigshafen am Rhein, Germany) on request.

2.2.2 Cultivation media

A complex medium was used for pre-cultures. The composition of the medium is listed in Table 2-1.

Table 2-1: Composition of pre-culture and main-culture complex medium.

The pre-culture complex medium contains 60 g/L maltose, and no buffer was used. The main-culture complex medium, called *Paenibacillus polymyxa* (Pbp) complex medium, contains 120 g/L maltose syrup instead of 60 g/L maltose, and additionally 0.1 M MES buffer. The letters in brackets indicate which components were prepared together in a stock solution. 3.21 g/L citric acid was added to the medium by the stock solution marked with (a) and 0.4 g/L was added by the stock solution marked with (c) to the final medium.

Ingredients		**Concentration in the medium [g/L]**
Main components		
Maltose (Maltose syrup)		60 (120)
Citric acid · H_2O	(a, c)	3.61
K_2HPO_4	(a)	1
$(NH_4)_2SO_4$	(a)	1.07
$MgSO_4$ · 7 H_2O	(a)	1.62
Yeast extract	(a)	5
Soy flour	(a)	10
Antifoam	(a)	0.2
$Ca(NO_3)_2$ · 4 H_2O		0.342
Vitamins		
Thiamin HCl	(b)	0.005
Nicotinic acid	(b)	0.005
Riboflavin	(b)	0.0002
Biotin	(b)	0.00005
Calcium pantothenate	(b)	0.001
Pyridoxine HCl	(b)	0.005
Vitamin B12	(b)	0.00005
Lipoic acid	(b)	0.00005
Trace elements		
$MnSO_4$ · H_2O	(c)	0.013
$CuSO_4$ · 5 H_2O	(c)	0.0046
Na_2MoO_4 · 2 H_2O	(c)	0.0028
$Fe_2(SO_4)_3$ · H_2O	(c)	0.015

The trace element, vitamin, and $Ca(NO_3)_2$ stock solutions were sterilized by filtration (0.2 µm). The maltose stock solution was autoclaved at 121 °C for 60 min. The pH of the stock solution containing citric acid, K_2HPO_4, $(NH_4)_2SO_4$, $MgSO_4$, yeast extract (Bio Springer, Maisons-Alfort, France), and soy flour (Sofarine Bic Protein, BiC, BC's-

Hertogenbosch, The Netherlands) was checked to be lower than 6.0. Then antifoam (Struktol J673, Schill+Silacher "Struktol" GmbH, Hamburg, Germany) was added and the solution was autoclaved at 121 °C for 60 min. Immediately before starting the cultivation, all stock solutions were combined, and the pH of the medium was adjusted to 6.5 using 25 % (w/w) NH_3 • aq and 40 % (w/w) H_3PO_4 solutions.

Main-cultures were performed in complex or in chemically defined medium. The complex medium was the same as for pre-cultures with some modifications and was here called *Paenibacillus polymyxa* (Pbp) complex medium (Table 2-1). This Pbp complex medium contained 120 g/L glucose syrup (C☆SweetTM M, Cargill Deutschland GmbH, Krefeld, Germany) instead of 60 g/L maltose and additionally 0.1 M 2-(*N*-morpholino)ethanesulfonic acid (MES) buffer. In the study presented herein, the glucose syrup is called maltose syrup. It contains around 50 % (w/w) dimeric maltose molecules, 21 % (w/w) maltose oligomers, and 2 % (w/w) glucose, resulting in an initial dimeric maltose concentration of around 60 g/L in the Pbp complex medium. The pH of the MES buffer stock solution was adjusted to 6.5 with 50 % (w/v) NaOH. Maltose syrup stock solution was autoclaved, and MES buffer was sterile filtered (0.2 µm). Preparation of the medium was performed as described for the pre-culture complex medium.

The chemically defined medium for main-cultures of *P. polymyxa* is called Moppa medium. This medium is based on a chemically defined medium after Müller et al. [68] and was modified. The composition of the Moppa medium and its variations are listed in Table 2-2. The maltose syrup, citric acid/ $(NH_4)_2SO_4$, and antifoam stock solutions were autoclaved at 121 °C for 60 min. All other stock solutions were sterile filtered. The MES buffer was prepared as for the complex medium, and the K_2HPO_4 solution was adjusted to a pH of 6.5 with a 40 % (w/w) H_3PO_4 solution. The pH of individual amino acid, vitamin and nucleobases/-sides stock solutions was changed with KOH or HCl solutions if they were not water soluble in the required concentration. The iron stock solution was frozen in aliquots at -20 °C after sterile filtration. Immediately before starting the cultivation, all medium stock solutions were combined except K_2HPO_4, and the pH was adjusted to 6.5 with a 25 % (w/w) NH_3 • aq solution and a 40 % (w/w) H_3PO_4 solution. After that, the K_2HPO_4 solution was added. The medium composition was adjusted for each experiment shown in the respective

figures, and the preparation of stock solutions was adapted for the investigated components. For the fermentation, the reduced Moppa medium, specified in Table 2-2, was prepared with 0.4 g/L D/L-methionine instead of 0.2 g/L L-methionine.

Table 2-2: Composition of chemically defined medium for *Paenibacillus polymyxa* (Moppa medium) for main-cultures and its variations.

The letters in brackets indicate which components were prepared together in a stock solution. In experiments with varying concentrations of medium components, the preparation of stock solutions was adapted according to the varying components.

Ingredients		**Concentration in Moppa medium [g/L]**	**Concentration in supplemented Moppa medium [g/L]**	**Concentration in reduced Moppa medium [g/L]**
Main components				
Maltose syrup		120	120	120
Citric acid · H_2O	(a)	3.61	3.61	3.61
K_2HPO_4		1	3	3
$(NH_4)_2SO_4$	(a)	1.07	3.21	3.21
$MgSO_4$ · 7 H_2O		1.62	1.62	1.62
MES buffer		19.5	39.0	39.0
Antifoam		0.2	0.2	0.2
$Ca(NO_3)_2$ · 4 H_2O		0.342	0.342	0.342
Vitamins				
Ascorbic acid		0.5	0.5	
Biotin		0.00006	0.00006	0.00006
Nicotinic acid	(b)	0.0011	0.013	0.013
Calcium pantothenate	(b)	0.001	0.001	
p-Aminobenzoic acid	(b)	0.01	0.01	
Pyridoxamine 2 HCl	(b)	0.006	0.006	
Pyridoxine HCl	(b)	0.002	0.002	
Vitamin B12	(b)	0.001	0.001	
Thiamin HCl	(b)	0.001	0.001	
Riboflavin		0.001	0.001	
Orotic acid		0.005	0.005	
Folic acid		0.001	0.001	
Inositol		0.0002	0.0002	
Amino acids				
L-Alanine		0.24	0.24	
L-Arginine		0.125	0.125	0.125

Ingredients		Concentration in Moppa medium [g/L]	Concentration in supplemented Moppa medium [g/L]	Concentration in reduced Moppa medium [g/L]
L-Aspartic acid		0.42	0.42	
L-Cysteine		0.13	0.13	
(S)-(+)-Glutamic acid		0.5	0.5	0.5
L-Glycine		0.175	0.175	
L-Histidine		0.15	0.15	0.15
L-Isoleucine		0.21	0.21	
L-Leucine		0.475	0.475	
L-Lysine		0.44	0.44	
L-Methionine		0.2	0.2	0.2
L-Phenylalanine		0.275	0.275	
L-Proline		0.675	0.675	0.675
L-Serine		0.34	0.34	
L-Threonine		0.225	0.225	
L-Tryptophane		0.05	0.05	
L-Tyrosine		0.25	0.25	
L-Valine		0.325	0.325	
Nucleobases/ -sides				
Adenine		0.01	0.01	
Guanine		0.01	0.01	
Inosine		0.005	0.005	
Xanthine		0.01	0.01	
Thymidine		0.005	0.005	
Uracil		0.01	0.01	
Trace elements				
$ZnSO_4 \cdot 7\ H_2O$	(c)	0.009	0.009	0.009
$CoSO_4 \cdot 7\ H_2O$	(c)	0.004	0.004	0.004
$CuSO_4 \cdot 5\ H_2O$	(c)	0.004	0.004	0.004
$(NH_4)_6Mo_7O_{24} \cdot 4\ H_2O$	(c)	0.003	0.003	0.003
$CaCl_2 \cdot 2\ H_2O$	(c)	0.066	0.066	0.066
$MnCl_2$	(c)	0.016	0.016	0.016
$FeCl_2$	(c)	0.005	0.005	0.005
$FeCl_3 \cdot 6\ H_2O$	(c)	0.005	0.005	0.005

2.2.3 Cultivation conditions

For pre-cultures, 30 mL medium was inoculated with 180 µL of cryo-culture in a baffled 250 mL shake flask closed with a plug (Silicosen®, Hirschmann Laborgeräte GmbH & Co. KG, Eberstadt, Germany). Cultivations were performed at 33 °C with a shaking diameter of 25 mm, and a shaking frequency of 150 rpm for 24-26 h.

Main-cultures were inoculated with 2.0 % (v/v) from pre-culture for the MTPs and fermenter cultivations. The main-cultures in MTPs were conducted in 48-round well MTPs without optodes (MTP-R48-B, Beckman Coulter GmbH, Krefeld, Germany) at 33 °C with a shaking diameter of 3 mm, a shaking frequency of 1000 rpm, and a filling volume of 0.8 mL in complex Pbp medium or chemically defined Moppa medium. MTPs were closed with a gas-permeable sealing foil (900371-T, HJ-Bioanalytik GmbH, Erkelenz, Germany). The in-house developed µRAMOS device was used for online monitoring of the OTR [73].

The fermentation was performed in a stirred tank reactor (1.8 L Benchtop fermentation system, DasGip, Eppendorf, Hamburg, Germany). The cultivation was conducted in batch mode with a liquid volume of 1 L at 33 °C. The DOT was controlled at 30 % with a stirrer-gas flow cascade (400 to 1400 rpm for a DOT of 0 to 40 % and 18-180 sL/h for a DOT of 40 to 100 %). The pH was controlled at 6.5 using 25 % NH_3 • aq and 40 % H_3PO_4 solutions. BlueSens sensors (Herten, Germany) were used for exhaust gas analytics. Antifoam addition (Struktol J673, Schill+Seilacher “Struktol” GmbH, Hamburg, Germany) was performed on demand by using an antifoam probe.

2.2.4 Offline analysis

For offline analysis, samples of at least three replicates of the wells from the MTP were pooled at the end of the experiments to increase sample volume to at least 2.0 mL. The OD was measured at a wavelength of 600 nm with a Genesys 20 photometer (Thermo Scientific, Darmstadt, Germany) or a Lambda photometer Bio+ (PerkinElmer, Rodgau, Germany). Samples were diluted with 0.9 % (w/v) NaCl to stay in the linear range of 0.1 to 0.3. The pH

of the culture broth was measured using a HI221 Basic pH meter (Hanna Instruments Deutschland GmbH, Vöhringen, Germany) or a pH-Meter 766 Calimatic (Knick, Berlin, Germany). For osmolality and high-performance liquid chromatography (HPLC) of sugars and metabolites, samples were centrifuged for 5 min at 13000g, and the supernatant was filtrated (0.2 µm). The osmolality of filtrated supernatant was determined with a freezing point Osmomat 3000 basic (Gonotec GmbH, Berlin, Germany) or an Advanced OsmoPro (Advanced Instruments, Norwood, MA, USA). For HPLC, samples were diluted with deionized water. Sample analysis for MTP experiments was performed with a Dionex UltiMate 3000 HPLC system (Thermo Scientific, Darmstadt, Germany). Measurements were conducted at 80 °C with 5 mM sulfuric acid as solvent with a flow of 0.8 mL/min and two connected organic acid-resin columns (300*7.8 mm, Phenomenex, Aschaffenburg, Germany). Refractive index (RI) measurement was performed for all components with a RI detector (RefractoMax 520, Shodex, Munich, Germany). Citrate was determined via UV signal with a Dionex UltiMate 3000 Diode Array Detector (Thermo Scientific, Darmstadt, Germany) or RI detector. HPLC analyses of fermentation samples were conducted with an Agilent HPLC system (Agilent, Santa Clara, CA, USA) at 30 °C using 5 mM sulfuric acid as solvent with a flow of 0.5 mL/min and an Aminex HPX-87 H column (300*7.8 mm, Bio-Rad Laboratories, Hercules, CA, USA). All components were detected via RI detector (G1362A from Agilent, Santa Clara, CA, USA). A comparative measurement of the two described methods above was performed, and the values in the fermenter were converted with a correlation (data not shown). Samples from the beginning of each experiment were analyzed by HPLC. The concentration ranges of those initial samples are specified in the corresponding figure captions. For cultivations in MTPs, evaporation was considered for OD and HPLC measurement by weighing the MTP filled with culture broth at the beginning and end of the cultivation.

2.2.5 Determination of lag-phase

The lag-phase was determined based on a method after Palmen et al. [142], with some modifications. The logarithm of the difference between the OTR and initial OTR was calculated and plotted over time. The initial OTR was determined as a mean value of OTR

values of a cultivation time between 1.6 to 3.0 h. This procedure was used to average low fluctuations of the initial measurement points. To specify the lag-phase, the intersection point of the regression line of the linear range was determined.

2.2.6 Depiction of experimental results of microtiter plate experiments

In MTP cultivations three to six replicates were performed, depending on the experiment. Mean values of the OTR are shown in the corresponding figures. Due to the very high density of the data of the OTR, not every measurement point over time could be represented as a symbol. Therefore, to clearly display the data, the OTR is only shown for a portion of the measured values as a symbol. The number of shown measuring points depends on the cultivation time of the experiment and is indicated in the respective figure caption. The standard deviation of the OTR data in MTP experiments is displayed as shadows. The total oxygen consumption (TOC) was determined based on the OTR of the replicates. The TOC is depicted as mean values of the replicates with error bars in bar charts. For offline analysis, samples (wells) of the replicates of the MTP cultivations were pooled at the end of the experiments. The results of measurements of pooled OD, pH, and sugar and metabolite concentrations of MTP experiments are displayed in bar charts. The OD of the pooled sample was measured in triplicate, represented as mean value with standard deviation as error bar. The pH and HPLC measurement of the pooled sample were performed in single determination and the single values are shown in bar charts.

2.2.7 Statistical analysis

Statistical analysis was performed using R (version 4.2.2, R Core Team, 2022, R Foundation for Statistical Computing, Vienna, Austria) with RStudio (version 2022.12.0, Posit team, 2022, Posit Software, PBC, Boston, MA, USA) as integrated development environment. To investigate statistical significance of differences of OTR peaks, a t-test (equal variances, two-sided) was conducted, when two samples were compared. An ANOVA followed by a Bonferroni post-hoc test was used, when more than two samples were investigated. A p-value of lower than 0.05 was determined to show significance in all statistical tests.

2.3 Results and Discussion

2.3.1 Comparison of cultivation in complex and chemically defined media

To assess the performance of the applied chemically defined medium for growth of *P. polymyxa*, the strain was initially cultivated in the Pbp complex medium. The composition is specified in Table 2-1. The chemically defined medium for *P. polymyxa* is called Moppa medium and is based on the complete modified Poolman medium after Müller et al. [68]. The composition of the Moppa medium is specified in Table 2-2. However, while using the medium of Müller et al. [68] as a starting point, the carbon-, nitrogen-, phosphate source, and buffer, and their concentrations were adapted to the concentrations of main components present in the Pbp complex medium, listed in Table 2-1. Nutrient concentrations added by soy flour and yeast extract were not considered in this adaption. Additionally, the methionine concentration was increased to 200 mg/L (originally 125 mg/L) based on internal data (not published) that methionine is growth-relevant for the applied *Paenibacillus* strain. The biotin concentration was reduced from 3 mg/L to 0.06 mg/L, due to observations that another *P. polymyxa* strain showed sensibility to high biotin concentrations (internal data, not published). Furthermore, inositol was added to the Moppa medium, to test its relevance for growth of *P. polymyxa*.

To compare the growth performance in the Pbp complex medium and the Moppa medium, the respiration activity, OD, pH, carbon source consumption, and overflow metabolite production of *P. polymyxa* were evaluated and are shown in Figure 2-1. The cultivations were performed at least in quadruplicates in the µRAMOS, and mean values with standard deviation as shadows are shown for the OTR (Figure 2-1A). The low standard deviations (on average <8.5 %) showed the good reproducibility of the measuring device and the metabolic activity of *P. polymyxa* in a single experiment. The offline values were determined after combining the content of at least four wells of the MTP.

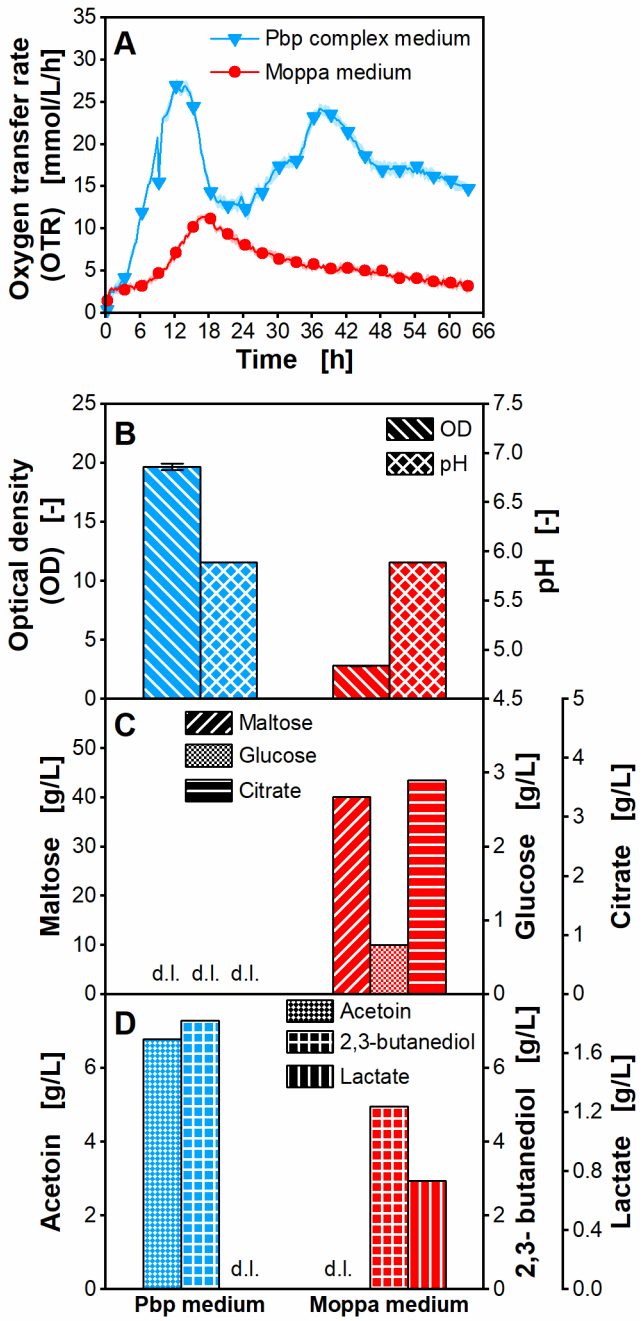

Figure 2-1: Cultivation of *Paenibacillus polymyxa* in complex medium and chemically defined Moppa medium in microtiter plate.

Pbp complex medium (specified in Table 2-1) or chemically defined Moppa medium (specified in Table 2-2). Initial concentrations were: 56.2-56.8 g/L maltose, 3.5-3.7 g/L glucose, 3.1-3.4 g/L citrate. **A:** Oxygen transfer rate (OTR), **B:** Final optical density (OD) and pH, **C:** Final maltose, glucose and citrate concentration, **D:** Final acetoin, 2,3-butanediol and lactate concentration. **A:** For clarity, only every 10th measuring point over time is marked as a symbol. Mean values for OTR of at least four replicates with standard deviations as shadows are shown. Standard deviations are not well recognizable, because they are small. **B-D:** For offline analysis, samples (wells) of the replicates of the OTR measurement were pooled at the end of the experiments. OD measurement of pooled samples was performed in triplicate and mean values with standard

deviations depicted as error bars are shown. pH and concentrations of sugars and metabolites were determined in a single measurement of pooled samples. **C, D:** d.l. means that concentrations of components were lower than the detection limit. Parameters in **B-D** were determined after 63 h. **B**: OD of complex medium prior to inoculation (3.6) is not subtracted from the final measured optical density. Initial osmolality in Pbp complex medium is 0.63 osmol/kg and osmolality after 63 h is 0.57 osmol/kg. Initial osmolality in Moppa medium is 0.69 osmol/kg and osmolality after 63 h is 0.73 osmol/kg. Cultivation conditions: temperature 33 °C, 48-round well plate, filling volume 0.8 mL, shaking frequency 1000 rpm, shaking diameter 3 mm, 0.1 M MES, initial pH 6.5.

During cultivations of *P. polymyxa* in complex medium, the course of the OTR showed three distinct peaks at 21 mmol/L/h after 9 h, at 27 mmol/L/h after 12 h, and at 24 mmol/L/h after 37 h (Figure 2-1A). An OD of 19.7 after 63 h of cultivation was achieved (Figure 2-1B). However, it must be considered that the complex medium itself had an initial OD of 3.6 prior to inoculation, as soy flour is not completely soluble. Citrate, as well as the carbon sources maltose and free glucose of the maltose syrup, were completely consumed after 63 h (Figure 2-1C). The maltose syrup mainly contains dimeric maltose molecules, maltose oligomers and free glucose. Maltose and maltose oligomers were reported to be metabolized intracellularly by *B. subtilis* [143]. Maltose is cleaved by a phospho-α-glucosidase after phosphorylation [144]. Maltose oligomers are hydrolyzed by a maltose phosphorylase, α-glucosidase, and neopullulanase [143]. Additionally, Hidaka et al. found a maltose phosphorylase in a *Paenibacillus* strain [145]. At 63 h, maltose oligomers may have remained in the complex medium. However, in this study, they were not quantified via HPLC.

The pH of the medium decreased to 5.9 after 63 h of cultivation, which was lower than the initial pH of 6.5 (Figure 2-1B). As found in *Bacillus* species [146], the decrease in pH is expected to be a result from the consumption of ammonium, which is supposed to be the major nitrogen source of the cultivation medium. Further influencing factors on the decreasing pH are acetate and lactate production, known for *P. polymyxa* [63, 147]. Acetate was not quantified via HPLC, due to overlapping peaks with the MES buffer in the medium. Lactate was not detected after 63 h (Figure 2-1D). Furthermore, *Paenibacillus* is well known to produce acetoin and 2,3-butanediol [63, 147]. An acetoin and 2,3-butanediol concentration of 6.8 g/L and 7.3 g/L, respectively, were measured (Figure 2-1D).

The fluctuating course of the OTR profile (Figure 2-1A) represents the metabolic activity of *P. polymyxa* during growth on various carbon sources of the Pbp complex medium, such as sugars and proteins from soy flour and yeast extract, but also from maltose syrup, and citrate. Additionally, in the later phase of the cultivation, consumption of produced overflow metabolites is possible. However, the undefined composition of the medium complicates the interpretation of the OTR peaks, indicating the necessity of applying a chemically defined medium.

In Figure 2-1, the growth of *P. polymyxa* in Pbp complex medium is compared to the chemically defined Moppa medium. The OTR peak reached in the chemically defined medium was 11 mmol/L/h after 18 h (Figure 2-1A); no additional peaks were observed. This peak value was 2.5-fold lower than in the complex medium. A statistically significant difference of the peak values in chemically defined medium after 18 h and in complex medium after 12 h was shown (Appendix Table A1). The growth rate, determined based on the slope of the logarithm of the OTR in Moppa medium, was 0.12 1/h compared to 0.29 1/h in Pbp complex medium (Appendix Figure A1).

The low respiration activity in Moppa medium is confirmed by the offline data. The OD reached only 2.8 in Moppa medium compared to 19.7 in Pbp complex medium after 63 h (Figure 2-1B). In contrast to the cultivation in complex medium, residual maltose, glucose, and citrate remained in Moppa medium after 63 h (Figure 2-1C). A lower amount of carbon source is consumed, due to obvious nutritional limitations in this medium. This resulted in lower concentrations of produced acetoin and 2,3-butanediol (Figure 2-1D). Only the final pH values were comparable (Figure 2-1B). In conclusion, the results in Figure 2-1 clearly indicate a limited growth of *P. polymyxa* in the chemically defined Moppa medium compared to the Pbp complex medium. Therefore, one or more nutrient limitations and growth inhibitions in the Moppa medium can be assumed. The nutritional limitations and growth inhibitions in the medium were systematically identified in the next step.

2.3.2 Identification of growth limitations and inhibitions in the chemically defined Moppa medium

A schematic overview of the experiments to identify growth limitations and inhibitions can be found in Appendix Figure A2. First, the nutrient groups were defined: amino acids, nucleobases/-sides, vitamins, and trace elements (Appendix Figure A2). Nutrients added in similar concentrations to both, the Moppa medium and Pbp complex medium, were not considered potentially limiting. These nutrients were: maltose syrup, citrate, K_2HPO_4, $(NH_4)_2SO_4$, $MgSO_4$, and $Ca(NO_3)_2$. The amino acids used in the Moppa medium were divided into six groups, as specified in Appendix Table A2. The division was adapted from the work of Müller et al. [68], based on the amino acid metabolism of *Escherichia coli* and *B. subtilis* [148], according to the Kyoto Encyclopedia of Genes and Genomes (KEGG) database. The grouping was based on intermediates or their precursors from glycolysis, citric acid cycle, or pentose phosphate pathway. Methionine was assigned to a separate group, based on internal data (not published) that it is growth-relevant for the applied *Paenibacillus* strain in this study. The vitamin grouping was also performed after Müller et al. [68], with some modifications. It is specified in Appendix Table A3. Biotin was assigned to a separate group, due to the observations that another *P. polymyxa* strain showed sensibility to high biotin concentrations (internal data, not published). Inositol was added to vitamin group 3.

To identify the limiting nutrient group(s), the concentration of each nutrient group was increased (Appendix Figure A3). Biotin was not increased, as the suggested sensitivity could mask growth-enhancing effects of the other vitamins (Appendix Figure A3A). Due to practical issues and the high number of amino acids, they were increased in single groups (Appendix Figure A3B). Only the increase of the vitamins resulted in a higher OTR peak (Appendix Figure A3A). Therefore, the next step was to identify the limiting vitamin(s).

In parallel cultivations, the concentrations of each single vitamin group were increased, to identify the possible limitation(s) (Appendix Figure A4). In these experiments, the concentration of biotin (vitamin group 4) was also increased. The cultivation with the three-fold higher concentration of vitamin group 1 resulted in a higher OTR peak of 19 mmol/L/h compared to 11 mmol/L/h in the cultivation with the one-fold concentration of all vitamins

(Appendix Figure A4A). The cultivations with increased concentrations of all other vitamin groups resulted in OTR courses similar to the cultivation with the one-fold concentration of all vitamins. There was no sensitivity observed at increased biotin concentrations for the strain of this study, as no growth inhibition was detected. The results of online monitoring of the OTR are in agreement with offline data (Appendix Figure A4B, C, and D). In the cultivation with the three-fold concentration of vitamin group 1, the OD and maltose consumption after 63 h was 2.1-fold and 1.1-fold, respectively, higher than in the cultivation with the one-fold concentration of all vitamins (Appendix Figure A4B and C). The 2,3-butanediol production was 1.2-fold lower and the lactate concentration was below the detection limit (Appendix Figure A4D). It can be concluded that at least one vitamin of group 1 is limiting in the Moppa medium.

Since the growth limitation was narrowed down to vitamin group 1, the next step was to increase the concentration of every single vitamin of this group in parallel cultivations (Appendix Figure A5). Only the increase of the nicotinic acid concentration resulted in a higher respiration activity (Appendix Figure A5A) and OD value after 66 h of cultivation (Appendix Figure A5B).

The influence of different nicotinic acid concentrations on growth is shown in more detail in Figure 2-2. The cultivations with the one-fold concentration of all medium components, in the legend referred to as Moppa medium, the three-fold concentration of vitamin group 1, and the three-fold concentration of nicotinic acid are shown in Figure 2-2A, B, C, and D. Similar courses of the OTR over time and TOC, OD values, maltose, and citrate consumption after 66 h were observed for the cultivations with the three-fold nicotinic acid concentration and the three-fold concentration of vitamin group 1 (Figure 2-2A, B, and C). The OTR peak of the cultivation with the three-fold nicotinic acid concentration was slightly higher than the OTR peak of the cultivation with the three-fold concentration of vitamin group 1. A statistically significant difference of the OTR peaks was shown (Appendix Table A4). The OTR peak was about two-fold higher for both cultivations than for the cultivation with the one-fold concentration of all components. This difference of the OTR peaks was statistically significant (Appendix Table A4). Hence, nicotinic acid is identified as the growth limiting vitamin of group 1.

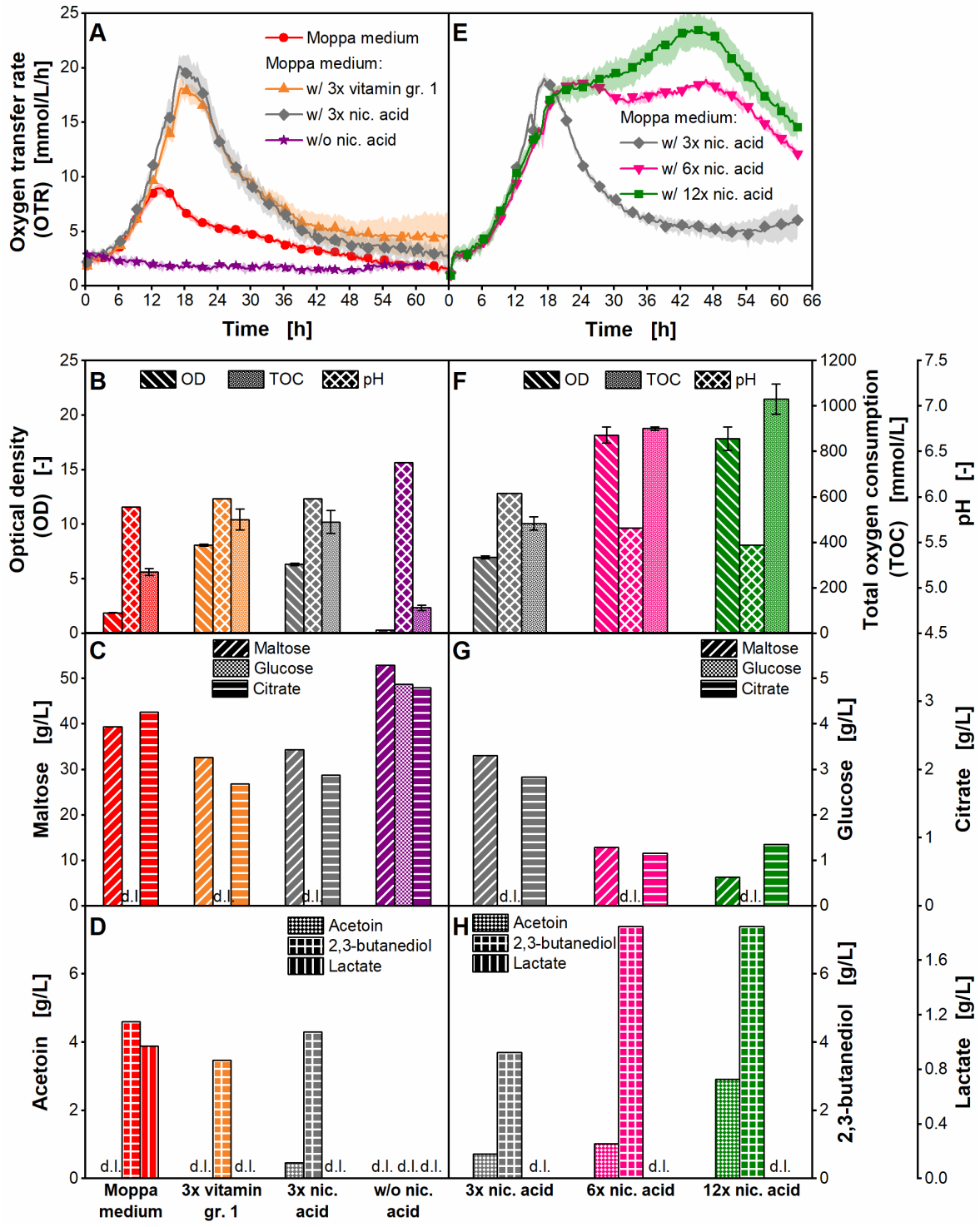

Figure 2-2: Cultivation of *Paenibacillus polymyxa* with increased concentrations of nicotinic acid in microtiter plate.

Moppa medium (specified in Table 2-2) without or with increased concentrations of all vitamins of group 1 or of nicotinic acid. Vitamin group (gr.) 1 is specified in Appendix Table A3. nic.: nicotinic. Initial concentrations were: 54.2-56.3 g/L **(A-D)** and 51.8-53.1 g/L **(E-H)** maltose, 4.2-4.5 g/L **(A-D)** and 4.1-4.3 g/L **(E-H)** glucose, 3.3-3.4 g/L **(A-D)** and 3.2-3.6 g/L **(E-H)** citrate. **A, E:** Oxygen transfer rate (OTR), **B, F:** Final optical density (OD), total oxygen consumption (TOC)

and pH, **C, G:** Final maltose, glucose and citrate concentration, **D, H:** Final acetoin, 2,3-butanediol and lactate concentration. **A, B:** For clarity, only every 10th measuring point over time is marked as a symbol. Mean values for OTR of at least three replicates with standard deviations as shadows are shown. **B, F:** TOC was determined based on OTR data of the replicates. Mean values for TOC of the replicates with standard deviations depicted as error bars are shown. **B-H:** For offline analysis, samples (wells) of the replicates of the OTR measurement were pooled at the end of the experiments. OD measurement of pooled samples was performed in triplicate and mean values with standard deviations depicted as error bars are shown. OD of pooled sample of the cultivation w/o nicotinic acid was measured in duplicate and the mean value without standard deviation is shown. pH and concentrations of sugars and metabolites were determined in a single measurement of pooled samples. **C-H:** d.l. means that concentrations of components were lower than the detection limit. Parameters in **C-H** were determined after 61 – 66 h. Cultivation conditions: temperature 33 °C, 48-round well plate, filling volume 0.8 mL, shaking frequency 1000 rpm, shaking diameter 3 mm, 0.1 M MES, initial pH 6.5.

Nicotinic acid is the precursor for nicotinamide adenine dinucleotide (NAD+), and various genes are involved in the synthesis of NAD+ [149, 150]. NAD+ is the cofactor for various cellular redox reactions, for example, in the citric acid cycle [151]. Therefore, it significantly impacts bacterial biomass formation. Another relevant metabolic pathway for *Paenibacillus* and *Bacillus* species is the production of acetoin and 2,3-butanediol as overflow metabolites [152]. Acetoin and 2,3-butanediol production are influenced by the NADH/NAD+ availability and ratio [153]. Since pyruvate acidifies the medium, the conversion of excess pyruvate from glycolysis to acetoin and 2,3-butanediol is a mechanism to prevent strong acidification of the medium [152, 154]. In the cultivations with the one-fold concentration of all medium components, the three-fold concentration of vitamin group 1, and the three-fold concentration of nicotinic acid, a pH drop of around 0.5 pH units was observed (Figure 2-2B).

In all cultivations, acetoin was produced in final concentrations lower than 1.0 g/L (Figure 2-2D). 2,3-butanediol concentrations were at similar levels of around 4.0 g/L in all cultivations despite the increased nicotinic acid concentration (Figure 2-2D). Hence, the increased concentration of nicotinic acid to three-fold resulted in higher activity of metabolic pathways for biomass formation, but not in the production of higher concentrations of overflow metabolites. Lactate was only detected in the cultivation with the one-fold concentration of all components (Figure 2-2D). Possibly, the *Paenibacillus* strain consumed the produced lactate in the other cultivations.

When nicotinic acid was left out of the medium, no growth of *P. polymyxa* was possible (Figure 2-2A, B, C, and D). Maltose, glucose, and citrate concentrations were on comparable levels at the beginning and at the end of the cultivation (Figure 2-2C). As no growth was observed in the cultivation without nicotinic acid, this vitamin is absolutely essential for the applied *P. polymyxa* strain, and an auxotrophy for this vitamin is proven. For example, in *E. coli*, nicotinic acid biosynthesis has been reported to occur via a 4-carbon dicarboxylic acid and a 3-carbon compound like glycerol [155]. The optimization of the applied *Paenibacillus* strain for industrial applications possibly led to a deletion of the relevant genes for nicotinic acid biosynthesis.

In Figure 2-2A, the OTR peak at 20 mmol/L/h of the cultivation in Moppa medium with the three-fold nicotinic acid concentration is still significantly lower than the OTR peak at 27 mmol/L/h in the cultivation using complex medium (Figure 2-1) (t-test, p-value < 0.001). Therefore, the nicotinic acid concentration was increased six-fold and twelve-fold (Figure 2-2E, F, G, and H).

The cultivations with the six-fold and twelve-fold nicotinic acid concentration showed an OTR peak after 22 h. Those peaks were on a comparable level as the peak of the cultivation with the three-fold nicotinic acid concentration after 17 h. There was no statistically significant difference of the OTR peaks (ANOVA, p-value = 0.484). Hence, the six-fold concentration of nicotinic acid did not increase the OTR peak, compared to the cultivation with the three-fold concentration (Figure 2-2E). Instead, after the first peak at 22 h, a plateau in the OTR course was observed. For the cultivation with the twelve-fold nicotinic acid concentration, a low increase of the OTR was visible after the OTR peak at 22 h. This indicates a limitation by a secondary substrate or a growth inhibition in the medium.

The TOC increased from 484 mmol/L in the cultivation with the three-fold nicotinic acid concentration to 901 mmol/L for the six-fold and 1031 mmol/L for the twelve-fold concentration of nicotinic acid (Figure 2-2F). Additionally, the OD after 63 h was 2.6-fold higher for both cultivations with increased nicotinic acid concentration than for the cultivation with the three-fold nicotinic acid concentration (Figure 2-2F).

P. polymyxa was metabolically active for a longer cultivation time when the nicotinic acid concentration was increased from three-fold to six- and twelve-fold. Additionally, the increase of the nicotinic acid concentration from three-fold to six-fold resulted in a higher biomass formation, represented in the OD (Figure 2-2F), and in the production of higher concentrations of acetoin and 2,3-butanediol (Figure 2-2H). The increase of the nicotinic acid concentration from six-fold to twelve-fold did not result in a higher OD and 2,3-butanediol concentration (Figure 2-2F and H). Only a higher acetoin production was observed (Figure 2-2H). Hence, at the highest investigated nicotinic acid concentration, a higher biomass formation, compared to the six-fold nicotinic acid concentration, was not possible, due to the suggested growth limitation or inhibition. Instead, excess pyruvate was used for overflow metabolite production. Lactate as a potential metabolic side product was not detected via HPLC in any sample taken after 63 h.

After 63 h of cultivation, the concentration of citrate was 2.4-fold and 2.1-fold lower for the cultivations with the six- and twelve-fold nicotinic acid concentration, respectively, than in the cultivation with the three-fold nicotinic acid concentration (Figure 2-2G). This higher consumption rate of citrate (Figure 2-2G) might be explained by an increased activity of the citric acid cycle due to elevated glycolysis.

Increasing the nicotinic acid concentration from one- to three-fold resulted in a similar pH value after 66 h (Figure 2-2B). Hence, the buffer capacity for the applied cultivation conditions was sufficient. A further increase of the nicotinic acid concentration resulted in a more substantial decrease of pH values (Figure 2-2F). In the cultivations with the six- and twelve-fold nicotinic acid concentration, a pH of 5.7 and 5.5 was measured after 63 h, respectively (Figure 2-2F). pH optima for *P. polymyxa* strains were reported to be 6.0 or higher [94, 95]. For example, Liu. et al. showed a pH optimum for growth of 6.0 for *P. polymyxa* EJS-3 [95]. Rafigh et al. reported a pH of 7.0 optimal for biomass formation of *P. polymyxa* ATCC 21830 [94]. In contrast to the cultivations with the one- and three-fold nicotinic acid concentrations, an insufficient buffer capacity is assumed for the six- and twelve-fold nicotinic acid concentrations. This might result in a subsequent growth inhibition in the cultivation.

To verify this hypothesis, the buffer capacity in the MTP cultivations was increased (Figure 2-3). The Moppa medium with the twelve-fold nicotinic acid concentration was used. The pK_a value of MES buffer is 6.0 at a cultivation temperature of 33 °C [156]. Therefore, the initial pH was increased, to better exploit the buffer capacity. Additionally, the buffer concentration was increased from 0.1 to 0.2 M MES.

The OTR peak was increased from 21 mmol/L/h in the cultivation with 0.1 M MES and an initial pH of 6.5 to a value of 33 mmol/L/h in the cultivation with 0.2 M MES and an initial pH of 7.0 (Figure 2-3A). A statistically significant difference of the OTR peaks was observed (Appendix Table A5). Additionally, a higher OD was achieved (Figure 2-3B), which is also represented in a higher consumption of maltose and citrate (Figure 2-3C). The acetoin concentration increased to 8.3 g/L in the cultivation with 0.2 M MES with an initial pH of 6.5 compared to 3.9 g/L in the cultivation with the lowest buffer capacity. A further increase of the buffer capacity (0.2 M MES, initial pH 7.0) resulted in a decreased acetoin concentration (Figure 2-3D). 2,3-butanediol concentrations decreased from 9.2 g/L in the cultivation with 0.1 M MES and an initial pH of 6.5 to a concentration of around 5.2 g/L in both cultivations with higher buffer capacity (Figure 2-3D). The decreased concentrations of overflow metabolites in the cultivation with the highest buffer capacity can be explained by a lower activity of overflow metabolism, since pyruvate is metabolized for biomass formation in the citric acid cycle and respiratory chain, represented in the higher OD.

The lag-phase using 0.2 M MES buffer and an initial pH of 7.0 increased by 4.7 h (Appendix Figure A6) compared to the cultivation with 0.1 M MES and an initial pH of 6.5. The longer lag-phase can be explained by an increase of the initial osmolality from 0.68 osmol/kg, which is similar to the osmolality in complex medium, to 0.94 osmol/kg using 0.2 M MES with an initial pH of 7.0 (Appendix Figure A6). It is well known that osmotic stress influences the growth of microorganisms [157, 158] and can prolong the lag-phase [92].

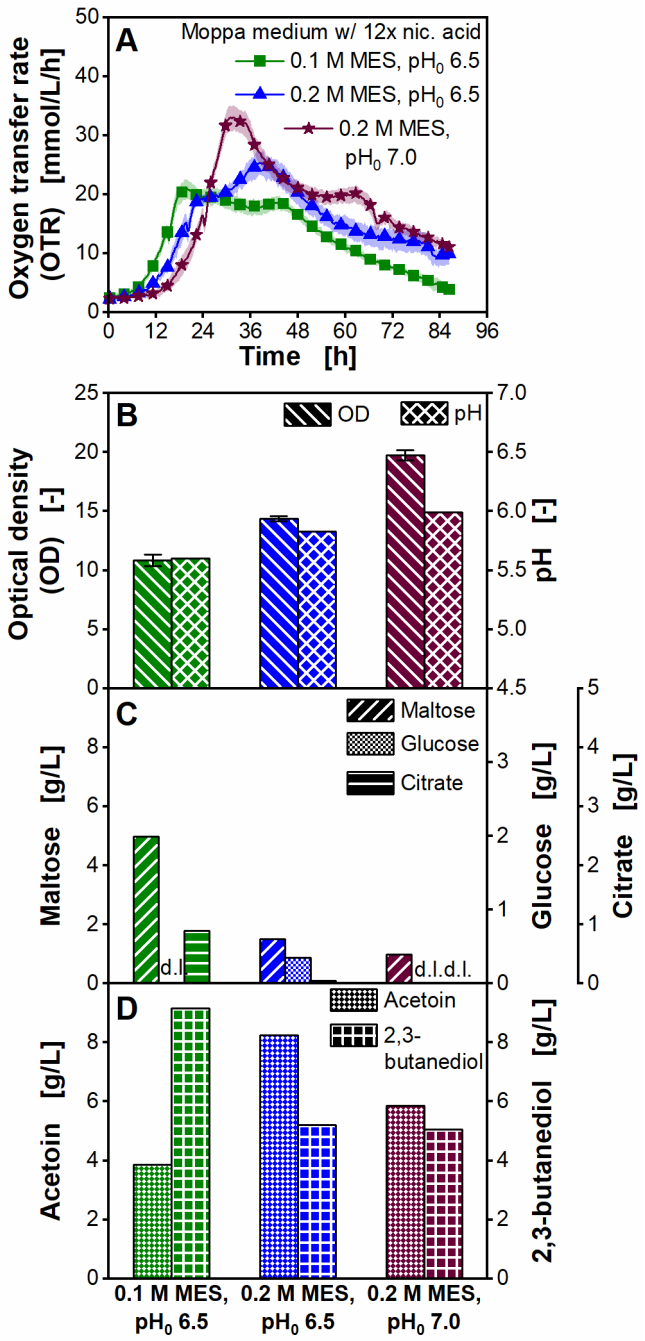

Figure 2-3: Cultivation of *Paenibacillus polymyxa* with increased pH - buffer capacity in microtiter plate. Moppa medium (specified in Table 2-2) with 12x nicotinic acid or Moppa medium with 12x nicotinic acid and with increased buffer concentration or with increased buffer concentration and initial pH. nic.: nicotinic, pH_0: initial pH. Initial concentrations were: 62.1-63.4 g/L maltose, 1.9-2.1 g/L glucose, 3.7-3.8 g/L citrate. **A:** Oxygen transfer rate (OTR), **B:** Final optical density (OD) and pH, **C:** Final maltose, glucose and citrate concentration, **D:** Final acetoin and 2,3-butanediol concentration. **A:** For clarity, only every 12th measuring point over time is marked as a symbol. Mean values for OTR of at least four replicates with standard deviations as shadows are shown. **B-D:** For offline analysis, samples (wells) of the replicates of the OTR measurement were pooled at the end of the experiments. OD measurement of pooled samples was performed in triplicate and

mean values with standard deviations depicted as error bars are shown. pH and concentrations of sugars and metabolites were determined in a single measurement of pooled samples. **C:** d.l. means that concentrations of components were lower than the detection limit. Final lactate concentrations were lower than the detection limit. Parameters in **C-D** were determined after 86 h. Osmolalities are shown in Appendix Figure A6. Cultivation conditions: temperature 33 °C, 48-round well plate, filling volume 0.8 mL, shaking frequency 1000 rpm, shaking diameter 3 mm.

The salt solutions (K_2HPO_4, $(NH_4)_2SO_4$, $MgSO_4$, $Ca(NO_3)_2$) and their concentrations in the chemically defined Moppa medium (Table 2-2), were similar to those added in the Pbp complex medium (Table 2-1). Therefore, only amino acids, nucleobases/-sides, vitamins, and trace elements were considered in the previous experiments. However, salts are added to the Pbp medium by the salt solutions itself, soy flour and yeast extract. To exclude that any salts, like the nitrogen and phosphate source are limiting in the Moppa medium, the composition of the elements of salts was calculated (Appendix Figure A7A). The nitrogen (N), magnesium (Mg), phosphorous (P), sulfur (S), and potassium (K) concentrations in the Moppa medium with the twelve-fold nicotinic acid concentration were calculated per amount of carbon source (C) in mol/mol (Appendix Figure A7A). Those elemental compositions were compared to other proven media known from literature for *Paenibacillus* and *Bacillus* species [68, 136, 138], *E. coli* [159], and lactic acid bacteria [135]. Compared to the other media, all elements (N, P, S, K), except Mg, were available in significantly lower amounts per amount of carbon in the Moppa medium (Appendix Figure A7A). Additionally, the elemental composition of trace elements was considered (Appendix Figure A7B). The comparison of the elemental composition of trace elements in Moppa medium compared to the other literature known media showed that those elements are available in sufficient amounts in Moppa medium (Appendix Figure A7B). Due to the low amount per carbon of N, P, S, and K in Moppa medium compared to the other media, cultivations with increased concentrations of $(NH_4)_2SO_4$ and K_2HPO_4 were performed (Appendix Figure A8). For this purpose, Moppa medium with the twelve-fold nicotinic acid concentration, 0.2 M MES buffer, and an initial pH of 7.0 was used. Respiration activities, ODs, final pH values, and 2,3-butanediol concentrations were comparable for all cultivations (Appendix Figure A8A, B, and D). Maltose and citrate were consumed entirely (Appendix Figure A8C). Only slight deviations in glucose and acetoin concentrations were observed (Appendix Figure A8C and D).

To avoid any limitations in fermenter experiments and to avoid a nitrogen limitation by reducing the amino acids to the growth-relevant ones, the Moppa medium with additional $(NH_4)_2SO_4$ and K_2HPO_4 was used for further experiments. From here on, the Moppa medium with the twelve-fold nicotinic acid concentration, 0.2 M MES, an initial pH of 7.0, and the three-fold $(NH_4)_2SO_4$ and K_2HPO_4 concentration is called supplemented Moppa medium.

2.3.3 Reduction of medium components to growth-relevant ones

Comparing the OTR peak of 35 mmol/L/h in the cultivation with supplemented Moppa medium (Appendix Figure A8A) with the OTR peak of 27 mmol/L/h in the cultivation with Pbp complex medium (Figure 2-1A), the OTR peak in the cultivation with supplemented Moppa medium was higher. However, the supplemented Moppa medium contains 53 components compared to 22 components in the complex medium. A high number of medium components leads to laborious medium preparation and high medium costs. Therefore, the medium components were reduced to the essential and growth-relevant ones. A schematic overview of the experiments performed in order to reduce the medium components is shown in Appendix Figure A9. A systematic approach by grouping the nutrients was chosen.

Preliminary experiments were performed to reduce the vitamins in Moppa medium with the three-fold nicotinic acid concentration, 0.1 M MES, an initial pH of 6.5, and the one-fold concentration of $(NH_4)_2SO_4$ and K_2HPO_4. An OTR peak of 15 mmol/L/h was achieved after 55 h in the cultivation without biotin compared to 19 mmol/L/h after 17 h in the cultivation with biotin (Appendix Figure A10). Leaving the other vitamins, listed in Appendix Table A3 (except nicotinic acid), out from the medium did not influence the respiration activity (data not shown). The results show that the *P. polymyxa* strain can grow without biotin in the medium, but the OTR peak is reached with a substantial time delay. Therefore, biotin enhances growth of *P. polymyxa*, but is not absolutely essential for the strain.

Based on these results, a cultivation in supplemented Moppa medium was performed, adding only nicotinic acid and biotin as vitamins. All other vitamins listed in Appendix Table A3 were left out of the medium (Figure 2-4).

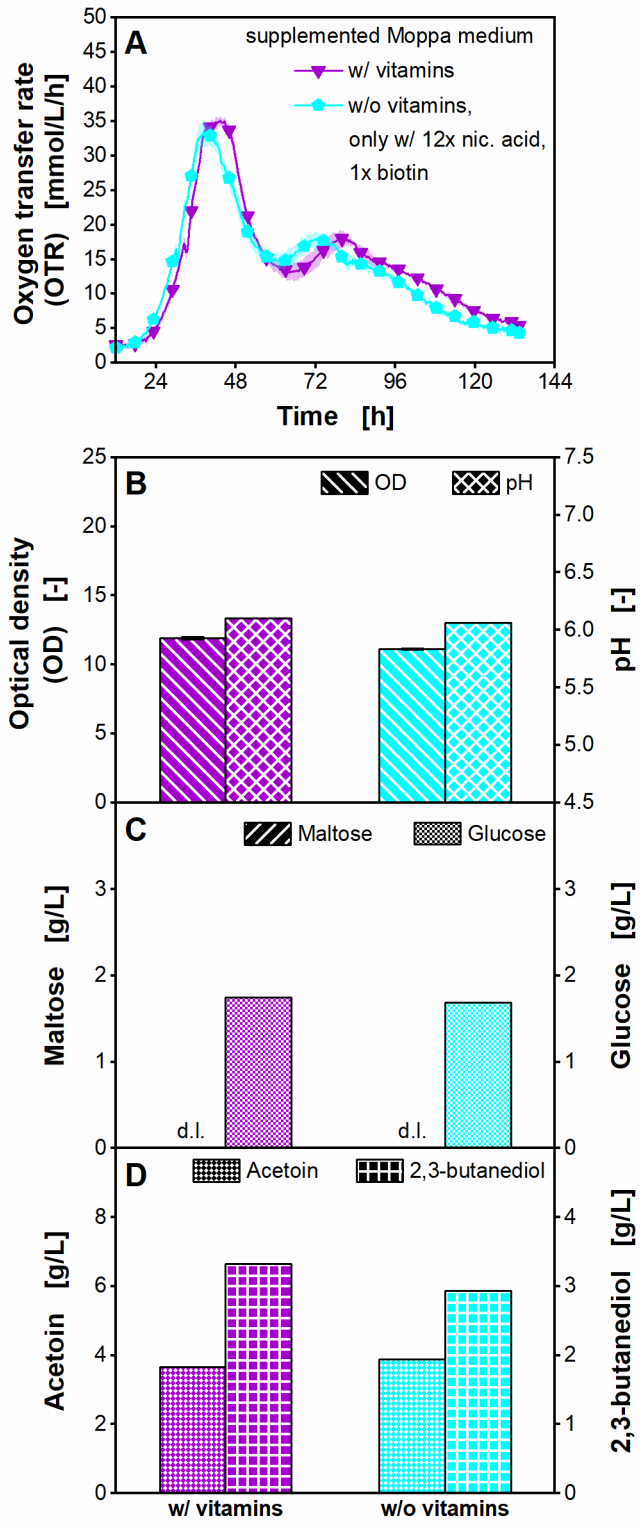

Figure 2-4: Cultivation of *Paenibacillus polymyxa* only with growth relevant vitamins in microtiter plate.

Supplemented Moppa medium (specified in Table 2-2) with or without vitamins (only with nicotinic acid and biotin). nic.: nicotinic. Initial concentrations were: 56.6-57.0 g/L maltose, 3.2-3.3 g/L glucose, 3.0 g/L citrate. **A:** Oxygen transfer rate (OTR), **B:** Final optical density (OD) and pH, **C:** Final maltose and glucose concentration, **D:** Final acetoin and 2,3-butanediol

concentration. **A:** For clarity, only every 18th measuring point over time is marked as a symbol. Mean values for OTR of four replicates with standard deviations as shadows are shown. Standard deviations are not well recognizable, because they are small. **B-D:** For offline analysis, samples (wells) of the replicates of the OTR measurement were pooled at the end of the experiments. OD measurement of pooled samples was performed in triplicate and mean values with standard deviations depicted as error bars are shown. pH and concentrations of sugars and metabolites were determined in a single measurement of pooled samples. **C:** d.l. means that concentrations of components were lower than the detection limit. Final citrate and lactate concentrations were lower than the detection limit. Parameters in **B-D** were determined after 133 h. Cultivation conditions: temperature 33 °C, 48-round well plate, filling volume 0.8 mL, shaking frequency 1000 rpm, shaking diameter 3 mm.

All measured parameters, the OTR course over time, the OD, the pH, and the sugar and metabolite concentrations after 133 h were similar to the cultivation with the addition of all vitamins. There was no statistically significant difference of the OTR peaks (Appendix Table A6). The results show that only nicotinic acid and biotin are growth-relevant vitamins.

In the next step, the amino acids were investigated. Therefore, only nicotinic acid and biotin were added as vitamins to the supplemented Moppa medium. The amino acids were divided into six groups, specified in Appendix Table A2. All amino acids were left out from the medium, while every single group was added (Figure 2-5). The *P. polymyxa* strain could not grow in a medium without any supplemented amino acid. By adding amino acid group 1, which contained only methionine, growth was possible, and an OTR peak at 22 mmol/L/h was observed (Figure 2-5A). Hence, methionine is an essential amino acid for the *P. polymyxa* strain, resulting in an auxotrophy for this amino acid.

In the cultivation supplemented with amino acid group 1, the OTR peak (Figure 2-5A) and the growth rate (Appendix Figure A11) were 1.6-fold and 1.8-fold lower, respectively, than in the cultivation with supplementation of all amino acids. The difference of the OTR peaks was statistically significant (Appendix Table A7). Nevertheless, the TOC was at comparable levels. In the cultivation supplemented with amino acid group 1, 1773 mmol/L oxygen was consumed, and in the cultivation supplemented with all amino acids, 1832 mmol/L was consumed (Figure 2-5B). In contrast, the OD in the cultivation with amino acid group 1 was 1.5-fold higher than that in the cultivation with all amino acids (Figure 2-5B). The reason for the higher OD is not yet clear. One possible explanation is an optical interference due to morphological changes. Those morphological changes might be caused by cell lysis due to

sporulation of *P. polymyxa*. It is known that amino acids influence the sporulation of *Bacillus* species [160].

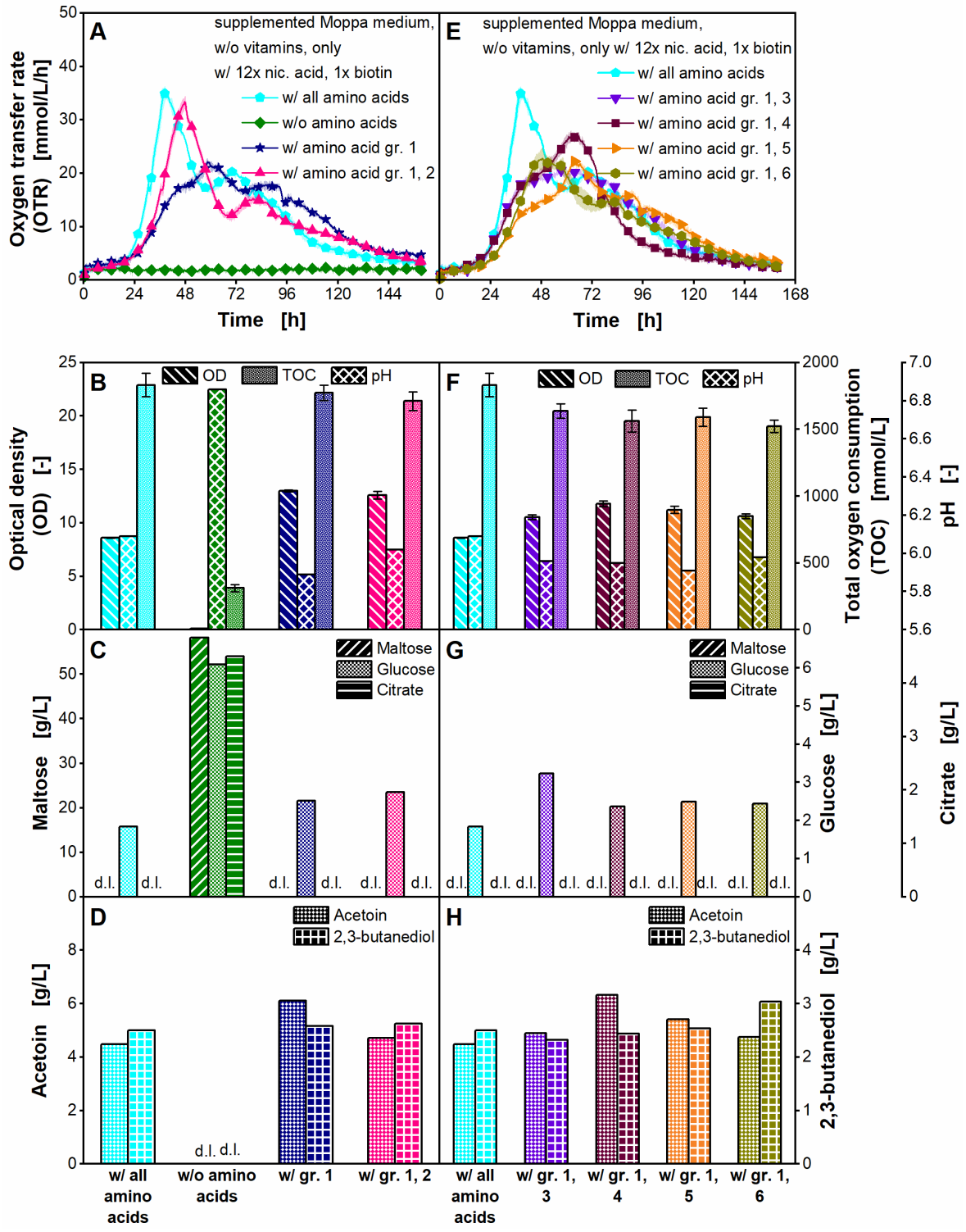

Figure 2-5: Cultivation of *Paenibacillus polymyxa* with varying amino acid composition in microtiter plate.

Supplemented Moppa medium (specified in Table 2-2) without vitamins (only with nicotinic acid and biotin) and with or without amino acid groups. nic.: nicotinic. Amino acid groups (gr.) are specified in Appendix Table A2. Initial concentrations were: 54.1-56.3 g/L **(A-D)** and 54.1-56.1 g/L **(E-H)** maltose, 2.9-3.2 g/L **(A-D)** and 2.9-3.1 g/L **(E-H)** glucose, 3.0-3.1 g/L **(A-D)** and 3.0-3.1 g/L **(E-H)** citrate. **A, E:** Oxygen transfer rate (OTR), **B, F:** Final optical density (OD), total oxygen consumption (TOC) and pH, **C, G:** Final maltose, glucose and citrate concentration, **D, H:** Final acetoin and 2,3-butanediol concentration. **A, B:** For clarity, only every 20th measuring point over time is marked as a symbol. Mean values for OTR of at least three replicates with standard deviations as shadows are shown. **B, F:** TOC was determined based on OTR data of the replicates. Mean values for TOC of the replicates with standard deviations depicted as error bars are shown. **B-H:** For offline analysis, samples (wells) of the replicates of the OTR measurement were pooled at the end of the experiments. OD measurement of pooled samples was performed in triplicate and mean values with standard deviations depicted as error bars are shown. OD of pooled sample of the cultivation w/o amino acids was measured in duplicate and the mean value without standard deviation is shown. pH and concentrations of sugars and metabolites were determined in a single measurement of pooled samples. **C, D, G:** d.l. means that concentrations of components were lower than the detection limit. Final lactate concentrations were lower than the detection limit. Parameters in **B-D** and **F-H** were determined after 159 h. Cultivation conditions: temperature 33 °C, 48-round well plate, filling volume 0.8 mL, shaking frequency 1000 rpm, shaking diameter 3 mm.

Maltose and citrate were entirely consumed in both cultivations (only amino acid group 1 and all amino acids), and around 2-3 g/L glucose was measured at the end of the cultivations (Figure 2-5C). 2,3-butanediol concentrations were on comparable levels after 159 h, and the acetoin concentration was 1.4-fold higher in the cultivation with only amino acid group 1 than in the cultivation with all amino acids (Figure 2-5D). The pH after 159 h was lower in the cultivation with only amino acid group 1 than in the cultivation containing all amino acid groups (Figure 2-5B). Possibly a higher amount of produced acetate, which was not measured in this study, led to the lower final pH in the cultivation containing only amino acid group 1.

The OTR course of the cultivation containing only amino acid group 1 is not entirely comparable to the OTR course of the cultivation containing all amino acids (Figure 2-5A). Hence, it is supposed that at least one amino acid was missing. To identify the limiting amino acid group, an individual supplementation of each group to the medium already containing amino acid group 1 was performed.

The addition of amino acid groups 1 and 2 resulted in a comparable OTR peak as in the cultivation containing all amino acid groups (Figure 2-5A). There was no statistically

significant difference of the OTR peaks (Appendix Table A7). However, the peak was measured 9 h later than in the cultivation with all amino acids. This delay was reflected in a slightly lower growth rate, which was 0.14 1/h in the cultivation with all amino acids and 0.10 1/h in the cultivation with only amino acid groups 1 and 2 (Appendix Figure A11). Adding only amino acid groups 1 and 2 to the cultivation medium, the observed OTR peak increased 1.5-fold compared to the cultivation with only amino acid group 1 (Figure 2-5A). A statistically significant difference of the OTR peaks was observed (Appendix Table A7). Offline data were similar (Figure 2-5B, C, and D).

The addition of amino acid group 3, 5, or 6 together with amino acid group 1 did not significantly increase the respiration activity compared to the cultivation with only amino acid group 1 (Figure 2-5E, Appendix Table A7). The addition of amino acid group 4 together with amino acid group 1 resulted in a slightly higher OTR peak, compared to the addition of only amino acid group 1. A statistically significant difference of these two OTR peaks was shown (Appendix Table A7). However, the TOC was on comparable levels. The results were also reflected in the offline data (Figure 2-5F, G, and H).

In the next step, each single amino acid of group 2 was investigated. The results are shown in Appendix Figure A12, Appendix Figure A13, and Appendix Figure A14. The OTR peak, growth rate, and lag-phases were evaluated as a criterion. Only the addition of histidine in combination with amino acid group 1 resulted in a similar peak of respiration activity as observed in the cultivation with amino acid groups 1 and 2 (Appendix Figure A12A). Growth rates were similar (Appendix Figure A13A). However, the lag phase was prolonged by 7.0 h compared to the cultivation with amino acid groups 1 and 2 (Appendix Figure A14A). The separate addition of proline and arginine resulted in a lower OTR peak value (Appendix Figure A12A), but a similar lag-phase as the cultivation supplemented with amino acid groups 1 and 2 (Appendix Figure A14A). Therefore, those two amino acids were each added to amino acid group 1 and histidine in parallel cultivations (Appendix Figure A12B). However, this did not result in entirely similar respiration activities to the cultivation with amino acid group 1 and 2 (Appendix Figure A12B, Appendix Figure A13B and Appendix Figure A14B). Additionally, a combination of amino acid group 1, histidine, proline, and arginine did not result in entirely comparable OTR courses (Appendix

Figure A12C, Appendix Figure A13C and Appendix Figure A14C). Therefore, all amino acids of group 2 were used in addition to amino acid group 1 in the supplemented Moppa medium.

The studies on amino acid supplementation resulted in a better understanding of the OTR peaks. Since the small peak after around 35 h is only present when arginine has been added to the medium, the peak can be attributed to arginine consumption as a carbon source (Appendix Figure A12A). Appendix Figure A15 shows the good reproducibility of growth of *P. polymyxa* in three experiments performed independently of one another.

The nucleobases/-sides were reduced after reducing the amino acids to the growth-relevant ones (Appendix Figure A16). As the strain was expected to produce the nucleobases/-sides by itself, they were not divided into groups. Therefore, *P. polymyxa* was cultivated in supplemented Moppa medium containing only nicotinic acid, biotin, amino acid groups 1 and 2, with and without nucleobases/-sides. The respiration activities and offline parameters were similar for both cultivations (Appendix Figure A16). Hence, *P. polymyxa* was able to synthesize the nucleobases/-sides by itself.

The number of components in the supplemented Moppa medium was reduced from 53 to 23, similar to the number of components in the complex medium. The Moppa medium only supplemented with nicotinic acid, biotin, methionine, the amino acids of group 2 and without nucleobases/-sides is called reduced Moppa medium from now on.

2.3.4 Comparability of cultivation in reduced Moppa medium in microtiter plate and laboratory fermenter scale

After screening optimized cultivation conditions in MTPs, the next step in bioprocess development may be the transfer to a laboratory fermenter scale, before the final scale-up to the production scale can be performed. To validate the results of this study obtained in MTPs, a cultivation in a laboratory fermenter was performed. The respiration activities and the measured offline parameters in the MTP and the fermenter are compared in Figure 2-6.

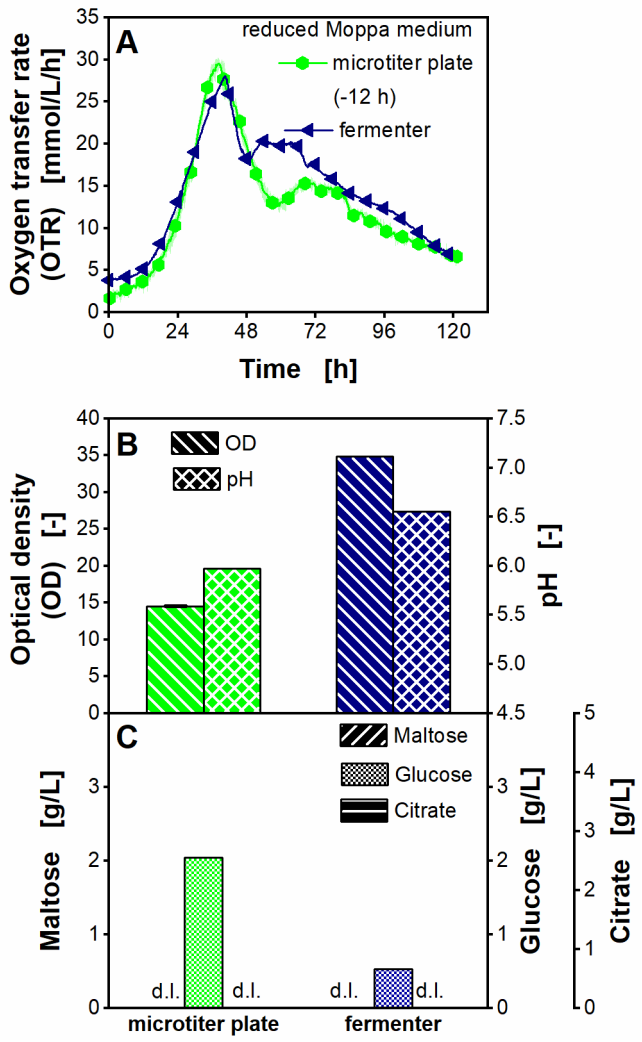

Figure 2-6: Cultivation of *Paenibacillus polymyxa* in reduced Moppa medium in microtiter plate and fermenter scale.

Reduced Moppa medium (specified in Table 2-2). Initial concentrations were: 55.7-58.2 g/L maltose, 2.7-3.3 g/L glucose, 3.1-3.8 g/L citrate. **A:** Oxygen transfer rate (OTR) in microtiter plate or fermenter, **B:** Final optical density (OD) and pH, **C:** Final maltose, glucose and citrate concentration. **C:** d.l. means that concentrations of components were lower than the detection limit. Final lactate concentrations were lower than the detection limit. Parameters in **B** and **C** were determined after 133 h in microtiter plate (corresponds to 121 h cultivation time after shift) and after 119 h in fermenter. Initial osmolality in reduced Moppa medium in microtiter plate is 0.95 osmol/kg and in fermenter is 0.48 osmol/kg. Cultivation conditions: microtiter plate: temperature 33 °C, 48-round well plate, filling volume 0.8 mL, shaking frequency 1000 rpm, shaking diameter 3 mm, 0.2 M MES, initial pH 7.0. For clarity, only every 18th measuring point over time is marked as a symbol. Mean values for OTR of four replicates with standard deviations as shadows are shown for microtiter plate. Standard deviations are not well recognizable, because they are small. **B-C:** For offline analysis, samples (wells) of the replicates of the OTR measurement were pooled at the end of the microtiter plate experiment. OD measurement of pooled sample was performed in triplicate and the mean value with standard deviation depicted as error bar is shown. pH and concentrations of sugars were determined in a single measurement of pooled sample. Fermenter: temperature 33 °C, filling volume 1 L, pH control at pH 6.5 with

NH_3 • aq and H_3PO_4 solutions, without MES buffer. For clarity, only every 720th measuring point is marked as a symbol. The cultivation in reduced Moppa medium in microtiter plate is also shown in Appendix Figure A16.

The OTR courses at both scales were comparable (Figure 2-6A). The OTR of the MTP was shifted by 12 h, as growth was delayed compared to the fermenter. The larger lag-phase might be driven by the two-fold higher initial osmolality in the cultivation in the MTP (0.95 osmol/kg in MTP and 0.48 osmol/kg in fermenter). Based on internal data (not published), increasing osmotic pressures (higher than 0.80 osmol/kg) were found to incrementally reduce growth of the *P. polymyxa* strain. The higher osmolality results from the used buffer in the MTP cultivation. In contrast, the pH in the fermenter was controlled by titration.

A higher OD was observed in the fermenter. This is likely the influence of the different pH control strategies. In the fermenter, pH was controlled to a value of 6.5 by titration with 25 % (w/w) NH_3 • aq and 40 % (w/w) H_3PO_4 solutions. In the MTP, the pH decreased to a value of 6.0 (Figure 2-6B). At the end of cultivation after 119 h, maltose was entirely consumed by the microorganisms in both, the fermenter and the MTP (Figure 2-6C).

To further characterize the fermentation of *P. polymyxa*, samples were sequentially taken every 6 h over the cultivation time (Figure 2-7). The OD increased throughout the whole cultivation time (Figure 2-7B). When the OTR peak was reached, maltose was still available at a concentration of at least 21.3 g/L (Figure 2-7C). After 119 h, maltose was completely consumed. A glucose concentration of 0.5 g/L was measured after 119 h (Figure 2-7C). The citrate concentration decreased to values lower than 0.5 g/L, when the OTR peak was reached. Lactate was produced in low concentrations and then consumed in the further course of the cultivation (Figure 2-7D). Lactate consumption started after the OTR peak was reached (Figure 2-7D). Thereby, the assumption that lactate was consumed in cultivations with increased nicotinic acid concentrations (Figure 2-2D) is confirmed here.

The DOT dropped to 30 % after 19 h and was kept constant by controlling the agitation speed in the fermenter (Appendix Figure A17). Therefore, the course of the agitation speed follows the course of the OTR curve.

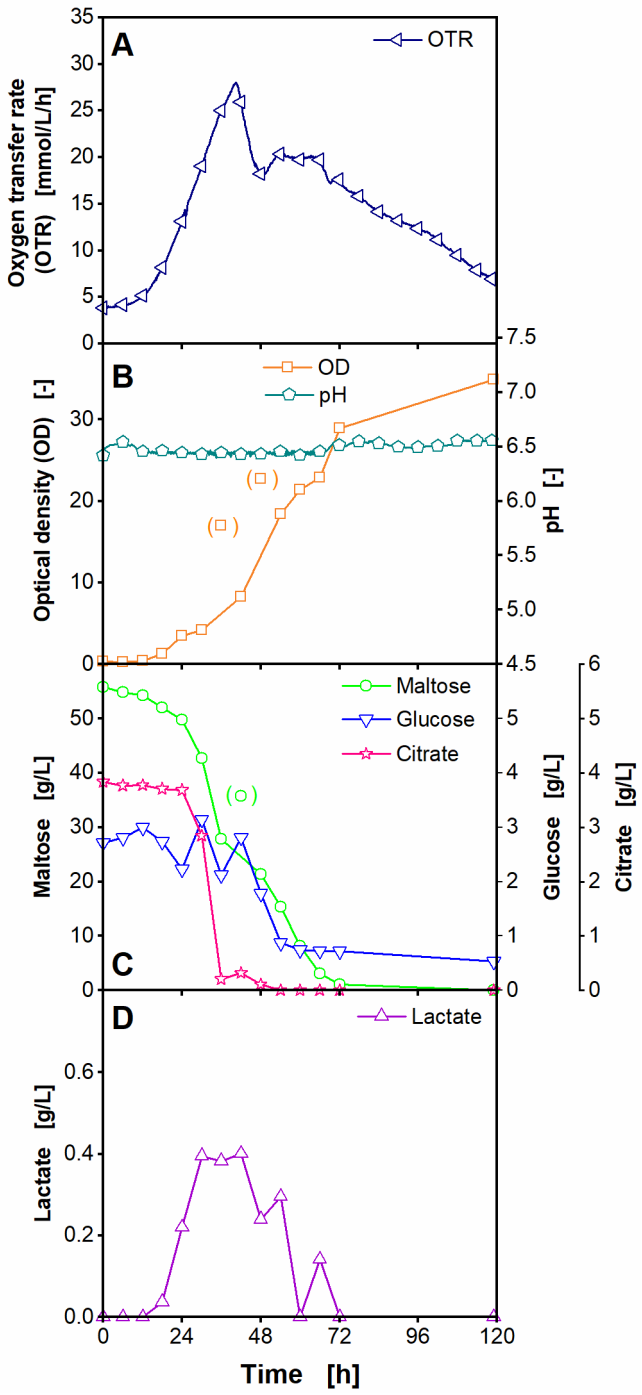

Figure 2-7: Characterization of the cultivation of *Paenibacillus polymyxa* in reduced Moppa medium in a fermenter.

Reduced Moppa medium (specified in Table 2-2). **A:** Oxygen transfer rate (OTR), **B:** Optical density (OD) and pH, **C:** Maltose, glucose and citrate concentration, **D:** Lactate concentration. Measuring points in brackets are considered outliers. For clarity, only every 720th measuring point is marked as a symbol for OTR. Cultivation conditions: temperature 33 °C, filling volume 1 L, pH control at pH 6.5 with NH_3 • aq and H_3PO_4 solutions, without MES buffer. The cultivation in the fermenter is also shown in Figure 2-6.

2.4 Conclusions

In this study, a chemically defined medium for a *P. polymyxa* strain was developed by combining a systematic experimental procedure and the small-scale high-throughput online cultivation system µRAMOS. In comparison to the Pbp complex medium, the respiration activity and OD in the chemically defined Moppa medium were low. Hence, the concentrations of the supplemented nutrient groups were systematically increased in the Moppa medium. Nicotinic acid was identified as a growth-limiting component. Furthermore, the use of the online monitoring technique revealed a pH-inhibition in the small-scale cultivations, which was traced back to an insufficient buffer capacity. By increasing the nicotinic acid concentration, the initial pH, and the buffer concentration in the Moppa medium, similar respiration activities to the Pbp medium were achieved. The next step was to reduce the medium components to the essential and growth-relevant ones. Auxotrophies for nicotinic acid and methionine were shown for the applied P. *polymyxa* strain. Biotin and the combination of histidine, arginine, proline, and glutamate showed growth-enhancing effects. Nucleobases /-sides do not have to be added to the medium. After reduction of the medium components to the essential and growth-relevant ones, a comparable number (23) of media components as in the Pbp complex medium (22) was achieved. The information obtained from the online monitored respiration activities in the MTP experiments could be verified by offline measured parameters (OD, pH, carbon source consumption, and metabolite production).

Finally, the cultivation of *P. polymyxa* in the chemically defined medium was successfully reproduced in a laboratory fermenter. The results showed a good transferability of the developed medium, based on online monitoring, although the method of pH-control was different. The reasons for the differences in OD have to be investigated in further studies.

This study shows that online monitoring of the respiration activity in high-throughput MTP cultivations in combination with a systematic experimental procedure is a valuable tool to optimize cultivation media. Compared to conventional methods, like OFAT, the number of experiments was reduced. A screening procedure was established for *P. polymyxa* in MTPs.

Finally, the good transferability of the MTP results to a laboratory fermenter highlights the importance of online monitoring the respiration activity in small-scale cultivation systems.

By the time of submission of this thesis, the following chapter is in preparation for submission as a journal article:

- Goldmanns J, Schulze M, Scholand T, May T, Haas EP, Boy M, Herold A, Büchs J. Application of online spectroscopic techniques for detection of *Bacillus* spores in cultivations with complex medium.

  The manuscript was adapted for this thesis.

Contributions to chapter 3:

The contributions are listed in the chapter “Funding, publications, and contributions”. More detailed experimental contributions from others: Monique Schulze and Theresa Scholand assisted with the experiments presented in chapter 3.3.2 (AVT – Biochemical Engineering, RWTH Aachen University, Aachen, Germany). Theresa Scholand assisted with the experiments shown in chapter 3.3.3 (AVT – Biochemical Engineering, RWTH Aachen University, Aachen, Germany).

3 Application of online spectroscopic techniques for detection of *Bacillus* spores in cultivations with complex medium

3.1 Introduction

High spore concentrations and sporulation efficiencies are needed for efficient industrial processes with spore formers. To increase spore concentrations and sporulation efficiencies of *Bacillus* species, parameters that influence sporulation need to be identified. For screening those parameters, spore detection methods are required. Counting spore numbers using the agar-plating method [103, 104] or microscopy in combination with a counting chamber [105, 106] are the most commonly applied conventional spore detection methods. However, these methods are time-consuming and laborious [161, 162]. Further disadvantages of spore quantification using the plating technique are miscounting, due colony clumping and susceptibility to high standard deviations [161, 162]. In addition, incubation of the agar plates for several days is necessary to enable reliable colony counting [162]. Several methods have been developed to measure the concentration of the spore-specific component DPA of the spore core, as an alternative to methods that determine spore concentrations directly. DPA concentration determination is, for example, performed by applying HPLC [163]. In addition, terbium dipicolinate photoluminescence assays were developed and optimized [164-166]. Furthermore, DPA was described to be detected and quantified by surface-enhanced Raman spectroscopy [167, 168]. The methods quantifying DPA require intensive sample preparation, for example, DPA extraction [163, 164, 167]. Only end-point measurements are possible for all spore detection methods mentioned above, or samples need to be taken during the cultivation. In addition, measurement results are only available

with a delay after sampling. In contrast, online detection methods allow monitoring of the progress and rate of sporulation over the whole cultivation time. For example, online monitoring of dielectric permittivity in combination with online measured OD was shown to represent the different cultivation states, like the sporulation phase of *Bacillus thuringiensis* in a bioreactor cultivation [169]. In another study, an electronic nose was used to monitor the sporulation of *B. subtilis* over the cultivation time in a bioreactor [170]. However, high-throughput methods are necessary for screening parameters that influence sporulation. Spectroscopic techniques might be a valuable tool for monitoring sporulation in MTPs. The scattered light of spores and the spectroscopic characteristics of DPA might be promising detection parameters.

Various studies have investigated the fluorescence characteristics of DPA. For DPA alone, no fluorescence emission has been observed in aqueous solution [171, 172]. In contrast, fluorescence emission at about 400 nm was reported for calcium-DPA at an excitation wavelength of about 300 nm in an aqueous solution [171], as well as for wet and dried calcium-DPA [172]. Fluorescence of DPA in *Bacillus* spores at an excitation wavelength of 345 nm and an emission wavelength of 410 nm was observed by Alimova et al. [173].

This study aimed to monitor *Bacillus* sporulation during cultivation using spectroscopic techniques. For demonstrating the method, the model organism *B. subtilis* was used. Two *B. subtilis* strains were cultivated, one spore-forming and one with a genetic knockout in sporulation. An increase in fluorescence during cultivation in the BioLector was qualitatively correlated to the course of sporulation. To highlight the broad applicability of this spore detection method, experiments with other spore-forming *Bacillus* species, namely *Bacillus licheniformis* and *Bacillus velezensis*, were performed.

3.2 Materials and Methods

3.2.1 Microbial strains

The experiments in this work were performed with various *Bacillus* strains. The *B. subtilis* strain PY79 [174-176] and *B. subtilis* strain KO7-S were both obtained from the *Bacillus* Genetic Stock Center (BGSC) by BASF SE (Ludwigshafen am Rhein, Germany) and kindly provided by BASF SE. In the study presented herein, the *B. subtilis* strain PY79 (BGSC ID: 1A747) is called spore former, and the *B. subtilis* strain KO7-S (BGSC ID: 1S145) is named knockout strain. The knockouts of the *B. subtilis* KO7-S strain are in a sporulation gene (*ΔsigF*) and seven protease genes (*ΔnprE*, *ΔaprE*, *Δepr*, *Δmpr*, *ΔnprB*, *Δvpr*, *Δbpr*). The industrially relevant *B. velezensis* strain (MBI600) was received from BASF SE. In addition, the *B. licheniformis* DSM8785 strain from Leibniz Institute DSMZ (German Collection of Microorganisms and Cell Cultures) was used. All cryo-cultures were stored at -80 °C with 125 g/L glycerin and 25 g/L saccharose.

3.2.2 Cultivation media

Lysogeny broth (LB) medium [177] was used for pre-cultures. It contained 5 g/L yeast extract (Karl Roth GmbH, Karlsruhe, Germany), 10 g/L tryptone (Karl Roth GmbH, Karlsruhe, Germany), and 5 g/L NaCl. After preparation, the pH of the medium was checked to be at 7.0 with a HI221 Basic pH meter (Hanna Instruments Deutschland GmbH, Vöhringen, Germany). The medium was autoclaved for 60 min at 121 °C.

Main-cultures were conducted in *Bacillus* complex (Bc) medium containing 10 g/L glucose, 5 g/L yeast extract (Bio Springer, Maisons-Alfort, France), 10 g/L soy flour (Sofarine Bic Protein, BiC, BC's-Hertogenbosch), and 10 g/L corn starch (Roquette Frères, Lestrem, France). A separate glucose stock solution and a main stock solution containing yeast extract, soy flour, and corn starch, were prepared for this medium. The pH of the main stock solution was adjusted to 7.0 with 25 % (w/w) NH_3 • aq and 40 % (w/w) H_3PO_4 solutions. The main

stock solution was autoclaved for 60 min at 121 °C. The glucose stock solution was sterilized by filtration (0.2 µm). Immediately before starting the experiment, the main stock solution was supplemented with glucose and deionized water to achieve the desired concentrations. The pH of the combined solution was adjusted to 7.0 with 25 % (w/w) NH_3 • aq and 40 % (w/w) H_3PO_4 solutions.

3.2.3 Cultivation conditions

Appendix Figure A18 shows an overview of the cultivation protocol. For all experiments, pre-cultures were performed in 250 mL shake flasks with a filling volume of 10 mL, a shaking frequency of 350 rpm, and a shaking diameter of 50 mm. Pre-cultures were stopped in the late exponential phase or beginning of the stationary phase (OTR of 10-20 mmol/L/h).

Main-cultures were inoculated with pre-culture to an OD of 0.1. The OD of the pre-culture was measured with a Genesys 20 photometer (Thermo Scientific, Darmstadt, Germany) in a standard 1 cm cuvette at a wavelength of 600 nm. The samples were diluted with 0.9 % (w/v) NaCl to an OD of 0.1 to 0.3 as this is the linear range of the photometer. The blank was measured with 0.9 % (w/v) NaCl. Cultivations were performed in 250 mL shake flasks, when a high sample volume was required for analysis at the end of the cultivation. Cultivations were conducted in 48-round well MTPs, when online spectroscopic measurement techniques were used, or a high-throughput was necessary. Shake flask cultivations were performed with a filling volume of 10 mL, a shaking frequency of 350 rpm, and a shaking diameter of 50 mm. In MTP experiments, a filling volume of 0.7 mL, a shaking frequency of 1000 rpm, and a shaking diameter of 3 mm were used.

3.2.4 Online monitoring techniques

An in-house developed RAMOS device [70, 71] was used to determine the OTR of pre- and main-cultures in shake flasks. The RAMOS device is commercially available from Adolf Kühner AG (Birsfeld, Switzerland) and HiTec Zhang GmbH (Herzogenrath, Germany). MTP cultivations were performed in a commercial BioLector I device (Beckman Coulter

GmbH, Krefeld, Germany) to monitor the DOT over cultivation time. MTPs with optodes (MTP-R48-BOH1, Beckman Coulter GmbH, Krefeld, Germany) were used. As measured DOT values exhibited an offset in the BioLector, the DOT was corrected as described in Appendix Section A1. The correction of DOT is shown exemplarily for four wells of the *B. subtilis* strains in Appendix Figure A19. In addition, the calculation of the OTR based on the DOT in MTP is described in Appendix Section A2. Fluorescence and scattered light monitoring in MTPs were performed in an in-house built BioLector [72, 75] coupled to a Fluoromax-4-spectrometer (HORIBA Jobin-Yvon GmbH, Bernsheim, Germany). The desired wavelengths can be selected using monochromators. The detailed measuring setup is described in Wandrey et al. [76]. The cultivations in the in-house BioLector were conducted in MTPs without optodes (MTP-R48-B, Beckman Coulter GmbH, Krefeld, Germany). The scattered light at 620 nm and the fluorescence at an excitation wavelength of 390 nm and an emission wavelength of 460 nm were recorded. The scattered light was measured with a slit width of 2 nm, and the fluorescence with a slit width of 4 nm. The integration time was 600 ms for both. Fluorescence and scattered light data over cultivation time in the in-house built BioLector were recorded using LabVIEW software developed by ZUMOLab GmbH (Wesseling, Germany). In all experiments, the MTPs were closed with a gas-permeable sealing foil with an evaporation-reducing layer (F-GPR48-10, Beckman Coulter GmbH, Krefeld, Germany).

3.2.5 Recording of 2D fluorescence spectra

2D fluorescence spectra of pure cultivation medium, inoculated cultivation medium, and culture broth at the end of the cultivation were recorded using the setup of the in-house built BioLector [72, 75, 76] coupled to a Fluoromax-4-spectrometer (HORIBA Jobin-Yvon GmbH, Bernsheim, Germany). When necessary, the culture broth of replicates of the shake flask cultivations or of replicates cultivated in different wells in a MTP was pooled at the end of the corresponding cultivation to increase sample volume. In addition, 2D fluorescence spectra of supernatant and pellet of *B. subtilis* were recorded. The supernatant was obtained after two centrifugation steps of the culture broth for 15 min at 18000 g. The pellet was resuspended in 0.9 % (w/v) NaCl. 2D spectra were recorded in a 48-round well MTP with a

filling volume of 700 µL using the software FluorEssence V3.5 (FluorEssenceTM for Windows, HORIBA Jobin-Yvon GmbH, Bernsheim, Germany). The positioning of the corresponding well of the MTP was performed utilizing LabVIEW software developed by ZUMOLab GmbH. Recording of the 2D spectra was performed at a temperature of 37 °C, a shaking frequency of 1000 rpm, and a shaking diameter of 3 mm. The increment of recorded wavelengths was set to 10 nm with a slit width of 2 nm and an integration time of 0.12 s. The difference in the 2D fluorescence spectra was calculated by subtracting the intensities of the 2D fluorescence scans at the beginning of the cultivation from the intensities of the 2D fluorescence scans at the end of the cultivation. Before measuring the samples, the spectrometer was calibrated with a quartz glass cuvette filled with deionized water. When a new calibration of the spectrometer was necessary, due to switching off the spectrometer between the beginning and end of the cultivation, the intensities at the end of the cultivation were corrected by a correction factor. The procedure is described in Appendix Section A3 and Appendix Figure A20.

3.2.6 Addition of iron to *Bacillus subtilis* supernatant

2D fluorescence spectra of the supernatant of *B. subtilis* culture broth at the end of the cultivation were recorded before and after the addition of iron. A schematic overview is shown in Appendix Figure A21. 2D fluorescence spectra of 700 µL supernatant for each well were obtained using the setup of the in-house built BioLector [72, 75, 76] coupled to a Fluoroxmax-4-spectrometer (HORIBA Jobin-Yvon GmbH, Bernsheim, Germany) with the settings described in chapter 3.2.5. Then, 100 µL supernatant was removed from the well of the MTP, and 100 µL of a 21 mM $FeCl_2 \cdot 4\ H_2O$ solution was added. A 2D fluorescence spectrum was recorded again. The same experiment was performed by adding 100 µL deionized water instead of the iron solution to the supernatant. The difference in the 2D fluorescence spectra was calculated by subtracting the intensities of the 2D fluorescence scans after adding iron from the intensities of the 2D fluorescence scans before adding iron.

In a further experiment, iron was added in different concentrations to the supernatant of *B. subtilis* culture broth. A schematic overview is shown in Appendix Figure A22. In this

case, the fluorescence intensity of the supernatant at the end of the cultivation was measured in a 48-round well MTP with a filling volume of 700 µL, a temperature of 37 °C, a shaking frequency of 1000 rpm, and a shaking diameter of 3 mm. The measurement was performed with the in-house built BioLector [72, 75, 76] coupled to a Fluoromax-4-spectrometer (HORIBA Jobin-Yvon GmbH, Bernsheim, Germany) and LabVIEW software developed by ZUMOLab GmbH. An excitation wavelength of 390 nm and an emission wavelength of 460 nm was used with a slit width of 4 nm and an integration time of 600 ms. After 4.2 h, 100 µL of the supernatant were removed from the well, and 100 µL of $FeCl_2 \cdot 4\ H_2O$ and $FeCl_3 \cdot 6\ H_2O$ solutions in different concentrations (0.7, 7, 21, 42, 63, 105, 350 mM) were added to the supernatant. For analysis, the fluorescence intensity before adding iron was determined by calculating a mean value of intensities before adding iron. The fluorescence intensity after adding iron was determined by calculating a mean value of intensities after adding iron. A period of 1.0 h was chosen for the mean value calculation. The mean fluorescence intensity before adding iron was subtracted from the mean fluorescence intensity after adding iron. For all experiments, fresh iron solutions were prepared.

3.2.7 Microscopic images

Phase contrast microscopy was performed with an Eclipse E600 (Nikon, Tokyo, Japan) with a 1000x magnification.

3.3 Results and Discussion

3.3.1 Comparison of *Bacillus subtilis* cultivations at different scales in complex medium

To develop the spore detection method, the *B. subtilis* spore former and knockout strain were cultivated in complex Bc medium in shake flask and MTP scale. A parallel cultivation was conducted in shake flasks and a MTP (Figure 3-1) to compare the growth of the strains at

these two scales. Figure 3-1A shows the OTR of duplicate cultivations of the *B. subtilis* spore former and knockout strain in Bc medium at shake flask scale.

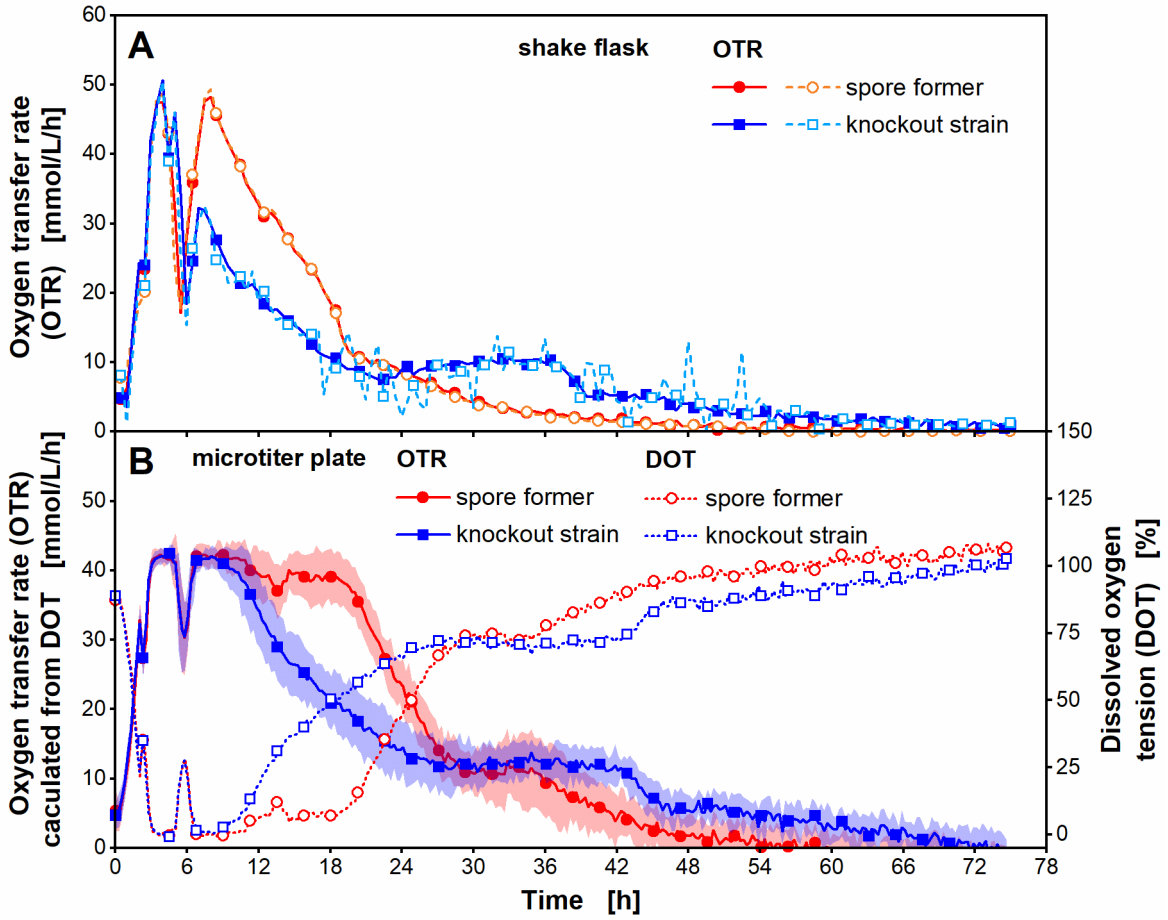

Figure 3-1: Cultivation of *Bacillus subtilis* PY79 spore former and KO7-S knockout strain in shake flask and microtiter plate scale.

(A) Oxygen transfer rate (OTR) in shake flasks, **(B)** dissolved oxygen tension (DOT) and OTR in a microtiter plate. **(A), (B)** For clarity, only every 10th measuring point over time is marked by a symbol. **(A)** Duplicates are shown for cultivations in shake flasks. **(B)** Mean values of 16 replicates with standard deviations as shadows are shown for cultivations in microtiter plate. The DOT was corrected as described in Appendix Section A1. Correction is shown for four wells of each strain as an example in Appendix Figure A19. The correction was performed for all 16 wells and the mean value of the corrected DOT of all 16 wells was calculated for each strain. The OTR in microtiter plate was calculated from the corrected DOT as described in Appendix Section A2 with a volumetric oxygen transfer coefficient (k_La) value of 194 1/h. Cultivation conditions in a RAMOS device [70, 71]: temperature 37 °C, 250 mL RAMOS shake flask, filling volume 10 mL, shaking frequency 350 rpm, shaking diameter 50 mm, Bc medium with 10 g/L glucose. Cultivation conditions in a commercial BioLector I device (Beckman Coulter GmbH): temperature 37 °C, 48-round well plate (MTP-R48-BOH 1), filling volume 0.7 mL, shaking frequency 1000 rpm, shaking diameter 3 mm, Bc medium with 10 g/L glucose.

The OTR of the spore former showed three distinct peaks at about 20 mmol/L/h after 2 h, at about 48 mmol/L/h after 4 h, and at about 49 mmol/L/h after 8 h (Figure 3-1A). The OTR of the knockout strain exhibited a similar course (Figure 3-1A). A difference in the OTR was observed in the last OTR peak. This peak, with a value of 32 mmol/L/h after around 7 h, was 1.5-fold lower than the OTR peak of the spore former after 8 h.

The OTR peaks of both strains represent the metabolization of the various carbon sources in the Bc medium, which are glucose, corn starch, and carbon sources contained in soy flour and yeast extract. The slight differences in the OTR profile between the spore former and knockout strain might be attributed to differences in protein cleavage. This difference in protein cleavage might be traced back to the protease knockouts of the knockout strain. The cultivation in shake flasks (Figure 3-1A) exhibited no oxygen limitation, which agrees with the calculated maximum oxygen transfer capacity (OTR_{max}) after Meier et al. [178]. The calculated OTR_{max} in shake flasks under the given cultivation conditions and with an osmolality of 0.12 osmol/kg in the Bc medium is 83 mmol/L/h. This is higher than the measured highest OTR peak of 49 mmol/L/h.

The results of the parallel cultivation in MTP for both strains are shown in Figure 3-1B. In addition, the OTR calculated based on the DOT in the MTP is presented. For this purpose, the volumetric oxygen transfer coefficient (k_La) in the MTP was determined in a separate cultivation to be 194 1/h (mean value of four replicates) under the given cultivation conditions. The k_La determination is presented, exemplarily for one replicate (well), in Appendix Figure A23.

The DOT of the spore former decreased to nearly zero after 3 h for around 2 h, then increased and again decreased to almost zero after 7 h until 11 h. Then the DOT increased until the end of the cultivation. The DOT of the knockout strain had a similar course until 8 h of cultivation. Afterward, it increased 3 h earlier than the DOT of the spore former. The OTR of both strains showed a mirrored course of the DOT. The range, in which the DOT for the first time was nearly zero, was observed as a plateau in the OTR at around 42 mmol/L/h, between 3 h and 5 h. When the DOT was nearly zero for the second time, the OTR exhibited another plateau at about 42 mmol/L/h.

The OTR of the cultivation in shake flasks (Figure 3-1A) and the DOT as well as the OTR of the cultivation in the MTP (Figure 3-1B), exhibit very similar profiles. In the MTP, the DOT decreased to nearly zero. Meanwhile the OTR in the MTP reached a plateau, which increased the total cultivation time compared to the shake flask experiment. This plateau indicates a short oxygen limitation during the cultivation in the MTP [70, 77], which was not observed during the cultivation in shake flasks. However, as this study aimed to develop a qualitative spore detection method, both cultivation scales were used, even though differences in oxygen supply were noticed.

An overview of all performed shake flask and MTP experiments for both *B. subtilis* strains is shown in Appendix Figure A24. The comparable courses of the OTR curves within an experiment and across experiments showed good reproducibility of the results from the RAMOS device (Appendix Figure A24A and B). This reproducibility could also be inferred from Appendix Figure A24C and D for the DOT courses in the MTP, which was represented in low standard deviations (on average 10 % for all shown experiments). The reproducibility of the corresponding pre-cultures of the experiments is depicted in Appendix Figure A25.

3.3.2 Screening for potential spore detection parameters

To monitor the sporulation of *Bacillus* species based on spectroscopic techniques, suitable wavelength combinations for online measurement need to be identified. Therefore, 2D fluorescence spectra (absolute values) of the *B. subtilis* spore former and knockout strain were recorded at the beginning and end of a shake flask cultivation. To compare the spectra of the *Bacillus* spore former and knockout strain, the difference in the fluorescence spectra was calculated for each strain (Figure 3-2). Calculating difference spectra in this experiment and the following experiments reduces variations between cultivations, and only changes in fluorescence intensities are investigated. Previous studies also applied this procedure [179, 180].

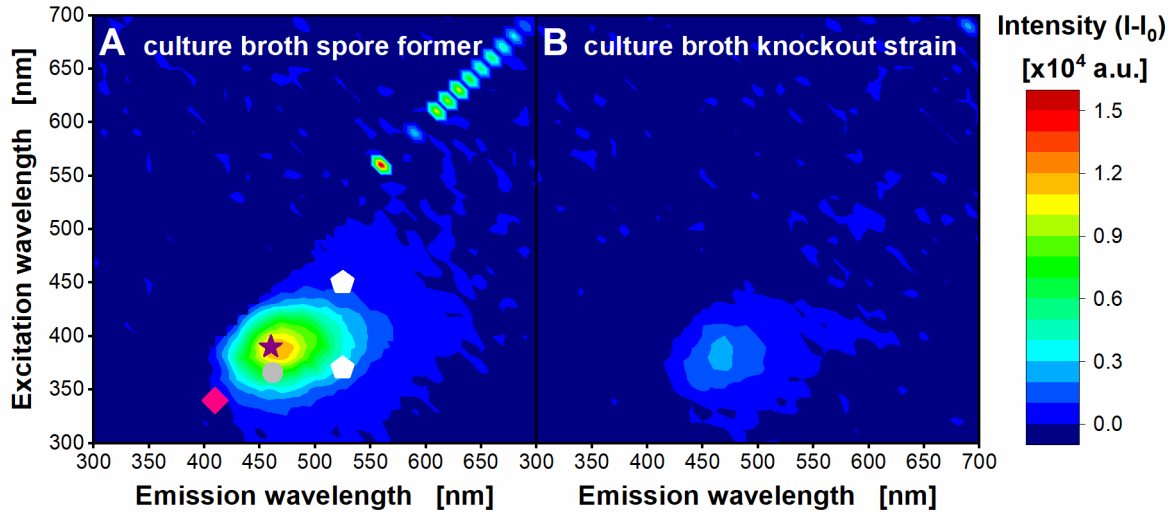

Figure 3-2: Difference of 2D fluorescence spectra of culture broth of *Bacillus subtilis* PY79 spore former and KO7-S knockout strain between the beginning and end of the cultivation.

(A) Spore former, **(B)** knockout strain. The wavelength combinations of fluorescence of fluorophore molecules ($\lambda_{ex}/\lambda_{em}$) are marked with symbols: Dipicolinic acid ($\lambda_{ex}/\lambda_{em}$=340/410 nm) [173] as pink diamond, NADH ($\lambda_{ex}/\lambda_{em}$=366/462 nm) [181] as grey circle, riboflavin ($\lambda_{ex}/\lambda_{em}$=270/525 nm (not marked), 370/525 nm and 450/525 nm) [182] as white pentagons, fluorescence maximum ($\lambda_{ex}/\lambda_{em}$=390/460 nm) as dark purple star. 2D fluorescence scans with excitation wavelengths from 300-700 nm and emission wavelengths from 300-700 nm were recorded at the beginning of the cultivation and after 67 h of cultivation using the setup of an in-house built BioLector device [72, 75, 76]. Intensities of 2D spectra after 67 h of cultivation were corrected with the correction factor as described in Appendix Section A3. Intensities of the 2D fluorescence scan from the beginning of the cultivation were subtracted from corrected intensities of the 2D fluorescence scan after 67 h of cultivation ($I-I_0$). The cultivations in shake flasks are shown in Appendix Figure A24.

The 2D fluorescence difference spectrum of the spore former culture broth exhibited a distinct fluorescence maximum at an excitation wavelength (λ_{ex}) of 390 nm and an emission wavelength (λ_{em}) of 460 nm (Figure 3-2A). This maximum was 5.3-fold lower in the 2D difference fluorescence spectrum of the knockout strain culture broth (Figure 3-2B). No other conspicuous fluorescence maxima were visible for either strain. A 2D difference fluorescence spectrum of pure Bc medium, which was not inoculated, did not show the fluorescence maximum (Appendix Figure A26). Microscopic images of the spore former exhibited free spores and some vegetative cells after 67 h (data not shown). Spores were not observed for the knockout strain (data not shown). As the fluorescence maximum at $\lambda_{ex}/\lambda_{em}$ = 390/460 nm was much higher in the 2D fluorescence difference spectrum of the spore former, a correlation of the fluorescence maximum to sporulation is assumed.

To classify the type of molecule causing the fluorescence, the wavelength combination of the fluorescence maximum was compared to the combinations of known fluorophore molecules. Neither the excitation and emission wavelengths of NADH ($\lambda_{ex}/\lambda_{em}$ = 366/462 nm) [181] nor riboflavin ($\lambda_{ex}/\lambda_{em}$ = 270/525 nm, $\lambda_{ex}/\lambda_{em}$ = 370/525 nm and 450/525 nm) [182] fit to the measured fluorescence maximum. This is not surprising, as it is known from literature that spores contain almost no high-energy compounds like NADH [31, 32]. Only the oxidized form NAD+ is found in dormant spores [31, 32]. In addition to NADH and riboflavin, the wavelength combination was compared to the spore-specific component DPA. Alimova et al. reported that DPA, which was assumed to be chelated with calcium, exhibited an excitation wavelength of 340 nm and an emission wavelength of 410 nm in fluorescence spectra of *B. subtilis* spores [173]. This wavelength combination is not comparable to the observed fluorescence maximum in this study.

To verify the hypothesis that the fluorescence maximum (λ_{ex}=390 nm, λ_{em}=460 nm) in the 2D fluorescence difference spectrum of the spore former is linked to sporulation, the wavelength combination was measured over time in an in-house built BioLector device (Figure 3-3A). The *B. subtilis* spore former and knockout strain were cultivated. In parallel, samples were taken, and microscopic images of those samples were recorded, to track the formation of spores (Figure 3-3B and C). Additionally, it was suspected that spores influence the scattered light signal. Hence, the scattered light signal at 620 nm was measured over cultivation time (Figure 3-3A).

The scattered light intensity of the spore former and knockout strain showed a comparable increase until 4.5 h of cultivation (Figure 3-3A). Then, the scattered light intensity of the knockout strain reached a more or less constant level, after a short drop at around 6 h of cultivation. In contrast, the scattered light intensity of the spore former increased after a decline. The scattered light intensity of the knockout strain started to decrease after around 26 h of cultivation, and the scattered light intensity of the spore former decreased after 21 h until a plateau after about 50 h was reached.

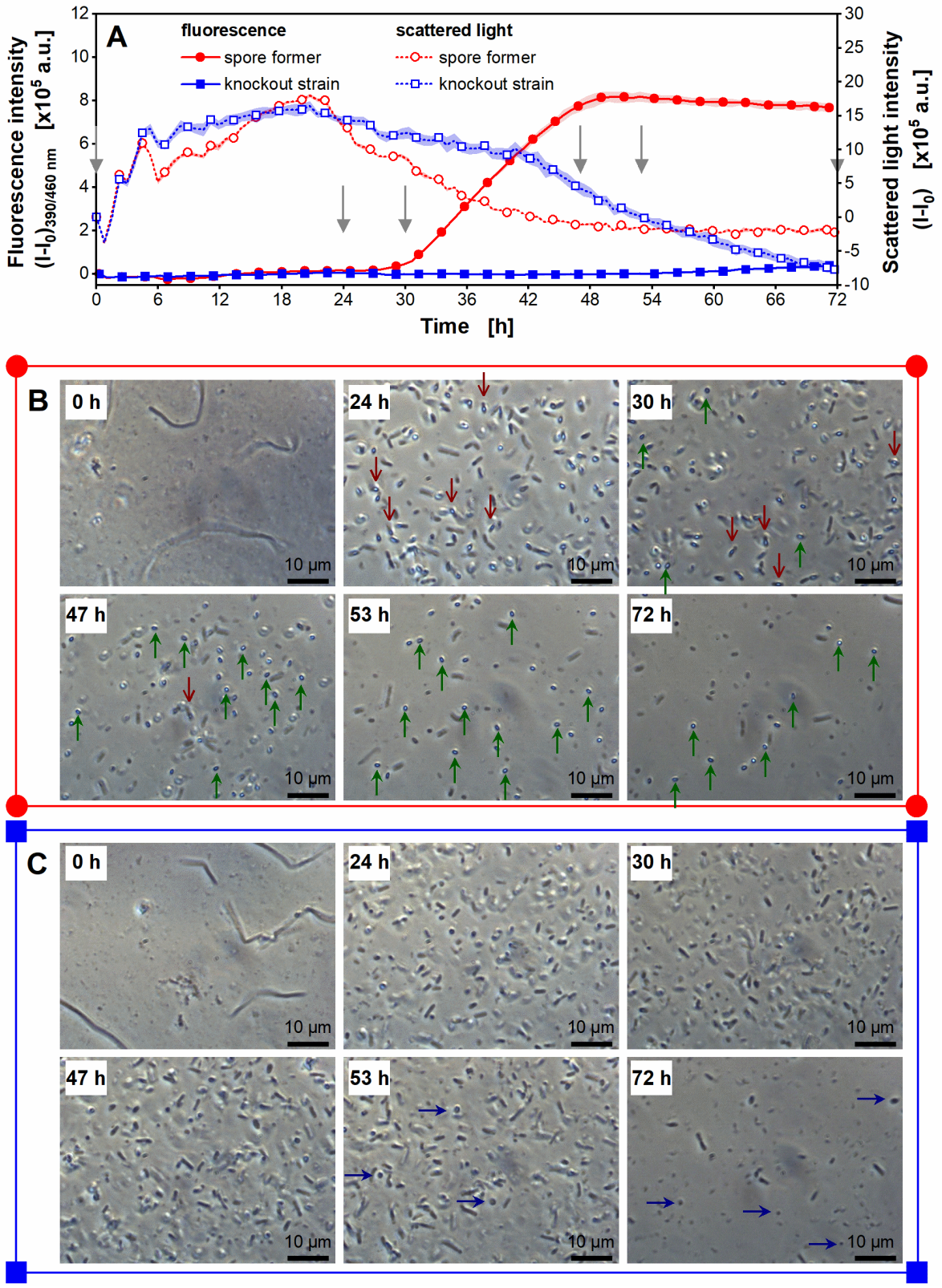

Figure 3-3: Online scattered light and fluorescence measurement of *Bacillus subtilis* PY79 spore former and KO7-S knockout strain with microscopic images.

(A) Scattered light intensity at 620 nm and fluorescence intensity with an excitation wavelength of 390 nm and an emission wavelength of 460 nm. Mean values of three replicates with standard deviations as shadows are shown. If the standard deviations are small, they are not well recognizable. For clarity, only every 4th measuring point over time is marked by a symbol. The initial intensity was subtracted from the measured intensities over time ($I-I_0$) for each strain. Grey arrows mark the time point of samples. Microscopic images of **(B)** spore former and **(C)** knockout strain at different time points with 1000x magnification. **(B), (C)** The color and symbol of the frame of the microscopic images correspond to the symbols and colors in **(A)**. Red arrows pointing downwards show spores inside the mother cells. Green arrows pointing upwards show free spores. Blue arrows pointing to the right show cells with round shape. Cultivation conditions in an in-house built BioLector device [72, 75, 76]: temperature 37 °C, 48-round well plate (MTP-R48-B), filling volume 0.7 mL, shaking frequency 1000 rpm, shaking diameter 3 mm, Bc medium with 10 g/L glucose.

The microscopic images of the spore former (Figure 3-3B) and knockout strain (Figure 3-3C) showed rod-shaped vegetative cells at the beginning of the cultivation. In the microscopic image of the sample taken after 24 h, for the spore former, spores inside the mother cells were observed together with vegetative cells, not containing spores. The microscopic image at 30 h of cultivation exhibited first released spores in an ellipsoidal form, which increased in number during the rest of the cultivation. The knockout strain did not show any spores. In contrast, cells with round shape were observed in the microscopic images taken after 53 h and 72 h of cultivation.

The increase in the scattered light intensity at the beginning of the cultivation of both strains represents the growth of the vegetative cells on the carbon sources in complex medium. Scattered light depends on various influencing factors, such as cell morphology [88] and the detection angle [183]. Therefore, it was hypothesized that the formation of spores can be followed by the scattered light signal. However, the inconclusive course of the scattered light intensity of both strains between 6 h of cultivation until the end of the cultivation did not show any correlation between scattered light and sporulation (Figure 3-3A). Additionally, the development of free spores in the microscopic images (Figure 3-3B), which started at around 30 h, did not show a distinct correlation to the scattered light intensity. Therefore, the above hypothesis was not confirmed in this study. As expected, the knockout strain did not exhibit any spores (Figure 3-3C). However, the microscopic images at the end of the cultivation showed that the knockout strain formed cells with round shape, and cell lysis was visible. These might influence the scattered light of this strain. The round cells of the knockout strain in Figure 3-3C are proposed to be the effect of an incomplete sporulation

process. The knockout strain might start the sporulation process under appropriate conditions as the spore former. After asymmetric septum formation [184], sporulation stops, as no sigma F factor (σ^F) is active due to the knockout in the gene *sigF*. This termination of sporulation could lead to pinch off the cells with round shape. Magill and Setlow showed the release of ellipsoid to coccoid forespores, called sporlets, of a *B. subtilis spoIIAC* (*sigF*) mutant in electron micrographs [185]. Due to the mutation, an additional septum was formed on the opposite side to the typical septum in the cells. Further incubation of the *B. subtilis spoIIAC* strain resulted in the lysis of the mother cells and release of the sporlets [185]. In addition, Defeu Soufo observed that round cells, called "dwarf cells", were formed by *B. subtilis* PY79, when incomplete sporulation took place in a minimal medium [186]. In their study, sporulation seemed to stop after the asymmetric septum was formed [186].

The fluorescence intensity (λ_{ex}=390 nm, λ_{em}=460 nm) of the spore former was almost constant until 24 to 26 h (Figure 3-3A). Afterwards, the fluorescence intensity of the spore former strongly increased, until a plateau was reached at around 50 h. The fluorescence intensity of the knockout strain was nearly constant during the whole cultivation.

Strong differences in fluorescence intensity were observed for the two strains. Therefore, the fluorescence is a more promising detection signal than the scattered light. The detection of some free spores in the microscopic image of the spore former after 30 h of cultivation (Figure 3-3B) corresponded well with the beginning of the increase in fluorescence intensity between 24 h and 30 h (Figure 3-3A). When the fluorescence intensity reached its plateau from around 50 h on, only free spores with a low portion of vegetative cells were visible in the microscopic image. Spores inside the mother cells were not observed anymore, in contrast to the time point of the beginning of the fluorescence increase. The fluorescence intensity of the knockout strain was nearly constant over the whole cultivation time (Figure 3-3A), and no spores were detected in microscopic images (Figure 3-3C). A slight increase in fluorescence after around 54 h was in parallel to the observation of the round cells in microscopic images. Concluding from the observations in this experiment, the hypothesis that the increase in fluorescence intensity at $\lambda_{ex}/\lambda_{em}$ =390/460 nm correlates with the sporulation process is emphasized. It is suggested that the increase in fluorescence

intensity is linked to the release of the spores from the mother cells and related cell lysis, as the fluorescence increase was observed during the development of the free spores.

Two different materials as the origin of the observed fluorescence are conceivable. The fluorescence could be caused by (a) the spores themselves (for example a spore-specific substance inside the spores) or (b) a substance produced during cultivation and released into the medium during lysis of the mother cells. Cell lysis did also take place for the knockout strain. Therefore, an intracellular substance produced by both strains is unlikely to cause the fluorescence, because it would also have been released into the medium for the knockout strain.

3.3.3 Identification of fluorescing chemical substance

To investigate, which chemical substance causes the fluorescence, the fluorescence source needs to be localized. Therefore, *B. subtilis* cells and spores were separated from the cultivation medium by centrifugation. 2D spectra of the pellet of the *B. subtilis* spore former diluted in NaCl and of the supernatant of the spore former were recorded at the beginning and end of the cultivation in shake flasks. 2D fluorescence difference spectra are shown in Figure 3-4.

The 2D fluorescence difference spectrum of the pellet of the *B. subtilis* spore former did not exhibit any fluorescence maximum (Figure 3-4B). Only the 2D difference spectrum of the supernatant (Figure 3-4A) showed the fluorescence maximum at the same wavelength combination ($\lambda_{ex}/\lambda_{em}$ =390/460 nm) as the culture broth of the spore former in Figure 3-2A. Due to the centrifugation steps, the supernatant is expected to contain no spores anymore. From this experiment, it can be concluded that a substance in the *Bacillus* spores, hence the spores themselves (a), does not cause the fluorescence. The assumption of chapter 3.3.2 that the fluorescence is not caused by the spore-specific substance DPA is underlined. The fluorescence is presumably caused by a substance produced during cultivation and released into the medium during lysis of the mother cells (b).

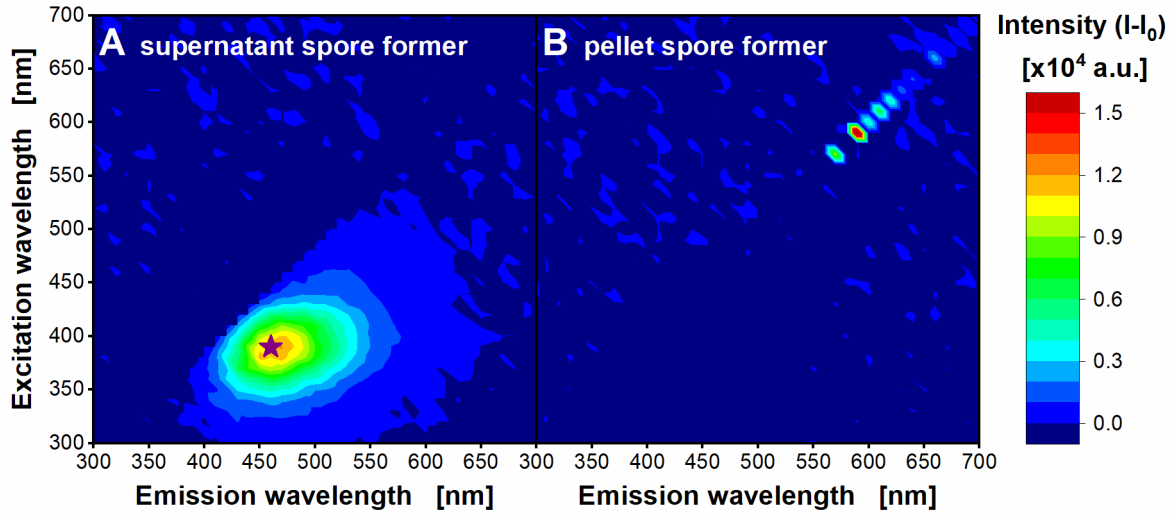

Figure 3-4: Difference of 2D spectra of supernatant and pellet of *Bacillus subtilis* PY79 spore former between the beginning and end of the cultivation.

(A) Supernatant, **(B)** pellet after resuspension in 9 g/L NaCl. The fluorescence maximum ($\lambda_{ex}/\lambda_{em}$=390/460 nm) is marked with a symbol as dark purple star. 2D fluorescence scans with excitation wavelengths from 300-700 nm and emission wavelengths from 300-700 nm were recorded at the beginning of the cultivation and after 67 h of cultivation using the setup of an in-house built BioLector device [72, 75, 76]. Intensities of the 2D spectra after 67 h of cultivation were corrected with the correction factor as described in Appendix Section A3. Intensities of the 2D fluorescence scan from the beginning of cultivation were subtracted from the corrected intensities of the 2D fluorescence scan after 67 h of cultivation ($I-I_0$). The cultivation in shake flasks is shown in Appendix Figure A24.

To further narrow down, which chemical substance causes the fluorescence, a literature review was carried out. In previous reports, the fluorescence of the siderophore pyoverdine was measured at a similar wavelength combination (λ_{ex} = 398-405 nm, λ_{em} = 452-470 nm) [187-190] as found in this study. Siderophores are low-molecular-weight iron-chelating molecules secreted into the medium, to facilitate iron uptake by the cells [191]. Several organisms produce siderophores under iron-limiting conditions [192-195]. *Pseudomonas* species produce, for example, pyoverdines [192], and *E. coli* produces, for example, enterobactin [195]. Also, *Bacillus* species are known to produce siderophores, like bacillibactin [193] and petrobactin [194]. Due to the similar wavelength combination for fluorescence of pyoverdines and the sought substance in this study, it is assumed that a siderophore causes the fluorescence.

The fluorescence of pyoverdines is known to be quenched after adding Fe^{2+} and Fe^{3+} [190]. To investigate the hypothesis of siderophore production by *B. subtilis*, ferrous iron (Fe^{2+} as

$FeCl_2$ solution) was added to the twice centrifuged supernatant of the spore former and knockout strain. A concentration of 3 mM Fe^{2+} was added to the supernatant. 2D fluorescence spectra were recorded before and after addition of $FeCl_2$ (Appendix Figure A27). The intensities of the 2D spectra (absolute values) before adding $FeCl_2$ were subtracted from the intensities of the 2D spectra after adding $FeCl_2$. The resulting 2D fluorescence difference spectra represent the fluorescence intensity change due to $FeCl_2$ addition (Figure 3-5).

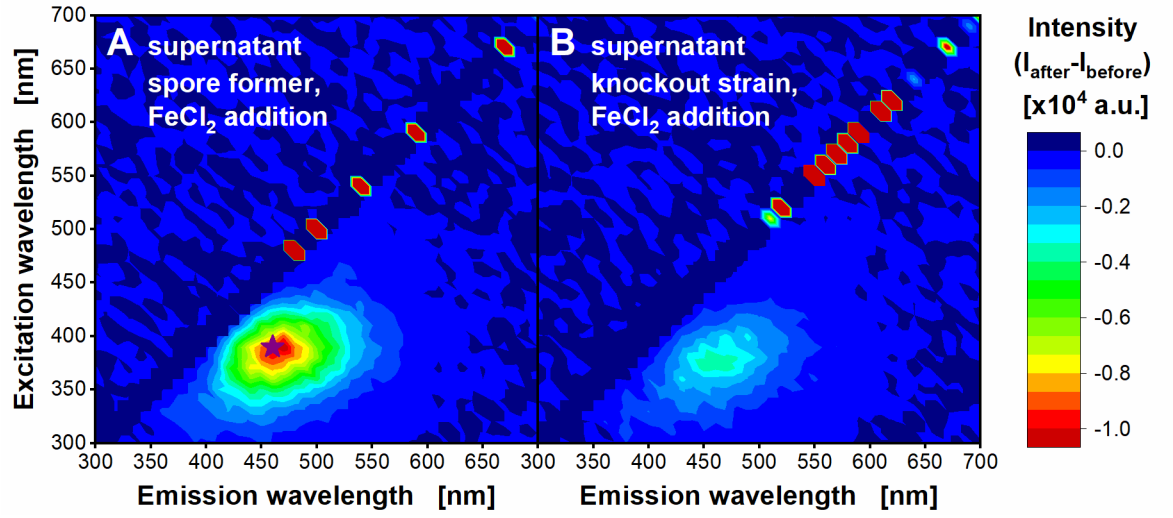

Figure 3-5: Difference of 2D fluorescence spectra of supernatant of *Bacillus subtilis* PY79 spore former and KO7-S knockout strain before and after adding $FeCl_2$.

(A) Spore former, **(B)** knockout strain. The fluorescence maximum ($\lambda_{ex}/\lambda_{em}$=390/460 nm) is marked with a symbol as a dark purple star. 2D fluorescence scans with excitation wavelengths from 300-700 nm and emission wavelengths from 300-700 nm were recorded of the supernatant after 66 h of cultivation before and after adding 3 mM $FeCl_2$ using the setup of an in-house built BioLector device [72, 75, 76]. Intensities of the 2D fluorescence scan before adding $FeCl_2$ were subtracted from the intensities of the 2D fluorescence scan after adding $FeCl_2$ (I_{after}-I_{before}). The scale of intensities shows negative values. Absolute spectra are shown in Appendix Figure A27. The cultivations in shake flasks are shown in Appendix Figure A24. Samples of cultivation were taken after 66 h and centrifuged for recording of 2D spectra of supernatant. A schematic overview for this experiment is shown in Appendix Figure A21.

Both strains exhibited a difference in the fluorescence intensity after addition of $FeCl_2$ compared to before addition of $FeCl_2$ (Figure 3-5). However, the difference of the fluorescence intensity of the spore former (Figure 3-5A) was four-fold stronger than the difference of the fluorescence intensity of the knockout strain (Figure 3-5B). A difference in the fluorescence intensity due to the dilution of the supernatant could be neglected for both

strains as difference spectra after addition of deionized water showed no difference in the fluorescence intensity (Appendix Figure A28).

As the fluorescence intensity was reduced after adding ferrous iron, the hypothesis that the *B. subtilis* spore former produces a siderophore is underlined. The slight fluorescence intensity difference for the knockout strain showed that it might produce the siderophore in very low quantities as well. In the study of Alimova et al., a similar fluorescence maximum at an excitation wavelength of 400 nm and an emission wavelength of 460 nm was reported in the fluorescence spectra of a *B. subtilis* strain [173]. The fluorescence was also quenched after adding $FeCl_2$ to the supernatant and the authors assumed a siderophore in their study to cause the fluorescence [173].

To investigate the fluorescence quenching in more detail, $FeCl_2$ was added in different concentrations to the supernatant of both *Bacillus* strains. Siderophores are known to chelate ferric iron with a higher affinity than ferrous iron [196, 197]. Therefore, the experiment was also performed with various concentrations of ferric iron in a $FeCl_3$ solution. The fluorescence intensity of the supernatant was measured at an excitation wavelength of 390 nm and an emission wavelength of 460 nm (absolute values) before and after the addition of iron instead of recording 2D spectra (Appendix Figure A29). The fluorescence difference was calculated as described in chapter 3.2.6. The results are presented in Figure 3-6.

The fluorescence intensity decreased to a comparable level for both types of iron species for the respective iron concentration. With increasing iron concentration, the difference in the fluorescence was stronger. For example, for a concentration of 9 mM $FeCl_3$, a 1.9-fold stronger decrease of the fluorescence signal was observed than for 3 mM $FeCl_3$ for the spore-forming strain. A saturation was observed for both strains for high iron concentrations (higher than 15 mM for the spore former and 9 mM for the knockout strain). The fluorescence decrease of the spore former was stronger for all ferrous and ferric iron concentrations investigated than the one of the knockout strain.

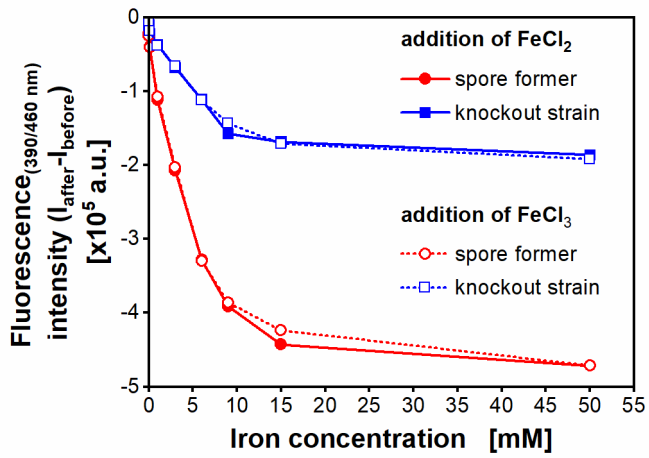

Figure 3-6: Difference of fluorescence intensity before and after adding different iron solutions and concentrations to the supernatant of *Bacillus subtilis* PY79 spore former and KO7-S knockout strain.

The fluorescence intensity of the supernatant was measured at an excitation wavelength of 390 nm and an emission wavelength of 460 nm, before and after adding $FeCl_2$ or $FeCl_3$ in an in-house built BioLector device [72, 75, 76]. The fluorescence intensity before adding $FeCl_2$ or $FeCl_3$ was subtracted from the fluorescence intensity after adding $FeCl_2$ or $FeCl_3$ (I_{after}-I_{before}). Absolute fluorescence intensities are shown in Appendix Figure A29. The cultivations in shake flasks are shown in Appendix Figure A24. Samples of the cultivation were taken after 66 h and centrifuged for measuring of the fluorescence intensity of the supernatant. $FeCl_2$ and $FeCl_3$ were added to the supernatant in different concentrations. Deionized water was added instead of iron so that no additional iron was added to the supernatant (0 mM). A schematic overview for this experiment is shown in Appendix Figure A22.

This experiment further underlines the assumption that a siderophore is the cause of the observed fluorescence. For the tested iron concentrations, no differences in the amount of fluorescence decrease were observed between $FeCl_2$ and $FeCl_3$. As the fluorescence difference for high iron concentrations increased only slightly, no more free siderophores were probably available to bind the higher amount of iron.

In this study, strong indications for *B. subtilis* producing a fluorescing siderophore, like pyoverdine, are found. The structure of pyoverdines is based on a fluorescing chromophore, a peptide ligand, and a carboxylic acid or carboxylic amid side chain [198]. *B. subtilis* strains are well known to produce the catecholic siderophore bacillibactin [193]. However, as reported by Alimova et al. [173] and to the best of our knowledge, reports about *B. subtilis* producing pyoverdine are not known. Only Oudega et al. showed that *B. subtilis* contains a gene similar to the pyoverdine synthetase from *Pseudomonas aeruginosa* [199]. Hence, further investigations are needed to determine the siderophore identified in this study.

The fluorescence measurement and the microscopic images in Figure 3-3 showed a correlation between the appearance of the fluorescence and the release of spores from the mother cells. Whether there is a causal relationship between sporulation and siderophore production or not, cannot yet be stated. Contradictory findings on the correlation of sporulation and siderophore production of *Bacillus* species can be found in literature. Santos et al. observed for *Bacillus megaterium* an increase in the concentration of the siderophore schizokinen before sporulation started [200]. The authors concluded that no correlation exists between sporulation and siderophore production in *B. megaterium* [200]. In contrast, Grandchamp et al. reported that the availability of the siderophore enterobactin, which *E. coli* produced in a co-culture with *B. subtilis*, promoted the sporulation of *B. subtilis* [201]. The authors traced this back to an increased iron availability due to siderophore production [201]. A further study investigated the association of siderophore production and sporulation with *B. anthracis* [202]. The authors reported that *B. anthracis* needs the siderophore petrobactin for sporulation. Production of petrobactin was started before sporulation, and the authors suggested that the siderophore was imported into the spore [202]. However, for *B. anthracis* it was also stated that petrobactin is produced during germination of spores [203].

3.3.4 Use of spore detection method with other *Bacillus* species

The spore detection method was demonstrated for the model organism *B. subtilis*. In the next step, the applicability of the fluorescence signal to monitor sporulation was investigated for other *Bacillus* species. The spore former *B. velezensis* MBI600 (reclassified, formerly *Bacillus amyloliquefaciens* [204]) was chosen as an industrially relevant example strain. Its spores are commercially applied, for instance, in biological plant protection [40]. There are also bioprocesses with spore-forming bacteria, in which spores are not desirable [205, 206]. For example, deleting sporulation genes can increase the yield of industrially relevant products [206]. Therefore, monitoring of sporulation during strain development is of great interest. As *B. licheniformis* is a workhorse for industrially relevant compounds, like proteases [206] and 2,3-butanediol [207], this species was also chosen in this study, to show the applicability of the spore detection method. *B. velezensis* MBI600 and *B. licheniformis*

DSM8785 were cultivated in parallel with the *B. subtilis* spore former and knockout strain. For high-throughput, this was performed in a MTP (Appendix Figure A30). 2D fluorescence spectra of the culture broth of all strains were recorded at the beginning and end of the cultivation. The 2D fluorescence difference spectra are shown in Figure 3-7A-D. Additionally, microscopy was performed at the end of the cultivation to assess the sporulation of the strains (Figure 3-7E-H).

Supporting the previous findings, the 2D fluorescence difference spectrum of the spore former showed the same fluorescence maximum as before. The knockout strain showed a 6.7-fold lower fluorescence intensity. In comparison, *B. velezensis* and *B. licheniformis* exhibited a fluorescence maximum with a 1.3-fold and 2.1-fold lower intensity, respectively, as the spore former strain. Free spores were found by microscopy for the *B. subtilis* spore former strain, but not for the knockout strain. Free spores were also observed for *B. velezensis* and *B. licheniformis*. However, based on the microscopic images, the spore concentration of *B. licheniformis* appears to be lower than that of *B. velezensis*, which in turn is lower than that of *B. subtilis* spore former.

The results underline the hypothesis that the fluorescence intensity at an excitation wavelength of 360 nm and an emission wavelength of 460 nm correlates with sporulation. The microscopic images indicated the highest spore concentration for the *B. subtilis* spore former strain, corresponding to the highest fluorescence intensity. Comparing *B. subtilis*, *B. licheniformis*, and *B. velezensis*, the microscopic image of the *B. licheniformis* strain suggests the lowest spore concentration (without consideration of the knockout strain), which corresponds to the lowest fluorescence intensity. This means that the newly developed method shows potential for quantitative detection of spores.

In previous reports, *B. licheniformis* and *B. velezensis* strains were shown to produce siderophores [208, 209]. In addition, in *B. velezensis*, the gene cluster for synthesis of bacillibactin was found [210]. However, to our knowledge, no reports exist that outline those two strains to produce pyoverdine. Finally, the fluorescence signal and sporulation correlation is confirmed for *B. velezensis* and *B. licheniformis*. Hence, the spore detection method was transferred to other *Bacillus* strains.

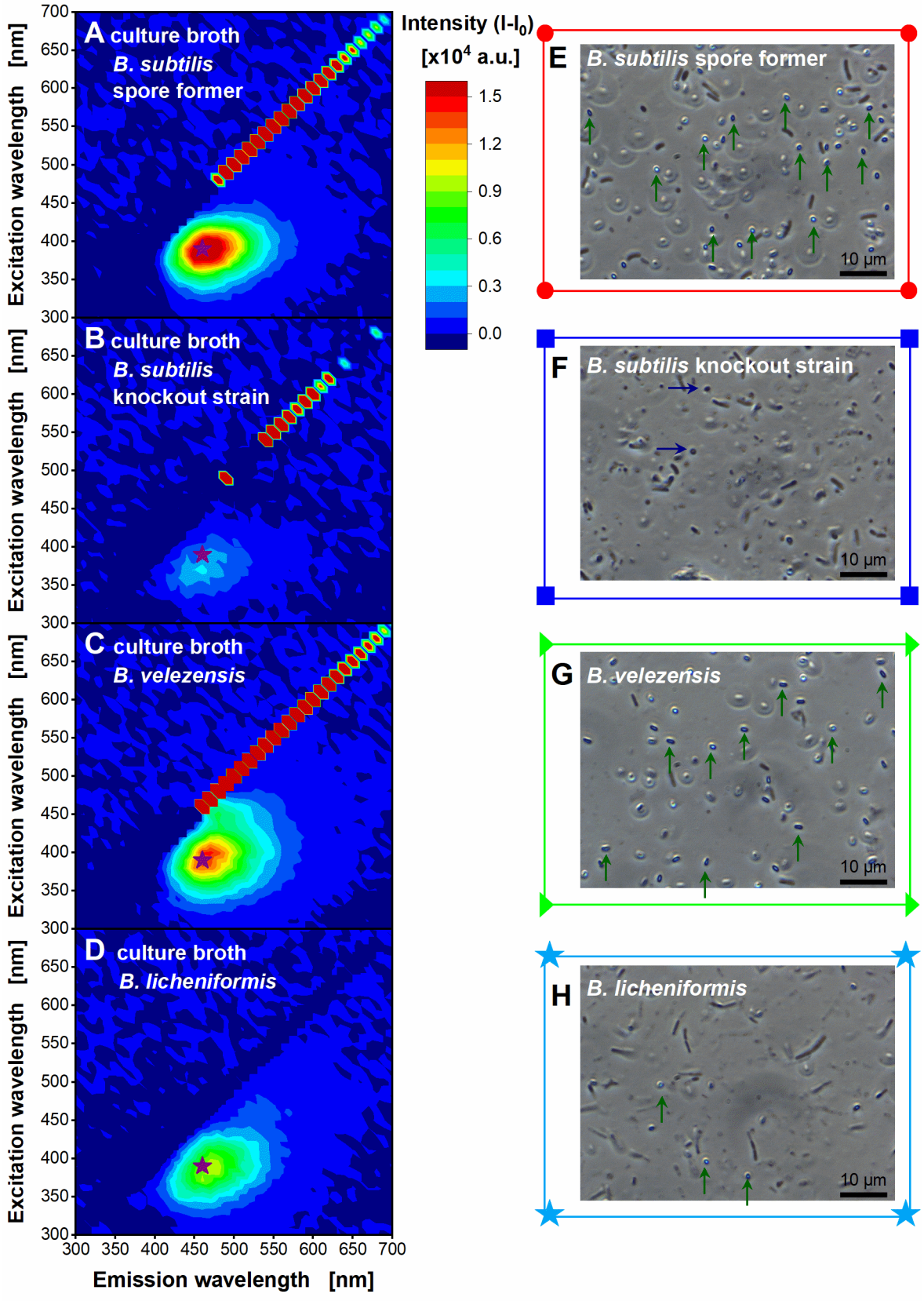

Figure 3-7: Transfer of spore detection method to other *Bacillus* strains.

Difference of 2D fluorescence spectra of culture broth between the beginning and end of the cultivation of **(A)** *Bacillus subtilis* PY79 (spore former), **(B)** *Bacilllus subtilis* KO7-S (knockout strain), **(C)** *Bacillus velezensis* (MBI600), **(D)** *Bacillus licheniformis* DSM8785. 2D fluorescence scans with excitation wavelengths from 300-700 nm and emission wavelengths from 300-700 nm were recorded at the beginning of the cultivation and after 66 h of cultivation using the setup of an in-house built BioLector device [72, 75, 76]. Intensities of the 2D fluorescence scan from the beginning of the cultivation were subtracted from intensities of the 2D fluorescence scan after 66 h of cultivation ($I-I_0$). **(A-D)** The fluorescence maximum ($\lambda_{ex}/\lambda_{em}$=390/460 nm) is marked with a dark purple star. Microscopic images of **(E)** *B. subtilis* spore former, **(F)** *B. subtilis* knockout strain, **(G)** *B. velezensis*, **(H)** *B. licheniformis* of samples after 66 h of cultivation with 1000x magnification. Green arrows pointing upwards show free spores. Blue arrows pointing to the right show cells with round shape. Cultivations in microtiter plate are shown in Appendix Figure A30. The color and symbol of the frame of the microscope images correspond to the symbols and colors in Appendix Figure A30.

3.4 Conclusion

In this study, spectroscopic techniques were applied to monitor sporulation of *Bacillus* species in a MTP. A spore-forming *B. subtilis* strain and a *B. subtilis* strain with a genetic knockout in sporulation were used to develop the method.

Recording of 2D fluorescence spectra showed that the *B. subtilis* spore former strain exhibited a distinct fluorescence maximum at an excitation wavelength of 390 nm and an emission wavelength of 460 nm, which was not observed for the *B. subtilis* knockout strain. This led to the assumption that the fluorescence is correlated to sporulation. Online monitoring of the fluorescence signal and microscopic images highlighted that the increase in fluorescence intensity correlates with the development of free spores and lysis of the mother cells.

2D fluorescence spectra of the pellet of the spore former, containing vegetative cells and spores, and of the supernatant revealed that the fluorescence was located in the supernatant. The 2D fluorescence spectra of the pellet did not show a notable fluorescence maximum. Hence, the fluorescence was not caused by the spores themselves (a spore-specific substance). The origin must rather be a chemical substance produced during cultivation and released into the medium during the lysis of the mother cells. Experiments, in which ferrous and ferric iron were added to the supernatant of the spore former, showed a significant

decrease in fluorescence after adding iron. Hence, most likely, a siderophore causes the observed fluorescence. Finally, the same wavelength combination correlated with sporulation in other *Bacillus* species and, therefore, applicability of the spore detection method to other *Bacillus* species was shown.

Through online fluorescence measurement, sporulation of *Bacillus* species can be detected in high-throughput screening experiments and qualitatively determined. The method is easy to use and less laborious than conventional spore detection methods. Thus, the established method is a valuable tool for monitoring sporulation. In addition to the use of the method for screening experiments in a MTP, the fluorescence could be measured with a novel probe for online monitoring of sporulation in industrial fermentations. Further investigations are required to identify the molecular mechanism of the identified correlation between the fluorescence and sporulation.

Contributions to chapter 4:

Jennifer Goldmanns wrote the chapter, prepared the figures, and designed and performed the experiments. Monique Schule and Theresa Scholand assisted with the experiments presented in chapter 4.3.1 and 4.3.2, respectively (AVT – Biochemical Engineering, RWTH Aachen University, Aachen, Germany).

4 Investigation of influence parameters on sporulation of *Bacillus subtilis* in complex medium applying the online spore detection method

4.1 Introduction

Sporulation is a complex process that is influenced by a multitude of different environmental factors. One of those crucial factors is the medium composition [104, 106, 110, 211]. In the past, various studies were performed to investigate and optimize medium compositions for the sporulation of different *Bacillus* strains [104, 106, 110, 211]. For example, Tian et al. investigated the influence of carbon and nitrogen sources on spore concentrations of *B. subtilis* BSNK-5 [104]. They reported that carbon and nitrogen sources, which are more difficult to metabolize (soluble starch in comparison to glucose and soybean in comparison to $(NH_4)_2SO_4$), enhance spore concentrations of *B. subtilis* BSNK-5 [104]. Sporulation takes place under starving conditions [114]. An excess of glucose represses the transcription of the *spo0A* gene [212]. As the Spo0A protein is a key regulator in the initiation of sporulation [213], the repression of transcription results in the inhibition of sporulation [212]. In addition to the choice of the carbon and nitrogen source, it was reported that the ratio of the carbon and nitrogen source (C/N) affects spore concentrations of *Bacillus* strains [106, 110].

Other media components with a relevant influence on sporulation are divalent cations as they are found in spores [214]. The most prominent cations are manganese and calcium. Manganese is essential for sporulation of various *Bacillus* species [215]. It is a cofactor for the enzyme phosphoglycerate phosphomutase, which is required for sporulation [216, 217]. Furthermore, manganese availability in the sporulation medium affects cortex biosynthesis

[218]. In most cases, calcium is associated with an increased heat resistance of *Bacillus* spores [107, 214]. This is mainly attributed to a reduction in the water content of the spores through mineralization [27, 219]. For *B. subtilis,* it was shown that the addition of calcium is required to achieve high spore concentrations in chemically defined media [109, 110]. Sinnelä et al. investigated the single and combined addition of calcium and manganese to nutrient broth medium for different *Bacillus* species [108]. In their study, the highest spore concentrations for *B. licheniformis* and *Bacillus cereus* were achieved in a nutrient broth medium supplemented with calcium. In contrast, the authors detected the highest spore concentrations for *B. subtilis* and *Bacillus coagulans* in a nutrient broth medium without supplementation of manganese and calcium [108].

Besides the medium composition, medium osmolality, pH, temperature, and oxygen availability are relevant fermentation parameters, which can influence the sporulation process [112-114, 220, 221]. It was shown for *B. subtilis* that a pH value in a range of 6.0-9.0 during batch cultivation in a fermenter with controlled pH increased sporulation efficiencies compared to an non-controlled pH [114]. In addition, pH values lower than 5.0 reduced sporulation efficiencies [114].

The oxygen supply in the cultivation of *Bacillus* species does not only affect the biomass, enzyme, and metabolite production [79, 222], but also the sporulation process [223]. Different cultivation strategies affect spore concentrations differently. Avignone-Rossa et al. presented that spore concentrations of *B. thuringiensis* were lower under oxygen-limited conditions compared to unlimited conditions during batch cultivations in a fermenter [111]. Sarrafzadeh and Navarro investigated the influence of oxygen on sporulation efficiencies for *B. thuringiensis* in a fermenter by varying the oxygen supply following the stop of substrate feeding after a fed-batch phase [112]. They showed that sporulation efficiencies (100 %) were higher during the absence of oxygen after the fed-batch phase compared to limited (93 %) and unlimited (84 %) oxygen conditions after the fed-batch phase [112]. In contrast, Boniolo et al. observed that spore concentrations of *B. thuringiensis* were reduced when the oxygen supply was interrupted during the sporulation and cell lysis phase in a batch fermentation [113]. They assumed that the remaining oxygen in the stationary phase did not provide enough energy for the sporulation process. Additionally, the investigation of

different constant DOT levels (5 %, 20 %, 50 %) throughout the fermentation, revealed an enhancement of spore concentrations for *B. thuringiensis* at higher DOT levels [113]. For *B. subtilis*, a controlled DOT level of 30 % resulted in slightly higher spore concentrations than DOT levels of 10 % and 50 % in a batch cultivation in a fermenter [114].

High spore concentrations and sporulation efficiencies are needed to run economic industrial processes. Therefore, a systematic screening of influence parameters on sporulation for a specific strain is indispensable. To reduce the laboratory effort, online detection methods in small-scale cultivations of spore formers are beneficial. In this study, the applicability of the spore detection method with fluorescence measurement at an excitation wavelength of 390 nm and an emission wavelength of 460 nm in MTPs, presented in chapter 3, was shown for investigating influence parameters on sporulation of the model organism *B. subtilis*. As calcium is a relevant element in sporulation and composition of *Bacillus* spores [107, 214], the influence of different calcium concentrations on spore concentrations of *B. subtilis* in complex Bc medium was tested. The other chosen parameter was oxygen, as it was shown in fermenter scale that it affects sporulation of different *Bacillus* strains [111-114]. However, in fermenter scale, experimental throughput is limited. Therefore, the aim was to investigate the influence of oxygen supply in-depth on a small-scale to allow multiple parallel conditions.

4.2 Materials and Methods

4.2.1 Microbial strains

For cultivations, *B. subtilis* PY79 (spore former) and *B. subtilis* KO7-S (knockout strain), mentioned in chapter 3.2.1, were used.

4.2.2 Cultivation media

The LB medium for pre-cultures and Bc medium for main-cultures described in chapter 3.2.2 were utilized.

For experiments with addition of different $CaCl_2$ concentrations, a 100 g/L $CaCl_2$ stock solution was prepared and sterile filtered (0.2 µm). The solution was added to the main stock solution of Bc medium together with glucose immediately before starting the experiments.

4.2.3 Cultivation conditions

The cultivation protocol used for this study is described in chapter 3.2.3. The figure captions indicate when the shaking frequency and the filling volume were varied.

4.2.4 Online monitoring techniques

Cultivations in shake flasks were conducted in a RAMOS device as described in chapter 3.2.4. Cultivations in MTPs were performed in a commercial BioLector I device (Beckman Coulter GmbH, Krefeld, Germany), in an in-house built BioLector device [72, 75, 76] or in an in-house built µRAMOS device combined with an in-house built BioLector (µRAMOS/BioLector combination) [77]. The commercial BioLector I measures the DOT over cultivation time in 48-round well MTPs with optodes (MTP-R-48-BOH1, Beckman Coulter GmbH, Krefeld, Germany). Due to an offset in the DOT in the BioLector, the DOT was corrected as described in Appendix Section A1. Cultivations in the in-house built BioLector [72, 75, 76] coupled to a Fluoromax-4-spectrometer (HORIBA Jobin-Yvon GmbH, Bernsheim, Germany) were performed to monitor the fluorescence intensity at an excitation wavelength of 390 nm and an emission wavelength of 460 nm in 48-round well MTPs without optodes (MTP-R48-B, Beckman Coulter GmbH, Krefeld, Germany). The slit width for fluorescence measurement was 2 nm, and the integration time was 600 ms. LabView software developed by ZUMOLab GmbH (Wesseling, Germany) was used for recording fluorescence data over cultivation time. For both BioLectors, MTPs were closed

with a gas-permeable sealing foil with an evaporation-reducing layer (F-GPR48-10, Beckman coulter GmbH, Krefeld, Germany). When OTR and fluorescence were monitored within one device, the µRAMOS/BioLector combination was used [77]. A gas-permeable sealing foil (900371-T, HJ-Bioanalytik GmbH, Erkelenz, Germany) was utilized to close the 48-round well MTP without optodes (MTP-R48-B, Beckman Coulter GmbH, Krefeld, Germany). Fluorescence measurement was conducted at the same excitation and emission wavelength with a slit width of 4 nm and an integration time of 600 ms.

4.2.5 Determination of (spore) colony forming units

The total cell concentration (vegetative cells and spores) and the spore concentration were determined at the end of the cultivations using the agar-plating technique. A salt-peptone stock solution containing 1.2 g/L K_2HPO_4, 0.34 g/L KH_2PO_4, 1 g/L Bacto peptone (Gibco™ Bacto™ Pepton, BD DIFCO™, Franklin Lakes, NJ, USA) and 0.1 g/L Tween 80 was prepared and sterile filtered (0.2 µm). Serial dilutions of the culture broth in the salt-peptone solution were prepared in quadruplicates. 100 µL of the dilution were pipetted onto ISP Medium 2 (BD DIFCO™, Franklin Lakes, NJ, USA) agar plates and smeared with a Drigalski spatula to determine the total cell concentration. Then, the diluted samples were heated at 60 °C for 30 min and 1000 rpm in a thermocycler to kill viable cells. After heating, 100 µL of the samples were pipetted onto the agar plate and smeared with a Drigalski spatula to determine the spore concentration. After plating, the plates were incubated at 37 °C for around 12 h, and colonies were counted. The total cell concentration was expressed as colony forming units per milliliter (CFU/mL) and the spore concentration was expressed as spore colony forming units per milliliter (SCFU/mL). The sporulation efficiency was calculated as the percentage of the spore concentration about the total cell concentration. Mass loss due to evaporation during shake flask and MTP cultivations was determined gravimetrically and considered in the data shown in the respective figures.

4.2.6 Determination of the start of the decrease in oxygen transfer rate and of the increase in fluorescence intensity

In chapter 4.3.3, the start of the decrease in the OTR and the increase in the fluorescence intensity of MTP cultivations was determined for different tested filling volumes. The procedure is shown exemplarily for one replicate for a filling volume of 0.7 mL for the decrease in the OTR in Appendix Figure A31A and for the increase in the fluorescence intensity in Appendix Figure A31B. A linear regression was performed on the almost constant values of the OTR plateau and on the values of the dropping flank of the OTR after the plateau. The start of the decrease in the OTR was the intersection point of those two regression lines. For the start of the increase in the fluorescence intensity, a linear regression was performed on the almost constant values of the fluorescence intensity before the increase and on the values of the linear increase in the fluorescence intensity. The start of the increase in the fluorescence intensity was the intersection point of those two regression lines. This procedure was performed for every replicate (well) of each tested filling volume. Mean values of points of intersection were calculated for each filling volume together with standard deviations to determine the start of the decrease in the OTR and the increase in the fluorescence intensity.

4.3 Results and Discussion

4.3.1 Influence of calcium concentration on sporulation of *B. subtilis* in microtiter plate scale

Microscopic images in Figure 3-3 of chapter 3.3.2 revealed that not all viable cells of *B. subtilis* PY79 sporulated in the applied Bc medium. As calcium is known to influence spore concentrations of *B. subtilis* strains [108-110], it was investigated if the addition of calcium results in higher spore concentrations in the Bc medium. Furthermore, the applicability of the online spore detection method for testing the influence of the $CaCl_2$ concentration was studied. Therefore, parallel cultivations were performed in a commercial

BioLector I device and in an in-house built BioLector device to allow measurement of DOT and fluorescence intensity in MTPs for *B. subtilis* PY79 spore former and *B. subtilis* KO7-S strain with a genetic knockout in sporulation. The cultivations were performed in four replicates without the addition of $CaCl_2$, with the addition of 0.2 g/L $CaCl_2$ and with the addition of 1.0 g/L $CaCl_2$. The total cell concentration and spore concentration were determined for the cultivation of the *B. subtilis* spore former in the in-house built BioLector. The DOT, fluorescence intensity, total cell concentration, spore concentration, and sporulation efficiency are presented in Figure 4-1.

Both *B. subtilis* strains exhibited similar DOT profiles with all tested $CaCl_2$ concentrations (without the addition of $CaCl_2$, with the addition of 0.2 g/L $CaCl_2$, and with the addition of 1.0 g/L $CaCl_2$) (Figure 4-1A). A rapid decrease of the DOT was observed from the beginning of the cultivations until about 2 h of cultivation, resulting in a DOT minimum of approximately 0 % for around 1.5 h. A second minimum was observed in the further course of the cultivations, which differed in the level for the two strains. The DOT of the spore former reached a second minimum of approximately 0 % after 7.5 h, whereas the DOT of the knockout strain had a minimum of about 25 % after 7 h. As expected, the fluorescence signal of the knockout strain did not show an increase in intensity for all $CaCl_2$ concentrations (Figure 4-1B). In contrast, in the cultivation without addition of $CaCl_2$, the fluorescence intensity of the spore former increased rapidly from about 30 h onwards until a plateau was reached after approximately 55 h. In the cultivations with 0.2 g/L and 1.0 g/L $CaCl_2$, a 3.5- to 4.0-fold lower fluorescence intensity was observed for both experiments, after 71 h of cultivation, than for the cultivation without the addition of $CaCl_2$. It was astonishing that the addition of 0.2 g/L and 1.0 g/L $CaCl_2$ reduced the total cell concentration of the spore former 4.6- and 3.2-fold, respectively, compared to the cultivation without the addition of $CaCl_2$ (Figure 4-1C), even though the DOT was comparable. The addition of $CaCl_2$ did not increase the spore concentration and sporulation efficiency. In contrast, the spore concentration was 12- and 17-fold lower in the cultivations with the addition of 0.2 g/L and 1.0 g/L $CaCl_2$, respectively, than in the cultivation without the addition of $CaCl_2$. The sporulation efficiency was only approximately 5 % in the cultivations with the addition of 0.2 g/L and 1.0 g/L $CaCl_2$ compared to about 17 % in the cultivation without the addition of $CaCl_2$.

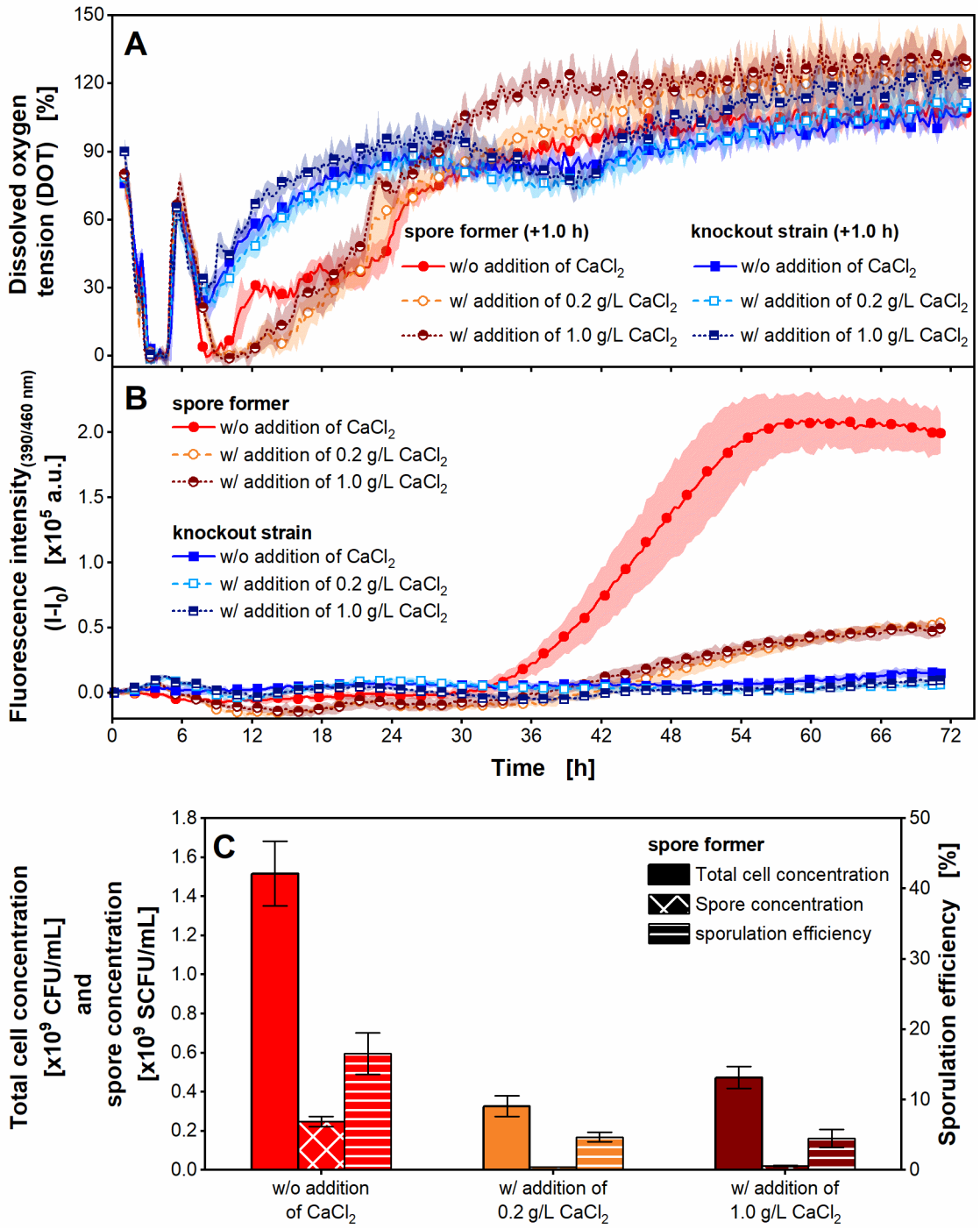

Figure 4-1: Cultivation of *Bacillus subtilis* PY79 spore former and KO7-S knockout strain in Bc medium with various calcium concentrations.

(A) Dissolved oxygen tension (DOT) measured in a commercial BioLector I device (Beckman Coulter GmbH), **(B)** fluorescence intensity with an excitation wavelength of 390 nm and an emission wavelength of 460 nm measured in an in-house built BioLector device [72, 75, 76], **(C)** total cell concentration, spore concentration, and sporulation efficiency. **(A), (B)** For clarity, only every 10th and 5th measuring point over time is marked by a symbol for DOT and fluorescence intensity, respectively. Mean values for DOT and fluorescence intensity of four replicates with standard deviations as shadows are shown. **(A)** The DOT was corrected as described in Appendix

Section A1. The DOT of the cultivation without addition of calcium for both strains is also shown in Appendix Figure A24. **(B)** The initial intensity was subtracted from the measured intensities over time ($I-I_0$) for each experiment. **(C)** Total cell concentration, spore concentration, and sporulation efficiency of one replicate (well) of the spore former for each $CaCl_2$ concentration after 71 h of cultivation in the in-house built BioLector were determined in quadruplicates. Mean values with standard deviations depicted as error bars are shown. CFU: colony forming unit, SCFU: spore colony forming unit. Cultivation conditions: temperature 37 °C, 48-round well plate (MTP-R48-BOH 1 in commercial BioLector I, MTP-R48-B in in-house built BioLector), filling volume 0.7 mL, shaking frequency 1000 rpm, shaking diameter 3 mm, Bc medium with 10 g/L glucose w/o addition of $CaCl_2$ or with addition of 0.2 g/L $CaCl_2$ (≙ 0.07 g/L Ca^{2+}) or 1.0 g/L $CaCl_2$ (≙ 0.36 g/L Ca^{2+}).

The DOT and fluorescence intensity in the cultivations of the *B. subtilis* spore former and knockout strain in Bc medium without the addition of $CaCl_2$ were comparable to the cultivations shown in Figure 3-1 and Figure 3-3 of chapter 3.3.1 and chapter 3.3.2. As suspected from the microscopic images in Figure 3-3B of chapter 3.3.2, the sporulation efficiency of the spore former after 71 h of cultivation in Bc medium was low (17 %) (Figure 4-1C) compared to sporulation efficiencies achieved in other complex media described in the literature [104, 221]. Widderich et al. observed a sporulation efficiency of about 90 % for *B. subtilis* JH642 in Difco Sporulation Medium (DSM) [221]. Tian et al. reported sporulation efficiencies of more than 80 % for *B. subtilis* BSNK-5 in optimized complex media formulations starting from LB medium [104].

For the *B. subtilis* spore former, a decrease in the total cell concentration while increasing the $CaCl_2$ concentration was detected (Figure 4-1C). Such an observation was also made for *B. coagulans* by Cho et al. [224]. It is noticeable that the DOT of the *B. subtilis* spore former was comparable despite the different total cell concentrations at varying $CaCl_2$ concentrations (Figure 4-1A and C). The cells were probably not viable anymore at higher $CaCl_2$ concentrations, and therefore, fewer colonies grew on the agar plates. The addition of $CaCl_2$ (addition of 0.07 g/L calcium and 0.36 g/L calcium) did not result in higher spore concentrations and sporulation efficiencies (Figure 4-1C). Monteiro et al. showed that up to a concentration of 0.6 g/L calcium within a tested range of 0.4 g/L to 1.2 g/L in a chemically defined medium, spore concentrations of a *B. subtilis* strain were increased [110]. Between 0.6 and 1.2 g/L calcium, they observed similar spore concentrations [110]. The total calcium concentration in the complex Bc medium was not determined in the work presented herein. However, as additional calcium did not increase the spore concentration, it is assumed that

there are already enough calcium ions in the complex medium. Furthermore, precipitation can occur at high calcium concentrations, which was observed in the study of Monteiro et al. [110]. Due to the turbidity of the Bc medium, precipitation was not detectable here. The decrease of the spore concentrations and sporulation efficiencies for the *B. subtilis* spore former in cultivations with additional $CaCl_2$ (addition of 0.07 g/L calcium and 0.36 g/L calcium) coincides with the results obtained by Sinnela et al. [108]. In their study, the addition of $CaCl_2$ to a nutrient broth medium resulted in lower spore concentrations for *B. subtilis* KCTC 3135 [108]. A conceivable influencing parameter on decreasing spore concentrations of the *B. subtilis* spore former could be chloride, negatively affecting the sporulation process. However, no studies investigating this in detail were found in literature. Another parameter potentially affecting sporulation of the *B. subtilis* spore former by the addition of $CaCl_2$ is the osmotic pressure. In the past, it was reported that an increase in osmolality results in lower sporulation efficiencies of *B. subtilis* strains [221, 225]. These hypotheses should be investigated in further studies with offline analysis (osmolality) and testing the addition of calcium with other counterions, like $CaSO_4$.

Looking at the fluorescence signal, a correlation is observed between spore concentrations and fluorescence intensity. Increasing the $CaCl_2$ concentration resulted in lower spore concentrations and lower sporulation efficiencies, and thus, in a lower level of fluorescence intensity for the spore former. Even though the spore concentrations could not be increased by increasing the calcium concentration, the applicability of the online sporulation detection method for screening of influence parameters on sporulation is emphasized here.

4.3.2 Influence of oxygen availability on sporulation of *B. subtilis* in shake flaske scale

The influence of the oxygen availability on sporulation was investigated for *B. subtilis* PY79 spore former in shake flasks. A two-stage cultivation protocol, developed by Heyman et al. [79], was applied. Cultivations were performed with different filling volumes (10 mL, 15 mL, 20 mL) in shake flasks under oxygen-unlimited conditions to gain biomass under comparable cultivation conditions. During exponential growth, the shaking frequency was

reduced from 350 to 150 rpm to induce oxygen limitations of different levels for the different filling volumes. Based on the calculation of the theoretical OTR_{max} according to Meier et al. [178] for cultivations in shake flasks with an osmolality of 0.12 osmol/kg in Bc medium, oxygen-limited conditions were expected for the filling volumes of 10 mL, 15 mL, and 20 mL at a shaking frequency of 150 rpm. For each experiment, the total cell and spore concentration were determined at the end of the cultivation. The results are shown in Figure 4-2. For reference, a cultivation with a shaking frequency of 350 rpm over the whole cultivation time is depicted.

The reference cultivation under oxygen-unlimited conditions (Figure 4-2A) had a similar course of the OTR as the cultivation presented in Figure 3-1A of chapter 3.3.1. The steep increase of the OTR was similar for all cultivations (filling volume of 10 mL, 15 mL, 20 mL) until 3.5 h (Figure 4-2A). When the shaking frequency was reduced to 150 rpm after 3.5 h in all cultivations, except in the reference cultivation (shaking frequency not reduced), a decrease in the OTR was followed by a plateau with a lower level for a higher filling volume (Figure 4-2A). This plateau ranged from 31 mmol/L/h for the cultivation with a filling volume of 10 mL to 19 mmol/L/h for the cultivation with a filling volume of 20 mL. The plateau indicates an oxygen limitation [70]. The measured OTR_{max} (average of measured OTR values of the plateau) for the different filling volumes coincided with the theoretical OTR_{max}, calculated after Meier et al. [178]. After the plateau, the OTR rapidly decreased, followed by a slowly gradual decrease until the end of the cultivation. The higher the filling volume was, the later the decrease of the OTR started.

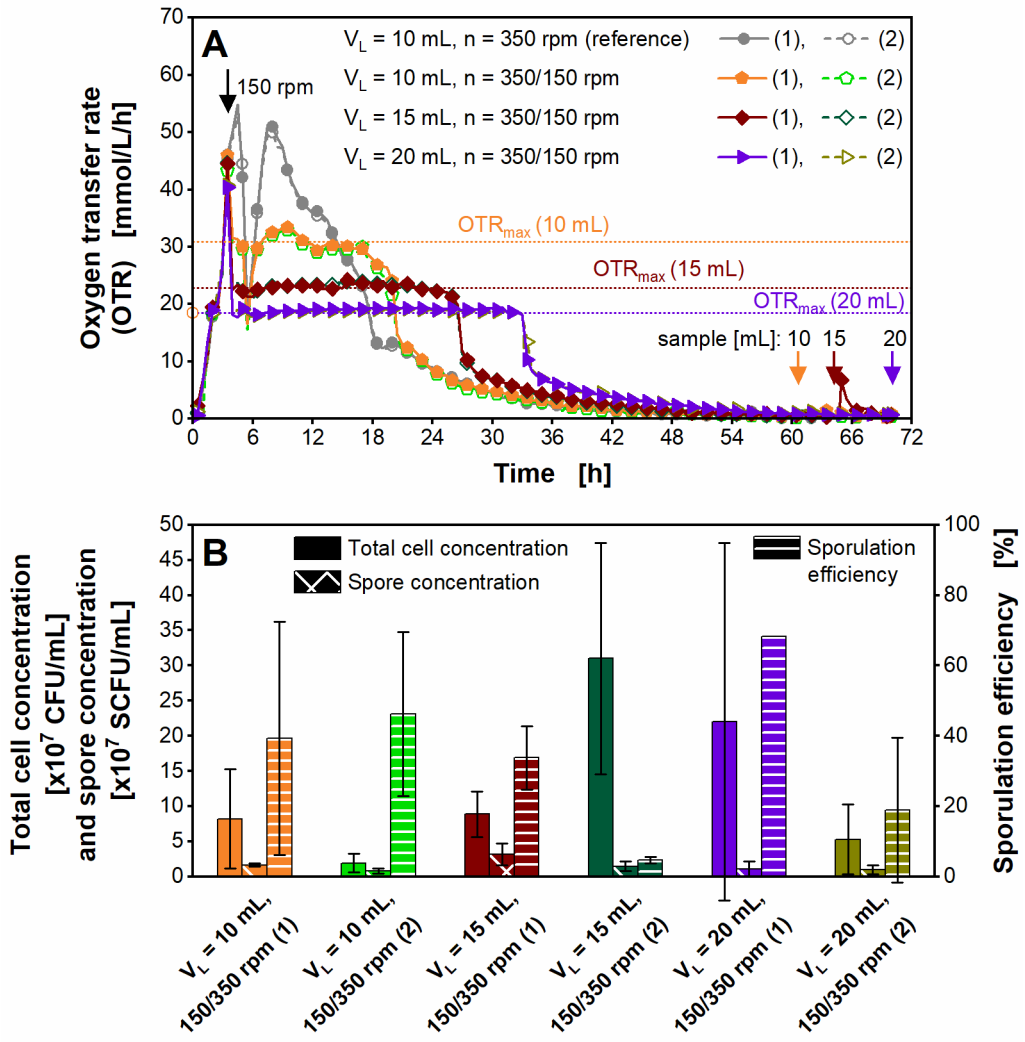

Figure 4-2: Cultivation of *Bacillus subtilis* PY79 spore former under different levels of oxygen limitation in shake flask scale.

(A) Oxygen transfer rate (OTR), **(B)** total cell concentration, spore concentration, and sporulation efficiency. **(A)** For clarity, only every 4th measuring point over time is marked by a symbol for OTR. Duplicates ((1) and (2)) are shown. The theoretical maximum oxygen transfer capacity (OTR_{max}) (horizontal dashed lines) was calculated for the applied cultivation conditions with an osmolality of 0.12 osmol/kg according to Meier et al. [178]. **(B)** For total cell concentration, spore concentration, and sporulation efficiency, mean values of quadruplicates for each shake flask with standard deviations depicted as error bars are shown. The total cell concentration and spore concentration were determined when the OTR was lower than 2 mmol/L/h for 19 to 23 h (time points marked by errors). The standard deviation for the sporulation efficiency of the cultivation with a filling volume of 20 mL (2) is not shown due to large fluctuations of the replicates. CFU: colony forming unit, SCFU: spore colony forming unit. Cultivation conditions in a RAMOS device [70, 71]: temperature 37 °C, 250 mL RAMOS shake flask, filling volume 10 mL, 15 mL, or 20 mL, shaking frequency 350 rpm/ 150 rpm after 3.5 h (marked with arrow), shaking diameter 50 mm, Bc medium with 10 g/L glucose. For comparison, a cultivation in duplicates with a shaking frequency of 350 rpm over the whole cultivation with a filling volume of 10 mL is shown (reference cultivation). This cultivation was conducted in parallel in a second RAMOS device. The OTR of the reference cultivation is also shown in Appendix Figure A24.

The total cell concentration, spore concentration, and sporulation efficiency were determined 19 to 23 h after the OTR was less than 2 mmol/L/h (Figure 4-2B). By this, comparability for the total cell concentration and spore concentration between the different filling volumes was achieved. The results showed large differences in the duplicates for the total cell concentration, spore concentration, and sporulation efficiency. In addition, large error bars were observed. Spore concentrations between $0.9 \cdot 10^7$ SCFU/mL and $3.2 \cdot 10^7$ SCFU/mL were achieved and sporulation efficiencies ranged between 4.8 % and 68.3 %.

No clear conclusions can be made about the influence of the level of oxygen limitation on the spore concentration and sporulation efficiency. This is due to the high variations within the duplicates and high standard deviations for the total cell concentrations and spore concentrations. Therefore, the experiment was repeated in MTP scale using the online spore detection method, presented in chapter 3.

4.3.3 Influence of oxygen availability on sporulation of *B. subtilis* in microtiter plate scale

In the following experiment, the influence of the oxygen availability on the sporulation of *B. subtilis* PY79 spore former was evaluated in MTP scale using the online spore detection method introduced in chapter 3. A cultivation in the MTP was conducted with different filling volumes (0.5 mL to 1.3 mL) with parallel measurement of the OTR and fluorescence intensity with an excitation wavelength of 390 nm and an emission wavelength of 460 nm in a µRAMOS/BioLector combination device. The cultivation was started at 1000 rpm, and the shaking frequency was reduced to 700 rpm at the end of the exponential growth phase. Based on the theoretical OTR_{max} calculation for cultivations in MTPs according to Lattermann et al. [226], oxygen limitations were expected for the different filling volumes at a shaking frequency of 700 rpm. The OTR and fluorescence signal are displayed in Figure 4-3. In addition, the OTR of a reference cultivation with a filling volume of 0.7 mL and a shaking frequency of 1000 rpm over the whole cultivation time is depicted.

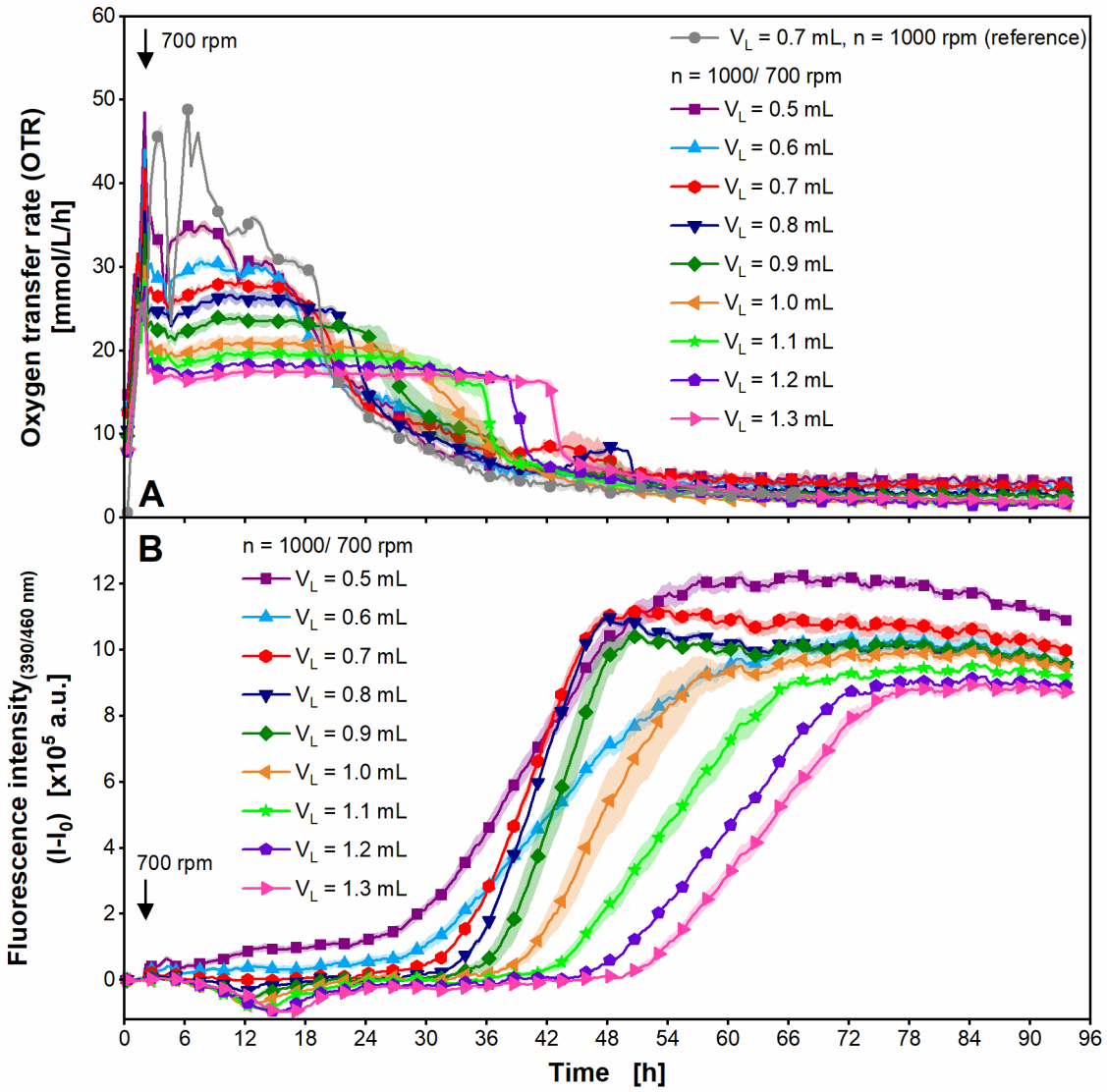

Figure 4-3: Cultivation of *Bacillus subtilis* PY79 spore former under different levels of oxygen limitation in microtiter plate scale by parallel monitoring of the fluorescence intensity.

(A) Oxygen transfer rate (OTR), **(B)** fluorescence intensity with an excitation wavelength of 390 nm and an emission wavelength of 460 nm. **(A), (B)** For clarity, only every 10th measuring point over time is marked by a symbol. Mean values of at least three replicates with standard deviations as shadows are shown. For the cultivation with a filling volume of 1.2 mL, no standard deviations are shown, as a mean value of a duplicate was calculated. **(B)** The initial intensity was subtracted from the measured intensities over time ($I-I_0$) for each filling volume. Cultivation conditions in a µRAMOS/BioLector combination device [77]: temperature 37 °C, 48-round well plate (MTP-R48-B), filling volume 0.5-1.3 mL, shaking frequency 1000 rpm/ 700 rpm after 2.1 h (marked with arrow), shaking diameter 3 mm, Bc medium with 10 g/L glucose. For comparison, a cultivation with a shaking frequency of 1000 rpm over the whole cultivation with a filling volume of 0.7 mL is shown (reference cultivation). This cultivation was conducted in another experiment with another pre-culture in the µRAMOS/BioLector combination device.

The cultivation of the spore former in the MTP with a filling volume of 0.7 mL and a shaking frequency of 1000 rpm (reference cultivation) over the whole cultivation time in the µRAMOS/BioLector combination device (Figure 4-3A, peaks are depicted more clearly in Appendix Figure A32B) showed three OTR peaks at about 26 mmol/L/h after 1.5 h, at about 46 mmol/L/h after 3.5 h and at about 49 mmol/L/h after 6.5 h. This OTR profile is comparable to the OTR profile of the cultivation in shake flasks with a filling volume of 10 mL and a shaking frequency of 350 rpm over the whole cultivation time in the RAMOS device (Appendix Figure A32A). In the cultivation with a filling volume of 0.7 mL and a shaking frequency of 1000 rpm over the whole cultivation time in the commercial BioLector I, a plateau for the calculated OTR from the DOT was observed (Appendix Figure A32B), which indicated a short oxygen limitation [70, 77], as described in chapter 3.3.1. This oxygen limitation was not observed in the cultivation in the µRAMOS/BioLector combination device (Appendix Figure A32B).

The OTR of the cultivations with the different filling volumes increased until the shaking frequency was reduced after 2.1 h (Figure 4-3A). After reducing the shaking frequency to 700 rpm, a higher filling volume resulted in a lower OTR plateau, ranging from 32 mmol/L/h for a filling volume of 0.5 mL to 17 mmol/L/h for a filling volume of 1.3 mL. Those OTR plateaus indicate oxygen limitations [70, 77]. The measured OTR_{max} (average of measured OTR values of the plateau) for the respective filling volume was on average 23 % higher than the theoretical OTR_{max}, calculated according to Lattermann et al. [226] (Appendix Figure A33). One parameter influencing the OTR_{max} is the osmolality of the medium [178], which is not taken into account in the calculation of the OTR_{max} according to Lattermann et al. [226]. This, most likely, explains the deviation of the measured OTR_{max} values from the theoretical values. The length of the plateau was greater, the lower the level of the plateau was. The OTR decreased slightly during the plateau in the cultivation with a filling volume of 0.5 mL.

The fluorescence intensity was almost constant during the first hours of the cultivation for all filling volumes (Figure 4-3B). Then, the fluorescence intensity increased. The time point of the start of the increase differed for the different filling volumes. An earlier increase in the fluorescence intensity was observed for the cultivations with lower filling volumes. The

increase in the fluorescence intensity always started after the OTR started to decrease at the end of the plateau (Figure 4-3A). Exemplarily, in the cultivation with a filling volume of 0.7 mL, the OTR started to decrease at approximately 18 h and the fluorescence intensity started to increase at approximately 33 h (Appendix Figure A31 shows an example of one replicate of the cultivation with a filling volume of 0.7 mL for determination of the time points). The decrease in the OTR can be attributed to the depletion of the available carbon sources [68, 227]. After the increase in the fluorescence intensity, an almost constant level of the fluorescence maximum was achieved. In general, it can be noted that the cultivations with lower filling volumes had a higher maximum fluorescence intensity than the cultivations with higher filling volumes. For example, the cultivation with a filling volume of 1.3 mL had a 1.1-fold lower fluorescence plateau than that of 0.6 mL. Figure 4-3B shows that the slope of the fluorescence increase varies for the different filling volumes. Therefore, the slope was determined (Appendix Figure A34) and plotted against the filling volume (Appendix Figure A35). However, there is no clear correlation between the slope of the fluorescence increase and the filling volume visible.

As described in chapter 3, the increase in the fluorescence signal is correlated to the release of spores from the mother cells and related cell lysis. Further, the fluorescence is most probably traced back to siderophore production. In Figure 4-3B, the maximum fluorescence intensity was, in general, lower for higher filling volumes, thus for a higher level of oxygen limitation. This effect indicates a lower spore concentration for higher levels of oxygen limitation. In addition, it is assumed that a lower siderophore production took place. However, it cannot be completely excluded that different biomass concentrations at the time point of the reduction of the shaking frequency caused the different fluorescence levels. At this time point, the level of the OTR curves differed for the different filling volumes (see the beginning of the cultivation in Appendix Figure A36). To verify the results, a further experiment with higher shaking frequencies at the beginning of the cultivation and an earlier reduction of the shaking frequency is proposed. This could allow comparable OTR levels at the time point of reducing the shaking frequency. In previous reports, the influence of oxygen on sporulation in fermenter scale was evaluated for *Bacillus* strains [111-114]. The authors applied different cultivation strategies [111-114]. The results of those reports and the MTP experiment with the *B. subtilis* PY79 spore former in this study show that the influence of

oxygen availability on sporulation is a complex issue. Depending on the *Bacillus* species and siderophore, different correlations have been published for siderophore production and oxygen supply. For *B. anthracis*, it was reported that more petrobactin was produced in an iron-depleted medium with a high oxygen supply compared to a low oxygen supply [228]. For bacillibactin of *B. anthracis*, a higher production was observed in an iron-depleted medium with a low oxygen supply than with a high oxygen supply [228]. An enhancement of siderophore production by *B. megaterium* under agitated conditions in shake flasks compared to static conditions was reported by Santos et al. [200]. *B. megaterium* is known to produce schizokinen [229]. Overall, the applicability of the fluorescence measurement to investigate the influence of oxygen availability on the sporulation of *B. subtilis* was shown in this study.

Based on the different time points of the start of the increase in the fluorescence intensity (Figure 4-3), it is concluded that the time point of the release of spores varied. The higher the filling volume was, the later the release of spores started. This can be traced back to a prolonged cultivation time due to the higher level of oxygen limitation. The increase in the fluorescence intensity was observed after the OTR started to decrease behind the end of the plateau. Therefore, it was investigated whether there was a correlation between the time points of the decrease in the OTR and the increase in the fluorescence intensity. The time point of the start of the increase in the fluorescence intensity was plotted against the time point of the start of the decrease in the OTR in Figure 4-4.

The cultivation with a filling volume of 0.5 mL was excluded from the regression since the plateau was not completely constant (Figure 4-3). The results show a linear correlation between the start of the decrease in the OTR and the increase in the fluorescence intensity (Figure 4-4). Therefore, it is possible to predict the time point of the release of spores from the mother cells based on the decrease in the OTR under oxygen-limited conditions. To support this approach, further experiments with different cultivation conditions should be conducted to investigate the correlations between the start of the decrease in the OTR and the increase in the fluorescence intensity.

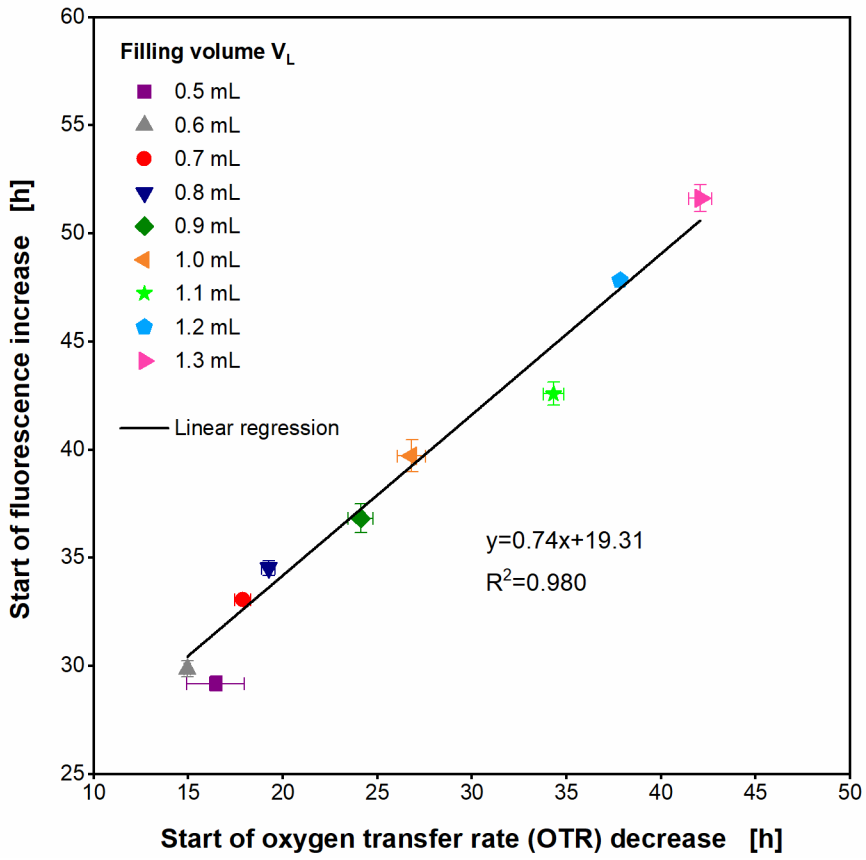

Figure 4-4: Correlation of start of the increase in fluorescence intensity and start of the decrease in oxygen transfer rate in oxygen-limited cultivations of *Bacillus subtilis* PY79 spore former in microtiter plate scale.

The start of the decrease in the oxygen transfer rate (OTR) and the increase in the fluorescence intensity was determined based on the cultivations shown in Figure 4-3. The time points were determined for each replicate (wells) for all filling volumes and mean values were calculated for each filling volume. The standard deviations are presented as error bars. For the cultivation with a filling volume of 1.2 mL, no standard deviations are shown, as a mean value of a duplicate was calculated. A linear regression was conducted for all time points excluding the cultivation with a filling volume of 0.5 mL. The determination of the time points of the start of the decrease in the OTR and the increase in the fluorescence intensity is shown in Appendix Figure A31, exemplarily for one well of the cultivation with a filling volume of 0.7 mL.

4.4 Conclusion

In this chapter, influence parameters on the sporulation of *B. subtilis* PY79 were investigated. Therefore, the plating technique and the measurement of the fluorescence intensity at an excitation wavelength of 390 nm and an emission wavelength of 460 nm were

applied. The medium component calcium and the oxygen supply were chosen as model parameters.

The increase of the $CaCl_2$ concentration in complex Bc medium did not increase the spore concentration and sporulation efficiency of the *B. subtilis* spore former. This demonstrated that the $CaCl_2$ concentration in the Bc medium was already sufficient for sporulation. Interestingly, spore concentrations and sporulation efficiencies decreased with higher $CaCl_2$ concentrations. A negative influence of chloride, the counter ion of the salt added, or an increased osmotic pressure was suspected.

The second parameter was the oxygen availability. A preliminary experiment in shake flasks did not allow any conclusions to be drawn due to the high standard deviations for spore concentrations. Therefore, in MTP scale, different levels of oxygen limitations were set based on different filling volumes in a two-stage cultivation protocol. Higher levels of oxygen limitation indicated a lower plateau of fluorescence intensity and thus, likely, a lower spore concentration.

The spore detection method using fluorescence measurement was applied for both tested parameters. The lower spore concentrations, determined based on the plating technique, with higher $CaCl_2$ concentrations coincided with a lower fluorescence intensity. In addition, conclusions were drawn on the influence of oxygen availability on the sporulation, based on the measured fluorescence intensity. Thus, the application of the online spore detection method for investigating influence parameters on sporulation in the complex medium was shown. The measurement of the fluorescence intensity is a promising tool for screening experiments in small-scale to better understand parameters influencing the sporulation and to optimize industrial processes.

A linear correlation of the start of the decrease in the OTR and the increase in the fluorescence intensity was observed in oxygen-limited cultivations. This correlation is a promosing step, which can be used in future experiments to derive the time point of spore release based on OTR measurement.

Contributions to chapter 5:

Jennifer Goldmanns wrote the chapter, prepared the figures, and designed and performed the experiments. Patrick Schminder assisted with the experiments presented in chapter 5.3 (AVT – Biochemical Engineering, RWTH Aachen University, Aachen, Germany).

5 Application of online spectroscopic techniques for detection of *Bacillus* spores in cultivations with a chemically defined medium

5.1 Introduction

Various complex media have been applied and optimized, for efficient spore production processes with *Bacillus* species in the past [104, 106, 114, 211, 230]. However, as described in chapter 2.1, a disadvantage of complex media worth highlighting is the fluctuating composition of complex components, leading to an inconsistent fermentation performance [96-98]. In contrast, chemically defined media can ensure a reproducible sporulation process and a reproducible sporulation onset. For example, de Vries et al. achieved synchronous sporulation of *B. cereus* in an airlift fermenter system using a chemically defined medium [231]. In addition, by adding nutrients in the desired and known concentrations, a higher control on the sporulation process can be achieved. By applying chemically defined media, parameters influencing sporulation can be investigated precisely. On the downside, applying chemically defined media often results in low spore concentrations and sporulation efficiencies [110, 232]. Therefore, optimization of those media is necessary. For example, Monteiro et al. observed 3.5- to 10-fold lower spore concentrations in different chemically defined media compared to the complex DSM [110]. The authors then optimized the best-performing chemically defined medium by investigating the carbon and nitrogen source and nutrients like calcium and vitamins. They reported a higher spore concentration in the optimized chemically defined medium compared to the DSM [110].

For studies investigating the influence of medium components on sporulation, spore concentrations are usually determined using laborious and time-intensive conventional methods, like agar-plating [110, 232]. These methods require sampling and only provide end-point measurements. To ensure a fast and reliable method to optimize chemically defined media regarding sporulation, online detection methods are of high interest. In this chapter, the application of the online spore detection method, presented in chapter 3, was investigated in cultivations of *B. subtilis* in a chemically defined medium. This online detection method uses fluorescence measurement with an excitation wavelength of 390 nm and an emission wavelength of 460 nm in MTP scale. In addition, in this chapter, it was evaluated whether a correlation between scattered light intensity and sporulation in chemically defined medium can be observed.

5.2 Materials and Methods

5.2.1 Microbial strains

Cultivations were conducted with *B. subtilis* PY79 (spore former) and *B. subtilis* KO7-S (knockout strain). Further information about the strains can be found in chapter 3.2.1.

5.2.2 Cultivation media

For pre-cultures, the LB medium listed in chapter 3.2.2 was applied. Main-cultures were conducted in the chemically defined complete modified Poolman medium after Müller et al. [68]. The composition is listed in Table 5-1.

Table 5-1: Composition of the chemically defined complete modified Poolman medium for main-cultures.

The letters in brackets (a-d) indicate which components were prepared together in a stock solution.

Ingredients		Concentration in complete modified Poolman medium [g/L]	Ingredients		Concentration in complete modified Poolman medium [g/L]
Main components			L-Isoleucine		0.21
Glucose		10	L-Leucine		0.475
Sodium acetate		1	L-Lysine		0.44
$(NH_4)_2SO_4$		7.49	L-Methionine		0.125
$MgCl_2 \cdot 6\ H_2O$		0.427	L-Phenylalanine		0.275
K_2HPO_4		1.7	L-Proline		0.675
MOPS buffer		20.93	L-Serine		0.34
Vitamins			L-Threonine		0.225
Ascorbic acid		0.5	L-Tryptophane		0.05
Biotin		0.002	L-Tyrosine		0.25
Nicotinic acid	(a)	0.0011	L-Valine		0.325
Calcium D-(+)-pantothenate	(a)	0.001	**Nucleobases/ -sides**		
p-Aminobenzoic acid	(a)	0.01	Adenine		0.01
Pyridoxamine 2HCl	(a)	0.006	Guanine		0.01
Pyridoxine HCl	(a)	0.002	Inosine		0.005
Vitamin B12	(a)	0.001	Xanthine		0.01
Thiamin HCl	(a)	0.001	Thymidine		0.005
Riboflavin		0.001	Uracil		0.01
Orotic acid		0.005	**Trace elements**		
Folic acid		0.001	$ZnSO_4 \cdot 7\ H_2O$	(b)	0.009
Amino acids			$CoSO_4 \cdot 7\ H_2O$	(b)	0.004
L-Alanine		0.24	$CuSO_4 \cdot 5\ H_2O$	(b)	0.004
L-Arginine		0.125	$(NH_4)_6Mo_7O_{24} \cdot 4\ H_2O$	(b)	0.003
L-Aspartic acid		0.42	$CaCl_2 \cdot 2\ H_2O$	(c)	0.066
L-Cysteine		0.13	$MnCl_2$	(c)	0.016
(S)-(+)-Glutamic acid		0.5	$FeCl_2$	(d)	0.005
L-Glycine		0.175	$FeCl_3 \cdot 6\ H_2O$	(d)	0.005
L-Histidine		0.15			

The $(NH_4)_2SO_4$, $MgCl_2$, and K_2HPO_4 stock solutions were autoclaved for 60 min at 121 °C. All other solutions were sterilized by filtration (0.2 µm). Before filtration, the pH of the 3-(*N*-morpholino)propanesulfonic acid (MOPS) buffer was adjusted to 8.1 with a 5 M NaOH solution. Since not all individual amino acids, vitamins, and nucleobases /-sides were soluble

in water, the pH of those components was adjusted with KOH or HCl. Aliquots of the iron stock solution were frozen at -20°C. The final complete modified Poolman medium was prepared immediately before the experiment. All stock solutions except the K_2HPO_4 stock solution were combined, and the pH was adjusted to 8.1 with 5 M NaOH and 40 % (w/w) H_3PO_4 solutions. After that, the K_2HPO_4 stock solution was added.

5.2.3 Cultivation conditions

The cultivation protocol used in this study for pre-cultures in shake flasks and main-cultures in MTPs is described in chapter 3.2.3.

5.2.4 Online monitoring techniques

Pre-cultures were conducted in shake flasks in a RAMOS device [70, 71] as described in chapter 3.2.4. For main-cultures in MTPs, the DOT was measured in a commercial BioLector I device (Beckman Coulter GmbH, Krefeld, Germany). Correction of the DOT was conducted as described in Appendix Section A1. In addition, scattered light intensity at a wavelength of 620 nm (gain = 20) was monitored in this device. MTPs with optodes (MTP-R48-BOH1, Beckman Coulter GmbH, Krefeld, Germany) were applied. The fluorescence intensity was detected at an excitation wavelength of 390 nm and an emission wavelength of 460 nm in an in-house built BioLector device [72, 75, 76] coupled to a Fluoromax-4-spectrometer (HORIBA Jobin-Yvon GmbH, Bernsheim, Germany) in MTPs without optodes (MTP-R48-B, Beckman Coulter GmbH, Krefeld, Germany). The fluorescence intensity was measured with a split width of 8 nm and an integration time of 600 ms. LabView software developed by ZUMOLab GmbH (Wesseling, Germany) was used for recording fluorescence data over cultivation time. An in-house built µRAMOS device [73] was used to measure the OTR in each well of a 48-round well MTP without optodes (MTP-R-48-B, Beckman Coulter GmbH, Krefeld, Germany), sealed with a gas-permeable sealing foil (900371-T, HJ-Bioanalytik GmbH, Erkelenz, Germany).

5.2.5 Recording of 2D fluorescence spectra

2D fluorescence spectra of pure cultivation medium, inoculated cultivation medium, and culture broth at the end of the cultivation were recorded using set up of the in-house built BioLector [72, 75, 76] coupled to a Fluoromax-4-spectrometer (HORIBA Jobin-Yvon GmbH, Bernsheim, Germany) as described in chapter 3.2.5.

5.2.6 Microscopic images

Microscopy was conducted as described in chapter 3.2.7.

5.2.7 Calculation of oxygen transfer rate from dissolved oxygen tension

The OTR was calculated from the DOT, measured in the commercial BioLector (after correction as described in Appendix Section A1), as described in Appendix Section A2. Therefore, equation 5 was applied. The oxygen solubility L_{O2} was calculated based on literature [233-235]. The medium components of the complete modified Poolman medium, for which the ion-specific parameters and parameters for organic components are listed in Weisenberger and Schumpe [234] and Rischbieter et al. [235], were considered for the calculation of L_{O2} calculation. The k_La was determined in a cultivation with complex Bc medium (Appendix Figure A23) (194 1/h) and was used for OTR calculations in the chemically defined medium. Thus, the calculated OTR is considered as an approximation.

5.3 Results and Discussion

5.3.1 Cultivation of *Bacillus subtilis* in a chemically defined medium

To transfer the online monitoring method for spore detection, presented in chapter 3, to a chemically defined medium, the complete modified Poolman medium after Müller et al. [68]

was used. The *B. subtilis* PY79 spore former and *B. subtilis* KO7-S strain with a genetic knockout in sporulation were cultivated in this medium in a MTP. First, the cultivation behavior in the medium was characterized. Therefore, the DOT was monitored over cultivation time in a commercial BioLector I device. The OTR was determined over cultivation time in a μRAMOS device in a separate cultivation with a separate pre-culture. The results are presented in Figure 5-1.

The DOT of both *B. subtilis* strains (Figure 5-1A) decreased from the beginning of the cultivation. A minimum of 14 % for the spore former and 25 % for the knockout strain was achieved after 2.5 h. After a short increase in the DOT, it reached almost zero between 3 h and 5 h for both strains, followed by an abrupt DOT increase to 88 % at 5 h cultivation time. The DOT started to decrease for both strains after 6 h. In the cultivation with the spore former, a local minimum of 23 % after 10 h was achieved, and in the cultivation with the knockout strain, a local minimum of 25 % after 9.5 h was reached. The subsequent slow DOT increase was interrupted by two local minima of 34 % after 14 h and 50 % after 18 h for the spore former. The DOT increase of the knockout strain was interrupted by two local minima of 37 % after 11.5 h and 59 % after 15 h.

The OTR calculated from the DOT (Figure 5-1A) mirrored the course to the DOT. The DOT minima were represented as OTR maxima. Between 3 and 5 h, a plateau of 41 mmol/L/h was achieved for both strains. For the spore former, a local maximum of 35 mmol/L/h after 2.5 h, of 32 mmol/L/h after 10 h, of 27 mmol/L/h after 14 h and of 21 mmol/L/h after 18 h was observed. The knockout strain reached a local maximum of 31 mmol/L/h after 2.5 h, of 31 mmol/L/h after 9.5 h, of 26 mmol/L/h after 11.5 h and of 17 mmol/L/h after 15 h.

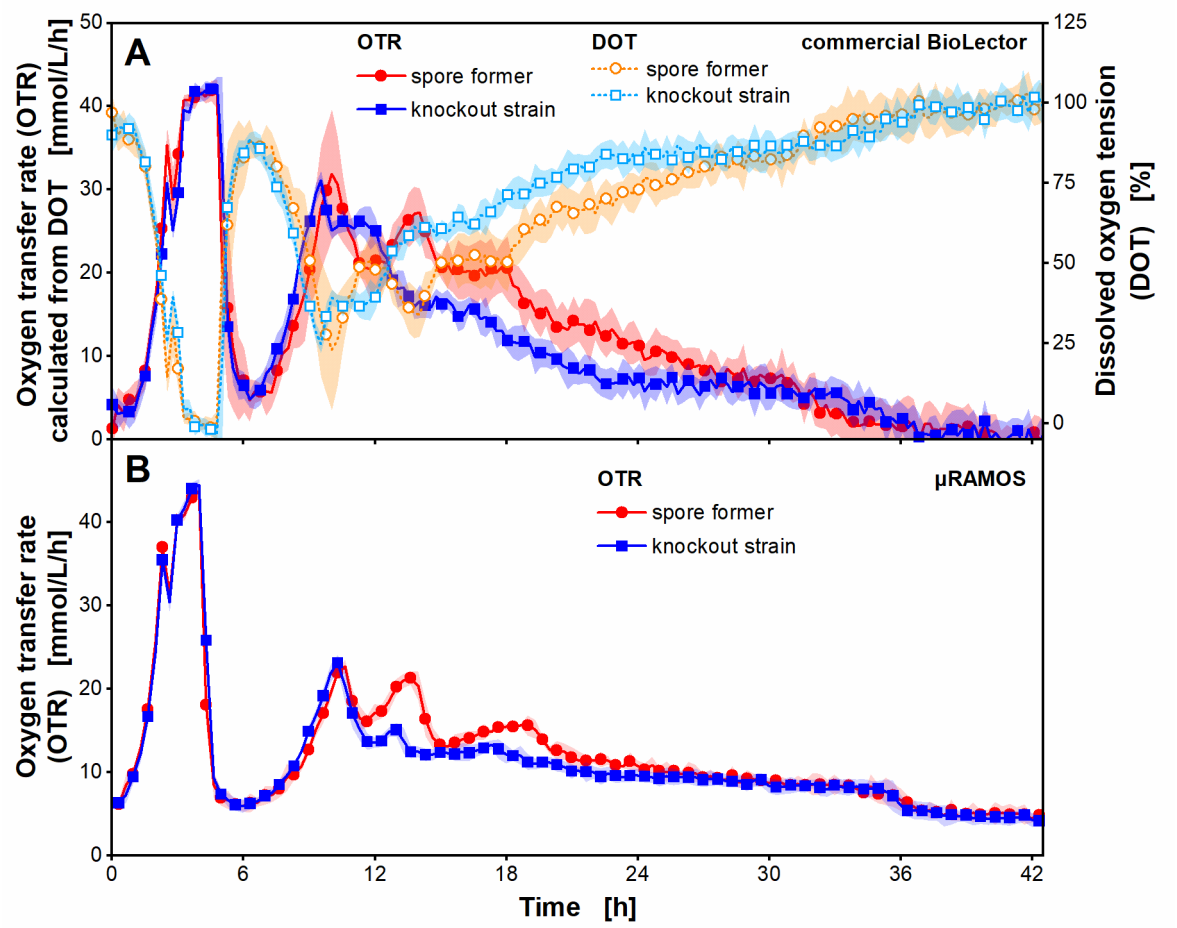

Figure 5-1: Cultivation of *Bacillus subtilis* PY79 spore former and KO7-S knockout strain in chemically defined complete modified Poolman medium in microtiter plate scale.

(A) Dissolved oxygen tension (DOT) and oxygen transfer rate (OTR) in a commercial BioLector I device (Beckman Coulter GmbH), **(B)** OTR in an in-house built µRAMOS device [73]. For clarity, only every 4th **(A)** and 3rd **(B)** measuring point over time is marked by a symbol. Mean values of eight **(A)** and three **(B)** replicates with standard deviations as shadows are shown. The DOT in **(A)** was corrected as described in Appendix Section A1. The OTR in **(A)** was calculated from the corrected DOT as described in chapter 5.2.7 with a volumetric oxygen transfer coefficient (k_La) value of 194 1/h (value was determined based on a cultivation in complex Bc medium). Cultivation conditions: temperature 37 °C, 48-round well plate (MTP-R48-BOH 1 in commercial BioLector I, MTP-R48-B in µRAMOS), filling volume 0.7 mL, shaking frequency 1000 rpm, shaking diameter 3 mm, complete modified Poolman medium with 10 g/L glucose. The cultivations in **(A)** and **(B)** were conducted with separate pre-cultures.

The OTR of the spore former and knockout strain, determined in the µRAMOS (Figure 5-1B), increased rapidly to 40 mmol/L/h until a cultivation time of 3 h. The fast OTR increase was interrupted by a peak of approximately 36 mmol/L/h after 2 h. Between 3 h and 4 h, a slight increase to a maximum of 45 mmoL/L/h was observed. A sharp OTR decrease to 6 mmol/L/h between 4 h and 6 h was observed for both strains. The following course of

the OTR showed three local OTR maxima. The first was similar for both strains with an OTR of 23 mmol/L/h after 10.5 h. The following two local maxima differed for the two strains. The spore former reached a maximum of 21 mmol/L/h after 13.5 h and of 16 mmol/L/h after 19 h. The knockout strain exhibited a maximum of 15 mmol//L/h after 13 h and of 13 mmol/L/h after 17 h. After the maxima were reached, the OTR decreased slowly for both strains until the end of the cultivation.

The OTR calculated from the DOT measured in the commercial BioLector (Figure 5-1A) and the OTR determined in the µRAMOS (Figure 5-1B) showed comparable profiles. Only slight deviations in the height of the maxima between 9 h and the end of the cultivation were observed. The slow OTR increase before reaching the maximum of 45 mmol/L/h could indicate a slight short oxygen limitation between 3 h and 4 h in the cultivation in the µRAMOS. In the cultivation in the BioLector, a more pronounced oxygen limitation, indicated by an OTR plateau [70, 77], between 3 h and 5 h was observed.

The DOT minima and OTR maxima represent the growth of the *B. subtilis* strains on the carbon sources in the complete modified Poolman medium. The highest OTR maximum and lowest DOT minimum at almost zero indicate the consumption of the main carbon source glucose. Consumption of glucose was proven with offline HPLC analysis in the cultivation of *B. pumilus* DSM18097 in complete modified Poolman medium by Müller et al. [68]. The other local OTR maxima and DOT minima between 9 h and 20 h can be connected to the consumption of previously produced overflow metabolites as carbon sources. Müller et al. demonstrated the production of acetoin and acetate by *B. pumilus* in complete modified Poolman medium, which was consumed in the following course of the cultivation [68]. *B. subtilis* strains also produce overflow metabolites [4, 236]. Dauner et al. showed the production of acetate and acetoin in a minimal medium by *B. subtilis* RB50::pRF69 under aerobic carbon-excess conditions [236]. In addition, Nakano et al. reported that under anaerobic conditions, *B. subtilis* JH642 produced acetate, ethanol, lactate, succinate, acetoin, and 2,3-butanediol in a defined medium [4]. Literature describes the consumption of acetoin in a complex medium by *B. subtilis* GD5 in the stationary phase when the preferred carbon source is depleted [237]. Besides the consumption of overflow metabolites, usage of the amino acids present in the complete modified Poolman medium is possible [238, 239].

Finally, the cultivation behavior of the *B. subtilis* spore former and knockout strain were characterized in cultivations with complete modified Poolman medium in MTPs based on DOT and OTR measurement while considering literature. This is the basis for exploring the possibilities of online spore detection in the chemically defined medium using spectroscopic techniques.

5.3.2 Online monitoring of *Bacillus subtilis* sporulation in a chemically defined medium

In chapter 3.3.2, a fluorescence maximum at an excitation wavelength of 390 nm and an emission wavelength of 460 nm was observed in 2D fluorescence difference spectra of the culture broth of the *B. subtilis* spore former after cultivation in complex Bc medium. Therefore, it was investigated whether this fluorescence maximum is also visible after cultivations in the chemically defined complete modified Poolman medium. 2D absolute fluorescence spectra of the culture broth of the *B. subtilis* spore former and knockout strain at the beginning and end of a MTP cultivation were recorded. The difference in fluorescence spectra was calculated (Figure 5-2).

Both, the 2D fluorescence difference spectrum of the spore former (Figure 5-2A) and of the knockout strain (Figure 5-2B) showed a distinct fluorescence maximum at an excitation wavelength of 390 nm and an emission wavelength of 460 nm. The fluorescence intensity of the maximum was 1.3-fold higher for the spore former than for the knockout strain. A 2D fluorescence difference spectrum of the complete modified Poolman medium that was not inoculated did not exhibit a fluorescence maximum at this wavelength combination (Appendix Figure A37).

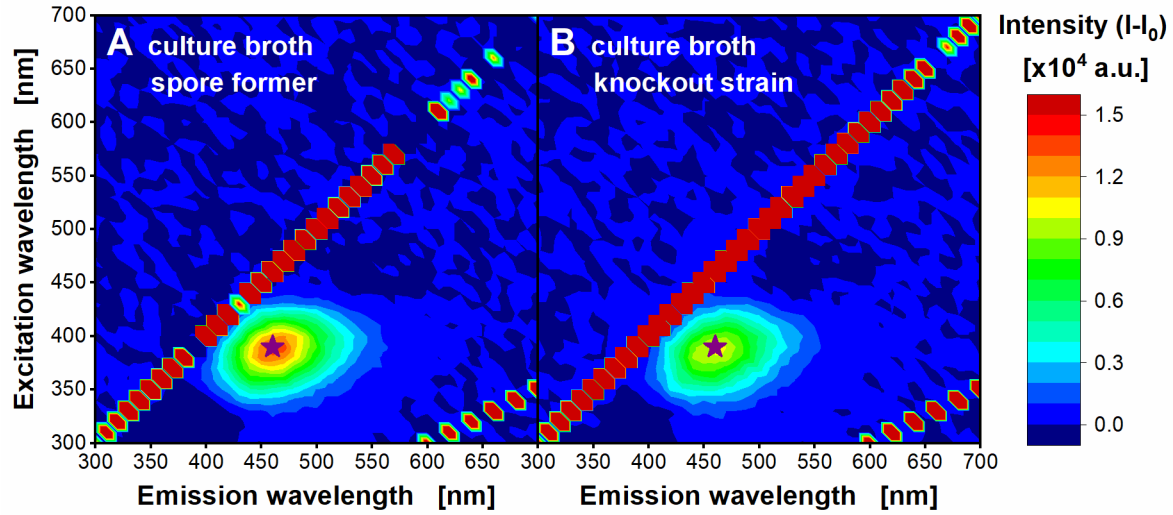

Figure 5-2: Difference of 2D fluorescence spectra of culture broth of *Bacillus subtilis* PY79 spore former and KO7-S knockout strain between the beginning and end of cultivation in complete modified Poolman medium.

(A) Spore former, **(B)** knockout strain. The wavelength combination of the fluorescence maximum ($\lambda_{ex}/\lambda_{em}$) is marked as dark purple star. 2D fluorescence scans with excitation wavelengths from 300-700 nm and emission wavelengths from 300-700 nm were recorded at the beginning of the cultivation and after 40 h of cultivation using the setup of an in-house built BioLector device [72, 75, 76]. Intensities of the 2D fluorescence scan from the beginning of cultivation were subtracted from intensities of the 2D fluorescence scan after 40 h of cultivation ($I-I_0$). Cultivation conditions in the in-house built BioLector device: temperature 37 °C, 48-round well plate (MTP-R48-B), filling volume 0.7 mL, shaking frequency 1000 rpm, shaking diameter 3 mm, complete modified Poolman medium with 10 g/L glucose.

As discussed in chapter 3.3.3, the fluorescence at an excitation wavelength of 390 nm and an emission wavelength of 460 nm is probably caused by a siderophore. Hence, the fluorescence maximum of the *B. subtilis* spore former and knockout strain at this wavelength combination in complete modified Poolman medium indicates that both strains produce siderophores in this medium. In contrast, in Bc medium, the distinct fluorescence maximum was only observed for the *B. subtilis* spore former (5.3-fold lower intensity for the knockout strain than for the spore former) (Figure 3-2 of chapter 3.3.2). Siderophore production is coupled to iron-limiting conditions for several microorganisms [188, 228, 240]. The iron conditions in the complete modified Poolman medium possibly lead to siderophore production for the *B. subtilis* knockout strain as well. The complete modified Poolman medium contains 0.005 g/L $FeCl_2$ (39 µM Fe^{2+}) and 0.005 g/L $FeCl_3 \cdot 6\ H_2O$ (18 µM Fe^{3+}). This corresponds to 0.0001 mol iron/ mol carbon in the complete modified Poolman medium. In contrast, in a previous study, at 0.0001 mol iron/ mol carbon (corresponded to

100 µM Fe^{3+} in the medium) and higher iron concentrations in modified sugar-aspartic acid medium, almost no siderophore production (hydroxamate type siderophore) by *B. subtilis* PZ-1 was observed [241]. The authors suggested that the threshold of the iron concentration at which siderophore production does not take place, is specific for the bacterium and the whole nutrient availability for the bacterium [241]. Further studies are needed to investigate the effect of different iron concentrations in complete modified Poolman medium on the fluorescence intensity of the *B. subtilis* spore former and knockout strain.

In chapter 3.3.2, a correlation between the increase in the fluorescence intensity and the release of spores and lysis of the mother cells was observed in the complex Bc medium. Such correlations were studied for the complete modified Poolman medium by taking microscopic images and monitoring of the fluorescence signal at an excitation wavelength of 390 nm and an emission wavelength of 460 nm in a MTP cultivation of the *B. subtilis* spore former and knockout strain. In addition, the scattered light at 620 nm as a potential spore detection parameter in a chemically defined medium was measured. The online parameters and the microscopic images are presented in Figure 5-3.

The scattered light intensity of the spore former and knockout strain (Figure 5-3A) increased to a maximum until a cultivation time of 5 h. Then, the scattered light intensity decreased until about 7.5 h. At this time point, the scattered light intensity of the spore former was slightly lower than the scattered light intensity of the knockout strain. The scattered light intensity of the knockout strain was characterized by slight increases and decreases until the end of the cultivation. The scattered light of the spore former stayed at almost the same value from 7.5 h cultivation time until the end of the cultivation.

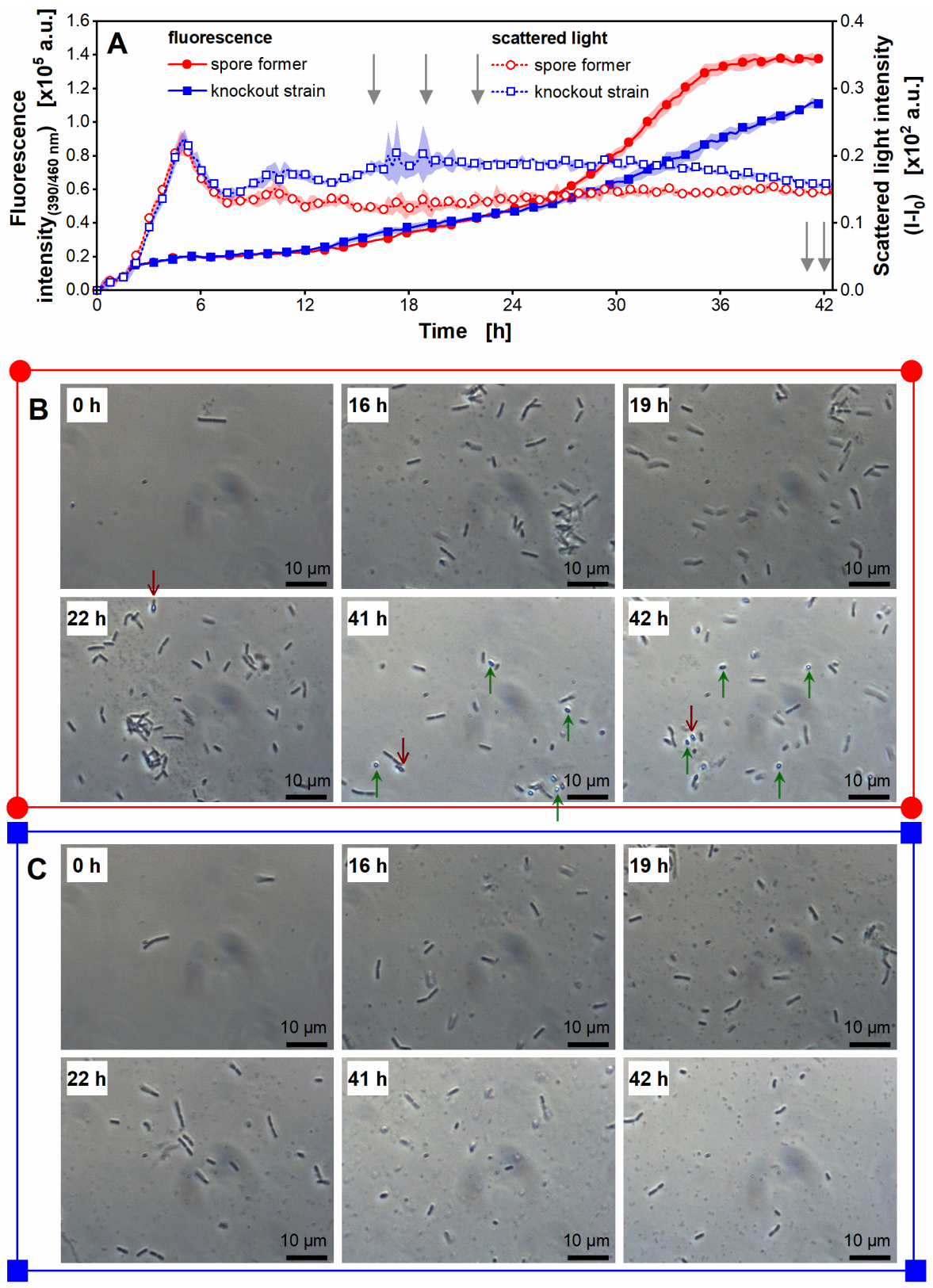

Figure 5-3: Online scattered light and fluorescence measurement of *Bacillus subtilis* PY79 spore former and KO7-S knockout strain in complete modified Poolman medium with microscopic images.

(A) Scattered light intensity at 620 nm in a commercial BioLector I device (Beckman Coulter GmbH) and fluorescence intensity with an excitation wavelength of 390 nm and an emission wavelength of 460 nm in an in-house built BioLector device [72, 75, 76]. For clarity, only every 4th measuring point over time is marked as a symbol. Mean values of eight (scattered light) and four (fluorescence) replicates with standard deviations as shadows are shown. Shaking of the cultivation in the in-house built BioLector was conducted around 2 h before online measurement was started. Therefore, no data points for the first 2 h are available and therefore, no initial intensity (I_0) for fluorescence. For scattered light in the commercial BioLector, initial intensities were subtracted from the measured intensities over time ($I-I_0$). Grey arrows mark the time point of samples. Microscopic images of **(B)** spore former and **(C)** knockout strain over cultivation time with 1000x magnification. **(B), (C)** The color and symbol of the frame of the microscopic images correspond to the symbols and colors in **(A)**. Red arrows pointing downwards show spores inside the mother cells. Green arrows pointing upwards show free spores. Cultivation conditions: temperature 37 °C, 48-round well plate (MTP-R48-BOH 1 in commercial BioLector I, MTP-R48-B in-house built BioLector), filling volume 0.7 mL, shaking frequency 1000 rpm, shaking diameter 3 mm, complete modified Poolman medium with 10 g/L glucose.

The fluorescence intensity (Figure 5-3A) increased over the whole cultivation time for both strains. Until about 12 h of cultivation, only a slight increase (1.6-fold between 2 h and 12 h) was observed. The course of the fluorescence intensity was almost comparable for the spore former and knockout strain until about 24 h. At 24 h, a 3.2-fold higher fluorescence intensity compared to a cultivation time of 2 h was reached for both strains. Then, a stronger increase in fluorescence intensity was observed for the spore former, reaching a plateau at 37 h. The fluorescence intensity of the knockout strain continued to increase almost constantly until the cultivation was stopped. At the end of the cultivation, a 1.2-fold higher fluorescence intensity was achieved for the spore former than for the knockout strain.

The microscopic images were taken at different time points by sampling (Figure 5-3B and C). At the beginning of the cultivation, some rod-shaped vegetative cells were observed for both strains. More rod-shaped cells were shown in microscopic images of both strains at 16 h and 19 h of cultivation. After 22 h of cultivation, the first spores inside the mother cells were seen in the microscopic image together with vegetative cells for the spore former (Figure 5-3B). At the end of the cultivation, the spore former exhibited mainly free spores and vegetative cells. Also some cells with spores inside the mother cells were visible. The knockout strain did not show spores inside mother cells or free spores (Figure 5-3C). In addition, round-shaped cells were not observed in the complete modified Poolman medium, contrary to the complex medium in chapter 3.3.2.

For a better overview, the DOT, OTR, scattered light intensity and fluorescence intensity are shown in one figure in Appendix Figure A38. The increase of the scattered light intensity to a maximum at 5 h cultivation time (Figure 5-3/ Appendix Figure A38), correlated well with the observed DOT level of 0 % and OTR plateau observed between 3 h and 5 h in Figure 5-1/ Appendix Figure A38. Hence, the scattered light measurement shows the growth on the carbon source glucose. However, like in the complex medium, the scattered light did not exhibit a significant difference in intensity for the spore former compared to the knockout strain during the sporulation process of the spore former. Thus, the presented results do not allow conclusions on a correlation between sporulation and scattered light intensity.

Based on the microscopic images, the release of spores from the mother cells took place between 22 h and 42 h in the cultivation of the *B. subtilis* spore former in complete modified Poolman medium. Additional samples are needed to determine a more accurate time frame for the release of spores from the mother cells. For the spore former, a strong increase in the fluorescence intensity was already observed from 12 h on; hence before the release of spores from the mother cells started. This contrasts with the observations in complex medium (chapter 3.3.2). In cultivations of the *B. subtilis* spore former in the complex Bc medium, the increase in the fluorescence intensity, probably caused by siderophores, started parallel to the release of spores from the mother cells and lysis of the mother cells. One hypothesis could be that the increase in the fluorescence intensity in complete modified Poolman medium, from 12 h on, took place during cannibalistic behavior of the *B. subtilis* spore former. *B. subtilis* is known to react with cannibalism to starving conditions to delay sporulation [242, 243]. Cannibalism means that sporulation is arrested by the production of extracellular killing factors, resulting in cell lysis of nonsporulating siblings to obtain nutrients [242, 243]. The distinct increase in the fluorescence intensity in the complete modified Poolman medium started about 7 h after the DOT level was 0 % and the end of the OTR plateau at 5 h was reached (Appendix Figure A38). Hence, the main carbon source glucose is expected to be already consumed during the increase in the fluorescence intensity. The fluorescence increase was parallel to the DOT minima and OTR maxima observed between 9 h and 20 h (Appendix Figure A38). Probably only overflow metabolites and amino acids are available during this time for catabolism. This indicates that starving conditions causing cannibalism were given. Possibly, the increase in the fluorescence

intensity, from 12 h on, of the knockout strain also took place during cannibalistic behavior and related cell lysis of this strain. Cannibalism is conducted by cells that can still resume growth before commitment to sporulation ("point of no return") [242]. Commitment to sporulation is reached after the asymmetric septum formation [244]. The genetic knockout of the knockout strain is in the gene *sigF*. The transcription factor σ^F is formed before septum formation, but becomes active after septum formation [245]. Therefore, the knockout strain might start the sporulation process as the spore former in complete modified Poolman medium, resulting in cannibalistic behavior, before sporulation is stopped due to the knockout in the gene *sigF*.

From 24 h on, a stronger increase in the fluorescence intensity was observed for the spore former than for the knockout strain. This correlates with the release of spores from the mother cells, as between 22 h and 42 h free spores developed for the spore former strain in the complete modified Poolman medium. Further studies are needed to investigate the correlations of cannibalistic behavior, sporulation, and the increase in fluorescence intensity in more detail. More samples should be taken over cultivation time and spore concentrations should be determined for a better overview on the sporulation process. In addition, cell lysis via protein analyses in the supernatant should be investigated. Moreover, the medium composition could be varied to study the effect of different spore concentrations on the increase in the fluorescence intensity (first trial see Appendix Figure A39).

5.4 Conclusion

In this chapter, online detection of *B. subtilis* spores was investigated in a chemically defined medium, termed complete modified Poolman medium. This was conducted with the same *B. subtilis* PY79 spore former and KO7-S knockout strain, which were used for the development of a spore detection method in complex medium in chapter 3.

Online scattered light measurement at 620 nm did not reveal correlations to sporulation. Recording of 2D fluorescence spectra suggested that the spore former and knockout strain produce siderophores in the complete modified Poolman medium, as a maximum at an

excitation wavelength of 390 nm and an emission wavelength of 460 nm was observed for both strains. In contrast to the Bc medium, iron conditions in the complete modified Poolman medium were assumed to be favorable for siderophore production by both strains. Online measurement of the fluorescence intensity of the spore former pointed out that the increase in the fluorescence intensity already started before spores were released from the mother cells. This needs to be investigated in further studies. During the sporulation process, a stronger increase in the fluorescence intensity was detected for the spore former than for the knockout strain. Hence, a correlation between the stronger increase in the fluorescence intensity and the development of free spores and lysis of the mother cells was proposed in the chemically defined medium.

In conclusion, promising results were shown for transferring the spore detection method used for a complex medium to a chemically defined medium. This is the basis for optimizing chemically defined media regarding sporulation in bioprocesses with spore formers. In the future, the correlation of sporulation and the increase in the fluorescence intensity should be investigated in more detail, for example by taking additional microscopic images and determining spore concentrations.

6 Summary and Outlook

Initial bioprocess development of microbial processes requires small-scale shaken cultivation systems for high-throughput screenings. For processes using spore-forming bacteria, a profound understanding of growth performance and sporulation behavior is indispensable. Online monitoring techniques in MTPs are of great interest to achieve this process insight as they allow fast and simple process optimization. Hence, the aim of this thesis was to assess the potential of online monitoring techniques in small-scale cultivations of spore-forming bacteria.

P. polymyxa has been mainly cultivated in complex media up to now [63, 93-95]. However, those media are associated with an inconsistent fermentation performance [96-98]. Chemically defined media, on the other hand, frequently lead to lower growth rates, cell densities and product yields [100-102]. Therefore, medium optimization of chemically defined media is necessary, yet laborious. In chapter 2, a previously reported systematic method involving online monitoring of the OTR [68] was applied and extended to develop a chemically defined medium for an industrially relevant *P. polymyxa* strain. As growth in the chemically defined Moppa medium was low compared to the previously used complex Pbp complex medium, nutrient limitations were identified by systematically increasing the concentration of nutrient groups with parallel monitoring of the respiration activity in the µRAMOS device. MTP experiments showed that nicotinic acid limits the growth of *P. polymyxa* in the Moppa medium. Thus, the concentration was increased to the twelve-fold concentration. In addition, an insufficient buffer capacity was detected. This issue was remedied by increasing the initial pH value from 6.5 to 7.0 to better exploit the MES buffer capacity and by doubling the MES concentration from 0.1 M to 0.2 M. Once the respiration activity in the supplemented Moppa medium was comparable to Pbp complex medium, the Moppa medium components were reduced from 53 to 23 components, resulting in a

comparable number of components as in Pbp complex medium (22). For vitamins, only nicotinic acid and biotin were added to the final medium, and for amino acids, only methionine, histidine, proline, arginine, and glutamate. The addition of nucleobases/-sides was not required for growth. Verification of the online monitoring results was based on offline parameters, like OD, pH, carbon source consumption, and metabolite production. The finally developed medium for *P. polymyxa* was successfully transferred from MTP to laboratory fermenter scale based on respiration activities. During the transfer to the laboratory fermenter, a higher OD was noticed in the fermenter than in the MTP. Differences in pH-control were assumed to be the reason. To verify this assumption, a fermentation without pH-control and with adding MES buffer could be performed as a future experiment. Alternatively, polymer beads, releasing the pH-active agent sodium carbonate, in RAMOS shake flasks [246, 247] could be used to mimic the pH-controlled fermentation conditions. The presented medium development method allows time-efficient optimization of chemically defined media. Through its use in the initial bioprocess development, nutrient limitations, oxygen limitations, and pH-inhibitions can be prevented during scale-up. To investigate the applicability of the developed medium for industrial processes, the next step would be a scale-up to higher fermentation scales.

Spores are often the target product in fermentations with spore-forming bacteria. High cell densities are not the only important factor in such bioprocesses. The characterization of sporulation to achieve high spore concentrations and sporulation efficiencies is also a central aspect. Spore concentrations must be determined when investigating influence parameters on sporulation. Conventional spore counting methods, like agar-plating or microscopy in combination with a counting chamber, are associated with a highly laborious effort [161, 162]. Therefore, online monitoring techniques are of great interest for tracking spore formation over cultivation time. In chapter 3, *B. subtilis* sporulation was monitored with spectroscopic techniques in a complex Bc medium. Contrary to expectations, scattered light measurement using the BioLector showed no conspicuous differences between the *B. subtilis* PY79 spore former and *B. subtilis* KO7-S strain with a genetic knockout in sporulation. Based on 2D fluorescence spectroscopy, a fluorescence maximum at an excitation wavelength of 390 nm and an emission wavelength of 460 nm was identified in the culture broth of the spore-forming *B. subtilis* strain. In contrast, the *B. subtilis* strain with

the knockout in sporulation did not exhibit such a pronounced fluorescence maximum. Online measurement of this fluorescence wavelength combination in a BioLector and sampling for microscopic images revealed a correlation between the increase in the fluorescence intensity and the development of free spores and lysis of the mother cells. The fluorescence maximum was also observed for other spore-forming *Bacillus* species, showing the broad applicability of the spore detection method. The results highlight the potential of spectroscopic online monitoring methods to track sporulation during cultivations non-invasively. The approach in chapter 3 was based on qualitative correlations of fluorescence intensity and spore release. Further studies could focus on quantitatively correlating the fluorescence signal with sporulation. In addition, to demonstrate the applicability of the method on an industrial scale, a novel online-fluorescence probe should be transferred into a fermenter.

Comparing 2D fluorescence difference spectra of the *B. subtilis* spore former pellet and supernatant, the fluorescence was only located in the supernatant. By adding iron to the supernatant of *B. subtilis* spore former culture broth, a decrease in the fluorescence intensity was observed in the 2D fluorescence spectra. This was a strong indication that a siderophore causes the fluorescence. Analytical measurements for structure elucidation, like HPLC/mass spectrometry, are proposed to prove this conclusion. Further, assays quantifying siderophore production should be used to investigate siderophore production during cultivation. By this, potential connections between siderophore production and sporulation could be investigated.

The online spore detection method was applied in chapter 4 for investigating influence parameters on sporulation. Calcium is a relevant element for the heat resistance of *Bacillus* spores [107, 214] and impacts spore concentrations [108-110]. In chapter 4, the influence of the $CaCl_2$ concentration was tested for *B. subtilis* in complex Bc medium in MTPs. Additional $CaCl_2$ in Bc medium in cultivations of the *B. subtilis* spore former did not influence the DOT, but the total cell concentration, spore concentration, and sporulation efficiency were strongly reduced. The reduction of the spore concentration was reflected in a reduced fluorescence intensity level during the BioLector cultivation. To verify whether the reduced spore concentration is due to an increase of osmolality or a negative influence of the chloride, further experiments with offline analysis and the addition of calcium with

other counterions, like $CaSO_4$, are recommended. The other tested influence parameter on sporulation was the oxygen availability. Different levels of oxygen limitation were set at a defined time point by reducing the shaking frequency in MTP cultivations with different filling volumes. The experiment implied that a higher level of oxygen limitation decreased the level of the fluorescence intensity, which suggests a lower spore concentration. To prove this, the spore concentration should be determined via conventional methods. Based on the results of chapter 4, it can be summarized that the method for online detection of sporulation is suited to investigate the parameters influencing sporulation in a time-efficient and reliable manner. In the future, further parameters, like the concentration of the complex components, the pH, and temperature, should be tested using this method to increase spore concentrations and sporulation efficiencies of *B. subtilis* in complex Bc medium.

A linear correlation between the start of the OTR decrease after the plateau and the start of the increase in the fluorescence intensity was observed in oxygen-limited cultures in the µRAMOS/BioLector combination device. This allows conclusions regarding the start of the spore release from the mother cells and related lysis of the mother cells to be drawn from the start of the OTR decrease.

In the last step, the online spore detection method was tested in the chemically defined modified Poolman medium with *B. subtilis* in chapter 5. Both *B. subtilis* strains, the spore former and the knockout strain, exhibited an increase in the fluorescence intensity at an excitation wavelength of 390 nm and an emission wavelength of 460 nm in a MTP cultivation. This indicated that both strains produce siderophores in the complete modified Poolman medium. The increase in the fluorescence intensity for the spore former was observed before spore release took place. However, the spore former exhibited a stronger increase in fluorescence intensity during the sporulation process compared to the knockout strain supporting the hypothesis that the release of spores from the mother cells can be correlated to the stronger increase in the fluorescence intensity. In further steps, more in-depth investigations of the chemically defined medium are needed using the online spore detection method. This means that, for example, spore concentrations should be determined quantitatively via conventional spore detection methods and correlated to the increase in the

fluorescence intensity. Furthermore, the medium composition should be varied to investigate the effect on spore concentrations and online determined fluorescence intensity.

In summary, methods were presented to optimize the growth of spore-forming bacteria by online monitoring of the respiration activity, and sporulation based on online monitoring of the fluorescence intensity. In the future, both methods can be combined for an easy and fast optimization of bioprocesses with spore formers like *Paenibacillus* and *Bacillus* species. This will provide a sound understanding of the processes, simplifying scale-up to industrial cultivation scale.

7 Bibliography

[1] Higgins D, Dworkin J. Recent progress in *Bacillus subtilis* sporulation. FEMS Microbiology Reviews. 2012;36(1):131-48.

[2] Riley EP, Schwarz C, Derman AI, Lopez-Garrido J. Milestones in *Bacillus subtilis* sporulation research. Microbial Cell. 2020;8(1):1-16.

[3] Galperin MY, Mekhedov SL, Puigbo P, Smirnov S, Wolf YI, Rigden DJ. Genomic determinants of sporulation in *Bacilli* and *Clostridia*: towards the minimal set of sporulation-specific genes. Environmental Microbiology. 2012;14(11):2870-90.

[4] Nakano MM, Dailly YP, Zuber P, Clark DP. Characterization of anaerobic fermentative growth of *Bacillus subtilis*: identification of fermentation end products and genes required for growth. Journal of Bacteriology. 1997;179(21):6749-55.

[5] Logan NA, de Vos P. *Bacillus*. In: Whitman WB, editor. Bergey's Manual of Systematics of Archaea and Bacteria: John Wiley & Sons, Inc., in association with Bergey's Manual Trust; 2015. p. 1-164.

[6] Cohn F. Untersuchungen über Bacterien. IV. Beiträge zur Biologie der Bazillen. In: Cohn F, editor. Beiträge zur Biologie der Pflanzen. 2. Breslau: J. U. Kerns Verlag; 1876. p. 249-76.

[7] Koch R. Untersuchungen über Bacterien. V. Die Aetiologie der Milzbrand-Krankheit, begründet auf die Entwicklungsgeschichte des *Bacillus anthracis*. In: Cohn F, editor. Beiträge zur Biologie der Pflanzen. 2. Breslau: J. U. Kerns Verlag; 1876. p. 277-310.

[8] Kay D, Warren SC. Sporulation in *Bacillus subtilis*. Morphological changes. The Biochemical Journal. 1968;109(5):819-24.

[9] Sonenshein AL, Hoch JA, Losick R. *Bacillus subtilis* and its closest relatives: from genes to cells. Washington, DC: ASM Press; 2002.

[10] Tan IS, Ramamurthi KS. Spore formation in *Bacillus subtilis*. Environmental Microbiology Reports. 2014;6(3):212-25.

[11] Setlow P. Spore germination. Current Opinion in Microbiology. 2003;6(6):550-6.

[12] Christie G, Setlow P. *Bacillus* spore germination: knowns, unknowns and what we need to learn. Cellular Signalling. 2020;74:109729.

[13] Errington J. Regulation of endospore formation in *Bacillus subtilis*. Nature Reviews Microbiology. 2003;1(2):117-26.

[14] Nicholson WL, Munakata N, Horneck G, Melosh HJ, Setlow P. Resistance of *Bacillus* endospores to extreme terrestrial and extraterrestrial environments. Microbiology and Molecular Biology Reviews. 2000;64(3):548-72.

[15] Setlow P. Spore resistance properties. Microbiology Spectrum. 2014;2(5).

[16] Setlow P. Spores of *Bacillus subtilis*: their resistance to and killing by radiation, heat and chemicals. Journal of Applied Microbiology. 2006;101(3):514-25.

[17] Warth AD, Ohye DF, Murrell WG. The composition and structure of bacterial spores. The Journal of Cell Biology. 1963;16(3):579-92.

[18] McKenney PT, Driks A, Eichenberger P. The *Bacillus subtilis* endospore: assembly and functions of the multilayered coat. Nature Reviews Microbiology. 2013;11(1):33-44.

[19] Stewart GC. The exosporium layer of bacterial spores: a connection to the environment and the infected host. Microbiology and Molecular Biology Reviews. 2015;79(4):437-57.

[20] Cortezzo DE, Setlow P. Analysis of factors that influence the sensitivity of spores of *Bacillus subtilis* to DNA damaging chemicals. Journal of Applied Microbiology. 2005;98(3):606-17.

[21] Murrell WG. The biochemistry of the bacterial endospore. Advances in Microbial Physiology. 1967;1:133-251.

[22] Powell JF, Strange RE. Biochemical changes occurring during the germination of bacterial spores. The Biochemical Journal. 1953;54(2):205-9.

[23] Powell JF. Isolation of dipicolinic acid (pyridine-2:6-dicarboxylic acid) from spores of *Bacillus megatherium*. The Biochemical Journal. 1953;54(2):210-1.

[24] Powell JF, Strange RE. Biochemical changes occurring during sporulation in *Bacillus* species. The Biochemical Journal. 1956;63(4):661-8.

[25] Setlow B, Atluri S, Kitchel R, Koziol-Dube K, Setlow P. Role of dipicolinic acid in resistance and stability of spores of *Bacillus subtilis* with or without DNA-protective α/β-type small acid-soluble proteins. Journal of Bacteriology. 2006;188(11):3740-7.

[26] Paidhungat M, Setlow B, Driks A, Setlow P. Characterization of spores of *Bacillus subtilis* which lack dipicolinic acid. Journal of Bacteriology. 2000;182(19):5505-12.

[27] Beaman TC, Gerhardt P. Heat resistance of bacterial spores correlated with protoplast dehydration, mineralization, and thermal adaptation. Applied and Environmental Microbiology. 1986;52(6):1242-6.

[28] Gerhardt P, Marquis RE. Spore thermoresistance mechanisms. In: Smith I, Slepecky RA, Setlow P, editors. Regulation of procaryotic development. Washington, DC: American Society for Microbiology; 1989. p. 43-63.

[29] Francesconi SC, MacAlister TJ, Setlow B, Setlow P. Immunoelectron microscopic localization of small, acid-soluble spore proteins in sporulating cells of *Bacillus subtilis*. Journal of Bacteriology. 1988;170(12):5963-7.

[30] Setlow P. I will survive: DNA protection in bacterial spores. Trends in Microbiology. 2007;15(4):172-80.

[31] Setlow B, Setlow P. Levels of oxidized and reduced pyridine nucleotides in dormant spores and during growth, sporulation, and spore germination of *Bacillus megaterium*. Journal of Bacteriology. 1977;129(2):857-65.

[32] Setlow P, Kornberg A. Biochemical studies of bacterial sporulation and germination. XXII. Energy metabolism in early stages of germination of *Bacillus megaterium* spores. The Journal of Biological Chemistry. 1970;245(14):3637-44.

[33] Cano RJ, Borucki MK. Revival and identification of bacterial spores in 25- to 40-million-year-old Dominican amber. Science. 1995;268(5213):1060-4.

[34] Setlow P. Mechanisms which contribute to the long-term survival of spores of *Bacillus* species. Journal of Applied Bacteriology Symposium Supplement. 1994;23:49S-60S.

[35] Zhang X, Al-Dossary A, Hussain M, Setlow P, Li J. Applications of *Bacillus subtilis* spores in biotechnology and advanced materials. Applied and Environmental Microbiology. 2020;86(17):e01096-20.

[36] Lee S, Lee J, Jin Y-I, Jeong J-C, Chang YH, Lee Y, et al. Probiotic characteristics of *Bacillus* strains isolated from Korean traditional soy sauce. LWT - Food Science and Technology. 2017;79:518-24.

[37] Damalas CA, Koutroubas SD. Current status and recent developments in biopesticide use. Agriculture. 2018;8(1):13.

[38] Kumar J, Ramlal A, Mallick D, Mishra V. An overview of some biopesticides and their importance in plant protection for commercial acceptance. Plants. 2021;10(6):1185.

[39] Shafi J, Tian H, Ji M. *Bacillus* species as versatile weapons for plant pathogens: a review. Biotechnology & Biotechnological Equipment. 2017;31(3):446-59.

[40] Dimopoulou A, Theologidis I, Liebmann B, Kalantidis K, Vassilakos N, Skandalis N. *Bacillus amyloliquefaciens* MBI600 differentially induces tomato defense signaling pathways depending on plant part and dose of application. Scientific Reports. 2019;9(1):19120.

[41] Alvarez F, Castro M, Príncipe A, Borioli G, Fischer S, Mori G, et al. The plant-associated *Bacillus amyloliquefaciens* strains MEP_218 and ARP_23 capable of producing the cyclic lipopeptides iturin or surfactin and fengycin are effective in biocontrol of sclerotinia stem rot disease. Journal of Applied Microbiology. 2012;112(1):159-74.

[42] Martínez-Absalón S, Rojas-Solís D, Hernández-León R, Prieto-Barajas C, Orozco-Mosqueda MdC, Peña-Cabriales JJ, et al. Potential use and mode of action of the new strain *Bacillus thuringiensis* UM96 for the biological control of the grey mould phytopathogen *Botrytis cinerea*. Biocontrol Science and Technology. 2014;24(12):1349-62.

[43] Sharma TK, Alazhari M, Heath A, Paine K, Cooper RM. Alkaliphilic *Bacillus* species show potential application in concrete crack repair by virtue of rapid spore production and germination then extracellular calcite formation. Journal of Applied Microbiology. 2017;122(5):1233-44.

[44] Wang H, Wang Y, Yang R. Recent progress in *Bacillus subtilis* spore-surface display: concept, progress, and future. Applied Microbiology and Biotechnology. 2017;101(3):933-49.

[45] Lin P, Yuan H, Du J, Liu K, Liu H, Wang T. Progress in research and application development of surface display technology using *Bacillus subtilis* spores. Applied Microbiology and Biotechnology. 2020;104(6):2319-31.

[46] Isticato R, Cangiano G, Tran HT, Ciabattini A, Medaglini D, Oggioni MR, et al. Surface display of recombinant proteins on *Bacillus subtilis* spores. Journal of Bacteriology. 2001;183(21):6294-301.

[47] Chen H, Tian R, Ni Z, Zhang Q, Zhang T, Chen Z, et al. Surface display of the thermophilic lipase Tm1350 on the spore of *Bacillus subtilis* by the CotB anchor protein. Extremophiles. 2015;19(4):799-808.

[48] He W, Jiang B, Mu W, Zhang T. Production of D-allulose with D-psicose 3-epimerase expressed and displayed on the surface of *Bacillus subtilis* spores. Journal of Agricultural and Food Chemistry. 2016;64(38):7201-7.

[49] Dai X, Liu M, Pan K, Yang J. Surface display of OmpC of *Salmonella* serovar Pullorum on *Bacillus subtilis* spores. PLoS One. 2018;13(1):e0191627.

[50] Ash C, Priest FG, Collins MD. Molecular identification of rRNA group 3 bacilli (Ash, Farrow, Wallbanks and Collins) using a PCR probe test. Proposal for the creation of a new genus *Paenibacillus*. Antonie van Leeuwenhoek. 1993;64(3-4):253-60.

[51] von der Weid I, Paiva E, Nóbrega A, van Elsas JD, Seldin L. Diversity of *Paenibacillus polymyxa* strains isolated from the rhizosphere of maize planted in Cerrado soil. Research in Microbiology. 2000;151(5):369-81.

[52] Guemouri-Athmani S, Berge O, Bourrain M, Mavingui P, Thiéry JM, Bhatnagar T, et al. Diversity of *Paenibacillus polymyxa* populations in the rhizosphere of wheat (*Triticum durum*) in Algerian soils. European Journal of Soil Biology. 2000;36(3-4):149-59.

[53] Lal S, Tabacchioni S. Ecology and biotechnological potential of *Paenibacillus polymyxa*: a minireview. Indian Journal of Microbiology. 2009;49(1):2-10.

[54] Langendries S, Goormachtig S. *Paenibacillus polymyxa*, a Jack of all trades. Environmental Microbiology. 2021;23(10):5659-69.

[55] Daud NS, Mohd Din ARJ, Rosli MA, Azam ZM, Othman NZ, Sarmidi MR. *Paenibacillus polymyxa* bioactive compounds for agricultural and biotechnological applications. Biocatalysis and Agricultural Biotechnology. 2019;18:101092.

[56] Raza W, Shen Q. Growth, Fe^{3+} reductase activity, and siderophore production by *Paenibacillus polymyxa* SQR-21 under differential iron conditions. Current Microbiology. 2010;61(5):390-5.

[57] Timmusk S, Nicander B, Granhall U, Tillberg E. Cytokinin production by *Paenibacillus polymyxa*. Soil Biology and Biochemistry. 1999;31(13):1847-52.

[58] Zhai Y, Zhu JX, Tan TM, Xu JP, Shen AR, Yang XB, et al. Isolation and characterization of antagonistic *Paenibacillus polymyxa* HX-140 and its biocontrol potential against Fusarium wilt of cucumber seedlings. BMC Microbiology. 2021;21(1):75.

[59] Mavingui P, Heulin T. In *vitro* chitinase and antifungal activity of a soil, rhizosphere and rhizoplane population of *Bacillus polymyxa*. Soil Biology and Biochemistry. 1994;26(6):801-3.

[60] Choi SK, Park SY, Kim R, Lee CH, Kim JF, Park SH. Identification and functional analysis of the fusaricidin biosynthetic gene of *Paenibacillus polymyxa* E681. Biochemical and Biophysical Research Communications. 2008;365(1):89-95.

[61] Hong J-H, Jung HK. Antioxidant and antitumor activities of β-glucan-rich exopolysaccharides with different molecular weight from *Paenibacillus polymyxa* JB115. Journal of the Korean Society for Applied Biological Chemistry. 2014;57(1):105-12.

[62] Prado Acosta M, Valdman E, Leite SGF, Battaglini F, Ruzal SM. Biosorption of copper by *Paenibacillus polymyxa* cells and their exopolysaccharide. World Journal of Microbiology and Biotechnology. 2005;21(6-7):1157-63.

[63] Nakashimada Y, Kanai K, Nishio N. Optimization of dilution rate, pH and oxygen supply on optical purity of 2, 3-butanediol produced by *Paenibacillus polymyxa* in chemostat culture. Biotechnology Letters. 1998;20(12):1133-8.

[64] Nakashimada Y, Marwoto B, Kashiwamura T, Kakizono T, Nishio N. Enhanced 2,3-butanediol production by addition of acetic acid in *Paenibacillus polymyxa*. Journal of Bioscience and Bioengineering. 2000;90(6):661-4.

[65] Song CW, Park JM, Chung SC, Lee SY, Song H. Microbial production of 2,3-butanediol for industrial applications. Journal of Industrial Microbiology and Biotechnology. 2019;46(11):1583-601.

[66] Lattermann C, Büchs J. Microscale and miniscale fermentation and screening. Current Opinion in Biotechnology. 2015;35:1-6.

[67] Wollborn D, Munkler LP, Horstmann R, Germer A, Blank LM, Büchs J. Predicting high recombinant protein producer strains of *Pichia pastoris* Mut^S using the oxygen transfer rate as an indicator of metabolic burden. Scientific Reports. 2022;12(1):11225.

[68] Müller J, Beckers M, Mußmann N, Bongaerts J, Büchs J. Elucidation of auxotrophic deficiencies of *Bacillus pumilus* DSM 18097 to develop a defined minimal medium. Microbial Cell Factories. 2018;17(1):106.

[69] Lapierre FM, Schmid J, Ederer B, Ihling N, Büchs J, Huber R. Revealing nutritional requirements of MICP-relevant *Sporosarcina pasteurii* DSM33 for growth improvement in chemically defined and complex media. Scientific Reports. 2020;10(1):22448.

[70] Anderlei T, Büchs J. Device for sterile online measurement of the oxygen transfer rate in shaking flasks. Biochemical Engineering Journal. 2001;7(2):157-62.

[71] Anderlei T, Zang W, Papaspyrou M, Büchs J. Online respiration activity measurement (OTR, CTR, RQ) in shake flasks. Biochemical Engineering Journal. 2004;17(3):187-94.

[72] Samorski M, Müller-Newen G, Büchs J. Quasi-continuous combined scattered light and fluorescence measurements: a novel measurement technique for shaken microtiter plates. Biotechnology and Bioengineering. 2005;92(1):61-8.

[73] Flitsch D, Krabbe S, Ladner T, Beckers M, Schilling J, Mahr S, et al. Respiration activity monitoring system for any individual well of a 48-well microtiter plate. Journal of Biological Engineering. 2016;10:14.

[74] Dinger R, Lattermann C, Flitsch D, Fischer JP, Kosfeld U, Büchs J. Device for respiration activity measurement enables the determination of oxygen transfer rates of microbial cultures in shaken 96-deepwell microtiter plates. Biotechnology and Bioengineering. 2022;119(3):881-94.

[75] Kensy F, Zang E, Faulhammer C, Tan RK, Büchs J. Validation of a high-throughput fermentation system based on online monitoring of biomass and fluorescence in continuously shaken microtiter plates. Microbial Cell Factories. 2009;8:31.

[76] Wandrey G, Bier C, Binder D, Hoffmann K, Jaeger KE, Pietruszka J, et al. Light-induced gene expression with photocaged IPTG for induction profiling in a high-throughput screening system. Microbial Cell Factories. 2016;15:63.

[77] Ladner T, Held M, Flitsch D, Beckers M, Büchs J. Quasi-continuous parallel online scattered light, fluorescence and dissolved oxygen tension measurement combined with monitoring of the oxygen transfer rate in each well of a shaken microtiter plate. Microbial Cell Factories. 2016;15(1):206.

[78] Bruder S, Reifenrath M, Thomik T, Boles E, Herzog K. Parallelised online biomass monitoring in shake flasks enables efficient strain and carbon source dependent

growth characterisation of *Saccharomyces cerevisiae*. Microbial Cell Factories. 2016;15(1):127.

[79] Heyman B, Lamm R, Tulke H, Regestein L, Büchs J. Shake flask methodology for assessing the influence of the maximum oxygen transfer capacity on 2,3-butanediol production. Microbial Cell Factories. 2019;18(1):78.

[80] Kottmeier K, Müller C, Huber R, Büchs J. Increased product formation induced by a directed secondary substrate limitation in a batch *Hansenula polymorpha* culture. Applied Microbiology and Biotechnology. 2010;86(1):93-101.

[81] Stöckmann C, Losen M, Dahlems U, Knocke C, Gellissen G, Büchs J. Effect of oxygen supply on passaging, stabilising and screening of recombinant *Hansenula polymorpha* production strains in test tube cultures. FEMS Yeast Research. 2003;4(2):195-205.

[82] Ihling N, Bittner N, Diederichs S, Schelden M, Korona A, Höfler GT, et al. Online measurement of the respiratory activity in shake flasks enables the identification of cultivation phases and patterns indicating recombinant protein production in various *Escherichia coli* host strains. Biotechnology Progress. 2018;34(2):315-27.

[83] Arain S, John GT, Krause C, Gerlach J, Wolfbeis OS, Klimant I. Characterization of microtiterplates with integrated optical sensors for oxygen and pH, and their applications to enzyme activity screening, respirometry, and toxicological assays. Sensors and Actuators B: Chemical. 2006;113(2):639-48.

[84] John GT, Klimant I, Wittmann C, Heinzle E. Integrated optical sensing of dissolved oxygen in microtiter plates: a novel tool for microbial cultivation. Biotechnology and Bioengineering. 2003;81(7):829-36.

[85] Brehl C, Brass HUC, Lüchtrath C, Böckmann L, Ihling N, Classen T, et al. Optimized prodigiosin production with *Pseudomonas putida* KT2440 using parallelized noninvasive online monitoring. Biotechnology Progress. 2022;38(3):e3245.

[86] Siepert EM, Gartz E, Tur MK, Delbrück H, Barth S, Büchs J. Short-chain fluorescent tryptophan tags for on-line detection of functional recombinant proteins. BMC Biotechnology. 2012;12:65.

[87] Finger M, Sentek F, Hartmann L, Palacio-Barrera AM, Schlembach I, Rosenbaum MA, et al. Insights into *Streptomyces coelicolor* A3(2) growth and pigment formation with high-throughput online monitoring. Engineering in Life Sciences. 2023;23(1):e2100151.

[88] Kottmeier K, Weber J, Müller C, Bley T, Büchs J. Asymmetric division of *Hansenula polymorpha* reflected by a drop of light scatter intensity measured in batch microtiter plate cultivations at phosphate limitation. Biotechnology and Bioengineering. 2009;104(3):554-61.

[89] Palacio-Barrera AM, Schlembach I, Finger M, Büchs J, Rosenbaum MA. Reliable online measurement of population dynamics for filamentous co-cultures. Microbial Biotechnology. 2022;15(11):2773-85.

[90] Klement T, Dankmeyer L, Hommes R, van Solingen P, Büchs J. Acetate-glycerol cometabolism: cultivating *Schizosaccharomyces pombe* on a non-fermentable carbon source in a defined minimal medium. Journal of Bioscience and Bioengineering. 2011;112(1):20-5.

[91] Ihling N, Uhde A, Scholz R, Schwarz C, Schmitt L, Büchs J. Scale-up of a Type I secretion system in *E. coli* using a defined mineral medium. Biotechnology Progress. 2020;36(2):e2911.

[92] Luchterhand B, Fischöder T, Grimm AR, Wewetzer S, Wunderlich M, Schlepütz T, et al. Quantifying the sensitivity of *G. oxydans* ATCC 621H and DSM 3504 to osmotic stress triggered by soluble buffers. Journal of Industrial Microbiology and Biotechnology. 2015;42(4):585-600.

[93] Häßler T, Schieder D, Pfaller R, Faulstich M, Sieber V. Enhanced fed-batch fermentation of 2,3-butanediol by *Paenibacillus polymyxa* DSM 365. Bioresource Technology. 2012;124:237-44.

[94] Rafigh SM, Yazdi AV, Vossoughi M, Safekordi AA, Ardjmand M. Optimization of culture medium and modeling of curdlan production from *Paenibacillus polymyxa* by RSM and ANN. International Journal of Biological Macromolecules. 2014;70:463-73.

[95] Liu J, Luo J, Ye H, Sun Y, Lu Z, Zeng X. Production, characterization and antioxidant activities *in vitro* of exopolysaccharides from endophytic bacterium *Paenibacillus polymyxa* EJS-3. Carbohydrate Polymers. 2009;78(2):275-81.

[96] Diederichs S, Korona A, Staaden A, Kroutil W, Honda K, Ohtake H, et al. Phenotyping the quality of complex medium components by simple online-monitored shake flask experiments. Microbial Cell Factories. 2014;13:149.

[97] Klotz S, Kuenz A, Prüße U. Nutritional requirements and the impact of yeast extract on the D-lactic acid production by *Sporolactobacillus inulinus*. Green Chemistry. 2017;19(19):4633-41.

[98] Sparviero S, Dicke MD, Rosch TM, Castillo T, Salgado-Lugo H, Galindo E, et al. Yeast extracts from different manufacturers and supplementation of amino acids and micro elements reveal a remarkable impact on alginate production by *A. vinelandii* ATCC9046. Microbial Cell Factories. 2023;22(1):99.

[99] Porter MA, Jones AM. Variability in soy flour composition. Journal of the American Oil Chemists' Society. 2003;80(6):557-62.

[100] Zhang G, Mills DA, Block DE. Development of chemically defined media supporting high-cell-density growth of lactococci, enterococci, and streptococci. Applied and Environmental Microbiology. 2009;75(4):1080-7.

[101] Görgens JF, van Zyl WH, Knoetze JH, Hahn-Hägerdal B. Amino acid supplementation improves heterologous protein production by *Saccharomyces cerevisiae* in defined medium. Applied Microbiology and Biotechnology. 2005;67(5):684-91.

[102] Battling S, Pastoors J, Deitert A, Götzen T, Hartmann L, Schröder E, et al. Development of a novel defined minimal medium for *Gluconobacter oxydans* 621H by systematic investigation of metabolic demands. Journal of Biological Engineering. 2022;16(1):31.

[103] Mitani T, Heinze JE, Freese E. Induction of sporulation in *Bacillus subtilis* by decoyinine or hadacidin. Biochemical and Biophysical Research Communications. 1977;77(3):1118-25.

[104] Tian Z, Hou L, Hu M, Gao Y, Li D, Fan B, et al. Optimization of sporulation conditions for *Bacillus subtilis* BSNK-5. Processes. 2022;10(6):1133.

[105] Kolodziej BJ, Slepecky RA. Trace metal requirements for sporulation of *Bacillus megaterium*. Journal of Bacteriology. 1964;88(4):821-30.

[106] Yuniarti A, Arifin NB, Fakhri M, Hariati AM. Effect of C:N ratio on the spore production of *Bacillus* sp. indigenous shrimp pond. IOP Conference Series: Earth and Environmental Science. 2019;236:012029.

[107] Sinnelä MT, Pawluk AM, Jin YH, Kim D, Mah JH. Effect of calcium and manganese supplementation on heat resistance of spores of *Bacillus* species associated with food poisoning, spoilage, and fermentation. Frontiers in Microbiology. 2021;12:744953.

[108] Sinnelä MT, Park YK, Lee JH, Jeong KC, Kim YW, Hwang HJ, et al. Effects of calcium and manganese on sporulation of *Bacillus* species involved in food poisoning and spoilage. Foods. 2019;8(4):119.

[109] O'Hara MB, Hageman JH. Energy and calcium ion dependence of proteolysis during sporulation of *Bacillus subtilis* cells. Journal of Bacteriology. 1990;172(8):4161-70.

[110] Monteiro SMS, Clemente JJ, Carrondo MJT, Cunha AE. Enhanced spore production of *Bacillus subtilis* grown in a chemically defined medium. Advances in Microbiology. 2014;4(8):444-54.

[111] Avignone-Rossa C, Arcas J, Mignone C. *Bacillus thuringiensis* growth, sporulation and δ-endotoxin production in oxygen limited and non-limited cultures. World Journal of Microbiology and Biotechnology. 1992;8(3):301-4.

[112] Sarrafzadeh MH, Navarro JM. The effect of oxygen on the sporulation, δ-endotoxin synthesis and toxicity of *Bacillus thuringiensis* H14. World Journal of Microbiology and Biotechnology. 2005;22(3):305-10.

[113] Boniolo FS, Rodrigues RC, Prata AM, López ML, Jacinto T, da Silveira MM, et al. Oxygen supply in *Bacillus thuringiensis* fermentations: bringing new insights on their impact on sporulation and δ-endotoxin production. Applied Microbiology and Biotechnology. 2012;94(3):625-36.

[114] Monteiro SM, Clemente JJ, Henriques AO, Gomes RJ, Carrondo MJ, Cunha AE. A procedure for high-yield spore production by *Bacillus subtilis*. Biotechnology Progress. 2005;21(4):1026-31.

[115] Goldmanns J, Röhling GA, Lipa MK, Scholand T, Deitert A, May T, et al. Development of a chemically defined medium for *Paenibacillus polymyxa* by parallel online monitoring of the respiration activity in microtiter plates. BMC Biotechnology. 2023;23(1):25.

[116] May T, Haas EP, Heinrich DC, Goldmanns J, Büchs J. Materials and methods for improving plant health. 2022. WO2022029027A1.

[117] Zhang J, Reddy J, Buckland B, Greasham R. Toward consistent and productive complex media for industrial fermentations: studies on yeast extract for a recombinant yeast fermentation process. Biotechnology and Bioengineering. 2003;82(6):640-52.

[118] Cromwell GL, Calvert CC, Cline TR, Crenshaw JD, Crenshaw TD, Easter RA, et al. Variability among sources and laboratories in nutrient analyses of corn and soybean meal. NCR-42 Committee on Swine Nutrition. North Central Regional-42. Journal of Animal Science. 1999;77(12):3262-73.

[119] L'Hocine L, Boye JI, Arcand Y. Composition and functional properties of soy protein isolates prepared using alternative defatting and extraction procedures. Journal of Food Science. 2006;71(3):C137-C45.

[120] Traina MS, Breene WM. Composition, functionality and some chemical and physical properties of eight commercial full-fat soy flours. Journal of Food Processing and Preservation. 1994;18(3):229-52.

[121] Charoenrat T, Khumruaengsri N, Promdonkoy P, Rattanaphan N, Eurwilaichitr L, Tanapongpipat S, et al. Improvement of recombinant endoglucanase produced in *Pichia pastoris* KM71 through the use of synthetic medium for inoculum and pH control of proteolysis. Journal of Bioscience and Bioengineering. 2013;116(2):193-8.

[122] Siedenberg D, Gerlach SR, Weigel B, Schugerl K, Giuseppin MLF, Hunik J. Production of xylanase by *Aspergillus awamori* on synthetic medium in stirred tank and airlift tower loop reactors: the influence of stirrer speed and phosphate concentration. Journal of Biotechnology. 1997;56(2):103-14.

[123] Kelle R, Laufer B, Brunzema C, Weuster-Botz D, Krämer R, Wandrey C. Reaction engineering analysis of L-lysine transport by *Corynebacterium glutamicum*. Biotechnology and Bioengineering. 1996;51(1):40-50.

[124] Zhang J, Greasham R. Chemically defined media for commercial fermentations. Applied Microbiology and Biotechnology. 1999;51(4):407-21.

[125] Zhang J, Marcin C, Shifflet MA, Salmon P, Brix T, Greasham R, et al. Development of a defined medium fermentation process for physostigmine production by *Streptomyces griseofuscus*. Applied Microbiology and Biotechnology. 1996;44(5):568-75.

[126] Singh V, Haque S, Niwas R, Srivastava A, Pasupuleti M, Tripathi CK. Strategies for fermentation medium optimization: an in-depth review. Frontiers in Microbiology. 2017;7:2087.

[127] Gonzalez R, Islas L, Obregon AM, Escalante L, Sanchez S. Gentamicin formation in *Micromonospora purpurea*: stimulatory effect of ammonium. The Journal of Antibiotics. 1995;48(6):479-83.

[128] Joy S, Rahman PKSM, Khare SK, Sharma S. Production and characterization of glycolipid biosurfactant from *Achromobacter* sp. (PS1) isolate using one-factor-at-a-time (OFAT) approach with feasible utilization of ammonia-soaked lignocellulosic pretreated residues. Bioprocess amd Biosystems Engineering. 2019;42(8):1301-15.

[129] Heo MS, Son HJ. Development of an optimized, simple chemically defined medium for bacterial cellulose production by *Acetobacter* sp. A9 in shaking cultures. Biotechnology and Applied Biochemistry. 2002;36(1):41-5.

[130] Parekh S, Vinci VA, Strobel RJ. Improvement of microbial strains and fermentation processes. Applied Microbiology and Biotechnology. 2000;54(3):287-301.

[131] Sharma S, Agarwal L, Saxena RK. Statistical optimization for tannase production from *Aspergillus niger* under submerged fermentation. Indian Journal of Microbiology. 2007;47(2):132-8.

[132] Shih IL, Van YT, Chang YN. Application of statistical experimental methods to optimize production of poly(γ-glutamic acid) by *Bacillus licheniformis* CCRC 12826. Enzyme and Microbial Technology. 2002;31(3):213-20.

[133] Cunha L, Martarello R, de Souza PM, de Freitas MM, Barros KVG, Ferreira Filho EX, et al. Optimization of xylanase production from *Aspergillus foetidus* in soybean residue. Enzyme Research. 2018;2018:6597017.

[134] Franceschini G, Macchietto S. Model-based design of experiments for parameter precision: state of the art. Chemical Engineering Science. 2008;63(19):4846-72.

[135] Poolman B, Konings WN. Relation of growth of *Streptococcus lactis* and *Streptococcus cremoris* to amino acid transport. Journal of Bacteriology. 1988;170(2):700-7.

[136] Wilming A, Begemann J, Kuhne S, Regestein L, Bongaerts J, Evers S, et al. Metabolic studies of γ-polyglutamic acid production in *Bacillus licheniformis* by small-scale continuous cultivations. Biochemical Engineering Journal. 2013;73:29-37.

[137] Kunze M, Roth S, Gartz E, Büchs J. Pitfalls in optical on-line monitoring for high-throughput screening of microbial systems. Microbial Cell Factories. 2014;13:53.

[138] Adlakha N, Pfau T, Ebenhöh O, Yazdani SS. Insight into metabolic pathways of the potential biofuel producer, *Paenibacillus polymyxa* ICGEB2008. Biotechnology for Biofuels. 2015;8:159.

[139] Schepers H-J, Bringer-Meyer S, Sahm H. Fermentation of D-xylose to ethanol by *Bacillus macerans*. Zeitschrift für Naturforschung C. 1987;42(4):401-7.

[140] von der Weid I, Alviano DS, Santos AL, Soares RM, Alviano CS, Seldin L. Antimicrobial activity of *Paenibacillus peoriae* strain NRRL BD-62 against a broad

spectrum of phytopathogenic bacteria and fungi. Journal of Applied Microbiology. 2003;95(5):1143-51.

[141] Alvarez VM, von der Weid I, Seldin L, Santos AL. Influence of growth conditions on the production of extracellular proteolytic enzymes in *Paenibacillus peoriae* NRRL BD-62 and *Paenibacillus polymyxa* SCE2. Letters in Applied Microbiology. 2006;43(6):625-30.

[142] Palmen TG, Scheidle M, Huber R, Kamerke C, Wilming A, Dittrich B, et al. Influence of initial pH values on the lag phase of *Escherichia coli* and *Bacillus licheniformis* batch cultures. Chemie Ingenieur Technik. 2013;85(6):863-71.

[143] Schönert S, Seitz S, Krafft H, Feuerbaum EA, Andernach I, Witz G, et al. Maltose and maltodextrin utilization by *Bacillus subtilis*. Journal of Bacteriology. 2006;188(11):3911-22.

[144] Thompson J, Pikis A, Ruvinov SB, Henrissat B, Yamamoto H, Sekiguchi J. The gene *glvA* of *Bacillus subtilis* 168 encodes a metal-requiring, NAD(H)-dependent 6-phospho-alpha-glucosidase. Assignment to family 4 of the glycosylhydrolase superfamily. The Journal of Biological Chemistry. 1998;273(42):27347-56.

[145] Hidaka Y, Hatada Y, Akita M, Yoshida M, Nakamura N, Takada M, et al. Maltose phosphorylase from a deep-sea *Paenibacillus* sp.: enzymatic properties and nucleotide and amino-acid sequences. Enzyme and Microbial Technology. 2005;37(2):185-94.

[146] Meissner L, Kauffmann K, Wengeler T, Mitsunaga H, Fukusaki E, Büchs J. Influence of nitrogen source and pH value on undesired poly(γ-glutamic acid) formation of a protease producing *Bacillus licheniformis* strain. Journal of Industrial Microbiology and Biotechnology. 2015;42(9):1203-15.

[147] de Mas C, Jansen NB, Tsao GT. Production of optically active 2,3-butanediol by *Bacillus polymyxa*. Biotechnology and Bioengineering. 1988;31(4):366-77.

[148] Akashi H, Gojobori T. Metabolic efficiency and amino acid composition in the proteomes of *Escherichia coli* and *Bacillus subtilis*. Proceedings of the National Academy of Sciences of the United States of America. 2002;99(6):3695-700.

[149] Kobayashi K, Ehrlich SD, Albertini A, Amati G, Andersen KK, Arnaud M, et al. Essential *Bacillus subtilis* genes. Proceedings of the National Academy of Sciences of the United States of America. 2003;100(8):4678-83.

[150] Sershon VC, Santarsiero BD, Mesecar AD. Kinetic and X-ray structural evidence for negative cooperativity in substrate binding to nicotinate mononucleotide

adenylyltransferase (NMAT) from *Bacillus anthracis*. Journal of Molecular Biology. 2009;385(3):867-88.

[151] Foster JW, Moat AG. Nicotinamide adenine dinucleotide biosynthesis and pyridine nucleotide cycle metabolism in microbial systems. Microbiological Reviews. 1980;44(1):83-105.

[152] Petrov K, Petrova P. Current advances in microbial production of acetoin and 2,3-butanediol by *Bacillus* spp. Fermentation. 2021;7(4):307.

[153] Bao T, Zhang X, Zhao X, Rao Z, Yang T, Yang S. Regulation of the NADH pool and NADH/NADPH ratio redistributes acetoin and 2,3-butanediol proportion in *Bacillus subtilis*. Biotechnology Journal. 2015;10(8):1298-306.

[154] Tsau JL, Guffanti AA, Montville TJ. Conversion of pyruvate to acetoin helps to maintain pH homeostasis in *Lactobacillus plantarum*. Applied and Environmental Microbiology. 1992;58(3):891-4.

[155] Ortega MV, Brown GM. Precursors of nicotinic acid in *Escherichia coli*. The Journal of Biological Chemistry. 1960;235(10):2939-45.

[156] Good NE, Winget GD, Winter W, Connolly TN, Izawa S, Singh RM. Hydrogen ion buffers for biological research. Biochemistry. 1966;5(2):467-77.

[157] Schroeter R, Hoffmann T, Voigt B, Meyer H, Bleisteiner M, Muntel J, et al. Stress responses of the industrial workhorse *Bacillus licheniformis* to osmotic challenges. PLoS One. 2013;8(11):e80956.

[158] Boch J, Kempf B, Bremer E. Osmoregulation in *Bacillus subtilis*: synthesis of the osmoprotectant glycine betaine from exogenously provided choline. Journal of Bacteriology. 1994;176(17):5364-71.

[159] Mühlmann M, Forsten E, Noack S, Büchs J. Optimizing recombinant protein expression via automated induction profiling in microtiter plates at different temperatures. Microbial Cell Factories. 2017;16(1):220.

[160] Doering JL, Bott KF. Differential amino acid requirements for sporulation in *Bacillus subtilis*. Journal of Bacteriology. 1972;112(1):345-55.

[161] Brugger SD, Baumberger C, Jost M, Jenni W, Brugger U, Mühlemann K. Automated counting of bacterial colony forming units on agar plates. PLoS One. 2012;7(3):e33695.

[162] Hazan R, Que YA, Maura D, Rahme LG. A method for high throughput determination of viable bacteria cell counts in 96-well plates. BMC Microbiology. 2012;12:259.

[163] Paulus H. Determination of dipicolinic acid by high-pressure liquid chromatography. Analytical Biochemistry. 1981;114(2):407-10.

[164] Pellegrino PM, Fell NF, Gillespie JB. Enhanced spore detection using dipicolinate extraction techniques. Analytica Chimica Acta. 2002;455(2):167-77.

[165] Rosen DL, Sharpless C, McGown LB. Bacterial spore detection and determination by use of terbium dipicolinate photoluminescence. Analytical Chemistry. 1997;69(6):1082-5.

[166] Cable ML, Kirby JP, Levine DJ, Manary MJ, Gray HB, Ponce A. Detection of bacterial spores with lanthanide-macrocycle binary complexes. Journal of the American Chemical Society. 2009;131(27):9562-70.

[167] Cowcher DP, Xu Y, Goodacre R. Portable, quantitative detection of *Bacillus* bacterial spores using surface-enhanced Raman scattering. Analytical Chemistry. 2013;85(6):3297-302.

[168] Zhang X, Young MA, Lyandres O, Van Duyne RP. Rapid detection of an anthrax biomarker by surface-enhanced Raman spectroscopy. Journal of the American Chemical Society. 2005;127(12):4484-9.

[169] Sarrafzadeh MH, Belloy L, Esteban G, Navarro JM, Ghommidh C. Dielectric monitoring of growth and sporulation of *Bacillus thuringiensis*. Biotechnology Letters. 2005;27(7):511-7.

[170] Clemente JJ, Monteiro SM, Carrondo MJ, Cunha AE. Predicting sporulation events in a bioreactor using an electronic nose. Biotechnology and Bioengineering. 2008;101(3):545-52.

[171] Nudelman R, Bronk BV, Efrima S. Fluorescence emission derived from dipicolinic acid, its sodium, and its calcium salts. Applied Spectroscopy. 2000;54(3):445-9.

[172] Sarasanandarajah S, Kunnil J, Bronk BV, Reinisch L. Two-dimensional multiwavelength fluorescence spectra of dipicolinic acid and calcium dipicolinate. Applied Optics. 2005;44(7):1182-7.

[173] Alimova A, Katz A, Savage HE, Shah M, Minko G, Will DV, et al. Native fluorescence and excitation spectroscopic changes in *Bacillus subtilis* and

Staphylococcus aureus bacteria subjected to conditions of starvation. Applied Optics. 2003;42(19):4080-7.

[174] Schroeder JW, Simmons LA. Complete genome sequence of *Bacillus subtilis* strain PY79. Genome Announcements. 2013;1(6):e01085-13.

[175] Youngman P, Perkins JB, Losick R. Construction of a cloning site near one end of Tn917 into which foreign DNA may be inserted without affecting transposition in *Bacillus subtilis* or expression of the transposon-borne *erm* gene. Plasmid. 1984;12(1):1-9.

[176] Zeigler DR, Prágai Z, Rodriguez S, Chevreux B, Muffler A, Albert T, et al. The origins of 168, W23, and other *Bacillus subtilis* legacy strains. Journal of Bacteriology. 2008;190(21):6983-95.

[177] Lennox ES. Transduction of linked genetic characters of the host by bacteriophage P1. Virology. 1955;1(2):190-206.

[178] Meier K, Klöckner W, Bonhage B, Antonov E, Regestein L, Büchs J. Correlation for the maximum oxygen transfer capacity in shake flasks for a wide range of operating conditions and for different culture media. Biochemical Engineering Journal. 2016;109:228-35.

[179] Boehl D, Solle D, Hitzmann B, Scheper T. Chemometric modelling with two-dimensional fluorescence data for *Claviceps purpurea* bioprocess characterization. Journal of Biotechnology. 2003;105(1-2):179-88.

[180] Ladner T, Beckers M, Hitzmann B, Büchs J. Parallel online multi-wavelength (2D) fluorescence spectroscopy in each well of a continuously shaken microtiter plate. Biotechnology Journal. 2016;11(12):1605-16.

[181] Duysens LN, Amesz J. Fluorescence spectrophotometry of reduced phosphopyridine nucleotide in intact cells in the near-ultraviolet and visible region. Biochimica et Biophysica Acta. 1957;24(1):19-26.

[182] Yang H, Xiao X, Zhao XS, Hu L, Xue XF, Ye JS. Study on fluorescence spectra of thiamine and riboflavin. MATEC Web of Conferences. 2016;63:03013.

[183] Koch AL, Ehrenfeld E. The size and shape of bacteria by light scattering measurements. Biochimica et Biophysica Acta (BBA) - General Subjects. 1968;165(2):262-73.

[184] Illing N, Errington J. Genetic regulation of morphogenesis in *Bacillus subtilis*: roles of σ^E and σ^F in prespore engulfment. Journal of Bacteriology. 1991;173(10):3159-69.

[185] Magill NG, Setlow P. Properties of purified sporlets produced by *spoII* mutants of *Bacillus subtilis*. Journal of Bacteriology. 1992;174(24):8148-51.

[186] Defeu Soufo HJ. A novel cell type enables *B. subtilis* to escape from unsuccessful sporulation in minimal medium. Frontiers in Microbiology. 2016;7:1810.

[187] Kang D, Kirienko DR, Webster P, Fisher AL, Kirienko NV. Pyoverdine, a siderophore from *Pseudomonas aeruginosa*, translocates into *C. elegans*, removes iron, and activates a distinct host response. Virulence. 2018;9(1):804-17.

[188] Meyer JM, Abdallah MA. The fluorescent pigment of *Pseudomonas fluorescens*: biosynthesis, purification and physicochemical properties. Journal of General Microbiology. 1978;107(2):319-28.

[189] Mureseanu M, Renard G, Galarneau A, Lerner DA. A demonstration model for a selective and recyclable uptake of metals from water: Fe(III) ions complexation and release by a supported natural fluorescent chelator. Talanta. 2003;60(2-3):515-22.

[190] Xiao R, Kisaalita WS. Fluorescent pseudomonad pyoverdines bind and oxidize ferrous ion. Applied and Environmental Microbiology. 1998;64(4):1472-6.

[191] Hider RC, Kong X. Chemistry and biology of siderophores. Nature Product Reports. 2010;27(5):637-57.

[192] Elliott RP. Some properties of pyoverdine, the water-soluble fluorescent pigment of the pseudomonads. Applied Microbiology. 1958;6(4):241-6.

[193] May JJ, Wendrich TM, Marahiel MA. The *dhb* operon of *Bacillus subtilis* encodes the biosynthetic template for the catecholic siderophore 2,3-dihydroxybenzoate-glycine-threonine trimeric ester bacillibactin. The Journal of Biological Chemistry. 2001;276(10):7209-17.

[194] Koppisch AT, Browder CC, Moe AL, Shelley JT, Kinkel BA, Hersman LE, et al. Petrobactin is the primary siderophore synthesized by *Bacillus anthracis* str. *Sterne* under conditions of iron starvation. BioMetals. 2005;18(6):577-85.

[195] O'Brien IG, Gibson F. The structure of enterochelin and related 2,3-dihydroxy-*N*-benzoylserine conjugates from *Escherichia coli*. Biochimica et Biophysica Acta (BBA) - General Subjects. 1970;215(2):393-402.

[196] Cornish AS, Page WJ. The catecholate siderophores of *Azotobacter vinelandii*: their affinity for iron and role in oxygen stress management. Microbiology (Reading, England). 1998;144(7):1747-54.

[197] Neilands JB. Microbial iron compounds. Annual Review of Biochemistry. 1981;50:715-31.

[198] Demange P, Wendenbaum S, Linget C, Mertz C, Cung MT, Dell A, et al. Bacterial siderophores : structure and NMR assignment of pyoverdins Pa, siderophores of *Pseudomonas aeruginosa* ATCC 15692. Biology of Metals. 1990;3(3-4):155-70.

[199] Oudega B, Vandenbol M, Koningstein G. A 12 kb nucleotide sequence containing the alanine dehydrogenase gene at 279° on the *Bacillus subtilis* chromosome. Microbiology (Reading, England). 1997;143 (Pt 5):1489-91.

[200] Santos S, Neto IF, Machado MD, Soares HM, Soares EV. Siderophore production by *Bacillus megaterium*: effect of growth phase and cultural conditions. Applied Biochemistry and Biotechnology. 2014;172(1):549-60.

[201] Grandchamp GM, Caro L, Shank EA. Pirated siderophores promote sporulation in *Bacillus subtilis*. Applied and Environmental Microbiology. 2017;83(10):e03293-16.

[202] Hagan AK, Plotnick YM, Dingle RE, Mendel ZI, Cendrowski SR, Sherman DH, et al. Petrobactin protects against oxidative stress and enhances sporulation efficiency in *Bacillus anthracis* Sterne. mBio. 2018;9(6):e02079-18.

[203] Wilson MK, Abergel RJ, Arceneaux JE, Raymond KN, Byers BR. Temporal production of the two *Bacillus anthracis* siderophores, petrobactin and bacillibactin. BioMetals. 2010;23(1):129-34.

[204] Dunlap CA, Kim SJ, Kwon SW, Rooney AP. *Bacillus velezensis* is not a later heterotypic synonym of *Bacillus amyloliquefaciens*; *Bacillus methylotrophicus*, *Bacillus amyloliquefaciens* subsp. *plantarum* and '*Bacillus oryzicola*' are later heterotypic synonyms of *Bacillus velezensis* based on phylogenomics. International Journal of Systematic and Evolutionary Microbiology. 2016;66(3):1212-7.

[205] Lücking G, Stoeckel M, Atamer Z, Hinrichs J, Ehling-Schulz M. Characterization of aerobic spore-forming bacteria associated with industrial dairy processing environments and product spoilage. International Journal of Food Microbiology. 2013;166(2):270-9.

[206] Zhou C, Zhou H, Zhang H, Lu F. Optimization of alkaline protease production by rational deletion of sporulation related genes in *Bacillus licheniformis*. Microbial Cell Factories. 2019;18(1):127.

[207] Jurchescu IM, Hamann J, Zhou X, Ortmann T, Kuenz A, Prüße U, et al. Enhanced 2,3-butanediol production in fed-batch cultures of free and immobilized *Bacillus licheniformis* DSM 8785. Applied Microbiology and Biotechnology. 2013;97(15):6715-23.

[208] Kalyan VSRK, Meena S, Karthikeyan S, Jawahar D. Isolation, screening, characterization, and optimization of bacteria isolated from calcareous soils for siderophore production. Archives of Microbiology. 2022;204(12):721.

[209] Wang C, Zhao D, Qi G, Mao Z, Hu X, Du B, et al. Effects of *Bacillus velezensis* FKM10 for promoting the growth of *Malus hupehensis* Rehd. and inhibiting *Fusarium verticillioides*. Frontiers in Microbiology. 2020;10:2889.

[210] Chen XH, Koumoutsi A, Scholz R, Eisenreich A, Schneider K, Heinemeyer I, et al. Comparative analysis of the complete genome sequence of the plant growth-promoting bacterium *Bacillus amyloliquefaciens* FZB42. Nature Biotechnology. 2007;25(9):1007-14.

[211] Chen ZM, Li Q, Liu HM, Yu N, Xie TJ, Yang MY, et al. Greater enhancement of *Bacillus subtilis* spore yields in submerged cultures by optimization of medium composition through statistical experimental designs. Applied Microbiology and Biotechnology. 2010;85(5):1353-60.

[212] Chibazakura T, Kawamura F, Takahashi H. Differential regulation of *spo0A* transcription in *Bacillus subtilis*: glucose represses promoter switching at the initiation of sporulation. Journal of Bacteriology. 1991;173(8):2625-32.

[213] Molle V, Fujita M, Jensen ST, Eichenberger P, González-Pastor JE, Liu JS, et al. The Spo0A regulon of *Bacillus subtilis*. Molecular Microbiology. 2003;50(5):1683-701.

[214] Slepecky R, Foster JW. Alterations in metal content of spores of *Bacillus megaterium* and the effect on some spore properties. Journal of Bacteriology. 1959;78(1):117-23.

[215] Charney J, Fisher WP, Hegarty CP. Managanese as an essential element for sporulation in the genus *Bacillus*. Journal of Bacteriology. 1951;62(2):145-8.

[216] Vasantha N, Freese E. The role of manganese in growth and sporulation of *Bacillus subtilis*. Journal of General Microbiology. 1979;112(2):329-36.

[217] Oh YK, Freese E. Manganese requirement of phosphoglycerate phosphomutase and its consequences for growth and sporulation of *Bacillus subtilis*. Journal of Bacteriology. 1976;127(2):739-46.

[218] Atrih A, Foster SJ. Analysis of the role of bacterial endospore cortex structure in resistance properties and demonstration of its conservation amongst species. Journal of Applied Microbiology. 2001;91(2):364-72.

[219] Cazemier AE, Wagenaars SF, ter Steeg PF. Effect of sporulation and recovery medium on the heat resistance and amount of injury of spores from spoilage bacilli. Journal of Applied Microbiology. 2001;90(5):761-70.

[220] Ryu JH, Kim H, Beuchat LR. Spore formation by *Bacillus cereus* in broth as affected by temperature, nutrient availability, and manganese. Journal of Food Protection. 2005;68(8):1734-8.

[221] Widderich N, Rodrigues CD, Commichau FM, Fischer KE, Ramirez-Guadiana FH, Rudner DZ, et al. Salt-sensitivity of σ^H and Spo0A prevents sporulation of *Bacillus subtilis* at high osmolarity avoiding death during cellular differentiation. Molecular Microbiology. 2016;100(1):108-24.

[222] Feng Y, He Z, Ong SL, Hu J, Zhang Z, Ng WJ. Optimization of agitation, aeration, and temperature conditions for maximum β-mannanase production. Enzyme and Microbial Technology. 2003;32(2):282-9.

[223] Elisashvili V, Kachlishvili E, Chikindas ML. Recent advances in the physiology of spore formation for *Bacillus* probiotic production. Probiotics and Antimicrobial Proteins. 2019;11(3):731-47.

[224] Cho J-H, Kim Y-B, Kim E-K. Optimization of culture media for *Bacillus* species by statistical experimental design methods. Korean Journal of Chemical Engineering. 2009;26(3):754-9.

[225] Ruzal SM, López C, Rivas E, Sánchez-Rivas C. Osmotic strength blocks sporulation at stage II by impeding activation of early sigma factors in *Bacillus subtilis*. Current Microbiology. 1998;36(2):75-9.

[226] Lattermann C, Funke M, Hansen S, Diederichs S, Büchs J. Cross-section perimeter is a suitable parameter to describe the effects of different baffle geometries in shaken microtiter plates. Journal of Biological Engineering. 2014;8:18.

[227] Wollborn D, Müller RL, Munkler LP, Horstmann R, Germer A, Blank LM, et al. Auto-induction screening protocol for ranking clonal libraries of *Pichia pastoris* Mut^S strains. Biotechnology and Bioprocess Engineering. 2022;27(4):572-85.

[228] Lee JY, Passalacqua KD, Hanna PC, Sherman DH. Regulation of petrobactin and bacillibactin biosynthesis in *Bacillus anthracis* under iron and oxygen variation. PLoS One. 2011;6(6):e20777.

[229] Lankford CE, Walker JR, Reeves JB, Nabbut NH, Byers BR, Jones RJ. Inoculum-dependent division lag of *Bacillus* cultures and its relation to an endogenous factor(s) ("schizokinen"). Journal of Bacteriology. 1966;91(3):1070-9.

[230] Amaha M, Ordal ZJ, Touba A. Sporulation requirements of *Bacillus coagulans* var. *thermoacidurans* in complex media. Journal of Bacteriology. 1956;72(1):34-41.

[231] de Vries YP, Hornstra LM, de Vos WM, Abee T. Growth and sporulation of *Bacillus cereus* ATCC 14579 under defined conditions: temporal expression of genes for key sigma factors. Applied and Environmental Microbiology. 2004;70(4):2514-9.

[232] Hageman JH, Shankweiler GW, Wall PR, Franich K, McCowan GW, Cauble SM, et al. Single, chemically defined sporulation medium for *Bacillus subtilis*: growth, sporulation, and extracellular protease production. Journal of Bacteriology. 1984;160(1):438-41.

[233] Wilhelm E, Battino R, Wilcock RJ. Low-pressure solubility of gases in liquid water. Chemical Reviews. 1977;77(2):219-62.

[234] Weisenberger S, Schumpe A. Estimation of gas solubilities in salt solutions at temperatures from 273 K to 363 K. AIChE Journal. 1996;42(1):298-300.

[235] Rischbieter E, Schumpe A, Wunder V. Gas solubilities in aqueous solutions of organic substances. Journal of Chemical and Engineering Data. 1996;41(4):809-12.

[236] Dauner M, Storni T, Sauer U. *Bacillus subtilis* metabolism and energetics in carbon-limited and excess-carbon chemostat culture. Journal of Bacteriology. 2001;183(24):7308-17.

[237] Suttikul S, Charalampopoulos D, Chatzifragkou A. Biotechnological production of optically pure 2,3-butanediol by *Bacillus subtilis* based on dissolved oxygen control strategy. Fermentation. 2023;9(1):15.

[238] Robbins JW, Jr., Taylor KB. Optimization of *Escherichia coli* growth by controlled addition of glucose. Biotechnology and Bioengineering. 1989;34(10):1289-94.

[239] Halvorson H. Utilization of single L-amino acids as sole source of carbon and nitrogen by bacteria. Canadian Journal of Microbiology. 1972;18(11):1647-50.

[240] Tindale AE, Mehrotra M, Ottem D, Page WJ. Dual regulation of catecholate siderophore biosynthesis in *Azotobacter vinelandii* by iron and oxidative stress. Microbiology (Reading, England). 2000;146 (Pt 7):1617-26.

[241] Yu S, Teng C, Bai X, Liang J, Song T, Dong L, et al. Optimization of siderophore production by *Bacillus* sp. PZ-1 and its potential enhancement of phytoextration of Pb from soil. Journal of Microbiology and Biotechnology. 2017;27(8):1500-12.

[242] González-Pastor JE, Hobbs EC, Losick R. Cannibalism by sporulating bacteria. Science. 2003;301(5632):510-3.

[243] González-Pastor JE. Cannibalism: a social behavior in sporulating *Bacillus subtilis*. FEMS Microbiology Reviews. 2011;35(3):415-24.

[244] Parker GF, Daniel RA, Errington J. Timing and genetic regulation of commitment to sporulation in *Bacillus subtilis*. Microbiology (Reading, England). 1996;142 (Pt 12):3445-52.

[245] Lewis PJ, Magnin T, Errington J. Compartmentalized distribution of the proteins controlling the prespore-specific transcription factor σ^F of *Bacillus subtilis*. Genes to Cells. 1996;1(10):881-94.

[246] Scheidle M, Dittrich B, Klinger J, Ikeda H, Klee D, Büchs J. Controlling pH in shake flasks using polymer-based controlled-release discs with pre-determined release kinetics. BMC Biotechnology. 2011;11:25.

[247] Keil DT. Polymer-based nutrient release system for small-scale microbial fed-batch cultivations. PhD thesis. RWTH Aachen University. 2020.

8 Appendix

Appendix Table A1: Statistically significance analysis of OTR peaks of cultivation in complex and chemically defined medium.

The statistical results correspond to the cultivation shown in Figure 2-1. A t-test (equal variances, two-sided) was performed. A p-value <0.05 was determined to show statistical significance.

	Pbp complex medium	Moppa medium
p-value	<0.001	

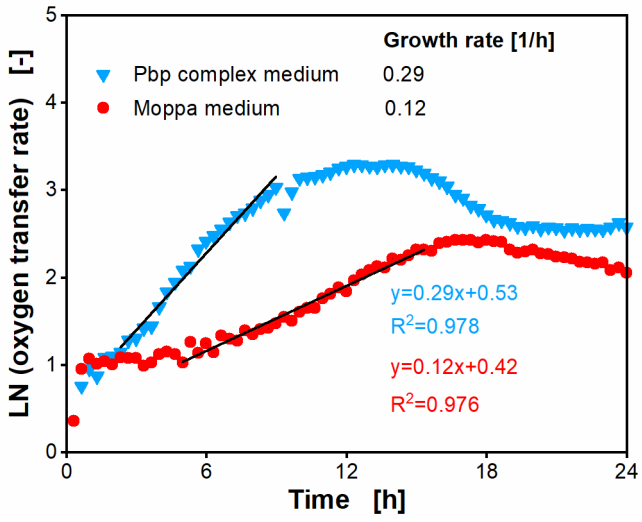

Appendix Figure A1: Determination of growth rate in complex and chemically defined Moppa medium.

Pbp complex medium (specified in Table 2-1) or chemically defined Moppa medium (specified in Table 2-2). Growth rates of *Paenibacillus polymyxa* were calculated based on regression of the linear range of logarithm of oxygen transfer rate (OTR). OTRs and cultivation conditions are shown in Figure 2-1.

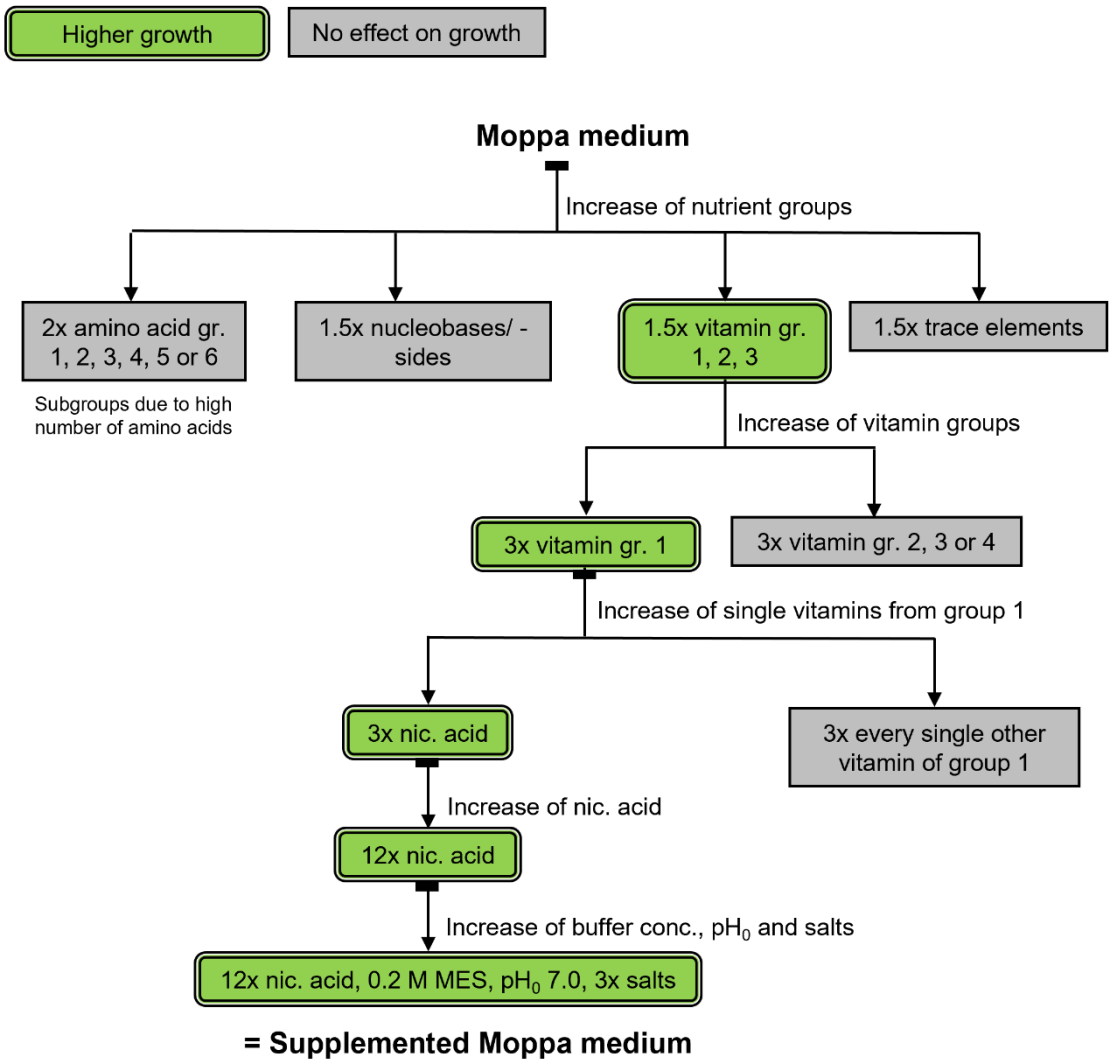

Appendix Figure A2: Schematic overview for systematic identification of growth limitations in Moppa medium for *Paenibacillus polymyxa*.

Compositions of Moppa medium and supplemented Moppa medium are specified in Table 2-2. Amino acid and vitamin groups are specified in Appendix Table A2 and Appendix Table A3, respectively. nic.: nicotinic, pH_0: initial pH, salts: $(NH_4)_2SO_4$, K_2HPO_4. Green boxes with double lined edging: growth and metabolic activity (Optical density and oxygen transfer rate peak or total oxygen consumed) are higher than in the reference cultivation. Grey boxes with single line edging: growth and metabolic activity are comparable to the reference cultivation. Bar at the end of the arrow marks the used medium reference, until a new arrow with bar is shown.

Appendix Table A2: Groups of amino acids in Moppa medium.

Group #	**1**	**2**	**3**	**4**	**5**	**6**
Amino acids	Methionine	Histidine	Aspartate	Cysteine	Phenylalanine	Alanine
		Proline	Isoleucine	Serine	Tyrosine	Leucine
		Glutamate	Threonine	Glycine	Tryptophane	Lysine
		Arginine				Valine

Appendix Table A3: Groups of vitamins in Moppa medium.

Group #	**1**	**2**	**3**	**4**
Vitamins	Nicotinic acid	Folic acid	Riboflavin	Biotin
	Pantothenic acid	Ascorbic acid	Orotic acid	
	p-Aminobenzoic acid		Inositol	
	Pyridoxamine			
	Pyridoxine			
	Thiamine			
	Vitamin B12			

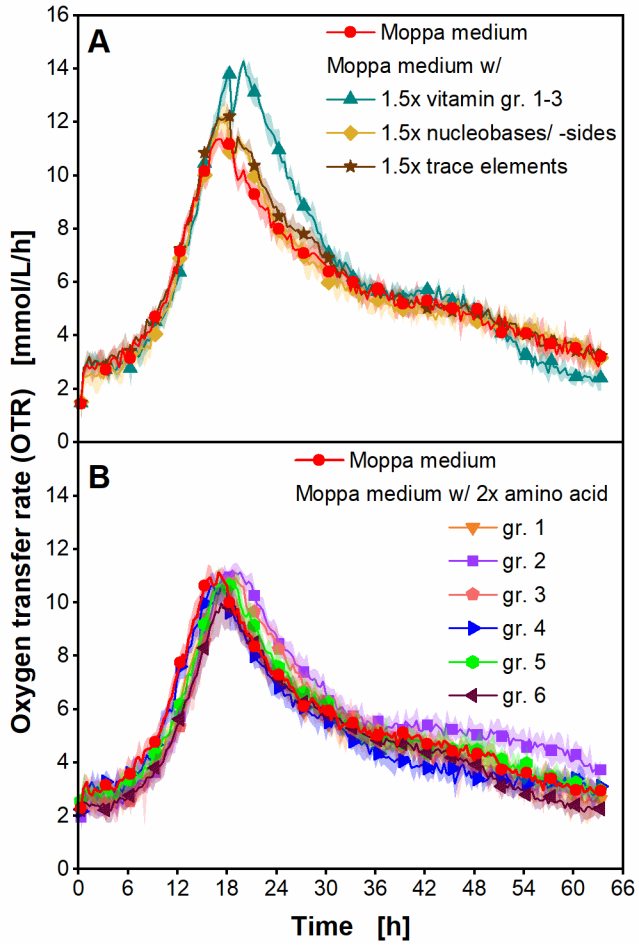

Appendix Figure A3: Cultivation of *Paenibacillus polymyxa* with increased concentrations of nutrient groups in microtiter plate.

Moppa medium (specified in Table 2-2) or Moppa medium with 1.5-fold concentration of vitamin group 1, 2 or 3 specified in Appendix Table A3, nucleobases/-sides or trace elements or Moppa medium with 2-fold concentration of amino acid groups specified in Appendix Table A2. **A, B:** Oxygen transfer rate (OTR). For clarity, only every 10th measuring point over time is marked as a symbol. Mean values for OTR of at least four replicates with standard deviations as shadows are shown. Cultivation conditions: Temperature 33 °C, 48-round well plate, filling volume 0.8 mL, shaking frequency 1000 rpm, shaking diameter 3 mm, 0.1 M MES, initial pH 6.5

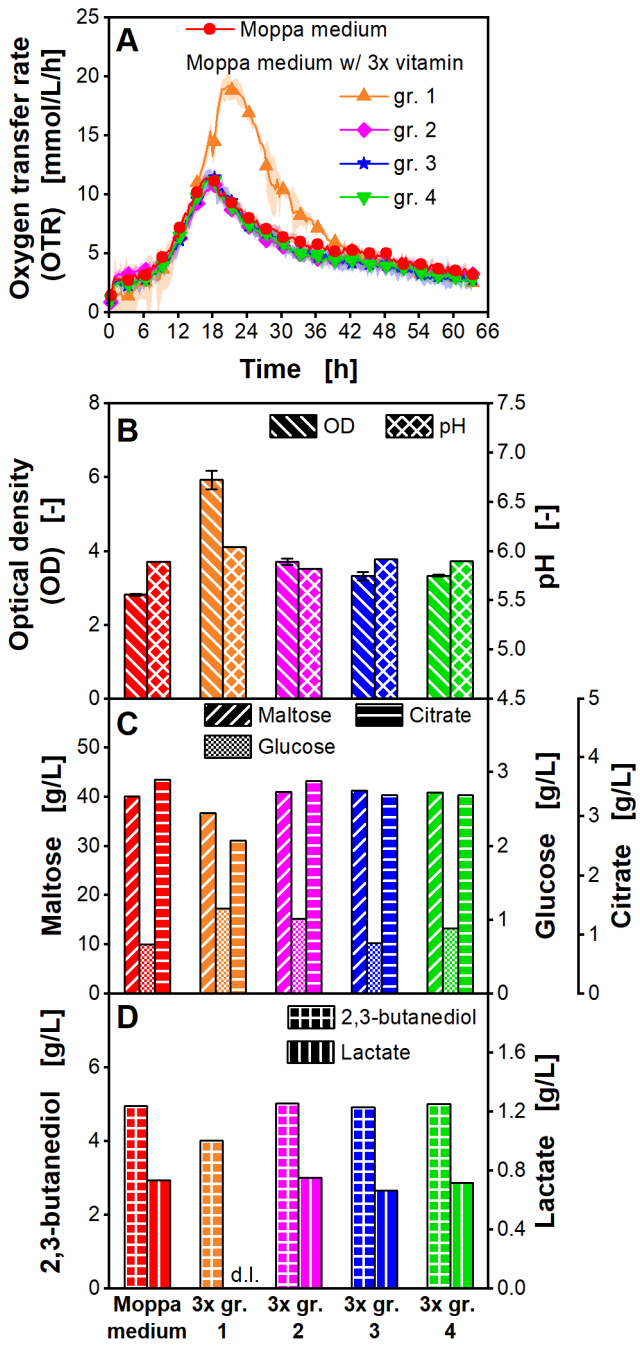

Appendix Figure A4: Cultivation of *Paenibacillus polymyxa* with increased concentrations of vitamin groups in microtiter plate.

Moppa medium (specified in Table 2-2) or Moppa medium with increased concentrations of vitamin groups. Vitamin groups (gr.) are specified in Appendix Table A3. Initial concentrations were: 55.0-56.7 g/L maltose, 3.5 g/L glucose, 3.0-3.1 g/L citrate. **A:** Oxygen transfer rate (OTR), **B:** Final optical density (OD) and pH, **C:** Final maltose, glucose and citrate concentration, **D:** Final 2,3-butanediol and lactate concentration. **A:** For clarity, only every 10th measuring point over time is marked as a symbol. Mean values for OTR of at least four replicates with standard deviations as shadows are shown. **B-D:** For offline analysis, samples (wells) of the

replicates of the OTR measurement were pooled at the end of the experiments. OD measurement of pooled samples was performed in triplicate and mean values with standard deviations depicted as error bars are shown. pH and concentrations of sugars and metabolites were determined in a single measurement of pooled samples. **D:** d.l. means that concentrations of components were lower than the detection limit. Final acetoin concentrations were lower than the detection limit. Parameters in **B-D** were determined after 63 h. Cultivation conditions: temperature 33 °C, 48-round well plate, filling volume 0.8 mL, shaking frequency 1000 rpm, shaking diameter 3 mm, 0.1 M MES, initial pH 6.5.

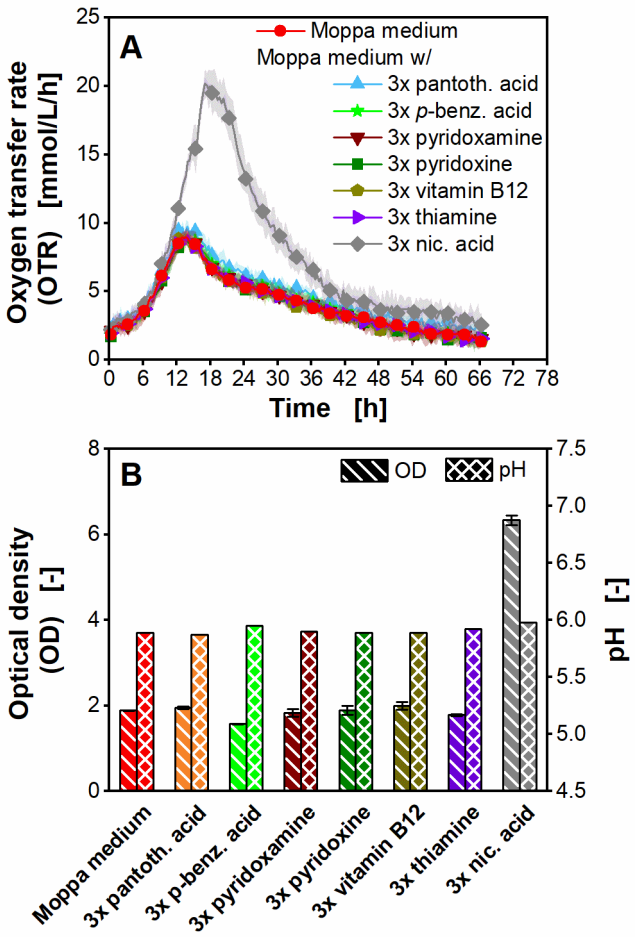

Appendix Figure A5: Cultivation of *Paenibacillus polymyxa* with increased concentrations of vitamins of group 1 in microtiter plate.

Moppa medium (specified in Table 2-2) or Moppa medium with increased concentrations of vitamins of group 1 specified in Appendix Table A3. Pantoth.: pantothenic, p-benz.: p-aminobenzoic, nic.: nicotinic. **A:** Oxygen transfer rate (OTR), **B:** Final optical density (OD) and pH. **A:** For clarity, only every 10th measuring point over time is marked as a symbol. Mean values for OTR of at least three replicates with standard deviations as shadows are shown. **B:** For offline analysis, samples (wells) of the replicates of the OTR measurement were pooled at the end of the experiments. OD measurement of pooled samples was performed in triplicate and mean values with standard deviations depicted as error bars are shown. pH was determined in a single measurement of pooled samples. Optical density and pH in **B** were determined after 66 h. The cultivation with the three-fold nicotinic acid concentration is shown in more detail in Figure 2-2A-D. Cultivation conditions: temperature 33 °C, 48-round well plate, filling volume 0.8 mL, shaking frequency 1000 rpm, shaking diameter 3 mm, 0.1 M MES, initial pH 6.5.

Appendix Table A4: Statistically significance analysis of OTR peaks of cultivation with increased concentration of nicotinic acid.

gr.: group, nic.: nicotinic. The statistical results correspond to the cultivations shown in Figure 2-2A. An ANOVA followed by a Bonferroni post-hoc test was performed. A p-value <0.05 was determined to show statistical significance. The p-value of ANOVA was <0.001.

	Moppa medium	**Moppa medium**	
		w/ 3x vitamin gr.1	**w/ 3x nic. acid**
Moppa medium	-	-	-
w/ 3x vitamin gr. 1	p-value <0.001	-	-
w/ 3x nic. acid	p-value <0.001	p-value = 0.012	-

Appendix Table A5: Statistically significance analysis of OTR peaks of cultivations with increased pH-buffer capacity.

nic.: nicotinic. The statistical results correspond to the cultivation shown in Figure 2-3. An ANOVA followed by a Bonferroni post-hoc test was performed. A p-value <0.05 was determined to show statistical significance. The p-value of ANOVA was <0.001.

	Moppa medium w/ 12x nic. acid		
	0.1 M MES, pH_0=6.5	**0.2 M MES, pH_0=6.5**	**0.2 M MES, pH_0=7.0**
0.1 M MES, pH_0=6.5	-	-	-
0.2 M MES, pH_0=6.5	p-value = 0.009	-	-
0.2 M MES, pH_0=7.0	p-value <0.001	p-value < 0.001	-

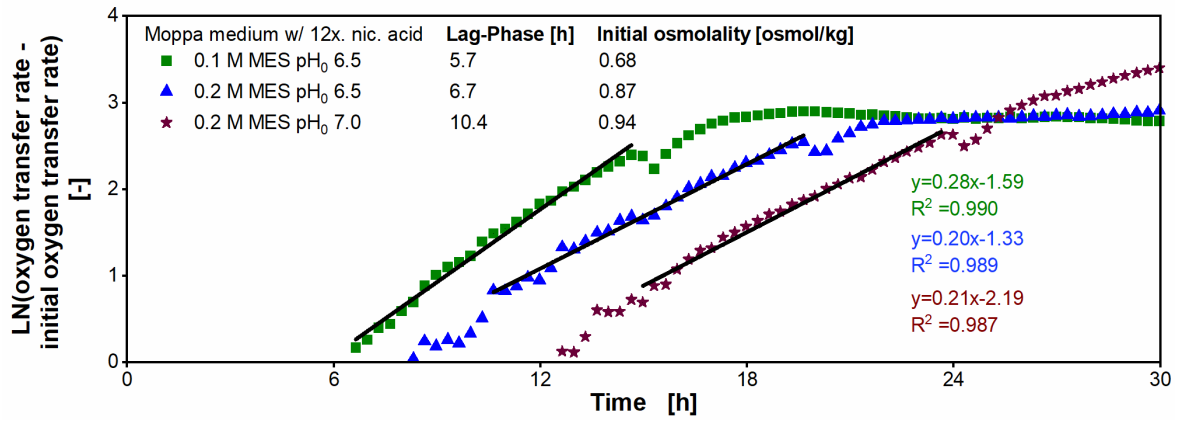

Appendix Figure A6: Determination of lag-phase for *Paenibacillus polymyxa* with increased pH - buffer capacity.

Moppa medium (specified in Table 2-2) with 12x nicotinic acid or Moppa medium with 12x nicotinic acid and with increased buffer concentration or with increased buffer concentration and initial pH. nic.: nicotinic, pH_0: initial pH. The logarithm of the difference of the oxygen transfer rate (OTR) and initial OTR was plotted over time. The initial OTR was determined based on the mean value of OTR values between 1.6 and 3.0 h. The lag-phases were calculated based on the intersection point of the regression line of the linear range. OTRs and cultivation conditions are shown in Figure 2-3. Osmolality after 86 h in Moppa medium with 12x nicotinic acid, 0.1 M MES and initial pH 6.5 is 0.64 osmol/kg. Osmolality after 86 h in Moppa medium with 0.2 M MES and initial pH 6.5 is 0.71 osmol/kg. Osmolality after 86 h in Moppa medium with 0.2 M MES and initial pH 7.0 is 0.73 osmol/kg.

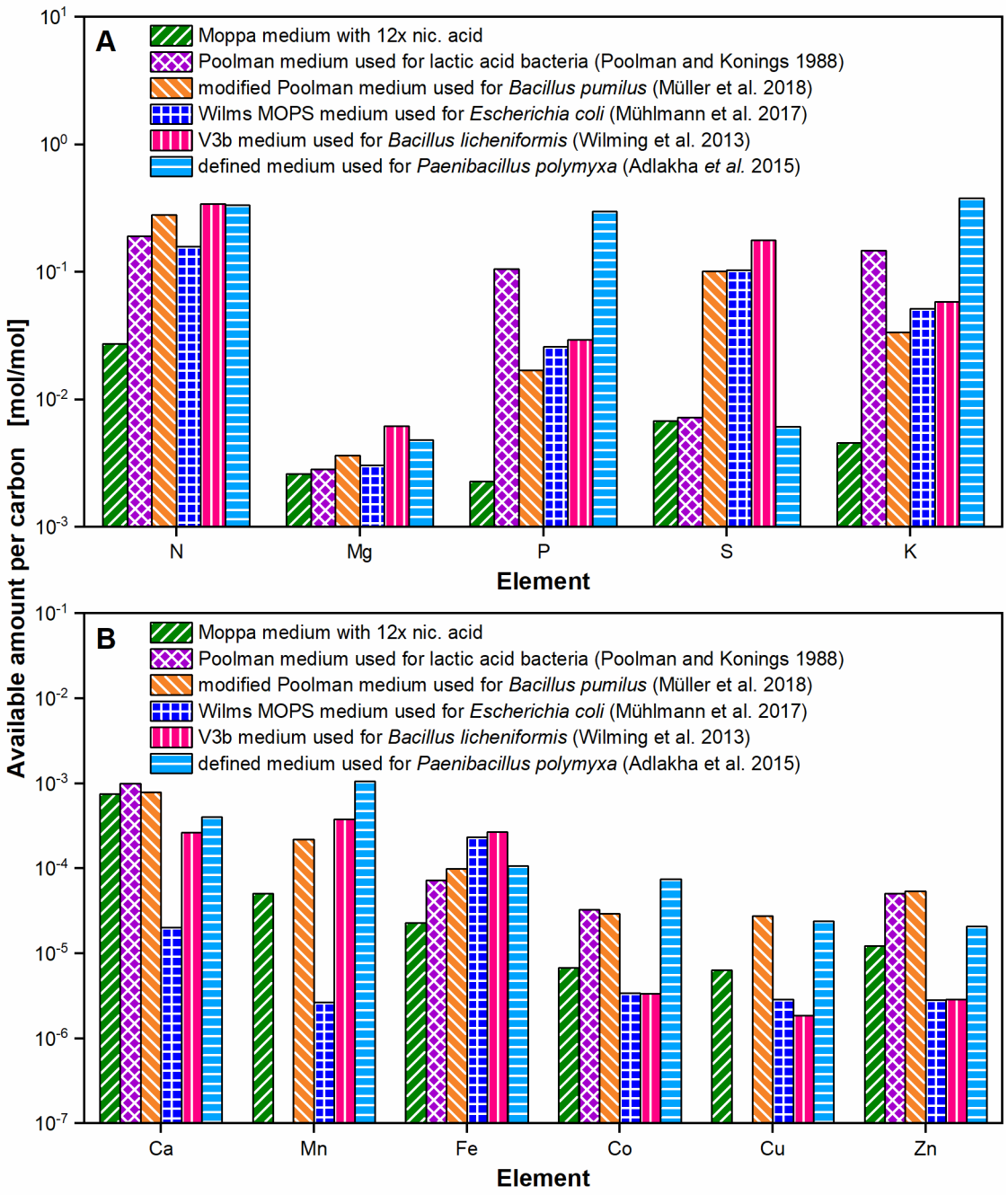

Appendix Figure A7: Elemental composition of Moppa medium, compared to established chemically defined media.

Moppa medium (specified in Table 2-2) with 12x nicotinic acid and literature known media for various bacteria [68, 135, 136, 138, 159]. **A:** Amounts were calculated in amount of nitrogen (N), magnesium (Mg), phosphor (P), sulfur (S), and potassium (K) per amount of carbon. **B:** Amounts were calculated in amount of calcium (Ca), manganese (Mn), iron (Fe), cobalt (Co), copper (Cu), and zinc (Zn) per amount of carbon. For calculation of the amount of carbon (C) in Moppa medium with 12x nicotinic acid, 60 g/L maltose, 2.6 g/L glucose, 3.6 g/L citrate, and carbon of amino acids, vitamins and nucleobases/-sides were considered. In all other media containing amino acids, vitamins and nucleobases/-sides, the carbon of those nutrients was also

considered. For calculation of the amount of N, Mg, P, S, K, Ca, Mn, Fe, Co, Cu, Zn, not only the amount of those elements in the salts and trace elements was considered, but also the amount of those elements in other medium components, like vitamins, amino acids and nucleobases/-sides. Y-axis: logarithmic scale.

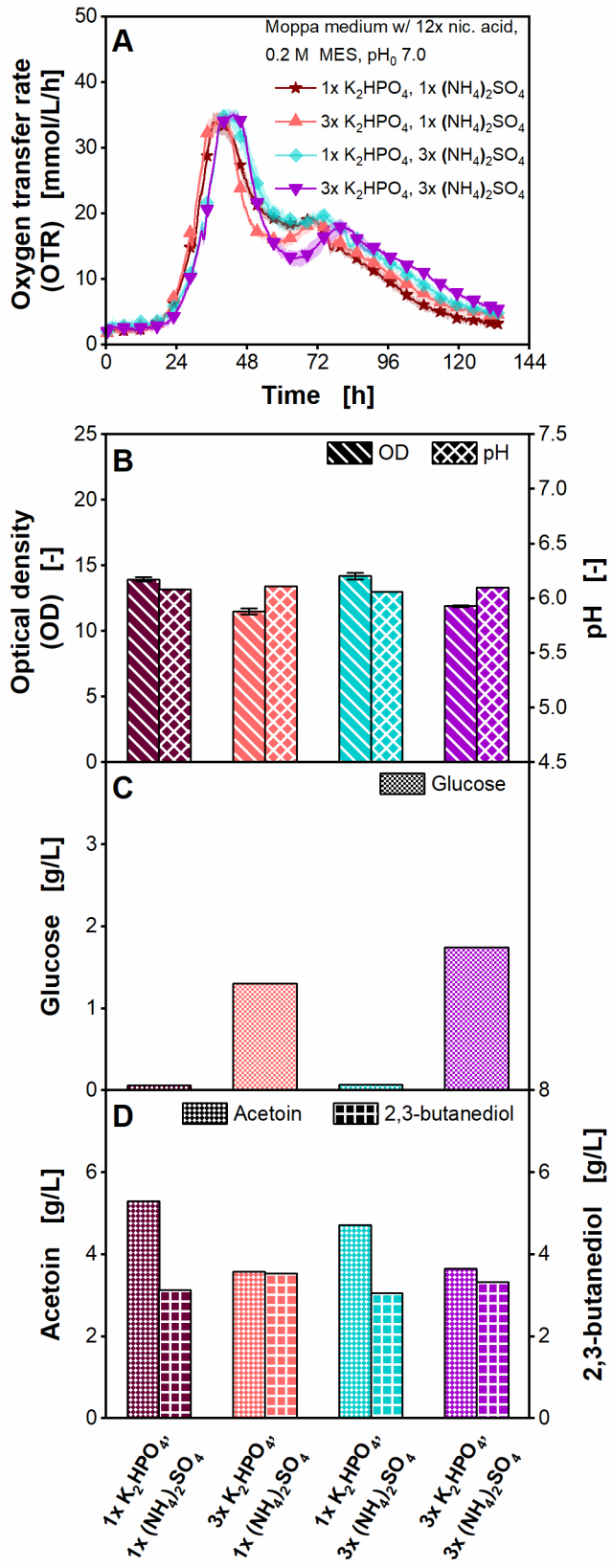

Appendix Figure A8: **Cultivation of *Paenibacillus polymyxa* with increased concentration of salts in microtiter plate.**

Moppa medium (specified in Table 2-2) with 12x nicotinic acid, 0.2 M MES, initial pH 7.0 or Moppa medium with 12x nicotinic acid, 0.2 M MES, initial pH 7.0 and with increased concentration of K_2HPO_4 and/ or $(NH_4)_2SO_4$. nic.: nicotinic, pH_0: initial pH. Initial concentrations were: 57.0-57.4 g/L maltose, 3.1-3.4 g/L glucose, 3.0-3.2 g/L citrate. **A:** Oxygen transfer rate (OTR), **B:** Final optical density (OD) and pH, **C:** Final glucose concentration, **D:** Final acetoin and 2,3-butanediol concentration. **A:** For clarity, only every 18^{th} measuring point over time is marked as a symbol. Mean values for OTR of at least four replicates with standard deviations as shadows are shown. **B-D:** For offline analysis, samples (wells) of the replicates of the OTR measurement were pooled at the end of the experiments. OD measurement of pooled samples was performed in triplicate and mean values with standard deviations depicted as error bars are shown. pH and concentrations of sugars and metabolites were determined in a single measurement of pooled samples. Final maltose, citrate and lactate concentrations were lower than the detection limit. Parameters in **C-D** were determined after 133 h. Cultivation conditions: temperature 33 °C, 48-round well plate, filling volume 0.8 mL, shaking frequency 1000 rpm, shaking diameter 3 mm. The medium with 3x K_2HPO_4 und 3x $(NH_4)_2SO_4$ is called supplemented Moppa medium.

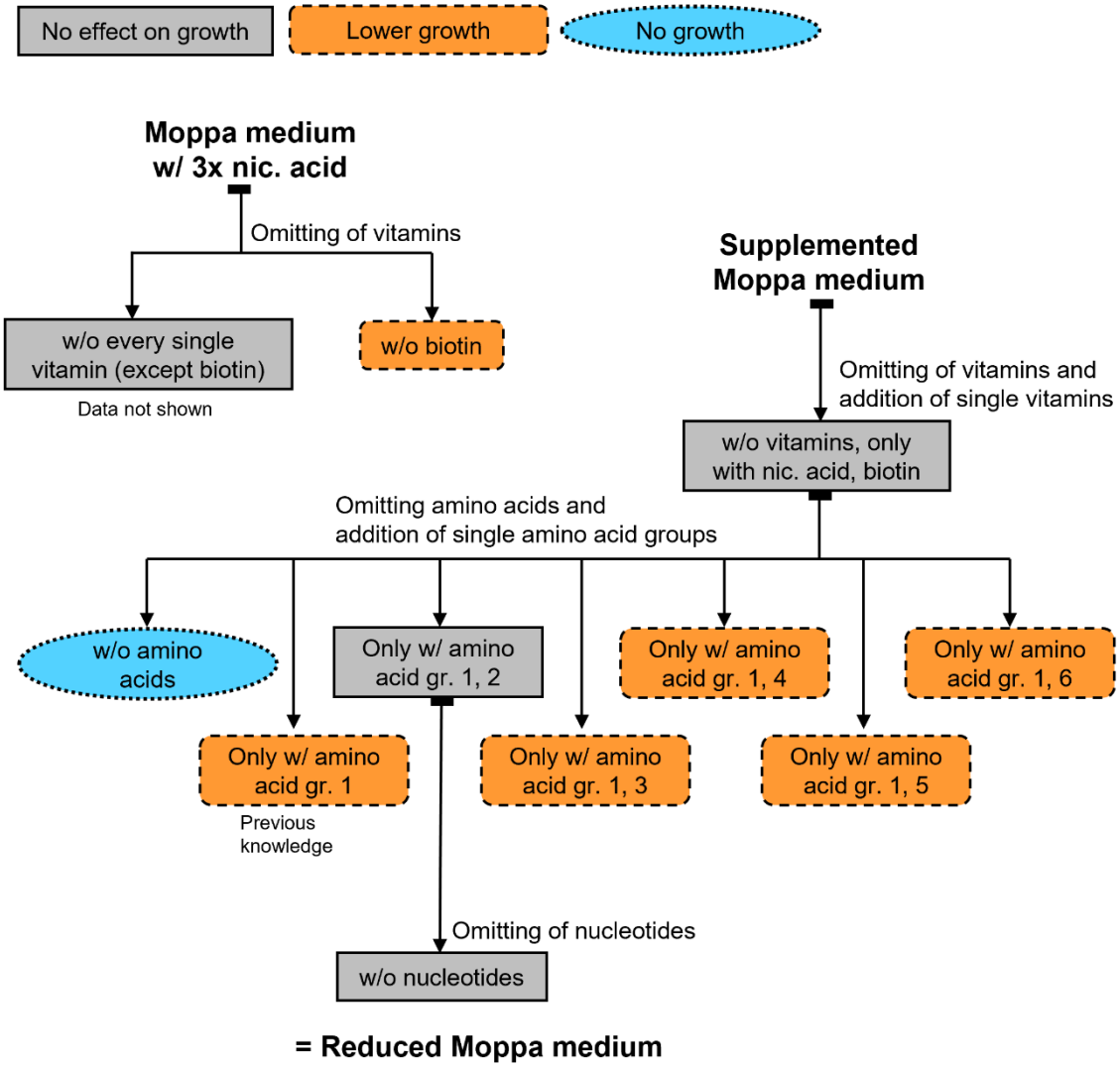

Appendix Figure A9: Schematic overview for systematic reduction of medium ingredients in supplemented Moppa medium for *Paenibacillus polymyxa*.

Compositions of Moppa medium, supplemented Moppa medium and reduced Moppa medium are specified in Table 2-2. Amino acid and vitamin groups are specified in Appendix Table A2 and Appendix Table A3, respectively. nic. acid: nicotinic acid. Grey boxes with solid single line edging: growth and metabolic activity (optical density and oxygen transfer rate peak or total oxygen consumed) is comparable to the reference cultivation. Light brown boxes with dashed line edging: Growth and metabolic activity is lower than in the reference cultivation. Blue ellipse with dotted line edging: No growth is observed. Bar at the end of the arrow marks the used medium reference until a new arrow with bar is shown.

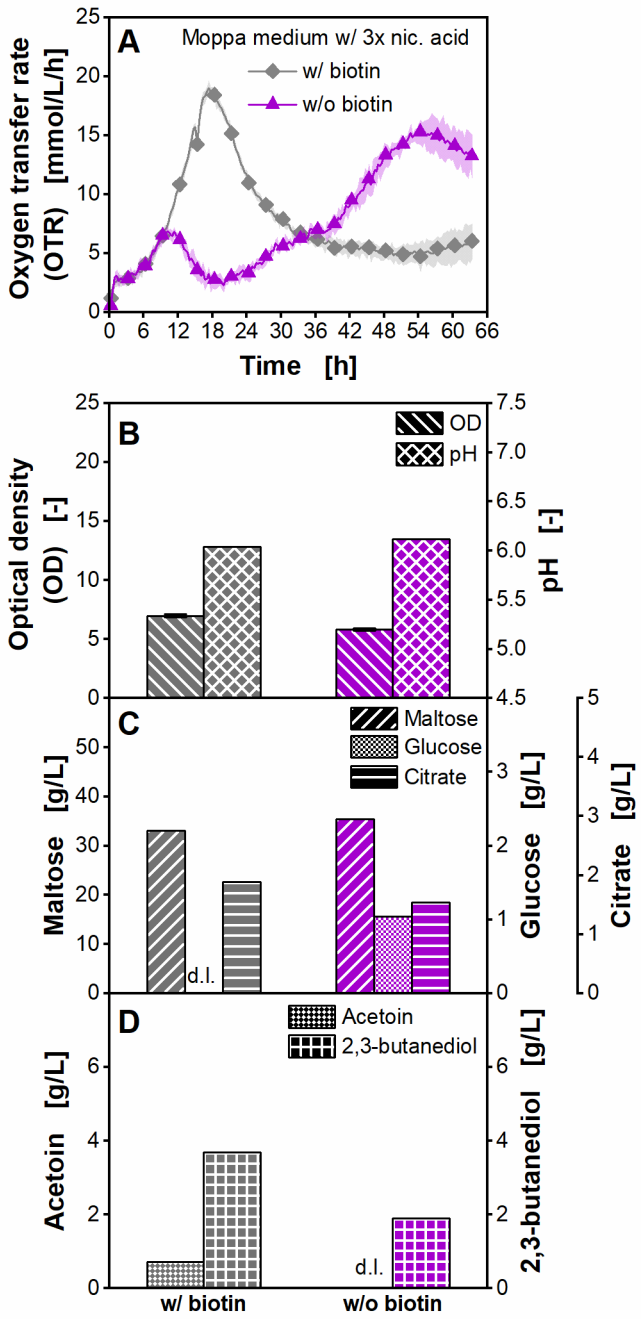

Appendix Figure A10: Cultivation of *Paenibacillus polymyxa* without biotin in microtiter plate.

Moppa medium (specified in Table 2-2) with 3x nicotinic acid with and without biotin. nic.: nicotinic. Initial concentrations were: 53.0-53.1 g/L maltose, 4.2-4.4 g/L glucose, 3.2-3.6 g/L citrate. **A:** Oxygen transfer rate (OTR), **B:** Final optical density (OD) and pH, **C:** Final maltose, glucose and citrate concentration, **D:** Final acetoin and 2,3-butanediol concentration. **A:** For clarity, only every 10th measuring point over time is marked as a symbol. Mean values for OTR of four replicates with standard deviations as shadows are shown. **B-D:** For offline analysis, samples (wells) of the replicates of the OTR measurement were pooled at the end of the experiments. OD measurement of pooled samples was performed in triplicate and mean values with standard deviations depicted as error bars are shown. pH and concentrations of sugars and

metabolites were determined in a single measurement of pooled samples. **C, D:** d.l. means that concentrations of components were lower than the detection limit. Final lactate concentration was lower than the detection limit. Parameters in **B-D** were determined after 63 h. Cultivation conditions: temperature 33 °C, 48-round well plate, filling volume 0.8 mL, shaking frequency 1000 rpm, shaking diameter 3 mm, 0.1 M MES, initial pH 6.5.

Appendix Table A6: Statistically significance analysis of OTR peaks of cultivation only with growth relevant vitamins.

nic.: nicotinic. The statistical results correspond to the cultivations shown in Figure 2-4. A t-test (equal variances, two-sided) was performed. A p-value <0.05 was determined to show statistical significance.

	Supplemented Moppa medium	
	w/ vitamins	**w/o vitamins, only w/ 12x nic. acid, 1x biotin**
p-value	0.137	

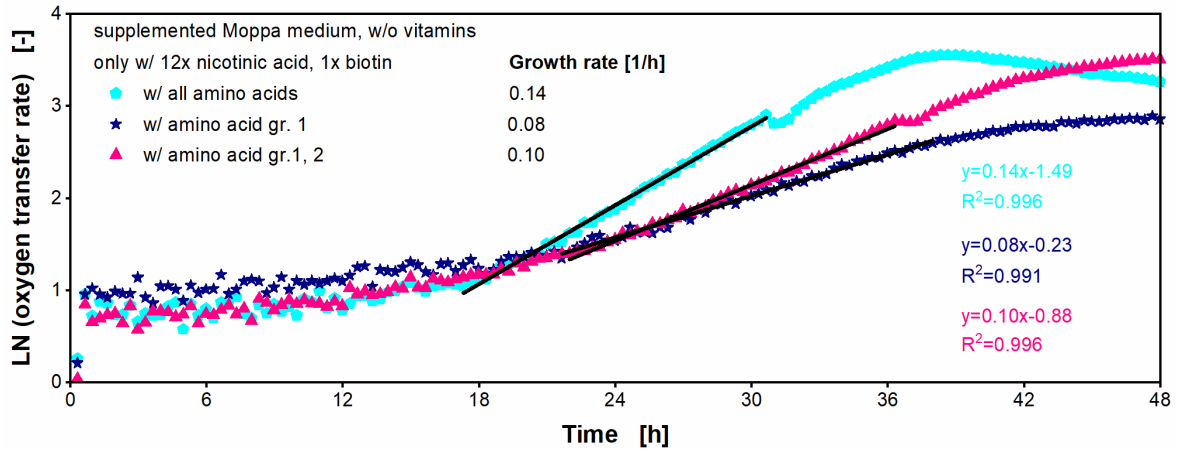

Appendix Figure A11: Determination of growth rate for *Paenibacillus polymyxa* cultivation with varying amino acid composition.

Supplemented Moppa medium (specified in Table 2-2) without vitamins (only with nicotinic acid and biotin) and with or without amino acid groups, specified in Appendix Table A2. Growth rates were calculated based on regression of the linear range of logarithm of oxygen transfer rate (OTR). OTRs and cultivation conditions are shown in Figure 2-5A.

Appendix Table A7: Statistically significance analysis of OTR peaks of cultivation with varying amino acid composition.

gr.: group, nic.: nicotinic. The statistical results correspond to the cultivations shown in Figure 2-5. An ANOVA followed by a Bonferroni post-hoc test was performed. A p-value <0.05 was determined to show statistical significance. The p-value of ANOVA was <0.001.

	Supplemented Moppa medium, w/o vitamins, only w/ 12x nic. acid, 1x biotin						
	w/ all amino acids	**w/ amino acid gr. 1**	**w/ amino acid gr. 1,2**	**w/ amino acid gr. 1,3**	**w/ amino acid gr. 1,4**	**w/ amino acid gr. 1,5**	**w/ amino acid gr. 1,6**
w/ all amino acids	-	-	-	-	-	-	-
w/ amino acid gr. 1	<0.001	-	-	-	-	-	-
w/ amino acid gr. 1,2	1.000	<0.001	-	-	-	-	-
w/ amino acid gr. 1,3	<0.001	1.000	<0.001	-	-	-	-
w/ amino acid gr. 1,4	<0.001	0.003	<0.001	<0.001	-	-	-
w/ amino acid gr. 1,5	<0.001	1.000	<0.001	1.000	0.002	-	-
w/ amino acid gr. 1,6	<0.001	1.000	<0.001	0.750	0.007	1.000	-

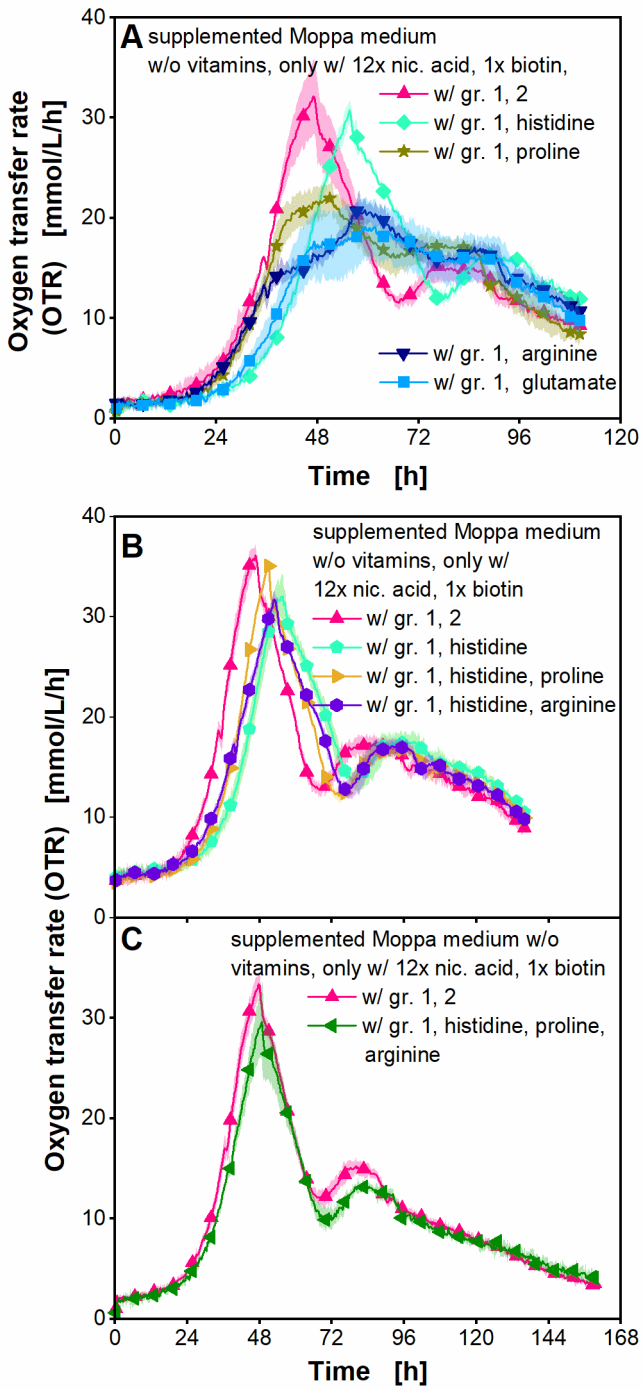

Appendix Figure A12: Cultivation of *Paenibacillus polymyxa* with single amino acids of group 2 in microtiter plate.

Supplemented Moppa medium (specified in Table 2-2) without vitamins (only with nicotinic acid and biotin) and without amino acids (only with amino acid group 1) and with or without amino acids of group 2 specified in Appendix Table A2. **A, B, C:** Oxygen transfer rate (OTR). For clarity, only every 20th measuring point over time is marked as a symbol. Mean values for OTR of at least four replicates with standard deviations as shadows are shown. Cultivation conditions: temperature 33 °C, 48-

round well plate, filling volume 0.8 mL, shaking frequency 1000 rpm, shaking diameter 3 mm.

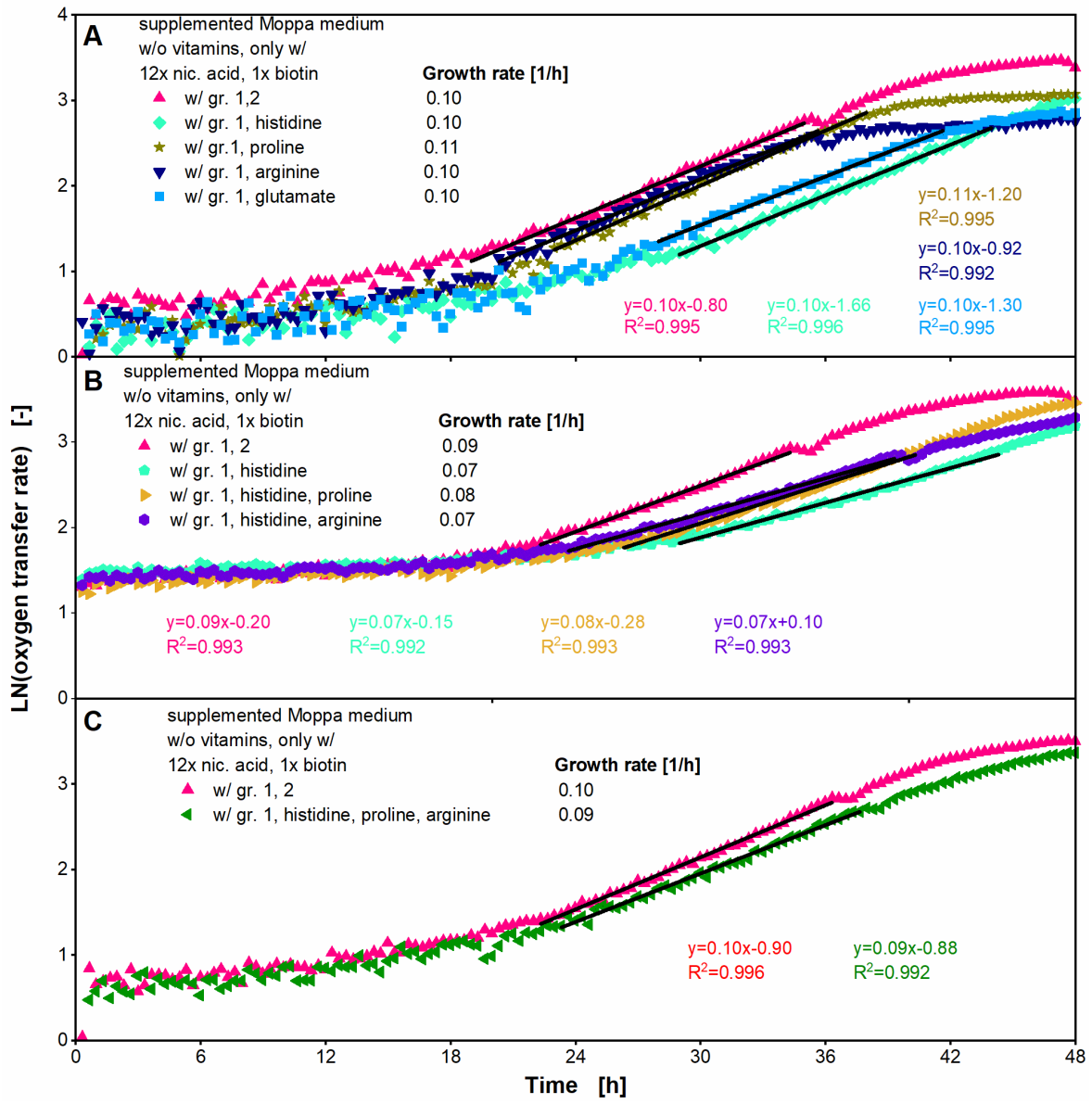

Appendix Figure A13: Determination of growth rate for *Paenibacillus polymyxa* cultivation with single amino acids of group 2.

Supplemented Moppa medium (specified in Table 2-2) without vitamins (only with nicotinic acid and biotin) and without amino acids (only with amino acid group 1) and with or without amino acids of group 2 specified in Appendix Table A2. **A, B, C:** Growth rates were calculated based on regression of the linear range of logarithm of oxygen transfer rate (OTR). OTRs and cultivation conditions are shown in Appendix Figure A12.

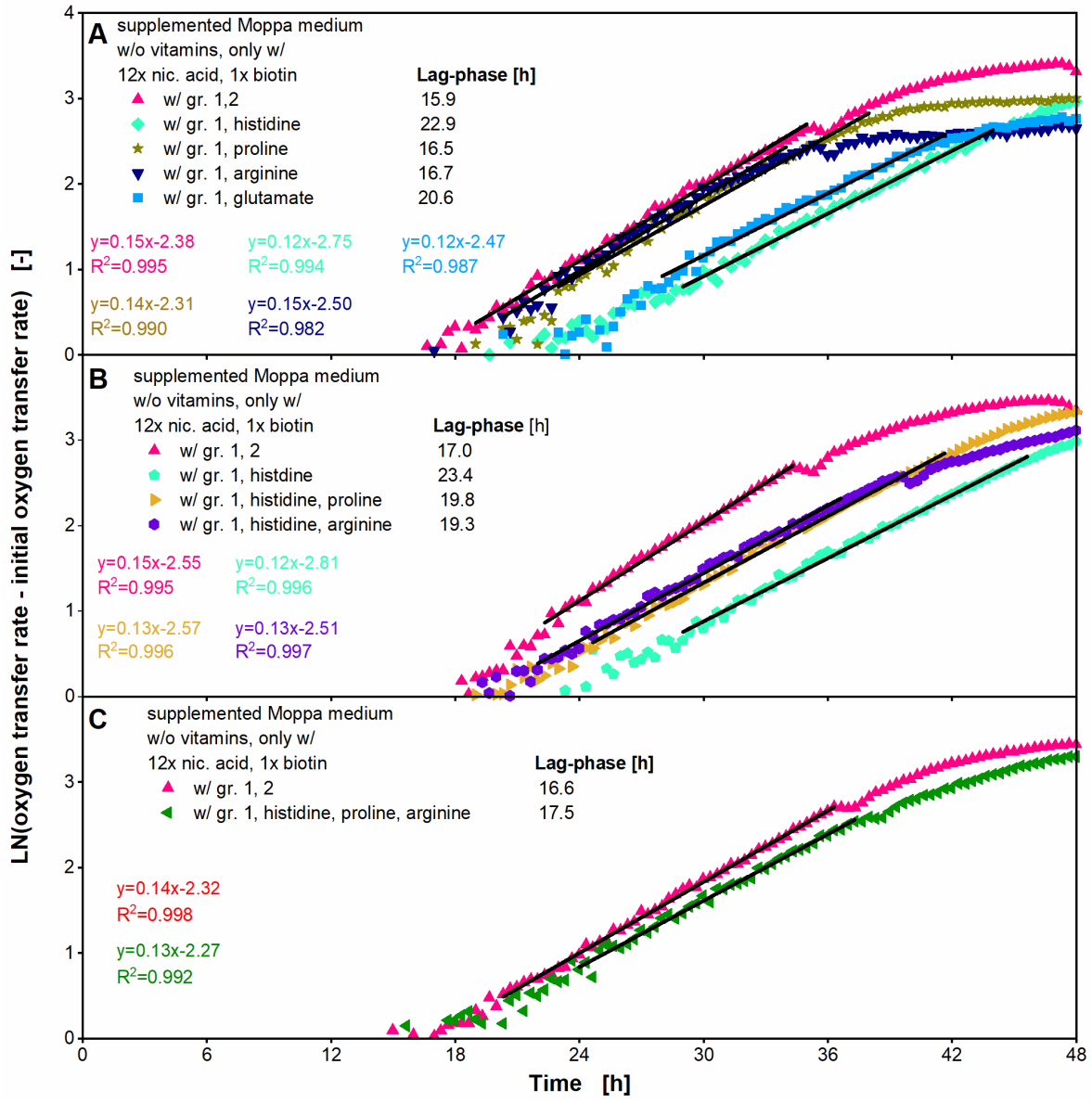

Appendix Figure A14: Determination of lag-phase for *Paenibacillus polymyxa* cultivation with single amino acids of group 2.

Supplemented Moppa medium (specified in Table 2-2) without vitamins (only with nicotinic acid and biotin) and without amino acids (only with amino acid group 1) and with or without amino acids of group 2 specified in Appendix Table A2. **A, B, C:** The logarithm of the difference of the oxygen transfer rate (OTR) and initial OTR was plotted over time. The initial OTR was determined based on the mean value of OTR values between 1.6 and 3.0 h. The lag-phases were calculated based on the intersection point of the regression line of the linear range. OTRs and cultivation conditions are shown in Appendix Figure A12.

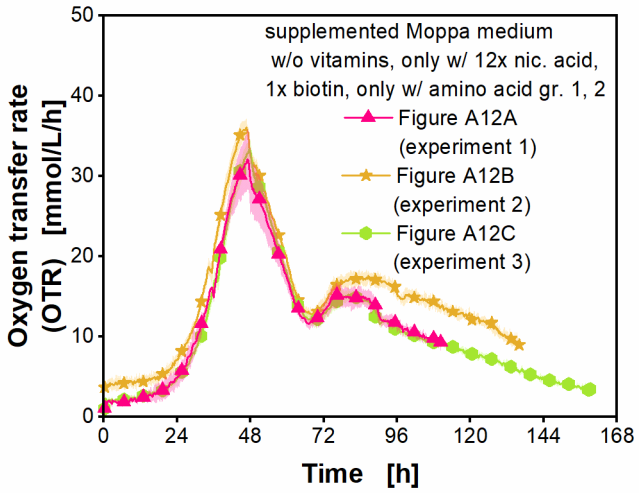

Appendix Figure A15: Reproducibility of respiration activity of *Paenibacillus polymyxa* in chemically defined medium in microtiter plate.

Supplemented Moppa medium (specified in Table 2-2) without vitamins (only with nicotinic acid and biotin) and without amino acids (only with amino acid group 1 and 2 specified in Appendix Table A2). Oxygen transfer rate (OTR). For clarity, only every 20th measuring point over time is marked as a symbol. Mean values for OTR of four replicates with standard deviations as shadows are shown. OTRs are also shown in Appendix Figure A12. Cultivation conditions are shown in Appendix Figure A12.

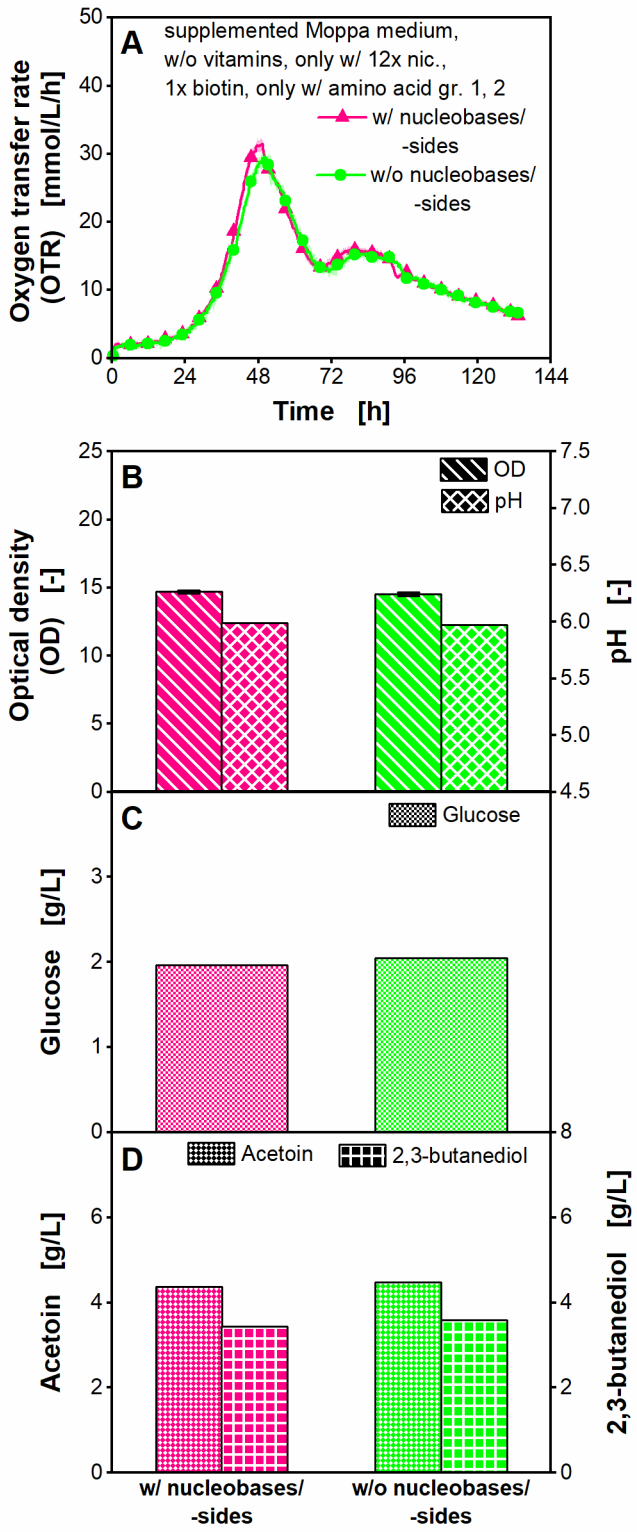

Appendix Figure A16: Cultivation of *Paenibacillus polymyxa* without nucleobases/ -sides in microtiter plate.

Supplemented Moppa medium (specified in Table 2-2) without vitamins (only with nicotinic acid and biotin) and without amino acids (only with amino acid group 1 and 2) and with or without nucleobases/-sides. nic.: nicotinic. Amino acids groups (gr.)

are specified in Appendix Table A2. Initial concentrations were: 57.4-58.2 g/L maltose, 3.3 g/L glucose, 3.1 g/L citrate. **A:** Oxygen transfer rate (OTR), **B:** Final optical density (OD) and pH, **C:** Final glucose concentration, **D:** Final acetoin and 2,3-butanediol concentration. **A:** For clarity, only every 18th measuring point over time is marked as a symbol. Mean values for OTR of at least four replicates with standard deviations as shadows are shown. Standard deviations are not well recognizable, because they are small. **B-D:** For offline analysis, samples (wells) of the replicates of the OTR measurement were pooled at the end of the experiments. OD measurement of pooled samples was performed in triplicate and mean values with standard deviation depicted as error bars are shown. pH and concentrations of sugars and metabolites were determined in a single measurement of pooled samples. Final maltose, citrate and lactate concentrations were lower than the detection limit. Parameters in **B-D** were determined after 133 h. Cultivation conditions: temperature 33 °C, 48-round well plate, filling volume 0.8 mL, shaking frequency 1000 rpm, shaking diameter 3 mm.

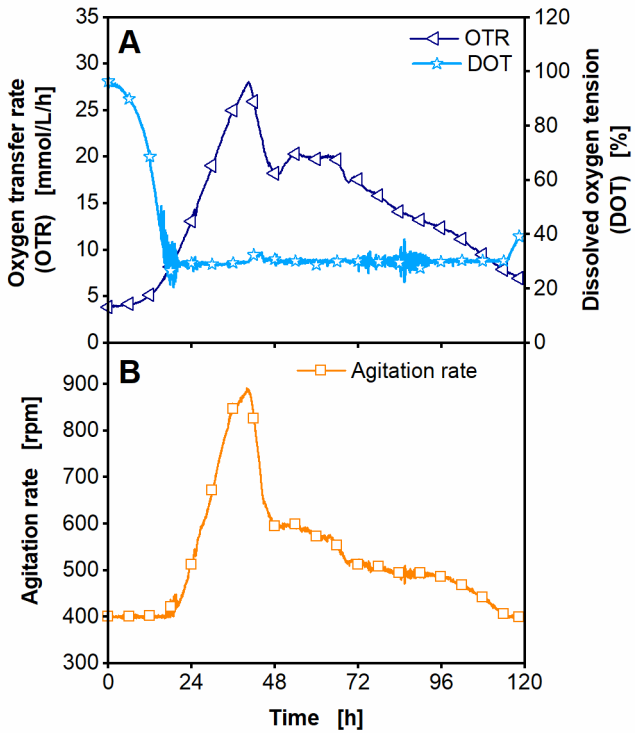

Appendix Figure A17: Dissolved oxygen tension and agitation speed in the cultivation of *Paenibacillus polymyxa* in fermenter.

The fermentation is shown in Figure 2-7. Reduced Moppa medium (specified in Table 2-2). **A:** Oxygen transfer rate (OTR) and dissolved oxygen tension (DOT), **B:** Agitation rate. For clarity, only every 720th measuring point is marked as a symbol for OTR, DOT and agitation rate. Cultivation conditions: temperature 33 °C, filling volume 1 L, pH control at pH 6.5, without MES buffer.

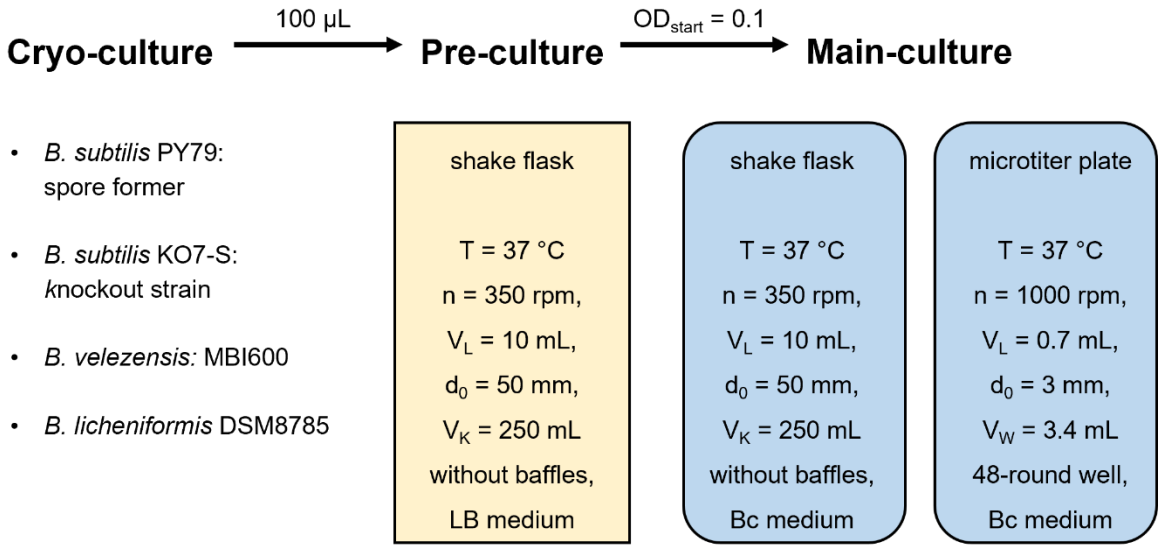

Appendix Figure A18: Cultivation protocol of *Bacillus subtilis* spore former and knockout strain, *Bacillus velezensis* and *Bacillus licheniformis*.

T = temperature, n = shaking frequency, V_L = filling volume, d_0 = shaking diameter, V_K = nominal volume of shake flask, V_W = volume of well of microtiter plate. Pre-cultures were inoculated from cryo-cultures and conducted in a RAMOS device [70, 71]. All recorded pre-cultures of experiments are shown in Appendix Figure A25. Main-cultures were inoculated from pre-culture and conducted in a RAMOS device or BioLector device (commercial BioLector I of Beckman Coulter GmbH or in-house built version [72, 75, 76]). All recorded main-cultures of experiments, in which oxygen transfer rate or dissolved oxygen tension was measured, are shown in Appendix Figure A24.

Appendix Section A1: Correction of DOT measured in commercial BioLector.

As the measured DOT values exhibited an offset in the commercial BioLector, the measured DOT was corrected as follows: A DOT maximum (DOT_{max}) and DOT minimum (DOT_{min}) were determined based on the measured DOT curves. Parallel to the cultivation of the *Bacillus* strains, non-inoculated pure medium was incubated in the same MTP. The non-inoculated medium was defined as DOT_{max}, as there was no respiration activity expected.

1. The DOT_{max} (green dashed horizontal line in Appendix Figure A19A and B) was calculated as the mean value of DOT values of all time points and replicates (wells) of non-inoculated medium.

2. The DOT_{min} (blue, turquoise, pink, and grey dotted horizontal lines in Appendix Figure A19A and B) was separately determined for each strain and each replicate (well). This minimum was determined as a mean value of the measured DOT between 3.5 and 4.5 h for *B. subtilis* (black dashed vertical lines in Appendix Figure A19A and B), between 4.5 and 5.3 h for *B. velezensis* and between 10.0 and 11.0 h for *B. licheniformis* for each replicate (well). The periods correspond to a plateau observed in the cultivations.

3. The DOT_{max} was regarded as 100 % and the DOT_{min} was regarded as 0 %. This led to equations (1) and (2) with a as the slope and b as the y-axis intercept.

$$100\ \% = a \cdot DOT_{max} + b \quad (1)$$

$$0\ \% = a \cdot DOT_{min} + b \quad (2)$$

4. The equations were solved for a and b for each replicate (well) in each experiment.

5. The corrected DOT (Appendix Figure A19C and D) was calculated for each replicate (well) of the corresponding experiment. The following equation (3) was used as a basis for DOT correction.

$$y = a \cdot x + b \quad (3)$$

with y as the corrected DOT, a as $\frac{100\ \%}{\mathrm{DOT_{max}} - \mathrm{DOT_{min}}}$, x as the measured DOT (Appendix Figure A19A and B) and b as $\frac{100\ \%}{\frac{\mathrm{DOT_{max}}}{\mathrm{DOT_{min}}} - 1}$.

6. This led to the following equation (4) for DOT correction.

$$corrected\ DOT = \frac{100\ \%}{DOT_{max} - DOT_{min}} \cdot measured\ DOT + \frac{100\ \%}{\frac{DOT_{max}}{DOT_{min}} - 1} \quad (4)$$

7. After performing the correction of DOT for each replicate (well), the mean value of the DOT of the replicates and standard deviation were calculated.

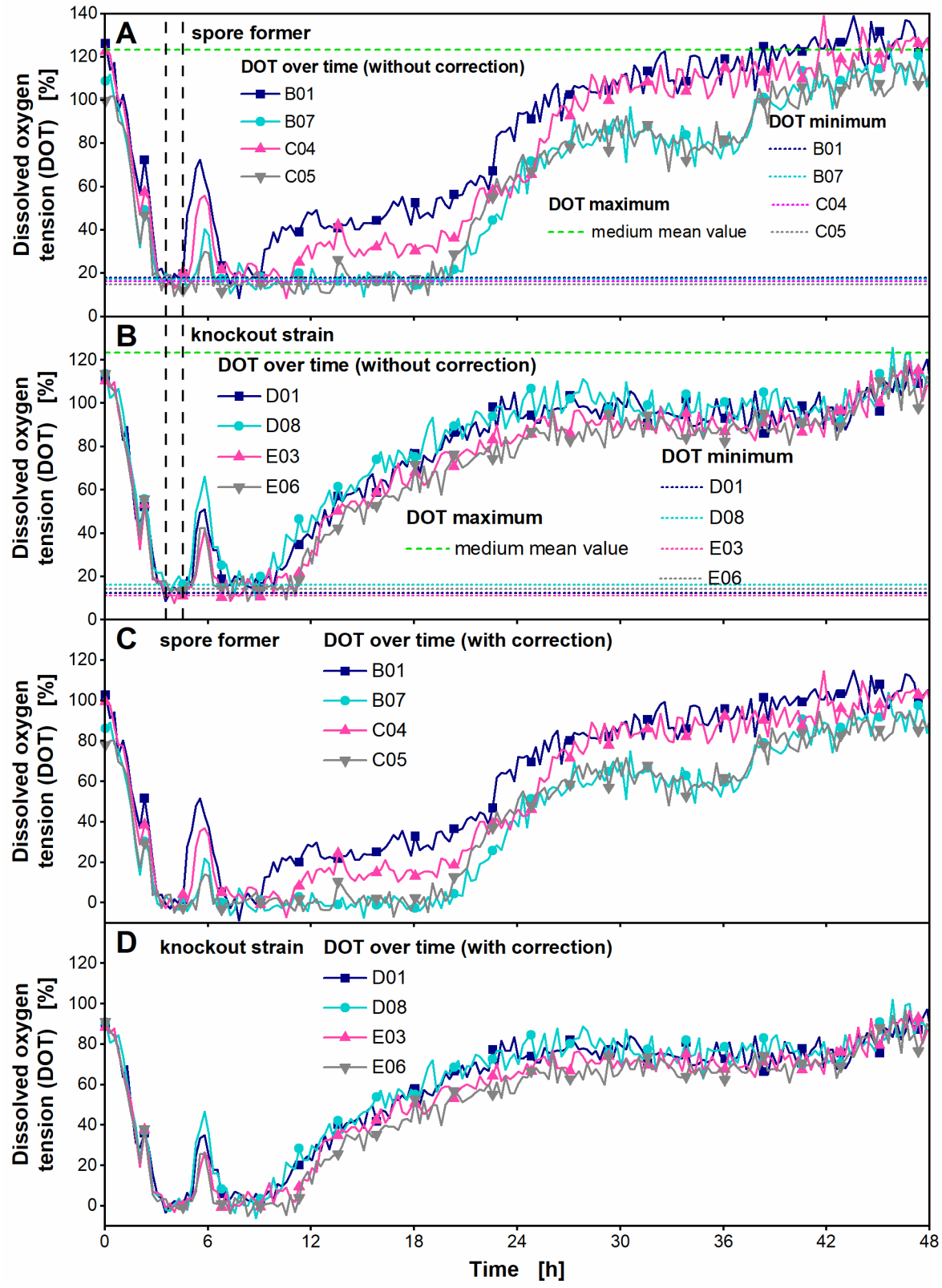

Appendix Figure A19: Determination of DOT minimum and correction of DOT values for cultivation of *Bacillus subtilis* PY79 spore former and KO7-S knockout strain.

(A) Uncorrected dissolved oxygen tension (DOT) of spore former, **(B)** uncorrected DOT of knockout strain, **(C)** corrected DOT of spore former, **(D)** corrected DOT of knockout strain. Exemplarily four replicates (wells) in microtiter plate are shown of the experiment depicted in Figure 3-1B. The DOT minimum was determined as a mean value of DOT values between 3.5 and 4.5 h (black vertical dashed lines). The horizontal dotted lines (blue, turquoise, pink, and grey) show the DOT minimum for each replicate. The green horizontal dashed line represents the DOT maximum, which is the mean value of non-inoculated pure medium of all time points and replicates (wells). For clarity, only every 10^{th} measuring point is marked by a symbol and only the first 48 h of cultivation are shown. The measured DOT was corrected as described in Appendix Section A1. Cultivation conditions in a commercial BioLector I device (Beckman Coulter GmbH): temperature 37 °C, 48-round well plate (MTP-R48-BOH 1), filling volume 0.7 mL, shaking frequency 1000 rpm, shaking diameter 3 mm, Bc medium with 10 g/L glucose.

Appendix Section A2: Calculation of OTR from DOT of commercial BioLector

The DOT measured in the commercial BioLector (after correction as described in Appendix Section A1) was used to calculate the OTR in the MTP. The calculation was performed based on equation (5):

$$OTR = k_L a \cdot L_{O_2} \cdot (pO_2{}^{gas} - \frac{DOT}{100} \cdot pO_2{}^{cal}) \quad (5)$$

with k_La as the volumetric oxygen transfer coefficient (1/h), L_{O2} as the oxygen solubility [mol/L/bar], pO_2^{cal} as the head space oxygen partial pressure during calibration (simplified assumption: 0.21 bar), pO_2^{gas} as the oxygen partial pressure in the head space of each well (simplified assumption: 0.21 bar). The oxygen solubility L_{O2} was calculated based on literature [233-235]. The medium component soy flour was neglected.

The k_La was calculated based on a parallel cultivation in the in-house built µRAMOS [73], in which the OTR was determined, and in the commercial BioLector I, in which the DOT was measured. The cultivation in the BioLector was performed as described in chapter 3.2.3 and 3.2.4. The cultivation in the µRAMOS was conducted using the same cultivation parameters. A gas-permeable sealing foil (900371-T, HJ-Bioanalytik GmbH, Erkelenz, Germany) was used for the MTP in the µRAMOS.

As measuring intervals were different for DOT and OTR, a spline interpolation (MATLAB function: interp1, spline, default settings) of the DOT was conducted to get value pairs for DOT and OTR using the software MATLAB (version R2021b 9.11.0.1769968, The Math Works, Inc., Natik, USA). This was performed for each replicate (well).

The k_La was calculated based on equation (6) for each value pair of DOT and OTR of the replicates.

$$k_L a = \frac{L_{O_2} \cdot (pO_2{}^{gas} - \frac{DOT}{100} \cdot pO_2{}^{cal})}{OTR} \quad (6)$$

As pO_2^{gas} is measured in the µRAMOS device, the measured pO_2^{gas} was used for calculating the k_La instead of the assumption of 0.21 bar. pO_2^{gas} values were determined as mean values of pO_2^{gas} measured in the µRAMOS in the aeration phase, before the corresponding OTR was determined in the following stop phase. After calculation of k_La values for each measuring point (value pair of DOT and OTR), a mean value based on k_La values over time was calculated for each replicate. Only k_La values for OTR values higher than 5 mmol/L/h were considered. The k_La used to calculate the OTR based on equation (5) was averaged for the replicates.

Appendix Section A3: Correction of intensities of 2D fluorescence spectra.

When a new calibration of the spectrometer was performed, a correction factor was determined for correction of the 2D fluorescence spectra at the end of the cultivation. Therefore, a bead suspension (1000 NTU) was prepared in triplicates (solution a, b, and c) by diluting the stock solution (4000 NTU calibration standard polymer bead, Sigma Aldrich Chemie GmbH, Taufkirchen, Germany) with deionized water. 2D spectra of those bead suspensions were recorded at the beginning and end of the cultivation under the same conditions as the cultivation samples (Appendix Figure A20). During cultivation, the bead suspensions were stored at 4 °C. The scattered light intensity for each measured scattered light wavelength of the 2D scan from the beginning of the cultivation was divided by the scattered light intensity for each measured scattered light wavelength of the 2D scan from the end of the cultivation (scattered light ratios for different wavelengths). The mean of those scattered light ratios for the different wavelengths for each bead suspension was calculated. Then, the mean value of the three bead suspensions (a, b, and c) was determined, which is called correction factor (Appendix Figure A20). This correction factor was used to multiply the intensities of the 2D fluorescence spectra of cultivation samples at the end of the cultivation.

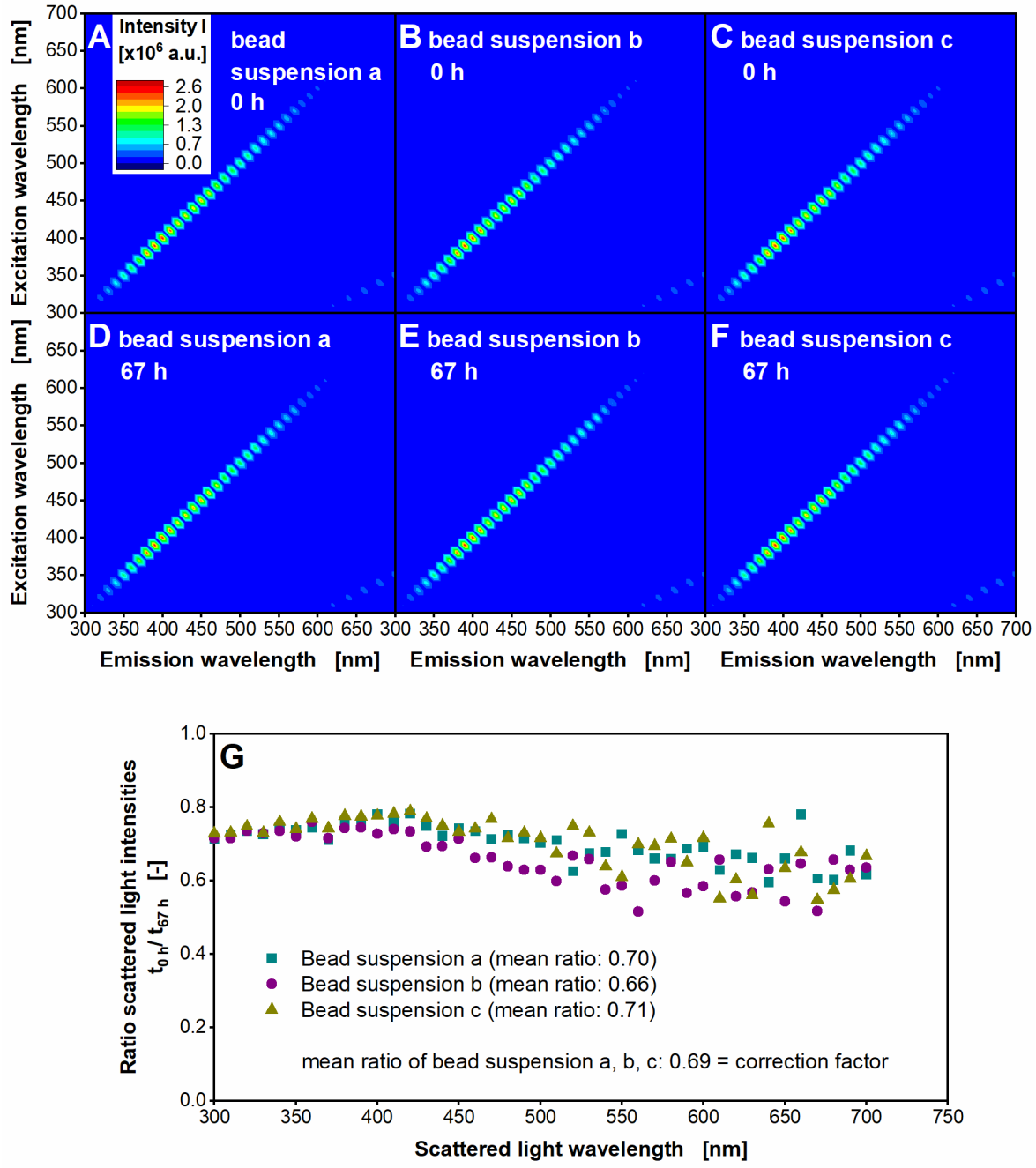

Appendix Figure A20: 2D absolute spectra of scattered light of a standard bead suspension.

2D absolute fluorescence spectrum of **(A)** bead suspension a, **(B)** bead suspension b and **(C)** bead suspension c measured at the beginning of the cultivation. 2D absolute fluorescence spectrum of **(D)** bead suspension a, **(E)** bead suspension b and **(F)** bead suspension c measured after 67 h of cultivation. During *Bacillus subtilis* cultivation the suspensions were stored at 4 °C. 2D fluorescence scans with excitation wavelengths from 300-700 nm and emission wavelengths from 300-700 nm were recorded using the setup of an in-house built BioLector device [72, 75, 76]. For calculation of the scattered light ratio in **(G)**, scattered light intensities of each suspension at the beginning of the cultivation ($t_{0\ h}$) were divided by scattered light intensities after 67 h of cultivation ($t_{67\ h}$). The mean value of these ratios was

calculated to obtain the correction factor. The correction factor is needed for correction of absolute 2D fluorescence spectra at the end of the cultivation of Figure 3-2 and Figure 3-4. Correction is necessary, because the spectrometer was switched off between the recordings of 2D spectra at the beginning and end of the cultivation of Figure 3-2 and Figure 3-4 and, thus, separate calibrations of spectrometer were performed for recording 2D spectra at the beginning and end of the cultivation.

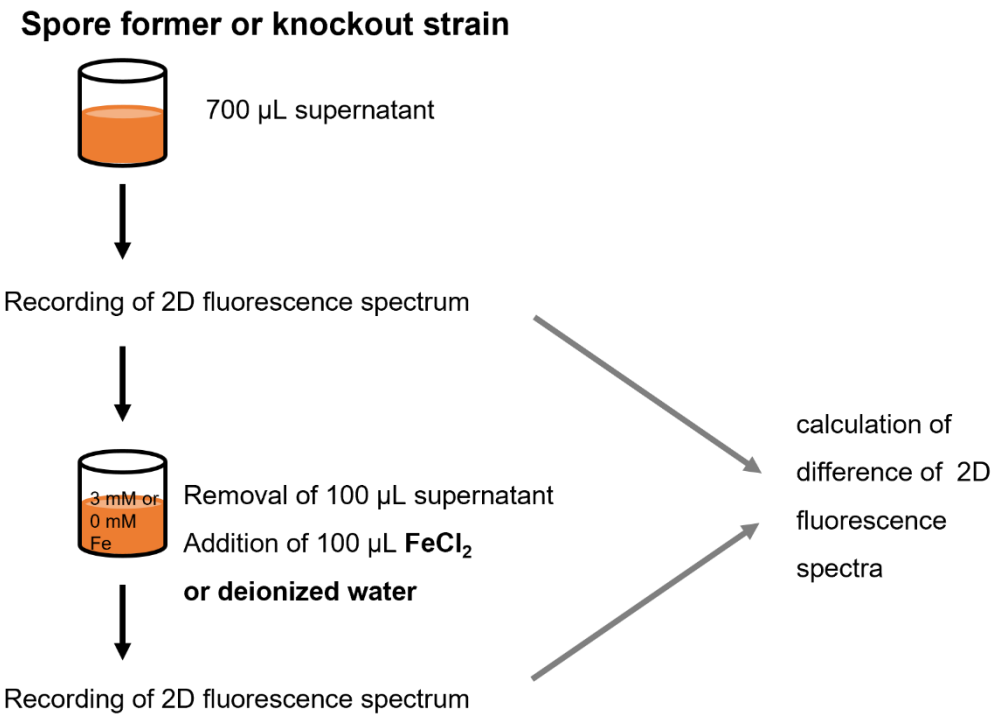

Appendix Figure A21: Schematic overview of recording of 2D fluorescence spectra with addition of $FeCl_2$.

This schematic overview is related to the experiment of Figure 3-5 and Appendix Figure A28. 700 µL supernatant of *Bacillus subtilis* PY79 spore former and KO7-S knockout strain were filled in a well of a 48-round well microtiter plate and a 2D fluorescence spectrum was recorded. Then, 100 µL of supernatant were removed from the well and 100 µL of a $FeCl_2$ solution or 100 µL deionized water were added to the well. When adding $FeCl_2$ to the supernatant a change in fluorescence could be caused by iron itself or by dilution of the sample by adding the solution. Therefore, the same volume of deionized water was added in another well. 2D fluorescence scans with excitation wavelengths from 300-700 nm and emission wavelengths from 300-700 nm were recorded using the setup of an in-house built BioLector device [72, 75, 76]. Intensities of the 2D fluorescence scan before adding $FeCl_2$ and deionized water were subtracted from intensities of the 2D fluorescence scan after adding $FeCl_2$ and deionized water. 3 mM $FeCl_2$ was added to the supernatant, which corresponds to 3 mM Fe.

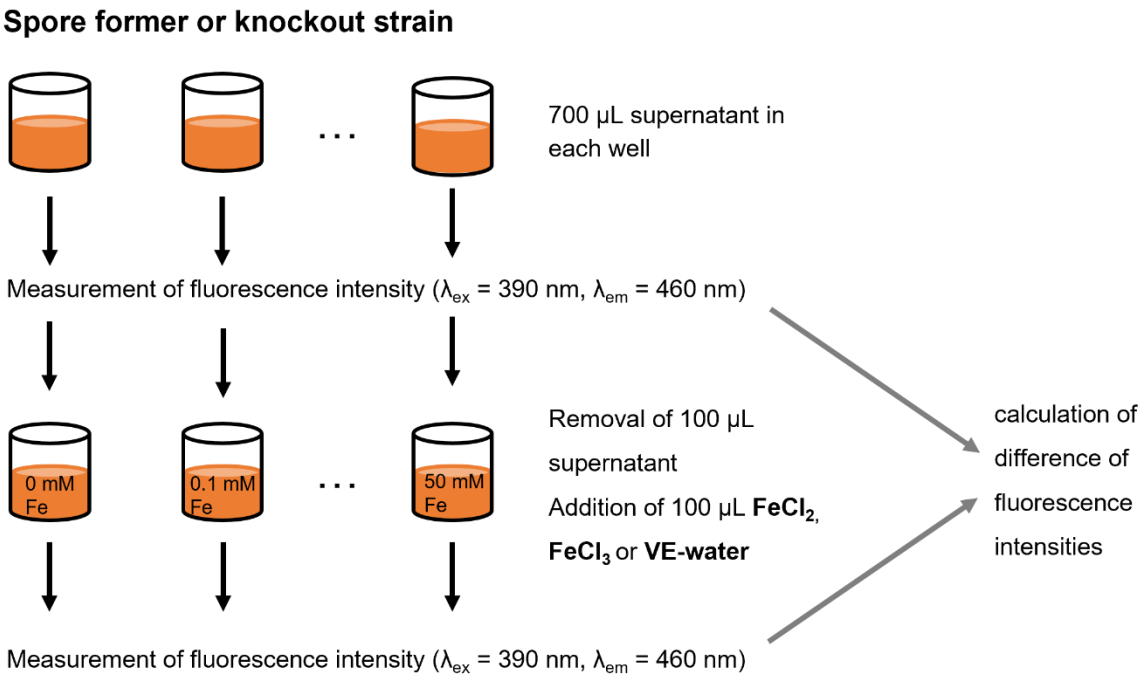

Appendix Figure A22: Schematic overview of recording of fluorescence intensities with different concentrations of $FeCl_2$ and $FeCl_3$.

This schematic overview is related to the experiment in Figure 3-6. 700 µL supernatant of *Bacillus subtilis* PY79 spore former and KO7-S knockout strain were filled in a well of a 48-round well microtiter plate and the fluorescence intensity at an excitation wavelength of 390 nm and an emission wavelength of 460 nm was measured in an in-house built BioLector device [72, 75, 76]. After 4.2 h, 100 µL of supernatant were removed from the well and 100 µL of a $FeCl_2$ or $FeCl_3$ solution in different concentrations (0.1, 1, 3, 6, 9, 15, and 50 mM $FeCl_2$ and $FeCl_3$, which corresponds to 0.1, 1, 3, 6, 9, 15, and 50 mM Fe) or 100 µL deionized water were added to the well. The fluorescence intensity before addition was determined by calculating a mean value of intensities measured before addition. A measurement period of 1.0 h was chosen for the mean value calculation. Fluorescence intensity after addition was determined by calculating a mean value of intensities after addition. A measurement period of 1.0 h was chosen for the mean value calculation. Mean fluorescence intensity before adding $FeCl_2$, $FeCl_3$ or deionized water was subtracted from mean fluorescence intensity after adding $FeCl_2$, $FeCl_3$ or deionized water.

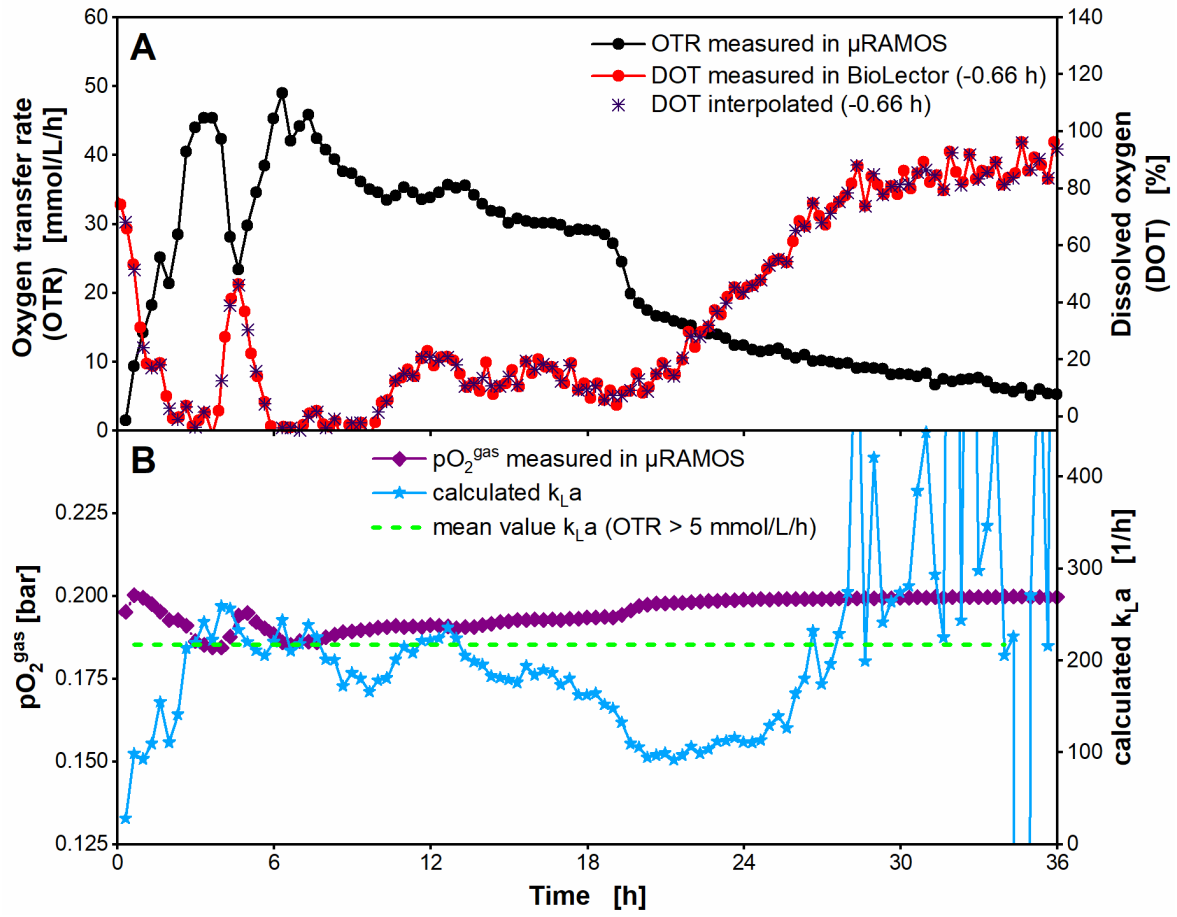

Appendix Figure A23: Cultivation of *Bacillus subtilis* PY79 spore former, to determine the volumetric oxygen transfer coefficient (k_La) value.

(A) Oxygen transfer rate (OTR) in a µRAMOS device [73] and corrected dissolved oxygen tension (DOT) in a commercial BioLector I device (Beckman Coulter GmbH), **(B)** oxygen partial pressure (pO_2^{gas}) measured in the µRAMOS device and calculated k_La. **(A), (B)** Exemplarily, one replicate (well) is shown. For clarity, only the first 36 h of cultivation are shown. Due to different measuring intervals of DOT and OTR, the DOT was interpolated as described in Appendix Section A2. The pO_2^{gas} values are shown as mean values of pO_2^{gas} measured in the aeration phase before the corresponding OTR was determined in the following stop phase in the µRAMOS device. The k_La was calculated as described in Appendix Section A2. The mean value of k_La over cultivation time for one replicate (green horizontal dotted line) was determined for all OTR values higher than 5 mmol/L/h. This was performed for all four replicates and a mean value was determined for k_La. The mean k_La value (194 1/h) of all replicates was used to calculate the OTR from DOT in Figure 3-1. Cultivation conditions in the commercial BioLector I device (Beckman Coulter GmbH) and µRAMOS device: temperature 37 °C, 48-round well plate (MTP-R48-BOH 1 for BioLector, MTP-R48-B for µRAMOS), filling volume 0.7 mL, shaking frequency 1000 rpm, shaking diameter 3 mm, Bc medium with 10 g/L glucose.

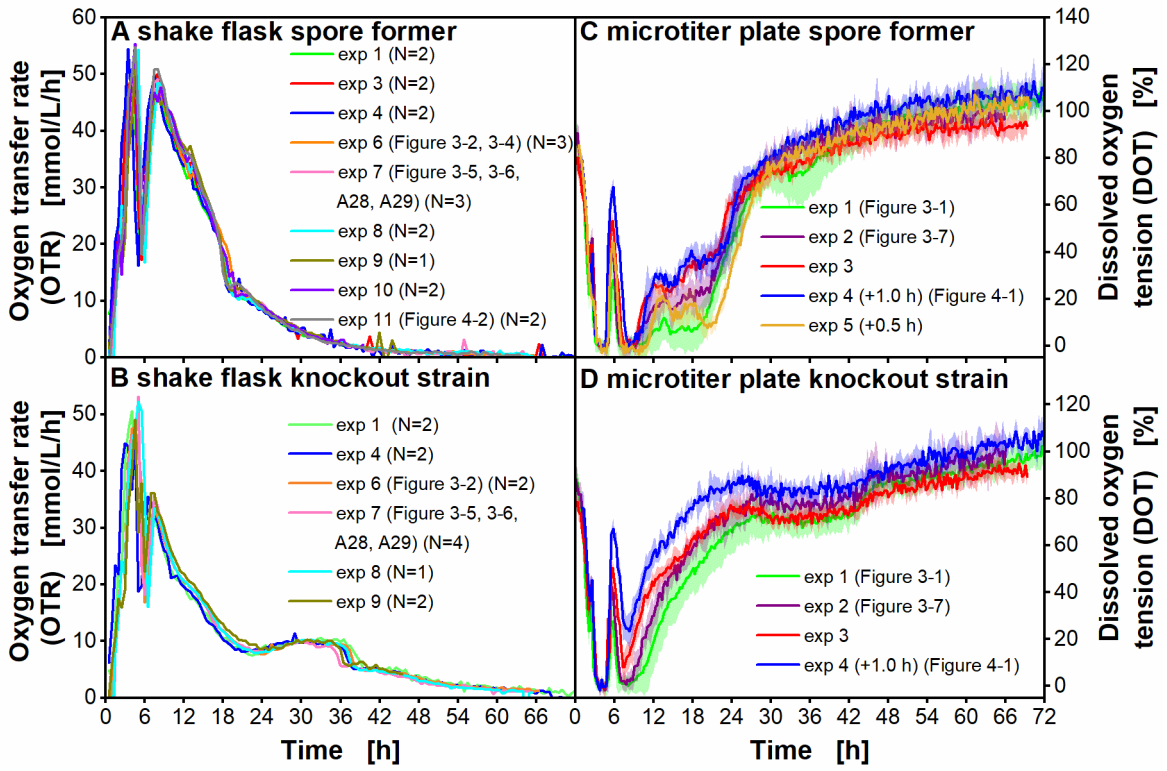

Appendix Figure A24: Reproducibility of all main-cultures of *Bacillus subtilis* PY79 spore former and KO7-S knockout strain performed in this study under the same cultivation conditions in shake flask and microtiter plate scale.

(A) Oxygen transfer rate (OTR) in shake flasks of the spore former **(B)** OTR in shake flasks of the knockout strain. **(C)** Dissolved oxygen tension (DOT) in microtiter plates of the spore former. **(D)** DOT in microtiter plates of the knockout strain. Cultivations of various experiments (exp) are shown. The figure numbers, to which the OTR or DOT data belong, are marked in the figure legends. **(A), (B)** One replicate is shown and N marks the available number of replicates with OTR curves in the experiment. **(C), (D)** Mean values of at least four replicates with standard deviations as shadows are shown. The DOT was corrected as described in Appendix Section A1. Cultivation conditions in a RAMOS device [70, 71]: temperature 37 °C, 250 mL RAMOS shake flask, filling volume 10 mL, shaking frequency 350 rpm, shaking diameter 50 mm, Bc medium with 10 g/L glucose. Cultivation conditions in a commercial BioLector I device (Beckman Coulter GmbH): temperature 37 °C, 48-round well plate (MTP-R48-BOH 1), filling volume 0.7 mL, shaking frequency 1000 rpm, shaking diameter 3 mm, Bc medium with 10 g/L glucose.

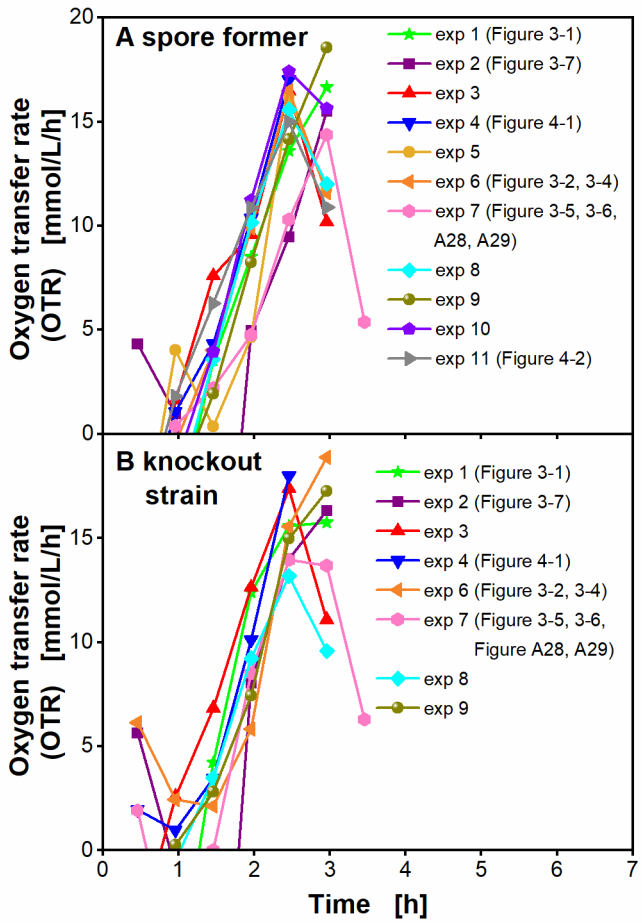

Appendix Figure A25: Reproducibility of all pre-cultures of *Bacillus subtilis* PY79 spore former and KO7-S knockout strain performed in this study under the same cultivation conditions.

(A) Oxygen transfer rate (OTR) in shake flasks of the spore former. **(B)** OTR in shake flasks of the knockout strain. exp: experiments. Pre-cultures of main-cultures in Appendix Figure A24 are shown. The figure numbers, to which the OTR data belong, are marked in the figure legend. Cultivation conditions in a RAMOS device [70, 71]: temperature 37 °C, 250 mL RAMOS shake flask, filling volume 10 mL, shaking frequency 350 rpm, shaking diameter 50 mm, LB medium.

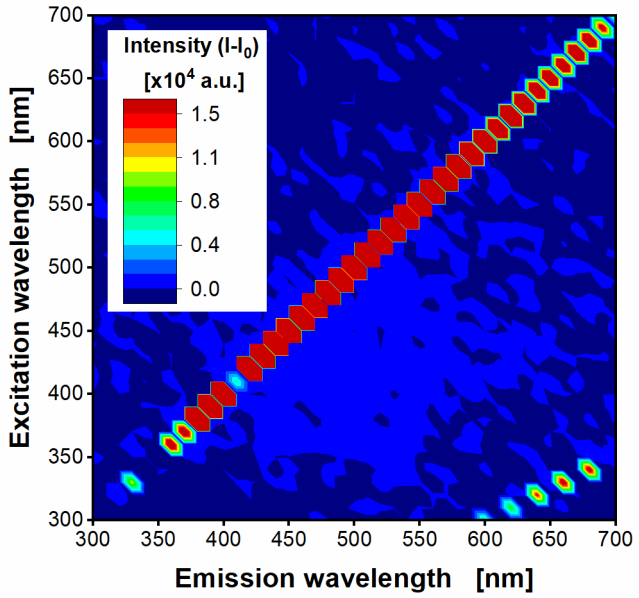

Appendix Figure A26: Difference of 2D fluorescence spectrum of pure Bc medium between the beginning and end of the experiment.

Bc medium was not inoculated. 2D fluorescence scan with excitation wavelengths from 300-700 nm and emission wavelengths from 300-700 nm was recorded at the beginning of the experiment and after 67 h of the experiment using the setup of an in-house built BioLector device [72, 75, 76]. Intensities of the 2D spectra after 67 h of the experiment were corrected with the correction factor as described in Appendix Section A3. Intensities of the 2D fluorescence scan from the beginning of the experiment were subtracted from corrected intensities of the 2D fluorescence scan after 67 h ($I-I_0$). Conditions of the experiment in a RAMOS device [70, 71]: temperature 37 °C, 250 mL RAMOS shake flask, filling volume 10 mL, shaking frequency 350 rpm, shaking diameter 50 mm, Bc medium with 10 g/L glucose without inoculation. The diagonal with high intensities in the lower right corner represents the 2nd order light scattering.

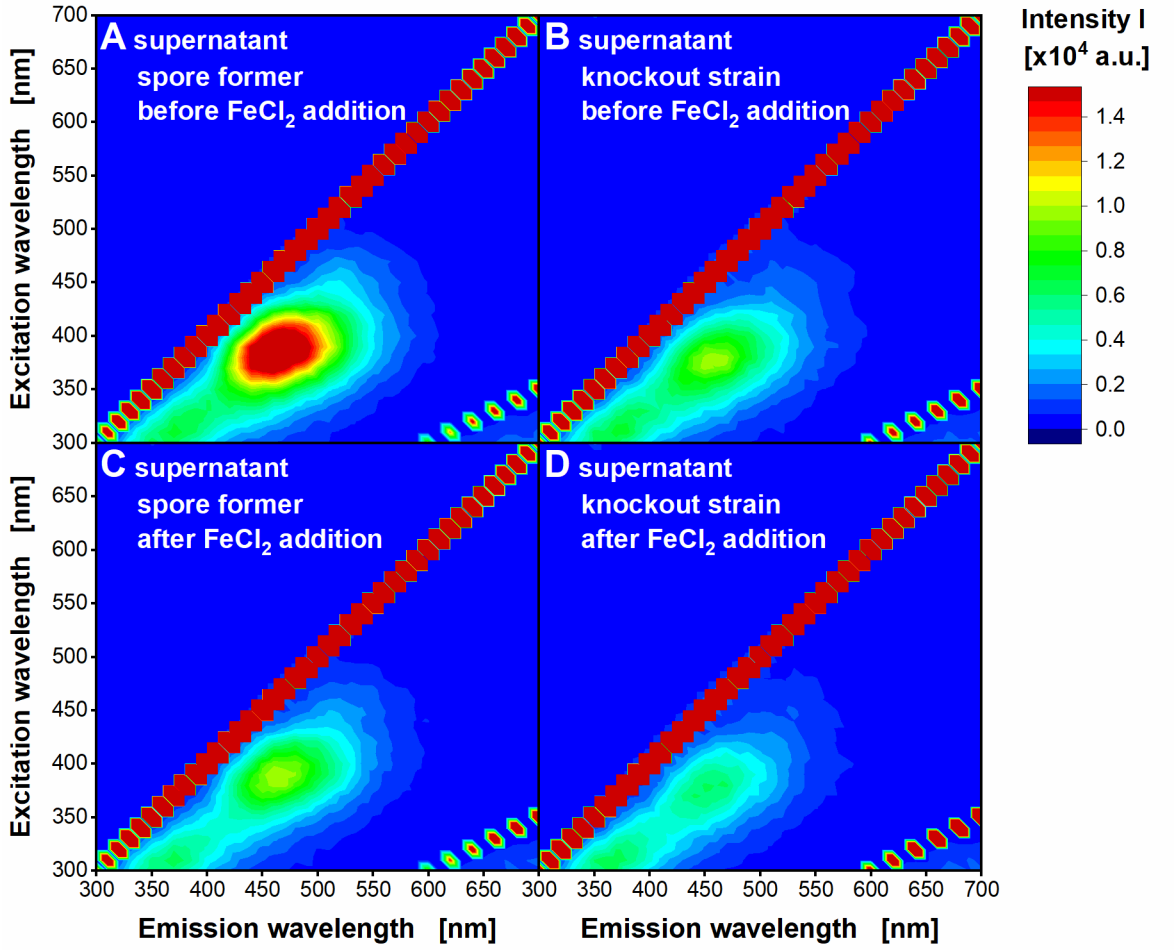

Appendix Figure A27: 2D absolute fluorescence spectra of supernatant of *Bacillus subtilis* spore former and knockout strain before and after adding $FeCl_2$.

2D absolute fluorescence spectra of Figure 3-5 are shown. **(A)** 2D absolute fluorescence spectrum of supernatant of **(A)** spore former before adding $FeCl_2$, **(B)** knockout strain before adding $FeCl_2$, **(C)** spore former after adding $FeCl_2$, **(D)** knockout strain after adding $FeCl_2$. 2D fluorescence scans with excitation wavelengths from 300-700 nm and emission wavelengths from 300-700 nm were recorded using the setup of an in-house built BioLector device [72, 75, 76]. Samples of the cultivation were taken after 66 h and centrifuged for recording of the 2D spectra of the supernatant. 3 mM $FeCl_2$ was added to the supernatant, which corresponds to 3 mM Fe.

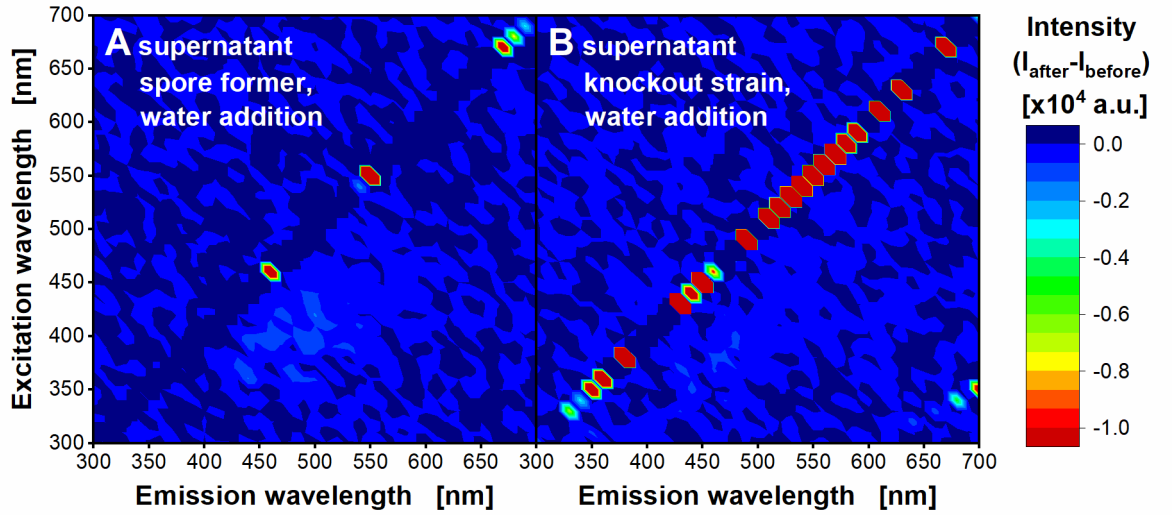

Appendix Figure A28: Difference of 2D fluorescence spectra of supernatant of *Bacillus subtilis* PY79 spore former and KO7-S knockout strain before and after addition of deionized water.

(A) Spore former, **(B)** knockout strain. 2D fluorescence scans with excitation wavelengths from 300-700 nm and emission wavelengths from 300-700 nm were recorded of the supernatant after 66 h of cultivation before and after adding deionized water using the setup of an in-house built BioLector device [72, 75, 76]. Intensities of the 2D fluorescence scan before adding deionized water were subtracted from the intensities of the 2D fluorescence scan after adding deionized water (I_{after}-I_{before}). The scale of intensities shows negative values. The cultivations in shake flask are shown in Appendix Figure A24. Samples of the cultivation were taken after 66 h and centrifuged for recording of the 2D spectra of the supernatant. Schematic overview for this experiment is shown in Appendix Figure A21.

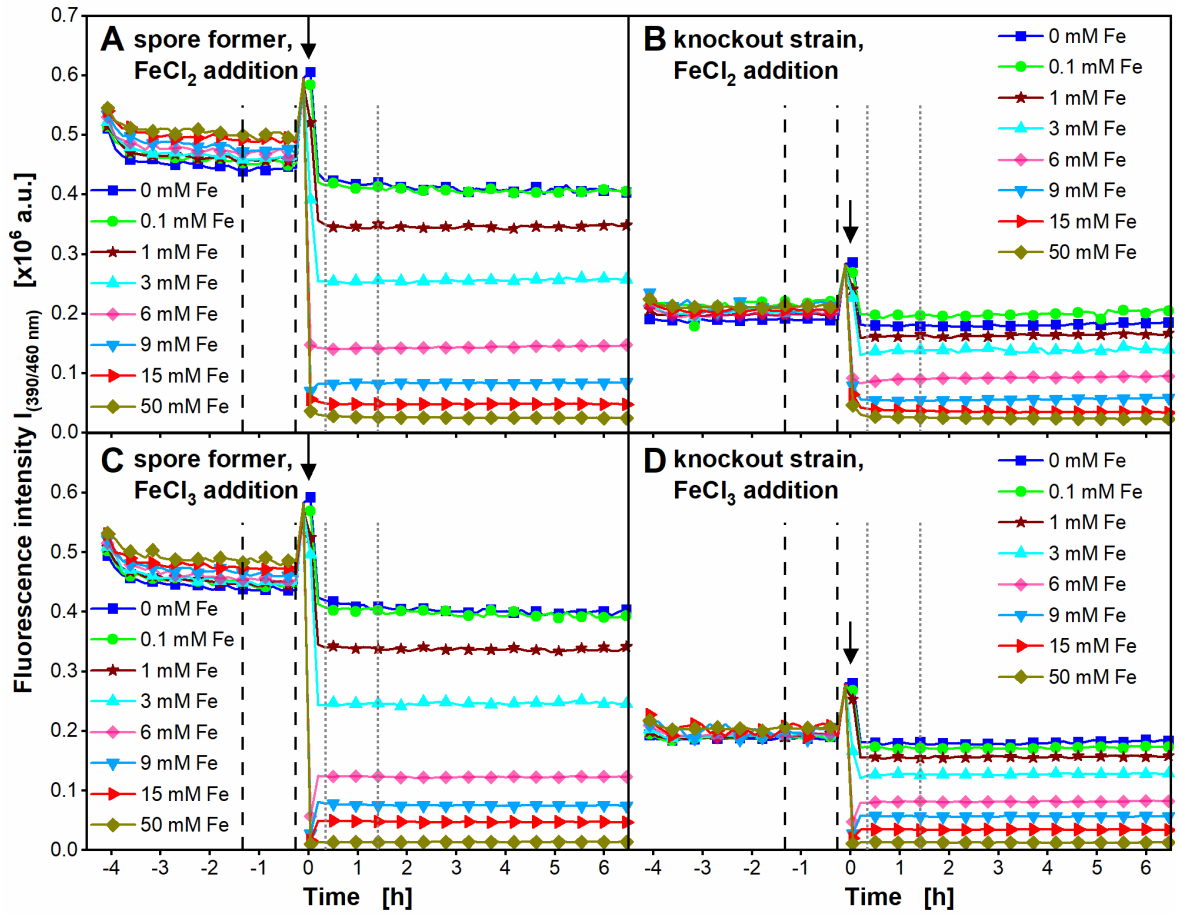

Appendix Figure A29: Absolute fluorescence intensities (390/460 nm) before and after adding different iron solutions and concentrations to the supernatant of *Bacillus subtilis* PY79 spore former and KO7-S knockout strain.

Absolute fluorescence intensities of Figure 3-6 are shown. Fluorescence intensity of supernatant of **(A)** spore former before and after adding $FeCl_2$, **(B)** knockout strain before and after adding $FeCl_2$, **(C)** spore former before and after adding $FeCl_3$, **(D)** knockout strain before and after adding $FeCl_3$. Fluorescence intensity was measured at an excitation wavelength of 390 nm and an emission wavelength of 460 nm in an in-house built BioLector device [72, 75, 76]. For clarity, only every 4th measuring point is marked by a symbol. $FeCl_2$ or $FeCl_3$ were added to the supernatant in different concentrations. Arrows mark the time point of adding $FeCl_2$ or $FeCl_3$, which was after 4.2 h of incubation of the supernatant in the microtiter plate. Fluorescence intensity before addition was determined by calculating a mean value of intensities in the period (0.4 – 1.4 h before addition of iron), marked with black dashed vertical lines. Fluorescence intensity after addition was determined by calculating a mean value of intensities in the period (0.4 – 1.4 h after addition of iron), marked with grey dotted vertical lines. Timing before addition is shown with negative time scale and timing after addition with positive time scale. Deionized water was added instead of iron so that no additional iron was added to the supernatant (0 mM). Samples of the cultivation were taken after 66 h and centrifuged for measuring the fluorescence intensity of the supernatant.

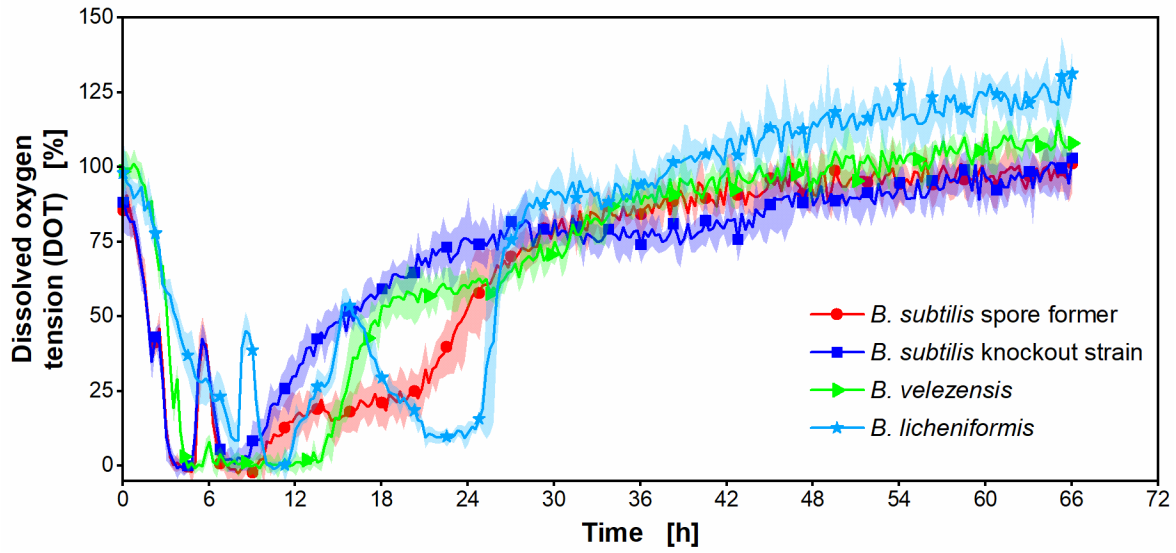

Appendix Figure A30: Cultivation of different *Bacillus* strains in microtiter plate scale.

Dissolved oxygen tension (DOT) of *Bacillus subtilis* PY79 spore former, *Bacillus subtilis* KO7-S knockout strain, *Bacillus velezensis* (MBI600), *Bacillus licheniformis* DSM8785. For clarity, only every 10th measuring point over time is marked by a symbol. Mean values of four replicates with standard deviations as shadow are shown. The DOT was corrected as described in Appendix Section A1. Cultivation conditions in a commercial BioLector I device (Beckman Coulter GmbH): temperature 37°C, 48-round well plate (MTP-R48-BOH 1), filling volume 0.7 mL, shaking frequency 1000 rpm, shaking diameter 3 mm, Bc medium with 10 g/L glucose.

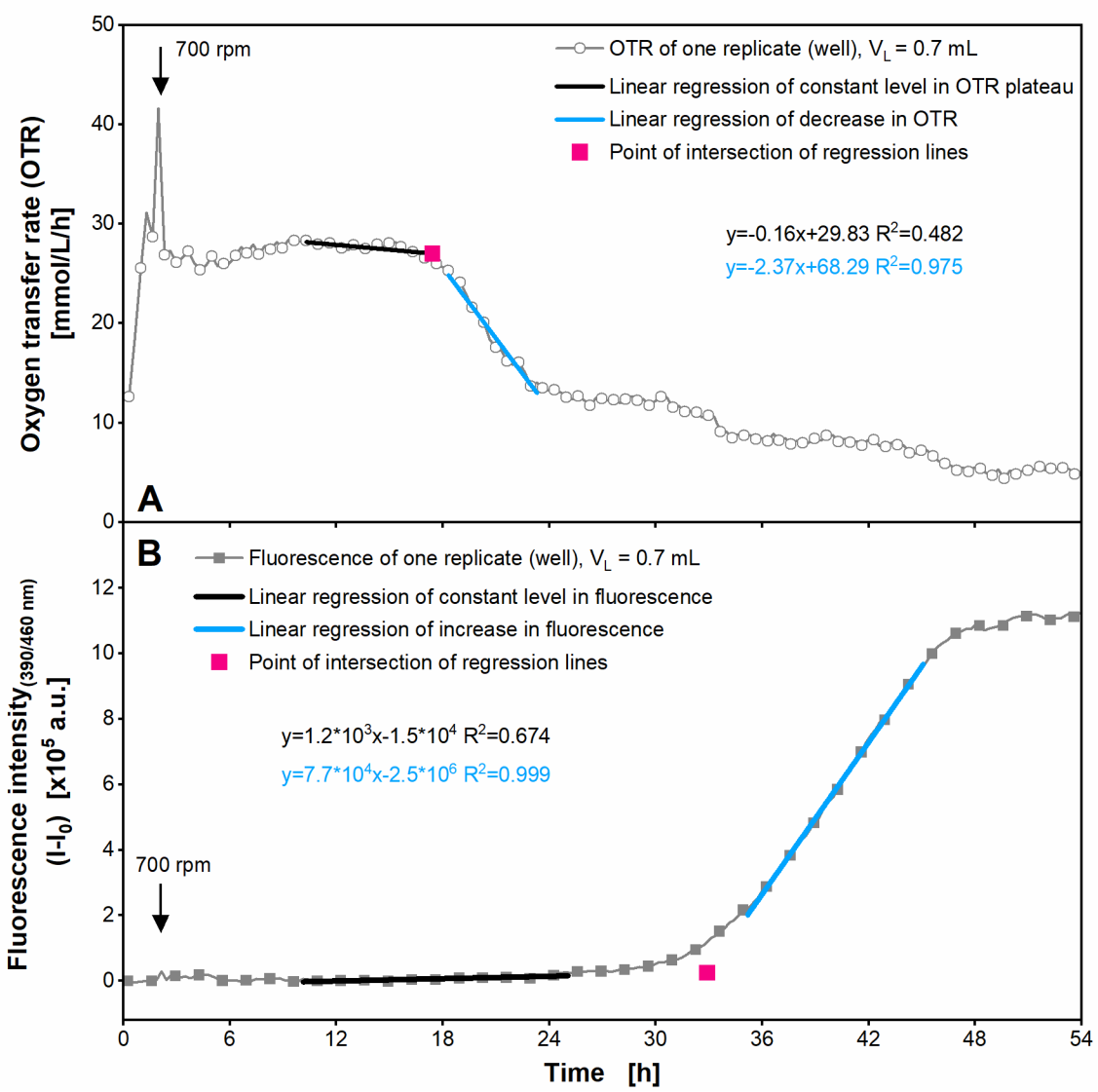

Appendix Figure A31: Determination of time point of start of decrease in OTR, and time point of start of increase in fluorescence intensity.

(A) Oxygen transfer rate (OTR) of one replicate (well) of the cultivation of *B. subtilis* PY79 spore former with a filling volume of 0.7 mL. For clarity, only every 3rd measuring point over time is marked as a symbol. A linear regression was performed on the almost constant values of the OTR plateau and on the values of the dropping flank of the OTR after the plateau. The start of the decrease in the OTR was the point of the intersection of those two regression lines. **(B)** Fluorescence intensity at an excitation wavelength of 390 nm and an emission wavelength of 460 nm of one replicate (well) of the cultivation of *B. subtilis* PY79 spore former with a filling volume of 0.7 mL. For clarity, only every 6th measuring point over time is marked as a symbol. The initial intensity was subtracted from the measured intensities over time ($I-I_0$). A linear regression was performed on the almost constant values of the fluorescence intensity before the increase and on the values of the linear increase in the fluorescence intensity. The start of the increase in the fluorescence was the point of intersection of those two regression lines. Cultivation conditions in a µRAMOS/BioLector combination: temperature 37 °C, 48 round well plate (MTP-

R48-B), filling volume 0.5-1.3 mL, shaking frequency 1000 rpm/ 700 rpm at 2.1 h, shaking diameter 3 mm, Bc medium with 10 g/L glucose. The replicate belongs to the cultivations shown in Figure 4-3.

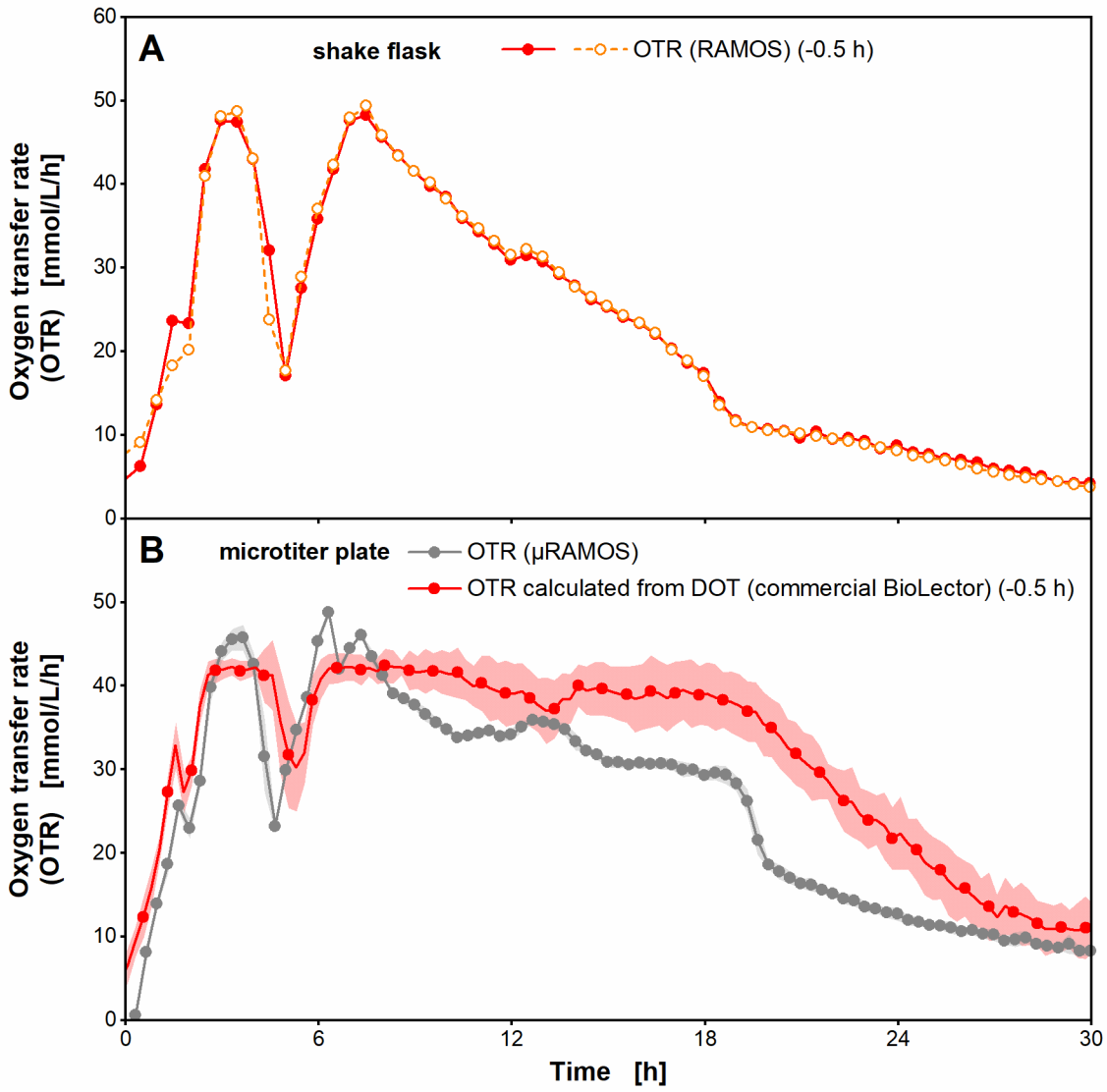

Appendix Figure A32: Cultivation of *Bacillus subtilis* PY79 spore former in shake flask (RAMOS) and microtiter plate (µRAMOS and commercial BioLector) scale.

(A) Oxygen transfer rate (OTR) in shake flasks measured in a RAMOS device [70, 71], **(B)** OTR in a microtiter plate measured in a µRAMOS/BioLector combination device [77] and OTR calculated from DOT in a microtiter plate measured in a commercial BioLector I device (Beckman Coulter GmbH). **(A), (B)** For a better overview, only the first 30 h of cultivations are shown. The cultivation in the RAMOS device and in the commercial BioLector I device were performed with the same pre-culture. The cultivation in the µRAMOS/BioLector combination device was performed in a separate experiment with a separate pre-culture. **(A)** Duplicates are shown for cultivations in shake flasks. **(B)** Mean values of four replicates (µRAMOS) and 16 replicates (commercial BioLector I) with standard deviations as shadows are shown for cultivations in microtiter plates. For clarity, only every 4th measuring point over time is marked by a symbol for the OTR calculated from the DOT (commercial BioLector I). The cultivation in the RAMOS device in **(A)** and the cultivation in the commercial BioLector I in **(B)** is also shown in Figure 3-1. The cultivation in the

µRAMOS/ BioLector combination device in **(B)** is also shown in Figure 4-3. Cultivation conditions are mentioned in the corresponding figure captions.

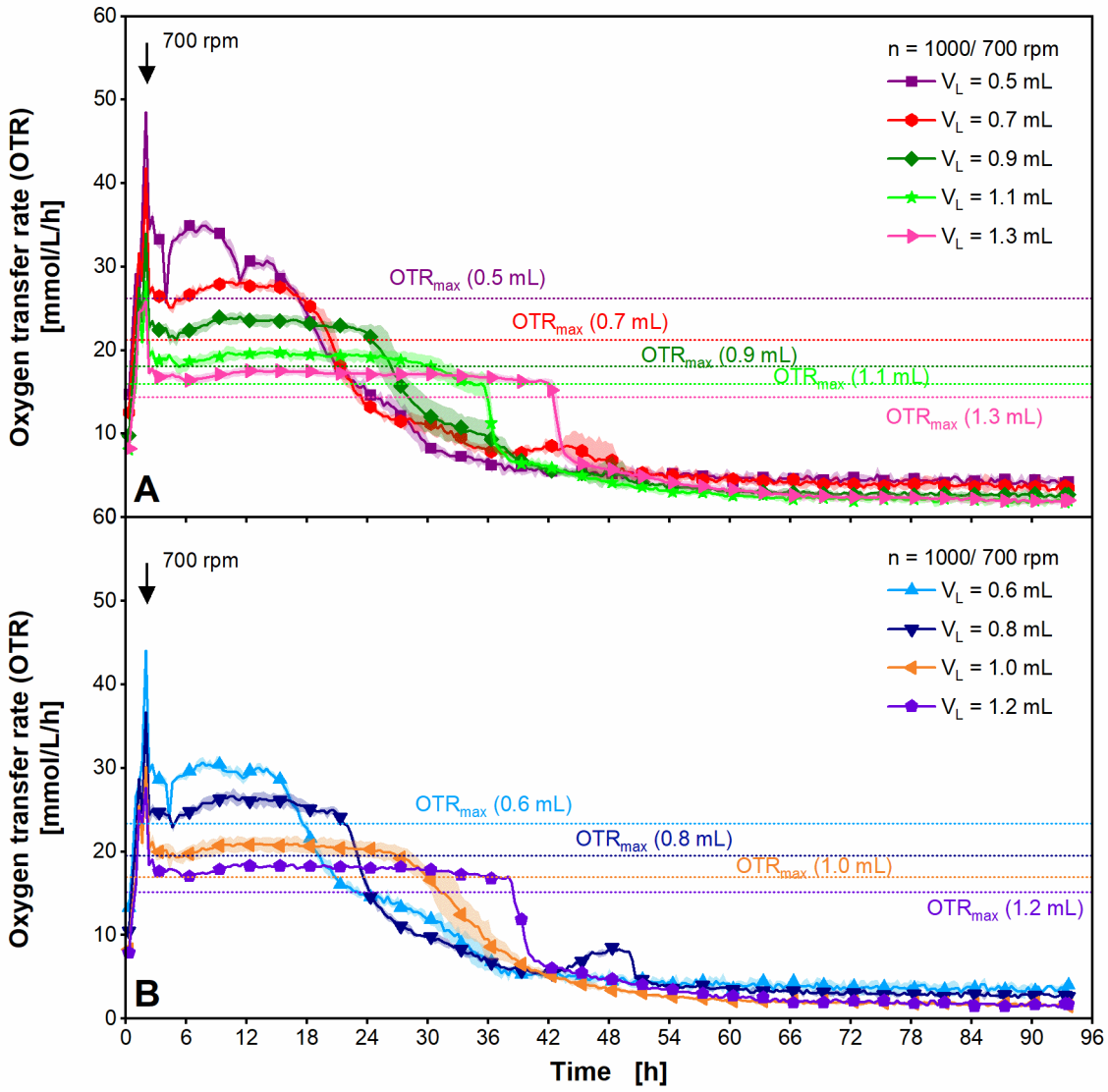

Appendix Figure A33: Cultivation of *Bacillus subtilis* PY79 spore former under different levels of oxygen limitation in microtiter plate scale with theoretical maximum oxygen transfer capacity.

(A), (B) Oxygen transfer rate (OTR). The OTR of the cultivations of Figure 4-3 is shown, except of the reference cultivation. For better overview, the cultivations of the filling volumes 0.5 mL, 0.7 mL, 0.9 mL, 1.1 mL and 1.3 mL are shown in **(A)**, and the cultivations of the filling volumes 0.6 mL, 0.8 mL, 1.0 mL and 1.2 mL are shown in **(B)**. **(A), (B)** For clarity, only every 4th measuring point of the OTR over time is marked by a symbol. Mean values of at least three replicates with standard deviations as shadows are shown. For the cultivation with a filling volume of 1.2 mL, no standard deviations are shown, as a mean value of two replicates was calculated. The theoretical maximum oxygen transfer capacity (OTR_{max}) (horizontal dashed lines)

was calculated for the applied cultivation conditions after Lattermann et al. [226]. The cultivation conditions are mentioned in Figure 4-3.

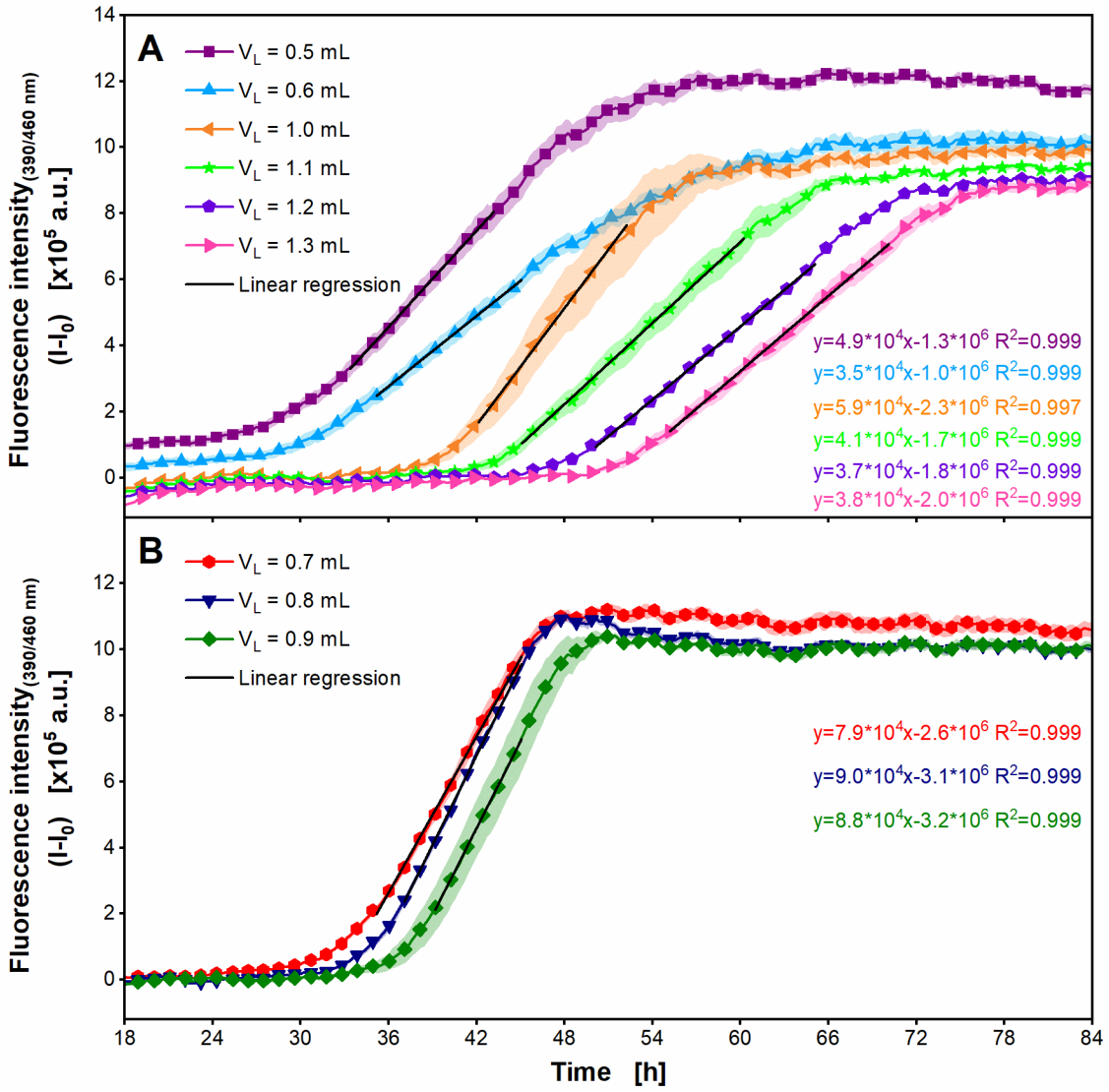

Appendix Figure A34: Determination of the slope of the increase in fluorescence intensity of the cultivation of *Bacillus subtilis* PY79 spore former under different levels of oxygen limitation in microtiter plate scale.

Fluorescence intensity with an excitation wavelength of 390 nm and an emission wavelength of 460 nm for a filling volume of **(A)** 0.5 mL, 0.6 mL, 1.0 mL, 1.1 mL, 1.2 mL, 1.3 mL and **(B)** 0.7 mL, 0.8 mL, 0.9 mL. For clarity, only every 5th measuring point over time is marked by a symbol. Mean values of at least three replicates with standard deviations as shadows are shown. For the cultivation with a filling volume of 1.2 mL, no standard deviations are shown, as a mean value of a duplicate was calculated. The slope of the increase in the fluorescence intensity was calculated based on regression of the linear range of the fluorescence intensity (black lines). The fluorescence intensity over the whole cultivation time is shown in Figure 4-3. The cultivation conditions are mentioned in Figure 4-3.

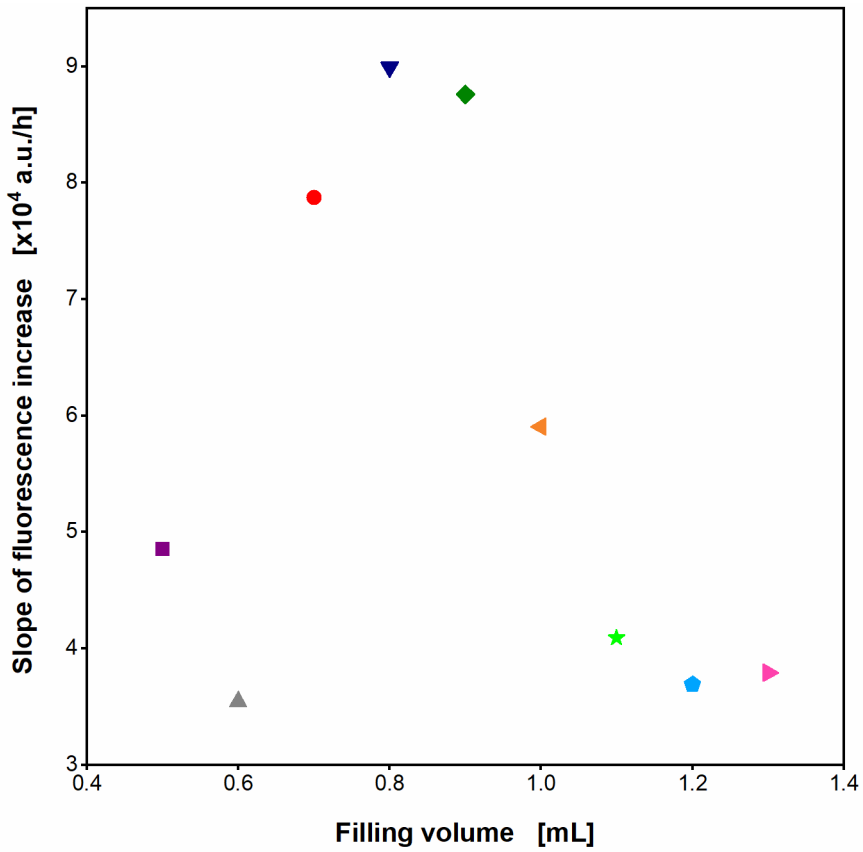

Appendix Figure A35: Slope of the increase in fluorescence intensity of the cultivation of *Bacillus subtilis* PY79 spore former under different levels of oxygen limitation in microtiter plate scale.

The slope of the increase in the fluorescence intensity of the cultivation shown in Figure 4-3 was determined for each filling volume as described in Appendix Figure A34.

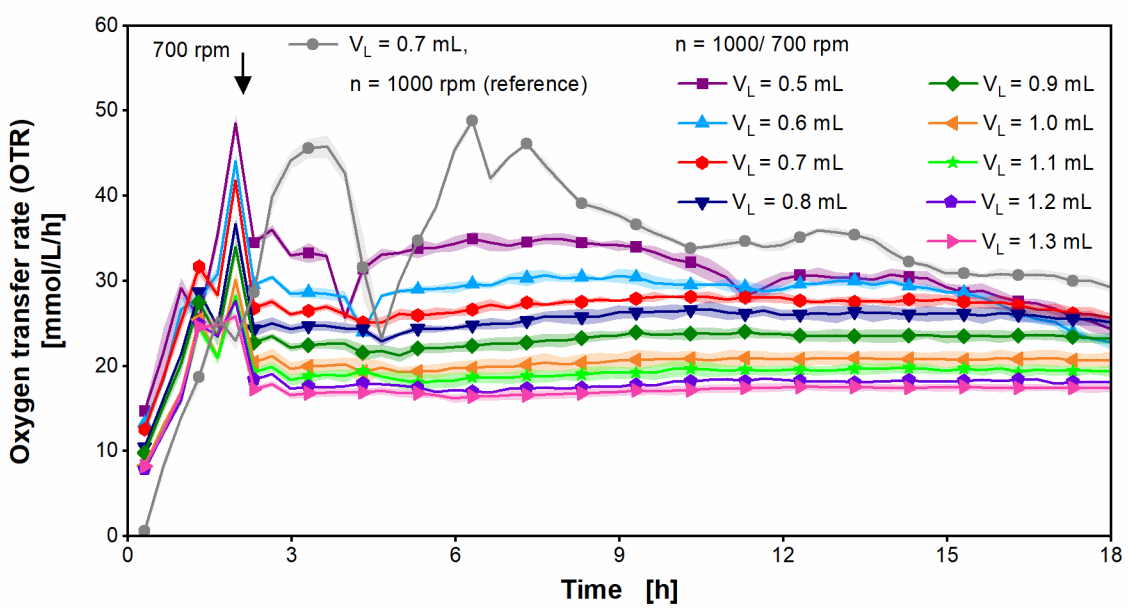

Appendix Figure A36: Higher resolution of the beginning of the cultivation of *Bacillus subtilis* PY79 spore former under different levels of oxygen limitation in microtiter plate scale.

The beginning (0 h -18 h) of the cultivations of Figure 4-3 is shown. For clarity, only every 4th measuring point of the oxygen transfer rate (OTR) over time is marked by a symbol. Mean values of at least three replicates with standard deviations as shadows are shown. For the cultivation with a filling volume of 1.2 mL, no standard deviations are shown, as a mean value of two replicates was calculated. The cultivation conditions are mentioned in Figure 4-3.

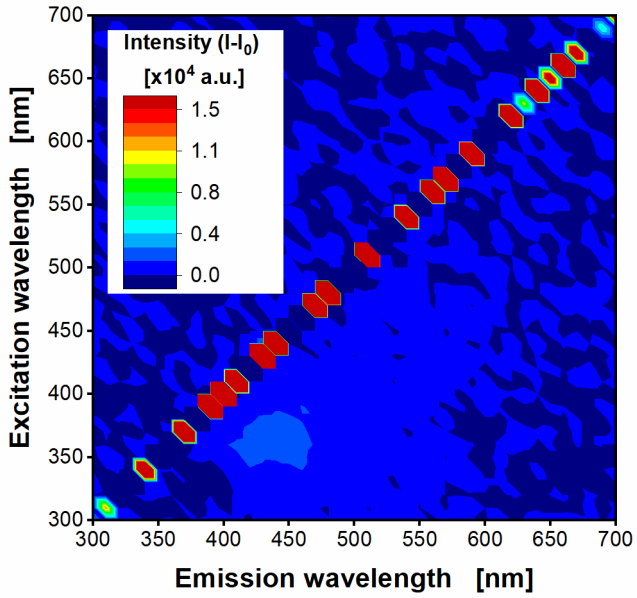

Appendix Figure A37: Difference of 2D fluorescence spectrum of pure complete modified Poolman medium between the beginning and end of the experiment.

Complete modified Poolman medium was not inoculated. 2D fluorescence scan with excitation wavelengths from 300-700 nm and emission wavelengths from 300-700 nm was recorded at the beginning of the experiment and after 40 h of the experiment using the setup of an in-house built BioLector device [72, 75, 76]. Intensities of the 2D fluorescence scan from the beginning of the experiment were subtracted from corrected intensities of the 2D fluorescence scan after 40 h ($I-I_0$). Conditions of the experiment in an in-house built BioLector device: temperature 37 °C, 48-round well plate (MTP-R48-B), filling volume 0.7 mL, shaking frequency 1000 rpm, shaking diameter 3 mm, complete modified Poolman medium with 10 g/L glucose.

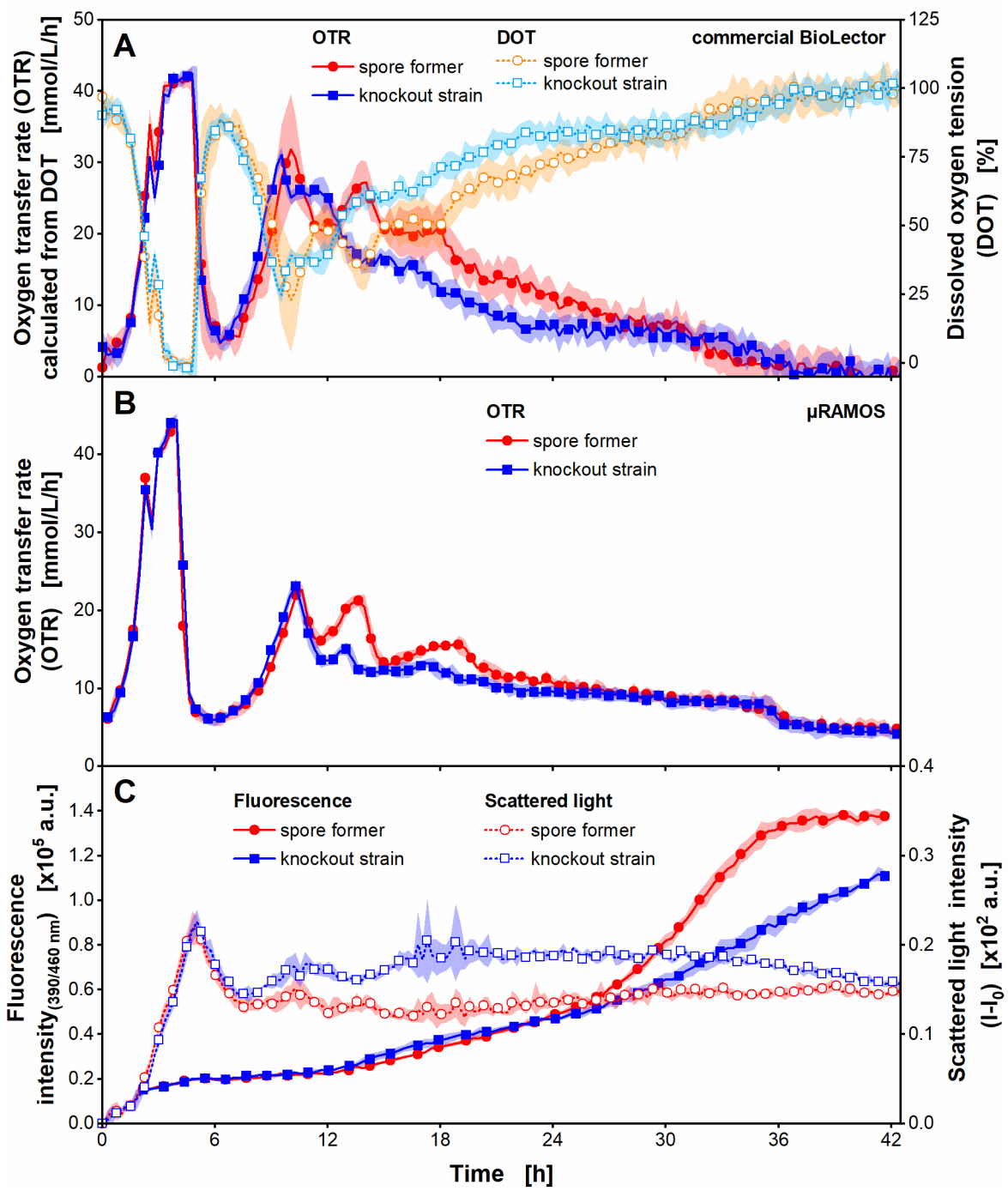

Appendix Figure A38: Dissolved oxygen tension, oxygen transfer rate, scattered light, and fluorescence measurement of *Bacillus subtilis* PY79 spore former and KO7-S knockout strain in complete modified Poolman medium.

(A) Dissolved oxygen tension (DOT) and oxygen transfer rate (OTR) in a commercial BioLector I device (Beckman Coulter GmbH), **(B)** OTR in an in-house built µRAMOS device [73], **(C)** scattered light intensity at 620 nm in the commercial BioLector I device and fluorescence intensity with an excitation wavelength of 390 nm and an emission wavelength of 460 nm in an in-house built BioLector device [72, 75, 76]. For clarity, only every 4th **(A, C)** and 3rd **(B)** measuring point over time

is marked by a symbol. Mean values of eight (**A,** scattered light in **C**), three **(B)** and four (fluorescence in **C**) replicates with standard deviations as shadows are shown. Shaking of the cultivation in the in-house built BioLector was conducted around 2 h before online measurement was started. Therefore, no data points for the first 2 h are available. The DOT in **(A)** was corrected as described in Appendix Section A1. The OTR in **(A)** was calculated from the corrected DOT as described in chapter 5.2.7 with a volumetric oxygen transfer coefficient (k_La) of 194 1/h (value was determined based on a cultivation in complex Bc medium). For scattered light **(C)**, the initial intensity was subtracted from the measured intensities over time ($I-I_0$) for each strain. The cultivations and the cultivation conditions in **(A)** and **(B)** are shown in Figure 5-1.The cultivations and the cultivation conditions in **(C)** are shown in Figure 5-3. The cultivations in the commercial BioLector I and in-house built BioLector were conducted in parallel, inoculated from the same pre-culture. The cultivation in the µRAMOS was conducted in a separate experiment with a separate pre-culture.

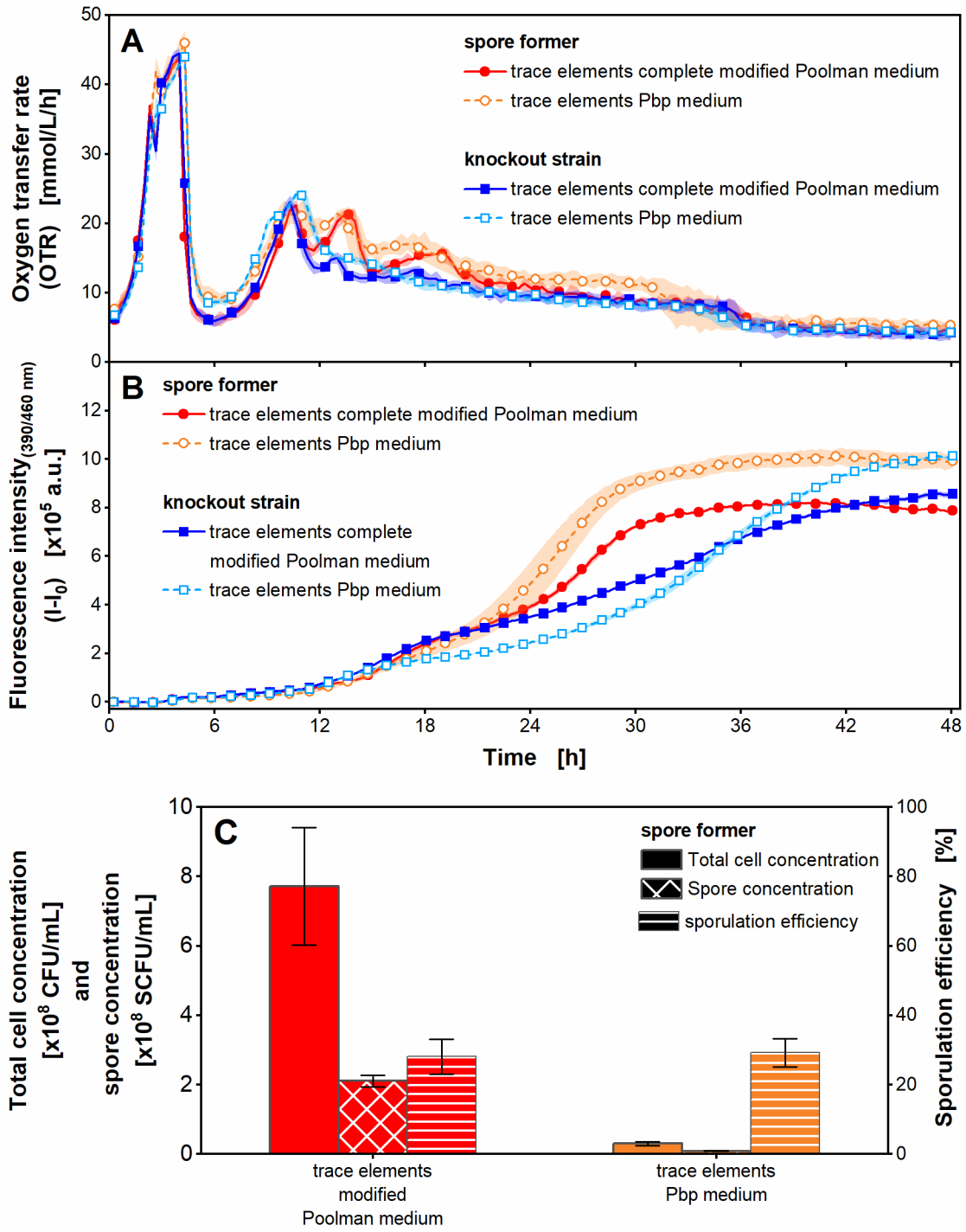

Appendix Figure A39: Cultivation of *Bacillus subtilis* PY79 and KO7-S knockout strain in complete modified Poolman medium with different trace element solutions.

(A) Oxygen transfer rate (OTR), **(B)** fluorescence intensity with an excitation wavelength of 390 nm and an emission wavelength of 460 nm, **(C)** total cell concentration, spore concentration, and sporulation efficiency. **(A), (B)** For clarity, only every 5th **(A)** and 6th **(B)** measuring point over time is marked by a symbol. Mean values for at least three replicates with standard deviations as shadows are shown. **(B)** The initial intensities were subtracted from the measured intensities over time ($I-I_0$)

for each experiment. The OTR and fluorescence measurement was performed in a µRAMOS/BioLector combination device [77]. Fluorescence measurement at an excitation wavelength of 390 nm and an emission wavelength of 490 nm in the BioLector was conducted with a slid width of 4 nm and an integration time of 600 ms. The OTR of the µRAMOS in **(A)** of the cultivation with trace elements of complete modified Poolman medium is also shown in Figure 5-1. **(C)** Total cell concentration, spore concentration, and sporulation efficiency of one replicate (well) of each experiment after 48 h of cultivation were determined in quadruplicates as described in chapter 4.2.5. Mean values with standard deviations depicted as error bars are shown. CFU: cell colony forming unit, SCFU: spore colony forming unit. Cultivation conditions in the in-house built µRAMOS/BioLector combination device: temperature 37 °C, 48-round well plate (MTP-R48-B), filling volume 0.7 mL, shaking frequency 1000 rpm, shaking diameter 3 mm, complete modified Poolman medium with 10 g/L glucose. Trace elements of complete modified Poolman medium (0.009 g/L $ZnSO_4 \cdot 7\ H_2O$, 0.004 g/L $CoSO_4 \cdot 7\ H_2O$, 0.004 g/L $CuSO_4 \cdot 5\ H_2O$, 0.003 g/L $(NH_4)_6Mo_7O_{24} \cdot 4\ H_2O$, 0.066 g/L $CaCl_2 \cdot 2\ H_2O$, 0.016 g/L $MnCl_2$, 0.005 g/L $FeCl_2$, 0.005 g/L $FeCl_3 \cdot 6\ H_2O$) or trace elements of Pbp medium (0.013 g/L $MnSO_4 \cdot H_2O$, 0.0046 g/L $CuSO_4 \cdot 5\ H_2O$, 0.0028 g/L $Na_2MoO_4 \cdot 2\ H_2O$, 0.015 g/L $Fe_2(SO_4)_3 \cdot H_2O$) were used. Results: In those cultivations, effects of different trace element solutions on the total cell concentration, spore concentration, sporulation efficiency, and fluorescence intensity were observed. The OTR curves were similar despite the different trace element solutions. In the cultivations, various trace elements were exchanged in parallel at the same time. The experiment should be repeated with the exchange of one trace element per experiment.